A Machine Learning Approach for Clinical Gait Analysis and Classification of Polymyalgia Rheumatica Using Myoelectric Sensors

A thesis submitted for the degree of Doctor of Philosophy

By

Anthony Bawa

Department of Electronic and Electrical Engineering

Brunel University London

December 2023

Abstract

The study focuses on Polymyalgia Rheumatica (PMR), an autoimmune musculoskeletal disease primarily affecting the shoulder blade and hip muscles in older adults, particularly women aged 50 and above. The research aims to address two main challenges: the need for more clarity on the disease's pathophysiology and the challenge of identifying disease severity in patients. The study introduces a novel approach involving movement assessment, by designing a low-cost MyoTracker system, and using electromyography (EMG) features to understand the impact on patients' hip muscles. A clinical trial was conducted at Komfo Anokye Teaching Hospital in Ghana, where the study employed a qualitative research approach to monitor movement patterns. Participants were tasked to perform exercises comprising of gait, knee lifting, and knee extension with sensors attached to the hip muscles.

This research unfolds in three iterations, the first investigation involved hip muscular imbalances where the significant difference between patients and healthy controls in the maximum voluntary contraction (MVC) values was recorded. The bilateral difference computed between the left and right hip in patients exhibited 15% MVC on average compared to the healthy control group's 6%, indicating substantial hip muscular imbalances. The second iteration involved a movement assessment to identify specific movement patterns in patients. Support Vector Machine (SVM) achieves 85% accuracy for gait exercises, while Decision Tree (DT) performs less efficiently at 70%. SVM also excels in knee lifting exercises (70% accuracy), outperforming DT (60%). Based on hip muscle activation, patients' movement patterns significantly differ from healthy controls. In the third iteration, deep learning techniques, specifically RNN-LSTM and Vision Transformer (ViT), classify PMR disease severity based on EMG features. The study's results carry significant clinical implications with the evidence of hip muscular imbalances aiding in designing tailored rehabilitation protocols. Importantly, this study uses a cost-effective method for determining disease severity, enabling predictions about patients with severe PMR conditions. The key contribution of this thesis is the identification of patients' specific movement patterns and the determination of PMR severity among patients. Other contributions are the detection of hip muscular imbalance in patients and the design of rehabilitation protocols to address hip

muscular imbalances and improve patients' range of motion, enhancing overall well-being. In conclusion, this comprehensive study leverages innovative approaches, from a MyoTracker system for movement assessment to deep learning models, to unravel the complexities of PMR disease. The collaboration with medical experts emphasises the potential real-world impact of this research in enhancing the treatment and recovery processes for individuals.

Table of Content

Abbreviations

EMG – Electromyography

CM- Confusion Matrix

ROC – Receiver Operating System

IMU – Inertia Measurement Unit

ML – Machine learning

PMR- Polymyalgia rheumatica

MS- Multiple Scoliosis

MKS- Microsoft Kinect Sensor

MCS- Motion Capture System

GCA – Giant Cell Arteritis

SVM – Support Vector Machine

DT – Decision Tree

RF – Rotation Forest

KNN- K-Nearest Neighbor

LSTM – Long Short-Term Memory

RNN – Recurrent Neural Networks

GRU – Gated Recurrent Units

FTF – Fourier Transform Techniques

MPF- Mean Power Frequency

RMS- Root Means Square

MVC – Maximum Voluntary Contraction

MAV – Mean Absolute Value

MEF – Median Frequency

DWT – Discrete Wavelet Transform

MCDCD – Maximum Cross Domain Classification Discrepancy

TA – Tibia Anterior

FOG- Freezing of Gait

RF- Rectus Femoris

VL – Vastus Lateralis

BF – Biceps Femoris

SC- Spearman's Correlation

SE – Semitendinosus

LCC – Linear Correlation Coefficient

ICC- Intra-Class Correlation

ViT- Vision Transformer

List Of Figures

List Of Tables

Dedication

I dedicate this work to the Almighty God for his grace and mercy throughout my research. I would also like to dedicate my work to my family, (Mr. Samuel Bawa and Mrs. Janet Bawa) who are far away in Ghana, who gave me emotional support and urged me to conduct this research. I also dedicate this to my siblings Martin, Sheila, Cletus, Rose, and Joseph for their diverse support in conducting this research. I also wish to dedicate this to fiancée Sarah Bachelle who has always been supportive to me.

Publications

The following papers are a result of the research work conducted in this thesis.

1. Anthony Bawa, Konstantinos Banitsas, Maysam Abbod, "A Review on the Use of Microsoft Kinect for Gait Abnormality and Postural Disorder Assessment", *Journal of Healthcare Engineering*, vol. 2021, https://doi.org/10.1155/2021/4360122

2. Bawa, A.; Banitsas, K. Design Validation of a Low-Cost EMG Sensor Compared to a Commercial-Based System for Measuring Muscle Activity and Fatigue. *Sensors* 2022, *22*, 5799. https://doi.org/10.3390/s22155799

3. Anthony Bawa, Konstantinos Banitsas, "MyoTracker: A Mobile Application to Monitor and Determine Muscles Strength" Proceedings of WRFER International Conference, Houston, August 2023

4. Bawa, A., Banitsas, K. (**2023**), 'An Assessment of the Hip Muscular Imbalance for Patients with Rheumatism', Proceedings of World Academy of Science, Engineering and Technology, Open Science Index 203, International Journal of Biomedical and Biological Engineering, 17(11), 300 – 306

5. A. Bawa, K. Banitsas, M. Abbod, M. van Gils, P.A. Moreno-Sanchez, "Classification of the Gait Pattern in Polymyalgia Rheumatica Patients Using Recurrent Neural Networks", Proceedings of the International Conference on Integrated Systems in Medical Technologies, ISMT 2023, Sept. 2023. doi: 10.25593/open-fau-354

6. Bawa, A.; Banitsas, K.; Abbod, M. A Movement Classification of Polymyalgia Rheumatica Patients Using Myoelectric Sensors. *Sensors* 2024, *24*, 1500. https://doi.org/10.3390/s24051500

Acknowledgement

I want to thank my supervisor, Dr. Konstantinos Banitsas, for his immense contribution and support in compiling this work. He has inspired me and provided good guidance in my research. I am also grateful to Prof. Maysam Abbod, Dr. Ioana Pisica, and Dr. Nicolas Boulgouris.

Secondly, I would like to thank the team of medical experts at Komfo Anokye Teaching Hospital in Ghana who collaborated on this research, comprising of Dr. Mensah Yeboah (rheumatologist), Dr. Evans Ansu-Yeboah (Medical Officer), and Mr. Baafi Sorti. I appreciate their efforts in conducting the critical trial in this research. Finally, I would like to acknowledge the support from my sponsors at the Ghana Scholarship Secretariat for funding this research work.

CHAPTER ONE: INTRODUCTION

1.1 Background

Telemedicine and artificial intelligence (AI) systems have revolutionised healthcare delivery by using communications in collaboration with special devices to provide accessible and efficient healthcare. Telemedicine and AI concepts have recently gained popularity, accelerated by global health challenges and the desire for new innovative solutions in healthcare. Both concepts offer advantages such as reducing patient travel time and costs, enabling medical expertise to provide medical solutions in underserved areas and facilitating timely patient intervention. The growth of telemedicine in particular, has been driven by expanding Internet connectivity and developing secure digital platforms that comply with health regulations. AI systems include a variety of technologies that enable machines to simulate human-like intelligence and decision-making processes. These systems are leveraged to identify patterns and analyse complex medical data to assist medical professionals in diagnosing diseases and recommending treatment plans. The convergence of telemedicine and AI systems has ushered in a new era of healthcare delivery characterised mainly by improved efficiency. In recent times, medical sensors have been applied in telemedicine, and some of these sensors are designed to capture essential patient data such as temperature, blood pressure, oxygen concentration, and glucose levels. These sensors can provide valuable tips on preventive measures to manage certain medical conditions. Medical sensors and wireless networks provide a communication backbone to aid in the delivery of desired health needs to patients remotely. The design of a personalised wireless network that uses intelligent sensors to gather essential data with a limited processing power has been illustrated in a study [1].

Biomechanics of musculoskeletal disease and neurological disorders has seen recent growth among researchers. It involves the analysis of the musculoskeletal systems that control the locomotion of humans. The biomechanics of human movement describes the forces that acts on the musculoskeletal system and how the rest of the body responds to these forces. The human movement is controlled by the muscles, bones, ligaments, tendons, and the central nervous system. Musculoskeletal disorders, such as osteoporosis, osteoarthritis, and traumatic muscle injury, are quite common. The biomechanics of

humans gives a better understanding of muscles and joint function or dysfunction, leading to improved designs of medical devices such as orthopaedic braces and the development of rehabilitation protocols. Clinicians and physiotherapists would normally use gait analysis to detect walking disabilities and decide on the appropriate exercise to improve movement. The use of motion capture systems provides effective tools to conduct gait assessments. Motion capture systems such as Microsoft Kinect and Viscon systems are used in gait analysis because they provide enhanced 3D skeletal and kinematic features to track human activity in determining gait disorder [2]. Currently, there is a lot of ongoing research on the biomechanics of musculoskeletal diseases and neurological disorders, with new diagnostic and treatment measures sought by medical professionals.

1.2 Motivation for the Study

This study focuses on the biomechanics of patients with Polymyalgia rheumatica in Ghana. Polymyalgia Rheumatica (PMR) is a disease that affects the inflammation of the muscles and joints that is characterised by stiffness and pain in the shoulder blade, hips, and around the pelvic girdle [3]. The pain is known to be severe in the mornings when patients undergo daily activities such as getting up from bed or climbing stairs. Polymyalgia rheumatic disease affects typically older adults, usually from the age of 50 years onwards [4]. The stiffness and pain characterised by the disease may severely affect the movement of people with the disease. However, it is not conclusive on how this condition could affects the movement pattern of patients.

The motivation for researching on the biomechanics of patients with polymyalgia rheumatica (PMR) is the potential benefits that possible solutions might offer for patients and the medical community. Firstly, movement analysis can objectively assess patients' disease progression and severity. It would shed some light on the underlying mechanisms of the impact of disease on muscle function joints and explore new avenues for therapeutic development. Another motivation for this study is to contribute to a broader scientific understanding of musculoskeletal disorders and inflammatory conditions regarding movement. The results generated from this work will inform clinicians to guide the development of new rehabilitation protocols. In addition, the study sheds some light on the link

between musculoskeletal function and disease pathology, that will be essential for healthcare professionals to pave the way for alternative diagnosis techniques.

1.3 Problem Statement

The detection of movement disorders is crucial in effectively managing musculoskeletal diseases, as it informs treatment strategies tailored to individual patient needs. However, the pathophysiology of polymyalgia rheumatica (PMR) remains inadequately understood, presenting challenges in developing targeted interventions. There exists a notable gap in the comprehension of PMR patients' pathophysiology and its broader impact, including its progression and influence on patient mobility. This knowledge deficiency poses difficulties for clinicians in accurately assessing treatment efficacy. Moreover, there is a notable absence of research examining whether strained hip muscles around the pelvic girdle contribute to mobility limitations in PMR patients. Additionally, objective measures for assessing hip muscles and joint movement in PMR patients are lacking, hindering precise quantification of the disease's effects during motion. This study aims to address these gaps by investigating the strained hip muscles around the pelvic girdle and analyzing patient movement patterns. Furthermore, it seeks to explore if strained hip muscle activation signals can serve as indicators of disease severity, offering a novel approach to differentiate between severe and mild PMR cases. Furthermore, the lack of consensus on PMR diagnostic criteria presents challenges in accurate detection. To tackle this issue, the study provides clinically relevant data that can facilitate the development of a decision support system for diagnostic purposes.

Moreover, the study delves into the potential muscular imbalances caused by inflamed hip muscles in PMR patients compared to healthy controls. By elucidating the complex interplay between PMR disease and movement assessment, this research aims to enhance our understanding of the condition and improve clinical management strategies. The research problem is structured into the following key points in a sequential order for more clarity.

Lack of Understanding of PMR Pathophysiology:

The pathophysiology of PMR is not thoroughly understood, posing challenges in developing effective treatments and interventions. This lack of understanding hampers clinicians' ability to address the disease comprehensively.

Uncertainty Regarding PMR Disease Progression and its Impact on Patient Movement:

The progression of PMR and its effect on patient movement remains largely unknown. This lack of knowledge complicates treatment evaluation and impedes clinicians' ability to gauge the efficacy of interventions.

Challenges in Objective Measurement of Hip Muscles of PMR Patients:

Objective measures to assess hip muscles and joint movement in PMR patients are lacking. This gap makes it difficult to accurately quantify the effects of the disease during motion, hindering treatment evaluation and outcome assessment.

Investigate Hip Muscle Activation Signals in PMR Severity Discrimination:

Current mechanisms to distinguish between severe and mild PMR cases are limited. This study aims to utilize hip muscle activation signals to discriminate between severe and mild cases, thereby enhancing diagnostic accuracy and treatment planning.

The breakdown down in a sequential order to provide a comprehensive understanding of the research problem and its significance in advancing knowledge and improving clinical care for PMR patients. There is a dearth of research on whether strained hip muscles around the pelvic girdle contribute to mobility limitations in PMR patients. Understanding this aspect is crucial for devising targeted interventions to improve mobility and quality of life.

1.4 Research Questions

The research questions within the scope of this study align with the broader research problem, aiming to address a critical gap in understanding and managing polymyalgia rheumatica (PMR) and its impact on movement disorders and musculoskeletal health. These questions are designed to shed light on specific aspects of PMR pathophysiology, its manifestation in patient movement, and potential diagnostic and therapeutic implications.

The main research question for this thesis: Is there a discernible modification in the gait pattern among patients with polymyalgia rheumatica based on hip muscle activation?

Investigating whether discernible modifications occur in the gait patterns of PMR patients due to hip muscle activation, to optimise rehabilitation protocols. Other research questions for the thesis which aimed to address the research problem are as follows.

ii) Are the movement patterns associated with polymyalgia rheumatica different from healthy control subjects? This question is answered by **c**omparing Movement Patterns Between PMR Patients and Healthy Controls**.**

iii) Is there a muscular imbalance between the hip muscles of patients with polymyalgia rheumatica compared to healthy control subjects? By **i**nvestigating muscular imbalance in PMR patients compared to Healthy Controls. This helps to address the problem of muscular imbalances.

iv) Can the muscle activation pattern be used to identify mild and severe conditions of polymyalgia rheumatica in patients? Assessing the feasibility of using muscle activation patterns to differentiate between mild and severe cases of polymyalgia rheumatica in patients.

v) What is the most efficient deep learning model that can support diagnosing polymyalgia rheumatica disease based on hip muscle activation? Identifying the optimal deep learning model capable of supporting the diagnosis of polymyalgia rheumatica based on hip muscle activation data.

vi) Can a newly designed low-cost EMG MyoTracker system serve as an alternative biomarker to monitor the progress of patients? Investigating the viability of utilizing newly designed low-cost EMG sensors as alternative biomarkers for monitoring the progress of PMR patients.

These research questions above are aligned with the overarching research problem, aiming to address key aspects of PMR pathophysiology, diagnosis, and management, thereby enhancing our understanding of the condition and improving clinical care strategies.

1.5 Research Hypothesis

Some hypotheses are inferred to facilitate the research's conduct in achieving the objectives. The hypotheses show the potential relationship between variables in the study. It is the guiding framework

for conducting this study through empirical data testing and analysis. Four hypotheses have been formulated in this study.

First Hypothesis:

Patients with polymyalgia rheumatica may exhibit modified movement patterns attributed to the strained hip muscles. This hypothesis directly addresses the lack of understanding regarding strained hip muscles' contribution to mobility limitations in PMR patients, aligning with the research problem's focus on investigating movement disorders in PMR diseases.

Second Hypothesis:

Substantial imbalance in hip muscular activity is anticipated in PMR patients as opposed to healthy control individuals. This hypothesis corresponds to the research problem's exploration of potential muscular imbalances caused by inflamed hip muscles in PMR patients compared to healthy controls.

Third Hypothesis:

Applying deep-learning models using EMG signals may effectively determine the severity of polymyalgia rheumatica conditions among patients. This hypothesis aligns with the research problem's aim to address the lack of consensus on PMR diagnostic criteria by exploring alternative diagnostic approaches, such as utilizing deep-learning models and EMG signals.

Fourth Hypothesis:

The diagnostic potential for polymyalgia rheumatica can be postulated by the analysis of patients' hip muscle activation patterns. This hypothesis is directly linked to the research problem's objective of utilizing hip muscle activation signals to enhance diagnostic accuracy and treatment planning for PMR patients.

The above research hypotheses are linked to the research problem, in providing empirical evidence to address the gaps in understanding PMR pathophysiology, disease progression, and its impact on patient movement, ultimately contributing to improved clinical management strategies.

1.6 Aim and Objectives of Study

1.6.1 Research Aim

The study's main aim is to investigate if polymyalgia rheumatica patients have altered gait patterns based on the hip muscles activation and determine the severity disease based on EMG signals. The thesis conducts a clinical gait analysis of PMR patients using surface EMG sensors to identify patients movement patterns compared to healthy control subjects. This is to provide a better understanding of the pathophysiology of PMR patients. The thesis also explores the use of EMG signals to determine the severity of the disease among patients. This would be used to segregate between mild and severe conditions of PMR for clinical interventions.

1.6.2 Objectives

The research objectives outlined below are designed to address specific gaps and challenges identified within the context of the provided research problem.

Objective 1: To comprehensively analyze existing literature and state-of-the-art for detecting gait disorders. The study critically evaluates previous works and summarizes the trends in biomechanics.

This thesis conducts a comprehensive analysis of current literature and cutting-edge research to detect gait disorders. This involves critical evaluation of prior studies to identify trends in biomechanics.

Objective 2: Design a low-cost EMG MyoTracker system to record muscle signals via a mobile application. The low-cost system would be calibrated with the standard EMG sensor to test its viability in capturing EMG data.

Developing an affordable EMG MyoTracker system for recording muscle signals using a mobile application. This system will undergo calibration with standard EMG sensors to evaluate its effectiveness in capturing EMG data. This addresses the problem of alternative biomarkers to measure muscle signals.

Objective 3: Compare the muscle co-activity of the strained hip muscles for patients and healthy control subjects to identify muscular imbalances. This will be useful to determine if the disease presents imbalances among patients compared to healthy individuals.

This addresses the problem of determining muscular imbalances by Investigating muscle co-activity in strained hip muscles among both PMR patients and healthy controls to detect potential muscular imbalances, aiding in understanding differences between patients and healthy individuals.

Objective 4: Apply deep learning techniques using recurrent neural networks with long-short-term memory (RNN-LSTM) and a vision Transformer model that will be useful for diagnostic purposes. This addresses the problem by identifying the optimal deep-learning techniques that can support the diagnostic capabilities of PMR conditions of EMG signals.

Objective 5: Propose new rehabilitation protocols to help in the recovery process of patients. This would lead to better outcomes for handling patients with PMR disease.

Develop novel rehabilitation protocols to support the recovery of PMR patients, aiming to improve treatment outcomes and enhance patient care strategies.

These objectives collectively aim to address the research problem identified in understanding PMR pathophysiology, and its impact on patient mobility, thereby contributing to advancements in clinical management strategies.

1.7 Scope of the Study

This research aims to conduct a comprehensive clinical movement classification and analysis of patients diagnosed with polymyalgia rheumatica (PMR) using advanced machine and deep-learning techniques. In addition to analyzing muscle activation patterns, this study seeks to investigate any discernible modifications in movement patterns exhibited by PMR patients compared to healthy individuals. To achieve this, the research employs electromyography (EMG) sensors as the primary data collection tool. Moreover, this study extends its scope to include the design and implementation of a low-cost MyoTracker system for recording muscle signals via a mobile application. The MyoTracker system

will be calibrated with standard EMG sensors to evaluate its effectiveness in capturing EMG data. This innovation in sensor technology aims to enhance accessibility to muscle signal recording, particularly in resource-constrained settings. In addition to the movement classification analysis, the research delves into assessing hip muscular imbalances among PMR patients in comparison to healthy controls. Specifically, the study investigates bilateral differences in muscle strength between the right and left hip muscles, shedding light on potential asymmetries that may contribute to mobility limitations in PMR patients. Furthermore, alongside the analysis of muscle activation patterns, this study explores the development of new rehabilitation protocols tailored to aid in the recovery process of PMR patients. These protocols aim to optimize patient outcomes by addressing specific movement impairments associated with PMR, ultimately leading to improved mobility and quality of life for affected individuals.

By integrating these multifaceted approaches, this research seeks to provide a comprehensive understanding of PMR-related movement disorders and contribute to the development of innovative solutions for both diagnosis and rehabilitation in PMR patients.

1.8 Clinical Trial

A clinical trial was conducted at the esteemed Komfo Anokye Teaching Hospital (KATH) in Ghana, aimed at investigating polymyalgia rheumatica (PMR) patients alongside healthy control subjects. Prior to participant recruitment, ethical approval was diligently obtained from both Brunel University and KATH, ensuring strict adherence to ethical standards and protocols throughout the study. The clinical trial was overseen by a team comprising a consultant rheumatologist and two medical doctors, all of whom provided expert guidance and supervision throughout the trial process. The recruitment phase spanned over two months and took place within the rheumatology department at KATH Hospital, where eligible participants were identified and invited to take part in the study. For the data collection process, state-of-the-art electromyography (EMG) sensors were employed to meticulously capture muscle activity in the strained hip muscles of both PMR patients and healthy control individuals. These EMG sensors served as the biomarkers for the data acquisition, providing valuable insights into muscle

activation patterns crucial for the analysis conducted in this study. This clinical trial not only adhered to stringent ethical guidelines but also employed cutting-edge technology and involved expert medical professionals to ensure the integrity and reliability of the data collected. Through meticulous planning and execution, the trial aimed to shed light on the intricate dynamics of PMR-related movement disorders, thereby contributing to advancements in clinical understanding and treatment strategies for this condition.

1.9 Structure of Thesis

The study has three main iterations to meet the main aims and objectives of the research. The first iteration is the muscular imbalances assessment, the second iteration is the movement classification of the two groups with machine learning algorithms and the third iteration is apply deep learning techniques for the analysis of EMG datasets. The rest of the thesis is organised into the following chapters,

Chapter Two Literature Review: This chapter presents the literature review focusing on movement of neurological and musculoskeletal disease and the state-of-the-art for movement assessment. The Literature review is divided into four subsections where the first section provides a general overview of the Polymyalgia rheumatica condition. The second subsection looks at the theoretical framework of gait analysis. The third subsection reviews the state-of-the-art in gait analysis for wearable and non-wearable sensors. This section examines the relevant papers and musculoskeletal disease, focusing on Osteoarthritis. The four subsection reviews the existing procedure for diagnosing Polymyalgia rheumatica disease. It also examines the traditional diagnostic methods and how deep learning techniques can serve as an alternative in diagnosing musculoskeletal disease.

Chapter Three: Design of Low-Cost MyoTracker EMG System- This chapter describes the design of a low-cost MyoTracker system for measuring muscle signals. It explains the approach in designing the low-cost EMG system and calibrating it with a standard Trigno Avanti sensor. The equipment used in developing the low-cost EMG system are described in this section.

Chapter Four: Methodology- This chapter describes the methods used in the study to achieve the study's aims. The study provides a mixture of quantitative and qualitative approaches in the research design. This chapter also describes the clinical trial process and the exercises conducted by participants. A clinical trial conducted at Komfo Anokye Teaching Hospital (KATH) in Ghana collected EMG data from participants. The primary EMG data collected from polymyalgia rheumatica patients and healthy control subjects were extraction. The techniques used for the analysis of the EMG data recorded is discussed.

Chapter Five: Muscular Imbalance Assessment and Movement Classification- This chapter describes the machine learning techniques for movement classification. The first part discusses the muscular imbalance assessment between patients and healthy control subjects. In the second part a number of traditional machines are applied for EMG classification from the extracted feature. The classification evaluation metrics are presented in this section.

Chapter Six: Deep Learning Approach Using RNN-LSTM and Vision Transformer-This chapter proposes the use of deep Learning techniques such as LSTM-RNN and vision Transformer model for the movement classification using EMG signals. The deep learning models are evaluated for their performance and address the limitations of traditional machine learning models. The chapter also describes the EMG features which can be used to distinguish between severe and mild conditions.

Chapter Seven: Discussion-This chapter discusses the findings of this study and the main contributions of this research work. It also compares the results obtained with previous similar works and the limitations of the findings The clinical and practical implication of the results for clinicians are discussed in this section. The chapter also proposes rehabilitation protocols based on the findings to help improve the well-being of patients.

Chapter Eight: Conclusion and Future Works- The final chapter contrasts the initial aims and objectives against the work performed. The research results and the clinical trial's main contributions to improving patients are outlined. Future research that other researchers can explore based on the findings is stated.

Figure 1. 1 Thesis Structure Overview

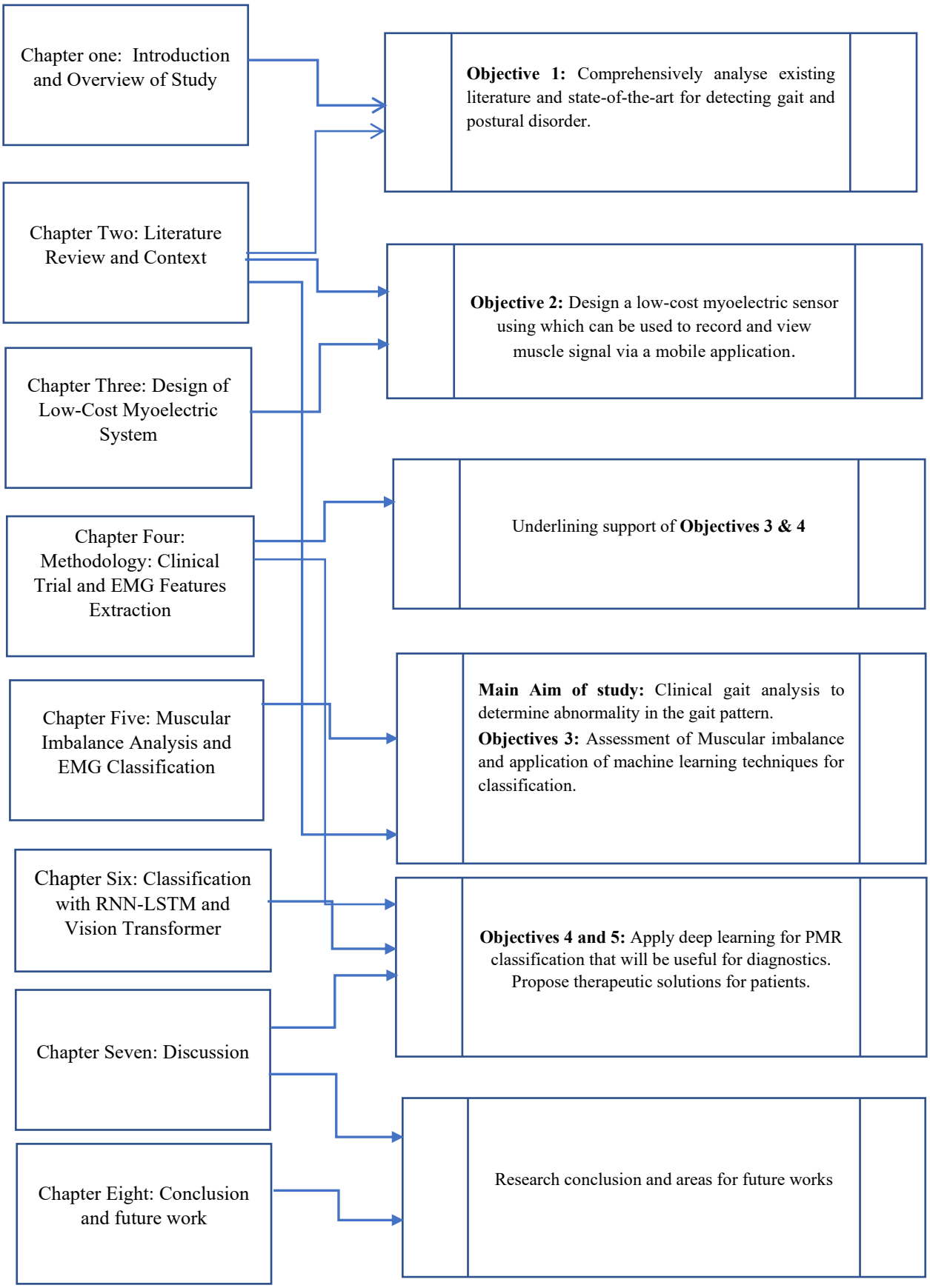

CHAPTER TWO: LITERATURE REVIEW

2.1 Overview

The chapter discusses a review conducted on the analysis of movement in patients with musculoskeletal conditions, particularly focusing on Polymyalgia Rheumatica (PMR) disease. It organizes various themes in the literature review into subsections, adopting a thematic approach. The chapter delves into the background of musculoskeletal disorders, honing in on PMR disease. It provides a theoretical framework for gait analysis and discusses the conceptual approach involved. Furthermore, it critically evaluates the state-of-the-art techniques used in movement analysis, including those utilizing both wearable and non-wearable sensors. Additionally, it explores the detection of gait abnormalities through machine and deep learning methods. Through this review, existing studies are analyzed in detail, leading to the identification of research gaps that form the foundation of the present study. The process of the literature review is depicted in a flow chart diagram (Figure 2.1), emphasizing the specific research gap targeted by this study.

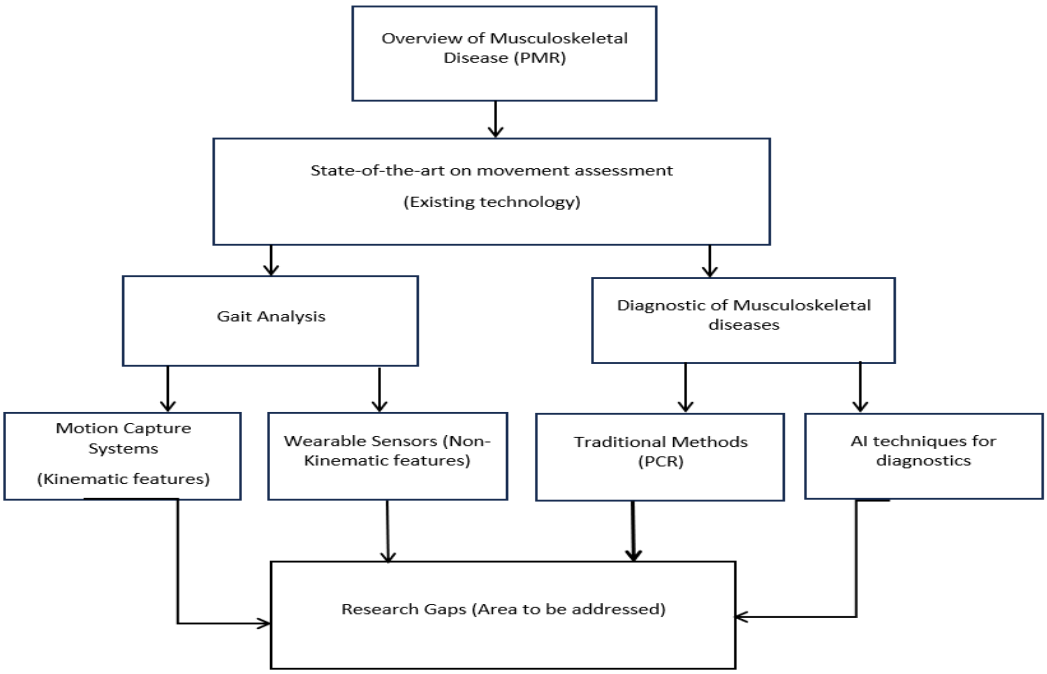

Figure 2. 1 A flow chart diagram of literature review

2.1.1 Technical Background of Literature Review

The literature review encapsulates the essence of the research problem, emphasizing the critical need for improved detection and understanding of movement disorders in the context of musculoskeletal diseases, particularly Polymyalgia Rheumatica (PMR). Highlighting the inadequacies in comprehending PMR's pathophysiology and its impact on patient mobility, it underscores the challenges clinicians face in tailoring effective treatment strategies. Moreover, the absence of research investigating the role of strained hip muscles in PMR-related mobility limitations and the lack of objective measures for assessing hip muscle function further exacerbate the problem. The study aims to bridge these gaps by delving into the intricate relationship between strained hip muscles and PMR, offering insights into patient movement patterns and potential indicators of disease severity.

Exploring the potential of machine learning and deep learning methodologies alongside wearable sensor technologies presents a promising avenue for examining gait irregularities among individuals with PMR disease. Machine learning models demonstrate adeptness in identifying subtle deviations indicative of abnormal gait, thereby aiding in the prompt detection and ongoing monitoring of musculoskeletal and neurological conditions impacting mobility in PMR patients. Deep learning methodologies, such as recurrent neural networks (RNNs), excel in capturing intricate relationships embedded within sensor-derived data, thereby enabling precise identification of abnormal gait dynamics. This comprehensive approach facilitates continuous monitoring and delivers personalized insights, equipping clinicians with invaluable resources to enhance diagnostic accuracy and tailor treatment strategies for individuals with PMR.

2.2 Background of Musculoskeletal Diseases

Musculoskeletal disease can be described as a group of conditions that affect the muscles, joints, and tissues [5]. Musculoskeletal diseases can result from various factors such as injury to the muscle, infections, autoimmune responses, and degeneration of the muscle tissues due to old age. Although the progression of musculoskeletal diseases may vary, this usually results in muscular weakness, pain,

sensory loss, and automatic dysfunction [6]. Some common examples of musculoskeletal diseases are osteoarthritis, rheumatoid arthritis, muscular dystrophy, polymyalgia rheumatica, fibromyalgia, etc. Patients with rheumatic conditions such as osteoarthritis (OA), rheumatoid arthritis (RA), ankylosis spondylitis (AS) and polymyalgia rheumatica (PMR) suffer from the distortion of muscle functions. A reduction in muscle functional capacity is quite common among patients in the hip and knee joints. Polymyalgia rheumatica (PMR) is a common autoimmune muscular disease among older people of 50 years and above [7]. PMR prevalence in the UK primary care population was recorded in 910 cases for 100,000 people, 1040 for women, and 780 for men [8]. In Ghana, where the setting of this research is situated, there are no available statistics on the prevalence of PMR disease among the elderly population. PMR disease creates an inflammation that causes pain and stiffness, usually worse in the mornings, gradually improving during the day [9]. PMR can result in difficulty doing daily activities such as getting up from bed, standing up from a chair, and climbing up a stair. Approximately 15% of patients with rheumatic conditions may develop Giant Cell Arteritis (GCA) and almost 50% of the patients with GCA are likely to get PMR over time [9]. The symptoms of PMR may vary among individuals, where some patients experience severe pain in muscles around the hip and shoulder joints. Below in [Figure 2.2] is an image of a patient with PMR illustrating the areas of pain [10].

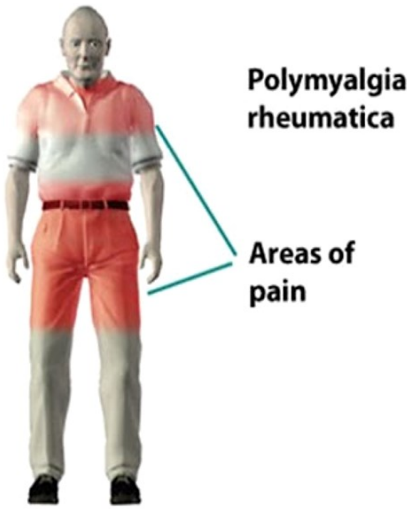

Figure 2. 2 Polymyalgia Rheumatica Patient

PMR treatment with Prednisolone helps reduce pain and stiffness experienced due to muscle inflammation [11]. Relapses of the disease are very often with the possibility of new symptoms, making the condition chronic. Even though most patients with PMR may respond well to the treatment of glucocorticoids, there is a high tendency for some patients to experience a relapse [11].

Movement assessment plays an essential role in diagnosing and managing musculoskeletal disease. The change in muscle strength, range of motion, and muscles coordination can be used in understanding and evaluating the movement of patients. It may help monitor the progression of the PMR disease in individuals. Gait analysis allows for measuring, processing, and interpreting biomechanical parameters that characterise human movement. It also provides valuable information on the impact of muscle diseases on an individual's mobility and functioning, enabling healthcare professionals to develop tailored interventions.

2.3 Theoretical Framework in Gait Analysis

The theoretical framework examines the basic principles and concepts that guide the study and interpretation of human gait patterns. The framework is synthesised based on the work by Pirker et al [12] which provided a clinical guide for gait studies in adults. Gait analysis is the systematic study of human movement, and it includes many different fields such as biomechanics, physiology, and motor control. The theoretical framework of gait helps clinicians and researchers to understand, interpret, and to apply information obtained from gait analysis. Analysis of gait and other movements relies heavily on biomechanical principles to understand the mechanical aspects of human movement, including forces, torques, joint movements, and the behaviour of muscles during movement. It also provides knowledge about the musculoskeletal system and nervous system by identifying the underlying cause of gait abnormalities. In movement analysis, kinematic and non-kinematic features are two distinct types of features for evaluating movement. Both kinematic and non-kinematic features providing insight into the movement patterns and fundamental forces involved in walking. Human gait combines the complex interaction of the human body's muscles, ligaments, tendons, bones, and neurons. Gait analysis measures kinematic features such as stride length, step size, velocity, and joint angles, which

are essential for movement assessment. It also includes an analysis of joint angles, forces, torques, muscle activity, and movement segmentation. Non-kinematic features such as EMG signals and muscle force can be used for movement assessment. The degree of movement variation is considered beneficial or adverse depending on the theoretical perspective chosen to explain underlying motor control. Pathological gait analysis assesses and diagnoses abnormal gait patterns due to neurological or musculoskeletal disorders. It also provides accurate and detailed information to understand patient gait mechanics comprehensively.

2.3.1 Conceptual Approach to Gait Analysis

The concept of gait assessment provides a systematic approach in examining movement such as walking or running. A typical gait starts with a heel strike, a loading stance, then a mid-stance, followed by a terminal stance, a pre-swing of the leg and toe-off, mid-sway of the leg, and finally, a terminal swing. [12] Factors that determine the gait of persons are pelvic tilt and rotation, lateral pelvic displacement, hips, and knee flexion. The hip muscles that connect the knee joint to the pelvic girdle play an essential role in movement. Figure 2.3 illustrates a diagrammatic approach to a gait cycle [12].

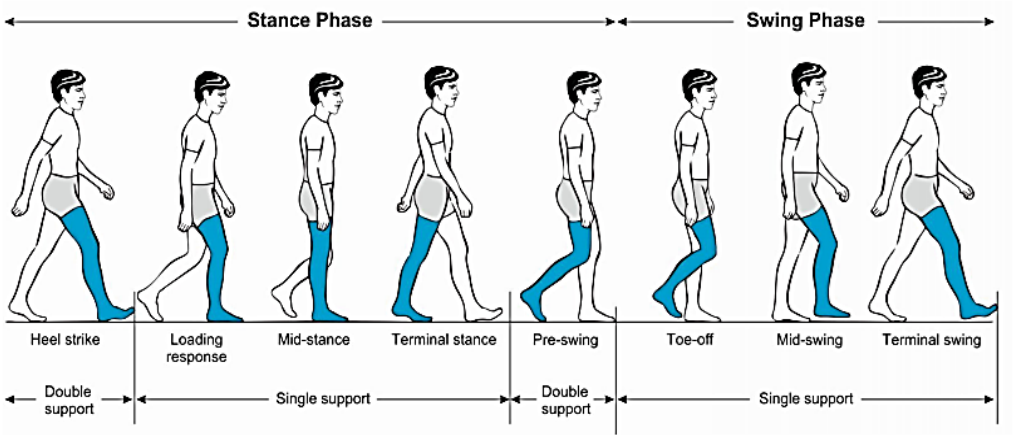

Figure 2. 3 Functional Gait Cycle

In the gait cycle [12], the first initial phase is the ***loading response***, with initial contact of the foot to the ground. The hamstrings control the hip muscle's activity, primarily the biceps femoris, vastus lateralis, rectus femoris, and gluteus maximus muscles. In the ***midstance phase***, the body is in motion,

where the quadriceps initiate the knee extension while the hip abductors continue their activities. At the ***pre-swing phase***, the rectus femoris acts in an isometric fashion, which limits the knee flexion to assist the hip muscle as a person moves faster. During slow walks, the joint and ground reaction is relatively small to initiate a knee flexion. In the ***swing phase***, the hip flexors, and the rectus femoris continue their pre-swing activity. While the activity varies among people, the hip abductors assist the initial swing and the pre-swing of the hip flexion. In the ***mid-swing*** phase, the muscle activity halts momentarily, while in the ***terminal swing***, the hamstring acts to reduce the swing extremity. The joints of the hip flexes during the swing phase and extend during the stance phase in walking. The hip abductors and the quadriceps initiate the muscle activity to complete the gait cycle. These processes illustrate the role of the hip muscles activity during movement [12].

2.3.2 Mathematical Analysis of Gait Process

Mathematical analysis of gait includes quantitative techniques to describe biomechanical aspects of human walking. This process includes a simulation and a statistical modelling of the motion process. As mentioned in previously, the human gait is controlled by internal muscles, nerve coordination, and external factors. Some studies have demonstrated the correlation between muscle activation and gait process. Miller et al [13] illustrated a Latency Correlation Ensemble Average (LCEA) computed for each stride in the muscle activation during a gait process. The mathematical model by Miller model allows for the quantification for each stride taken during motion. The LCEA for each stride is in the equations below [13].

$$\bar{y}[p] = \frac{1}{N}\sum_{n=1}^{N} y_n[p] p = 1 \rightarrow 128 \tag{2.1}$$

The LCEA is computed by the average of individual stride profiles after time shifting for each profile with an original correlation phase.

$$\hat{y}[p] = \frac{1}{N}\sum_{n=1}^{N} y_n[p+\theta_n] \tag{2.2}$$

The variability magnitude, Vm and phase Vp is calculated using the average phase variability is also calculated on the absolute for the phase shift in a single stride.

$$V_m = 1.0 - \frac{1}{N}\sum_{n=1}^{N} Max\left\{\rho_{\hat{}_{yy_n}}(t)\right\} \tag{2.3}$$

$$V_P = \frac{1}{N}\sum_{n=1}^{N} abs\{\tau\} \max\left\{r_{\hat{}_{yy_n}}(\tau)\right\} \tag{2.4}$$

These equations above illustrate the mathematical expression for the strides taken during walking. During movement, the torques at the hip and knee joints are determined using the hip joints. The hip muscles create hip flexion in a forward-swinging motion of the lower leg. Based on the anatomical model shown in [Figure 2.4], the human lower limb is measured as a serial manipulator with rigid links to estimate the internal forces of the lower limb joints [14].

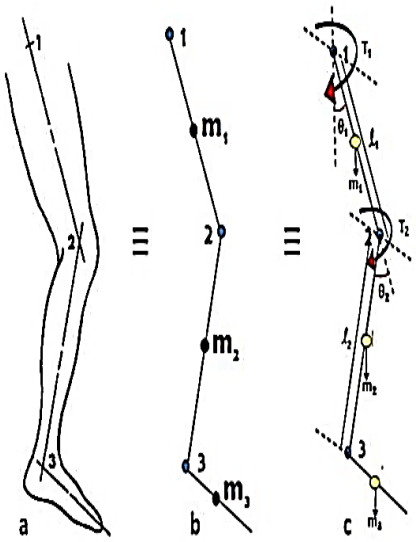

Figure 2. 4 Anatomical Model of the human lower limb

2.4 State of the art for Gait Analysis

The equipment for movement analysis is categorised into wearable and non-wearable (contactless) sensors [15]. Non-wearable sensors are motion capture devices that digitally record movement using

built-in sensors with cameras to track 3D human body joints and kinematic features. These motion capture (mocap) systems can also capture skeletal joints of the human body during motion. On the other hand, wearable sensors are electronic devices attached to the body to capture spatiotemporal parameters such as muscle activity. Wearable sensors can record other physiological features required in gait analysis. Both motion capture systems and contactless sensors are effective tools for gait analysis in research. There have been several advancements in studies conducting clinical gait analysis using wearable sensors such as inertia measuring units (IMU), electromyography (EMG), and foot pressure plate sensors. Contactless motion recording systems and wearable sensors can be used for movement analysis to detect abnormal gait. The connection between these two technologies lies in the common goal of recording and analysing gait patterns in complementary ways. Motion capture systems can synchronously collect data along with wearable sensors, which can validate the data captured. Motion recording systems quantify the movement of humans, and recent innovations in optical motion recording systems have added unprecedented to assess gait impairment. Gold standard techniques are applied to perform gait analysis against system and motion recording markers. The type of data collected from these devices is tailor-specific and appropriate for rehabilitation treatments.

2.4.1 Motion Capture Systems for Gait Analysis

Motion capture (mocap) systems provide detailed information on body positions, joint angles, and corresponding linear and angular velocities. Some motion capture systems for movement assessments are Vicon, Qualisys, OptiTrack, Kinect Xbox, etc. Kinematic data recorded from mocap, such as joint angles, swing angles, gait speed and velocity, stride length, stride width, step angle, and cadence or rhythm, are essential for gait analysis [15].

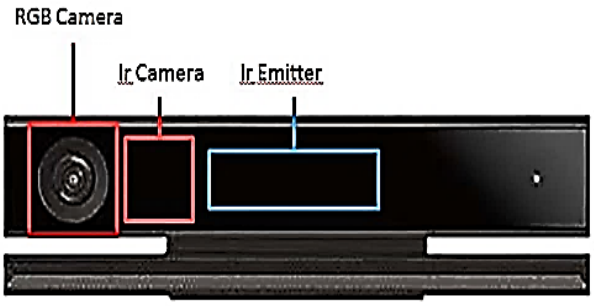

Figure 2. 5 Microsoft Kinect version 2 sensor

Microsoft Kinect presents some capabilities for gait research beyond the initial design as a game console [16]. The key features of the Kinect sensor in [Figure 2.5] are the RGB camera used for capturing colour images of the simulation environment and the IR camera and IR emitter function together to calculate depth. Kinect sensors also allow for interaction through voice commands and gesture recognition, which are unique components of the technology. Kinect sensor has been presented as an effective tool for capturing skeletal information in gait analysis [16]. Using Kinect sensors, the relative distance of lower extremities and joint angles can be used for gait recognition. Prathap et al [17] presented gait recognition using Kinect's skeletal data, which serves as a digital eye. Dynamic and static features were extracted using the sensor with two distinctive algorithms for gait recognition. A Lovenberg-Marquardt backpropagation and correlation algorithms achieved 94% and 90% accuracy, respectively. One challenge with this work is the small dataset used. A large dataset is required to test the reliability of the algorithms. Hassain et al [18] demonstrated a novel technique using Kinect and a deep neural network for gait recognition. The authors used feature vectors from the joints forming triangle area and relative cosine of dissimilar triangles as the dataset. This method is an improvement of the previous work by Prathap [17], with an accuracy of 98.0% recorded. The results were promising and could be replicated in a natural environment to monitor movement. A novel approach for detecting foots-offs and foot-contacts in a gait cycle with a Kinect V2 sensor was demonstrated in [19] using participants' foot contact, foot-off phases, and knee joint angles. The results were good with an accuracy of 86.52% achieved in the study. Below in [Figure 2.6] is a picture of a participant using Kinect sensor to measure gait kinematics [19].

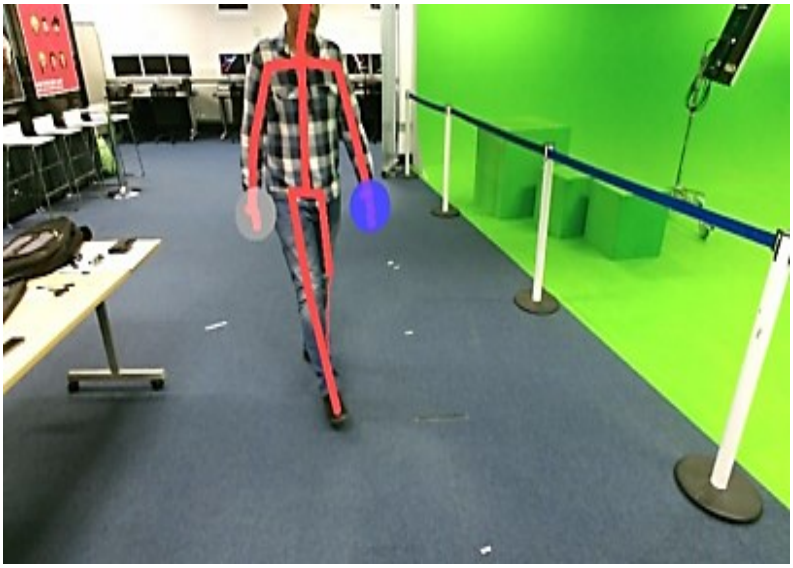

Figure 2. 6 Using Kinect sensor to track body joints.

Gait analysis plays an essential role in detecting and evaluating gait abnormalities in patients with musculoskeletal diseases [19]. The link between gait analysis and musculoskeletal disorders lies in its ability to provide valuable information on how muscular conditions affect a person's walking habits and overall mobility. Abnormal gait analysis can be detected by evaluating various gait-related parameters, such as stride length, step width, speed, joint angle, and pressure distribution in the foot. A comparison of these gait parameters with established standards can help identify deviations from typical gait patterns that may be indicative of gait abnormalities.

2.4.2 Abnormal Gait Detection Using Motion Capture Systems

Gait abnormality is the asymmetric movement in individuals which may be a result of physical injury or damage to the central nervous system [20]. As already explained in the previous session the skeletal system and muscles play key roles during movement. Muscle disorders create damage, weakness of muscles, and joint problems in patients. The literature survey first considers the use of a motion capture system for movement assessment for neurological and musculoskeletal diseases.

2.4.2.1 Machine learning Techniques with Motion Capture Systems

Machine learning techniques, when integrated with motion capture systems, offer a powerful approach to detecting gait abnormalities. By leveraging data obtained from these systems, machine learning algorithms can analyze various gait parameters such as stride length, step width, joint angles, and pressure distribution to identify deviations from typical gait patterns indicative of abnormalities. Studies have demonstrated the effectiveness of machine learning in this context, utilizing motion capture data from sensors like Kinect to classify abnormal gait patterns with significant accuracy. These methods enable automated and objective assessment of gait disorders, providing valuable insights for clinicians in diagnosing and monitoring musculoskeletal and neurological conditions affecting mobility. The

integration of machine learning with motion capture systems not only enhances the detection of gait abnormalities but also paves the way for personalized treatment strategies tailored to individual patient needs.

Some studies have demonstrated motion capture (mocap) for abnormal gait detection with significant results achieved. Sun Bei et al [20] presented gait disorder detection with multiple Kinect sensors. This approach used gait symmetry which was calculated based on the correlation between angles of the leg swing, locations of ankle joints of the knee and hip. The gait cycle and length were extrapolated using a Zero-cross detection method. The extracted gait features were able to report gait disorder among participants. The approach used was significant in detecting gait symmetry to distinguish between normal and abnormal gait.

Aleš Procházka et al [21] presented a novel technique with Bayesian model to determine gait disorder in Parkinson disease. Images captured from Kinect sensor with 3D skeletal tracking joints and process signals were used to evaluate gait features in identifying movement disorders. The authors achieved an accuracy of 94.1% for gait disorder classification based on the gait features. Even though the study achieved good accuracy, some key joint angles were not considered with the Bayesian model for abnormal gait recognition. Also, the dataset used in the study was limited and did not provide sufficient reliability with the approach used. Nevertheless, the results indicated a good approach in recognising gait disorder.

In [22] the authors illustrated the use of machine learning techniques and kinematic data for early detection of gait abnormality. The gait cycle captured from patients were compared with normal gait frames to distinguish the two classes. The authors set up 70% threshold in gait asymmetric to distinguish normal and abnormal gait using a cross-correlation between existing recorded database. Two limitations to this work were the criteria for setting up 70% threshold which was low and the second was the validation of gait asymmetric in the study. Further testing is required using this approach to validate the results.

A study by Tsukagoshi et al [23] demonstrated a non-invasive technique using depth sensor to detect movement disorder. This approach allowed gait features to be extracted from ataxia, Parkinson,

and healthy control subjects for evaluation using machine learning techniques. Kinematic features such as gait rhythm, stride length, and ratio of walking route length were assessed to determine walking disorders in patients. The results were significant in identifying gait disorders among patients with Parkinson and ataxia, but the accuracy achieved with this method was not stated. Another challenge is that some key gait parameters and joint angle were not considered which is important for patients with ataxia.

A study by Kazlow et al [24] demonstrated gait abnormality among participants. Gait features such as stride length, cadence, and joint angles were extracted from multiple Kinect sensors. The authors applied a dynamic Bayesian Network and the recorded kinematic features for different abnormal gaits. An accuracy of 88.68% was obtained in classifying distinct gait abnormalities. This study is similar to work done by Procházka [21], which used a Bayesian network for abnormal gait classification. The challenge with this work is the relatively small dataset and the divergent distinctive features extracted were not adequately addressed. Furthermore, the model does not provide sufficient reliability in identifying gait abnormality.

2.4.2.2 Deep Learning Techniques with Motion Capture Systems

Deep learning techniques, when coupled with motion capture systems, offer a sophisticated approach to detecting gait abnormalities. By processing vast amounts of kinematic data obtained from motion capture sensors, deep learning models such as recurrent neural networks (RNNs) and long short-term memory (LSTM) networks can learn intricate patterns in gait dynamics. These models excel at recognizing complex relationships within the data, enabling accurate identification of abnormal gait patterns. Studies have demonstrated the efficacy of deep learning in this domain, achieving high accuracy rates in classifying various gait abnormalities. By leveraging the capabilities of deep learning, motion capture systems can provide clinicians with valuable insights into patients' gait mechanics, aiding in the diagnosis and treatment of musculoskeletal and neurological disorders affecting mobility. This integration holds great promise for advancing the field of gait analysis and improving patient care through more precise and personalized interventions.

Deok-Won et al [25] presented RNN-LSTM model capable of recognising five different abnormal gait patterns using multiple Kinects sensors. The RNN-LSTM model was trained with the extracted kinematics data to distinguish irregular gait patterns from normal gait depending on the sequence lengths. The challenge with this method is that the RNN-LSTM model could only recognise the abnormal gait used in training the model but is deficient in detecting other gait disorders. Nevertheless, the results obtained were significant in detecting abnormal gaits with an accuracy of 97%. This work is an improvement of previous studies by Procházka [21] and Kazlow [24] using the Bayesian model for abnormal gait detection.

In a study by Elkholy et al [26], a new technique was used to detect abnormal actions by neuromuscular patients. Extracted skeletal features were used to build an automatic system for abnormal gait detection and determine the quality of activity performed. The motion asymmetry between the right and left body joints were used to distinguish between normal and abnormal patterns. The average stride distance and joint angles were computed using Euclidean distance in the equation (2.5) below.

$$D_{ij}^{p} = \frac{\sum_{t=1}^{n} \sqrt{(x_{it} - x_{jt})^2 + (y_{it} - y_{jt})^2 + (z_{it} - z_{it})^2}}{n} \tag{2.5}$$

Dρ represents the left and right of the average distance of a subject while x_{it}, y_{it}, and z_{it} represent the 3D coordinates of the joint *i* of an issue of frame *t,* and *n* is the number of frames of action sequence. Np is the set of joints for the left and right body parts. The velocity magnitude feature was computed to detect slow action performed by the subject. The equation used to calculate this is given by equation (2.6) below.

$$V = \frac{\sum_{t=1}^{n-1} \sum_{i=1}^{N} \sqrt{(x_{i(t+1)} - x_{it})^2 + (y_{i(t+1)} - yit)^2 + (z_{i(t+1)} - z_{it})^2}}{(n-1)N} \tag{2.6}$$

Equation (2.6) is essential in computing the displacement magnitude for each body joint between two successive frames where N represents the number of joints and n represents the number of frames.

Corina et al [27] presented the gait pattern classification in osteoarthritis patients using kinematic data from the Viscon MX13 system and two force measuring plates with LSTM model. Instrumented gait analysis was conducted for 15 healthy control subjects and eight asymmetric ankle osteoarthritis patients. The results indicated that the asymmetric ankle osteoarthritis had reduced hindfoot dorsiflexion with lower motion rotation than healthy controls. An accuracy of 97.8% was reported in discriminating the gait pattern between healthy control and the affected ankle of patients. The significance of this work is that it will help clinicians understand the movement mechanism in the early stages of ankle osteoarthritis. The approach used in this study can be replicated in clinical settings to detect ankle osteoarthritis for immediate attention.

The survey above illustrates the use of non-contactless motion capture systems for the movement assessment of patients with various conditions. Predominantly, Kinect sensors have been widely used in a number of studies with kinematic data. Even though motion capture systems are suitable for detecting gait abnormality, there are some limitations to using motion capture systems for musculoskeletal disease. The main challenge is that motion capture cannot capture intrinsic muscle features and activation patterns based on muscle signals, which is essential for patients with muscle diseases. In addition, mocap requires subjects to be in a controlled environment for movement assessment. Wearable sensors have emerged as an alternative technology for gait analysis to detect muscle activity and abnormalities in musculoskeletal disease. Wearable sensors can be used to measure kinematics, and electromyography (EMG) data for gait during movement.

2.4.3 Gait Analysis Using Wearables Sensors

Wearable sensors are non-invasive electronic devices designed to human body contact in collecting data directly. An electromyography (EMG) device is a wearable sensor that measures electrical muscle activities during contraction. EMG sensors can be used as diagnostic tools to detect musculoskeletal disease, assess muscle pain, and for kinesiology [28]. These sensors could be invasive or non-invasive used to measure muscle signals. When placed on the skin surface, a non-invasive sensor allows current

to flow through the electrode by electrolytic induction. It allows electrical muscle signals to be captured with sensor electrodes. Invasive EMG sensors, on the other hand, are inserted into the muscle tissue to capture the electric activity of muscles. Invasive sensors are used where deep muscle activities are required for research in kinesiology. Figure 2.7 is the Trigno Avanti sensor from Delsys used for capturing muscle signals [29].

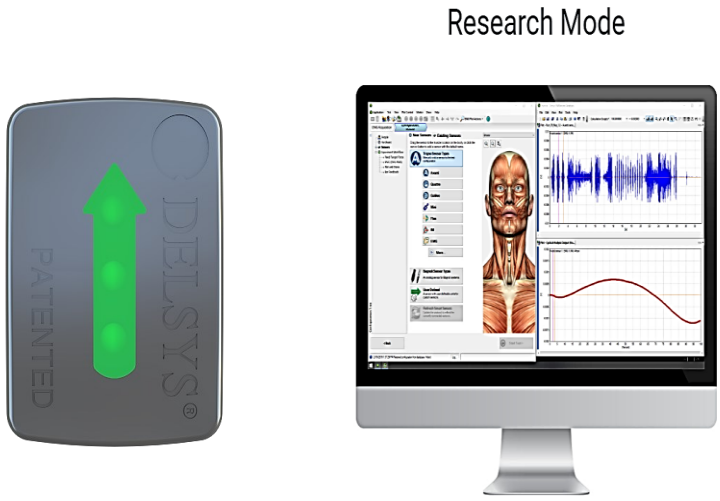

Figure 2. 7 Delsys Trigno Avanti System

2.6.4 Abnormal Gait Detection Using Wearable Sensors

Abnormal gait detection using wearable sensors represents a cutting-edge approach in healthcare technology. By harnessing data from accelerometers, gyroscopes, and electromyography (EMG) sensors embedded in wearable devices, such as smartwatches or specialized motion trackers, abnormalities in walking patterns can be accurately identified. These sensors capture subtle changes in movement dynamics, allowing for the early detection of musculoskeletal and neurological disorders affecting mobility. Through sophisticated algorithms and machine learning techniques, wearable sensors can analyze gait parameters and patterns in real time, providing clinicians with valuable insights into patients' movement patterns.

2.6.4.1 Machine learning Techniques with Wearable Sensors

Machine learning techniques, when integrated with wearable sensors, offer a promising approach to detecting gait abnormalities. By leveraging data collected from wearable sensors, such as accelerometers, gyroscopes, and electromyography (EMG) sensors, machine learning algorithms can analyze various gait parameters and patterns to identify deviations indicative of abnormal gait. Studies have demonstrated the effectiveness of machine learning in this context, utilizing wearable sensors to measure kinematic and EMG data during walking exercises. These methods enable automated and objective assessment of gait disorders, providing valuable insights for clinicians in diagnosing and monitoring musculoskeletal and neurological conditions affecting mobility. The integration of machine learning with wearable sensors not only enhances the detection of gait abnormalities but also facilitates remote monitoring and real-time analysis, allowing for more personalized and timely interventions tailored to individual patient needs.

EMG sensors have been used to detect gait abnormalities in patients with muscular disorders in previous studies. Reza et al [30] developed an inertial measurement unit (IMU) sensor used to identify gait asymmetry extracted from a muscle. In the study, an Android app was designed to collect EMG data with an IMU sensor from the lower extremities of participants. The results showed that the designed sensor was a viable tool to determine gait abnormalities. An accuracy of 97.73% was significant to illustrate the reliability of the model. A study by Nardo et al [31] presented occurrence frequency as a key parameter for assessing muscles during walking. EMG signals were acquired from the tibialis anterior, rectus femoris, gastrocnemius, and biceps femoris muscle of participants. The results illustrated that the occurrence frequency is suitable for evaluating muscle activity during walking. Based on the findings, some studies have proceeded to use EMG data as the feature for gait analysis.

2.6.4.2 Deep Learning Techniques with Wearable Sensors

The integration of deep learning techniques with wearable sensors heralds a significant advancement in gait abnormality detection. By leveraging data captured by accelerometers, and electromyography

(EMG) sensors embedded in wearable devices, deep-learning models can discern intricate patterns indicative of abnormal gait. These models, such as recurrent neural networks (RNNs) and convolutional neural networks (CNNs), excel at capturing complex relationships within the sensor data, enabling accurate identification of deviations from normal walking patterns. This approach enables real-time analysis of gait dynamics, allowing for early detection of musculoskeletal and neurological disorders affecting mobility. By providing continuous monitoring and personalized insights, the fusion of deep learning and wearable sensors offers clinicians a powerful tool for improving diagnostic accuracy and treatment efficacy in patients with gait abnormalities.

Some studies illustrated the use of deep learning techniques using deep models to detect gait abnormality. Yao Guo et al [32] presented EMG sensors used to detect gait abnormality detection. In this study, the authors employed multiple wearable sensors to measure the intrinsic features of the muscles used in detecting gait disorders. The raw EMG signals were extracted using the Discrete Wavelet Transform (DWT) in a time domain series. The support vector machine (SVM) and the Bidirectional Long Short-Term Memory (Bi-LSTM) algorithms were used in this study. In order to demonstrate the effectiveness of the model, the authors compared EMG data with the kinematic data from a motion capture system. The results indicate that the EMG data was sufficient for abnormal gait recognition. This was an improvement for abnormal gait recognition based on the previous work. However, the challenge with this study is that the accuracy and reliability of this method were not stated. Further experiment is required using this method to determine the accuracy of this process. Bryan et al [33] implemented a dynamic neural network to detect freeing of gait (FOG) for patients with Parkinson disease. The design sensors were placed on the shin and thigh of patients to measure muscle signals. The authors proposed a model to train FOG data collected from different participants. The results indicated that the EMG device can detect FOG with high accuracy. The study had an overall sensitivity of 83% and a specificity of 97%. Mohd et al [34] presented an analysis of EMG signals from the gastrocnemius (GAS) and tibialis anterior (TA) muscles in detecting gait abnormality among children with autism. The EMG data obtained from the lower limbs of participants provided significant information to distinguish the gait of children with autism against normal children. The results were

promising in distinguishing the gait pattern for the two groups. Ivan et al [35] proposed EMG sensors to detect and analyse the freezing of gait for patients with Parkinson disease with deep learning models. The developed system could monitor and identify FOG in a free environment. The novelty of this work is that the designed device could merge information from gyroscopes and EMG sensors. This work is very similar to the work by Bryan [33] in detecting FOG. The only difference is that this study illustrates the ability of FOG to be detected abnormality with higher reliability. This improvement of the earlier work allows FOG to be identified in a constrained environment. Furthermore, this work provided feedback to patients in real-time based on motor performance and FOG detection.

Sasanka et al [36] presented a wearable sensor that combines a planter pressure measuring unit and IMU to detect gait abnormality among participants. The authors designed a wearable sensor with a pressure-measuring insole based on piezo-resistivity technology in the study. RNN-LSTM was used to train datasets in classifying gait abnormality among participants. The results indicated that the developed system was feasible for identifying different gait disorders. This was novel as different gait abnormalities, such as Parkinson, ataxia, and hemiplegia, were detected from the designed system. Chakraborty et al [37] used inertial sensors and deep neural networks to illustrate gait abnormality detection. The study recorded the walking pattern of children with cerebral palsy and healthy control children with two inertial sensors. DNN model was used to train and automate gait features to identify abnormal gait patterns. An accuracy of 90.97% and 96.4% for subject-wise evaluation and segment-wise were recorded, respectively. This work is similar to the study done by Mohd [34] in identifying abnormal gait for children with autism. The neural network used by Chakraborty achieved higher accuracy for abnormal gait recognition compared to the work by Mohd.

Nair et al [38] presented EMG pattern recognition for patients with arthritis. The two forms of arthritis considered were osteoarthritis (OA) and rheumatoid arthritis (RA). The authors employed two classification algorithms, namely the Least-square kernel (LSK) and the Neural Network algorithm, to automatically classify the EMG patterns for the two groups. LSK showed superior performance in the EMG classification compared to neural networks. The study illustrated the novelty of using the LSK algorithm for classifying the EMG pattern in OA and RA patient, which support diagnostic purposes.

Furthermore, this approach allows for identifying strained muscles critical in designing corrective rehabilitation measures for patients. The findings were significant and can be replicated with the kernel algorithm to identify severely affected muscles. Appropriate rehabilitation protocols were designed to strengthen affected muscles based on this approach. Ankit et al [39] presented a hybrid technique to identify abnormal arthritis knee based on surface EMG data recorded. In this paper, a wavelet denoising-ensemble empirical mode decomposition (WD-EEMD) was used to analyse surface EMG signals to identify lower knee abnormality and healthy control subjects based on the muscle activities of the lower limbs. Even though the proposed work achieved significant results, this study has two limitations. Firstly, the dataset used in the study was relatively small, so the proposed method needs to be validated with a large dataset. The second challenge is that the method was done with an offline dataset. There is a need for further research for real-time analysis that will be useful to clinicians.

Based on the literature [31-35], the best way to detect movement patterns of musculoskeletal diseases is to use wearable sensors using deep learning models. Although motion capture systems are suitable for detecting gait disorders, they have limitations when it comes to musculoskeletal disorders. Motion capture systems are not able to detect muscle characteristics and activation patterns which are essential for patients with PMR disease. Furthermore, motion capture systems require individuals to be in a controlled environment for movement assessment. Wearable sensors serve as an alternative technology to gait analysis to detect abnormalities in muscle activity and musculoskeletal diseases. These can be used to measure kinematic and electromyographic (EMG) data on gait during exercise and can also remotely monitor the gait of patients recovering from musculoskeletal disorders.

From this survey, the position of this study is that wearable sensors are the best tool for the movement assessment of musculoskeletal disorders specifically PMR disease. Wearable sensors have shown significant potential in monitoring and detecting gait abnormality in Parkinson, ataxia, etc. This study adopted the use of wearable EMG sensors for the data collection from participants. Even though a study by Ankit [39] examined the movement pattern of patients with Osteoarthritis with mocap, there is no evidence of using EMG sensors to monitor the movement of patients with PMR disease. Furthermore, there is no empirical evidence to show the potential of EMG sensors to determine the

severity of PMR conditions. Even though in [39], abnormal arthritis knee was detected with slight variation in the disease manifestation of individual patients, the study did provide the severity among patients. This study is focused on investigating the hip muscle activation of PMR patients that is compared with healthy control subjects to determine whether patients have altered movement. Recent studies [32][37] have shown that wearable sensors generate robust and valid gait parameters compared to motion recording systems intended for patients. The relationship between wearable sensors and the diagnosis of musculoskeletal conditions is multifaceted. EMG data provided valuable insight into how PMR diseases affect a person's mobility and functioning. Wearable sensors can help detect subtle changes in movement patterns and biomechanics, which can be early signs of musculoskeletal problems.

Utilizing machine learning and deep learning techniques with wearable sensors presents a promising avenue for investigating gait abnormalities in patients with PMR disease. By integrating data from accelerometers and electromyography (EMG) sensors these advanced algorithms can effectively analyze gait patterns and parameters. Machine learning models can discern subtle deviations indicative of abnormal gait, aiding in the early detection and monitoring of musculoskeletal and neurological disorders affecting mobility in PMR patients. Deep learning techniques, such as recurrent neural networks (RNNs), excel at capturing complex relationships within sensor data, enabling accurate identification of abnormal gait dynamics. This approach facilitates continuous monitoring and personalized insights, offering clinicians valuable tools for improving diagnostic precision and tailoring treatment strategies for PMR patients. By leveraging the muscle synergy between wearable sensors and advanced computational methods, researchers can enhance understanding of PMR-related gait abnormalities. Machine and deep learning algorithms can analyze datasets of patient movement patterns, muscle activation signals, and clinical data to identify patterns that may not be immediately evident to human clinicians. This can help in understanding the relationship between strained hip muscles, movement limitations, and PMR severity. By training predictive models on collected data, machine learning can help in forecasting disease progression and severity based on various factors, including hip muscle strain and movement patterns. Furthermore, machine learning algorithms can be employed to develop a decision support system for diagnosing PMR. By leveraging clinically relevant

data collected from patient assessments, these systems can provide valuable insights to aid in accurate and timely diagnosis. In addition, deep learning techniques, particularly those involving neural networks, can learn complex relationships between strained hip muscle activation signals and PMR severity.

2.7 Musculoskeletal Diagnostic Systems

Musculoskeletal diagnostics identifies conditions affecting muscles, ligaments, joints, and bones. The diagnostics of muscular disease may be complex because of varying systems and their effect on muscles. A traditional way of diagnosing musculoskeletal conditions is a thorough physical examination of the affected joint or muscle. It involves assessing motion range, strength, and the stability of body joints. Joint movement gives further insight into the muscle activities around the affected joint. In medical settings, image tests such as X-rays, magnetic resonance imaging (MRI), or computed tomography (CT) scans are used to diagnose musculoskeletal disorders [40]. These tests can provide detailed images of the bones, muscles, and joints which have been affected. Another way of examining muscular disorders is laboratory testing of blood samples to detect musculoskeletal conditions that affect the entire body. For instance, blood sample tests can help diagnose rheumatoid arthritis, which can affect joints. AI systems can also be used to diagnose and improve efficiency in musculoskeletal imaging [41]. This technique helps detect muscle disorders in real time with high accuracy. Additionally, AI systems can use imaging techniques to classify patients based on the severity of musculoskeletal disease quickly. AI techniques are increasingly being applied to diagnose musculoskeletal disorders and can help improve diagnostic accuracy, cost savings, and provide better outcomes for patients.

There are primarily no particular tests to diagnose PMR disease but rather a group of diagnostic tests and classifications to determine the disease within an individual [42]. Even though there are no specific tests in diagnosing PMR disease, the determination of PMR symptoms is based on clinical grounds. Using images, such as MRI, ultrasound, and 18F-fluorodeoxyglucose positron emission tomography (FDG-PET) for diagnosis is being studied increasingly [43]. However, these methods are

not specific to the disease diagnoses based on image capture. The imaging, particularly with FDG-PET/CT, provides hints on underlying GCA in patients with an incomplete response to glucocorticoid therapy. In diagnosing PMR using 18F-fluorodeoxyglucose positron emission tomography, demonstrate that an FDG-PT scan before the commencement of glucocorticoid treatment can help increase the diagnostic accuracy of people suspected to have PMR disease. An average score of 85.1% sensitivity and 87.1% specificity were recorded for people having Polymyalgia Rheumatica [44].

Dasgupta et al [45] developed European League Against Rheumatism (EULAR)/American League of Rheumatism (ACR) criteria for diagnosing. A 6-month clinical trial with 125 PMR patients and 169 non-PMR. A scoring algorithm was developed based on morning stiffness of more than 45 minutes (2 points), hip pain range of motion (1 point), the absence of RF and/or ACPA (2 points), and finally, the absence of peripheral joint pain (1 point). From the designed criteria, a score ≥4 had a sensitivity of 68% and a specificity of 78% to discriminate all compared subjects from PMR. Specificity was high, up to (88%) for differentiating shoulder disease of PMR and with a lower (65%) for determining RA from PMR. When ultrasound was added, the sensitivity increased to 66% and specificity to 81% for scores greater than 5 points. From this work, patients older than 50 years with bilateral shoulder pain and elevated CRP and/or ESR are diagnosed with PMR in the presence of morning stiffness lasting >45 minutes and new hip pain in the absence of peripheral nerve symptoms. This study's results significantly classified PMR patients based on sores of hip muscles and joint pains. Fors et al [46] adopted a similar approach used by Dasgupta [45] in validating patients diagnosed with polymyalgia rheumatica based on the EULAR/ACC classification criteria. The results obtained in this work illustrated an overall accuracy of 60% was achieved to confirm individuals diagnosed with PMR disease.

In this research work, the thesis focuses on the muscle activation patterns of PMR patients and their effects on the range of motion based on the strained hip muscles. Below in Table 2.1 are some selected key papers from the literature survey discussed.

Table 2. 1 Selected reviewed papers.

Authors	Year of Publication	Data Type	Algorithms	Findings
Bei et al [20]	2018	Kinematic features	K-means and Bayesian	A novel technique was illustrated to detect movement disorder based on gait symmetry.
Tsukagoshi et al [23]	2019	Kinematic features	Clinical scale measure	Depth sensors were used to identify the interference of gait patterns in patients.
Procházka et al [21]	2020	Kinematic features	Skeletal tracking	A system was developed to detect gait abnormality in Parkinsonia.
Sasanka et al [38]	2019	EMG signals	LSTM-RNN	The authors developed a novel system to identify different abnormal gait patterns.
Chakraborty [37]	2020	EMG signals	DNN	The walking patterns of children with cerebral palsy and healthy control children were recorded with two inertial sensors.
Guo et al [32]	2020	EMG signals	SVM and Bi-LSTM	The study employed the intrinsic muscle signals to identify abnormal gait patterns.
Ankit et al [39]	2021	EMG signals	LDA classifier	A hybrid technique was used to discriminate the gait patterns between healthy controls and arthritis knee patients.

2.8 Research Gap to Address

From the above literature survey, several literatures have conducted movement assessments for different kinds of conditions. To the best of our knowledge, no available study has investigated the intrinsic muscular activity of patients with polymyalgia rheumatica. No work has reported the movement patterns of patients with PMR disease. This study investigates if the strained hip muscle activities around the pelvic girdle of patients with PMR disease create mobility challenges. There are two main problems this study seeks to address; the first problem is to identify patients' specific movement patterns to determine if they have altered movement patterns based on muscle activation. The second problem addresses the severity of the disease by measuring the hip muscle signals in patients. The research gap is addressed by using EMG signal features to classify PMR disease with deep learning techniques and determining the severity of the disease in patients.

The significance of the gap in this study is to provide helpful information to clinicians and physiotherapists in designing new and improved rehabilitation protocols for people with PMR disease and hip joint problems. The relevant information is used in designing appropriate exercises to relieve pain in the hip muscles and joints to improve the range of movement. This would lead to further studies exploring different dynamics in the biomechanics of PMR disease. Furthermore, the study helps examine the movement pattern of patients to explore deep learning models for classification that will support development of a decision support system for diagnostic purposes. The significant impact of motion analysis of patients with PMR would help improve patient well-being and give a better understanding of the pathophysiology of PMR disease and its effect on movement. Overall, there is some impact of patients and clinicians in the larger community.

CHAPTER 3: DESIGN AND CALIBRATION OF LOW-COST MYOELECTRIC SYSTEM

3.1 Overview

This chapter discusses the design and implementation of a low-cost myoelectric system for measuring muscle signals. The objective is to design a low-cost EMG MyoTracker system that can be used as an alternative to commercial-based EMG sensors, along with the accompanying software, capable of running on a mobile phone. The MyoTracker system is designed with inexpensive electronic components making it accessible to all healthcare budgets. The chapter is divided into two main parts. The first section is the development of the low-cost MyoTracker sensor, which works with an Android application to record muscle signals recorded in real-time. In the second section, the developed MyoTracker is compared to the golden standard commercial-based Trigno Avanti system to test for its reliability. The two systems are used concurrently to measure muscle signals to determine the correlation between them and the validity of the low-cost EMG sensor.

3.2 Background on Low-Cost EMG Sensors

Low-cost EMG systems are affordable sensors designed to measure muscle activity. These sensors can be applied in various applications, such as gait analysis, hand movement recognition, and therapeutic purposes. These sensors can also be used in clinical settings to record muscle activities, which is helpful in the detection of musculoskeletal diseases. In the recent past, some work has been done in the design and implementation of low-cost sensors. Wu et al [47] designed a low-cost surface EMG sensor to recognise hand motion. Extracted features from the raw EMG signals were trained using back propagation neural network (BPNN) to classify different hand gestures. The designed system could recognise hand gestures with an accuracy rate of 96.09%. J. Fu et al [48] presented the development of a low-cost surface EMG sensor that can be used to predict wrist gestures. The developed system provided a convenient human-machine interaction of hand gestures, which could be applied in biometric control applications in industry. Supuk et al [49] developed a low-cost surface EMG sensor

to record muscular activities in gait analysis. The designed hardware was made up of two components, a bio amplifier, and a band-pass filter, which could be used to filter muscle signals between 3-500Hz. Dombele et al [50] proposed a mobile application for monitoring the status of muscles using an Android app and a built low-cost system. The designed system was used to determine abnormality of the muscles among participants. The challenge with this design is that the strength of muscles was not determine in real-time.

Even though there are some significant works in designing low-cost EMG sensors, previous low-cost systems did not measure muscle strength in real-time. There is a gap to be addressed in the design of low-cost EMG sensors. Earlier designed low-cost systems were stationary and not portable for convenient use and as such, did not provide a standalone application that could be used to monitor muscle signals. A proposed MyoTracker system is designed to monitor muscle signals in real time and categorises muscle strength into weak and strong muscles. A mobile-based Android application is designed to interact with a microcontroller-based EMG sensor to monitor and measure muscle strength.

3.3 System Design and Hardware Components

The system design describes the architecture and user interfaces, in developing the low-cost MyoTracker system to meet its specification. This involves creating a system architecture by designing a user-friendly interface and providing data useful for testing the system. The designed MyoTracker sensor has three phases, the first phase creates a high-level structure for the system, and it describes the electronic components used. This includes identifying the system's core modules, subsystems, and their relationship. The second phase involves defining the interfaces and communication protocols between the different components of the system. The third phase involves developing a plan to test the MyoTracker system to ensure it meets the specified requirements. The system testing of the designed MyoTracker allows for defects to be corrected and to help users acceptance the system.

3.3.1 System Architecture

The system architecture diagram is an abstract representation of the low-cost MyoTracker component. It describes the system in terms of structure, functions, and relationships between components. The system architecture diagram in [Fig 3.1] forms the foundation of the MyoTracker system and serves as a guide in developing the system. In the design of the proposed MyoTracker architecture, the hardware components: Arduino Uno board, Myoware sensor module, HC-05 Bluetooth and battery. The battery can power up the entire hardware component of the system, which can last about four hours continuously. An Android application is designed that allows users to operate the sensor via a Bluetooth connection to measure muscle signals and stored signals in a centralised database system.

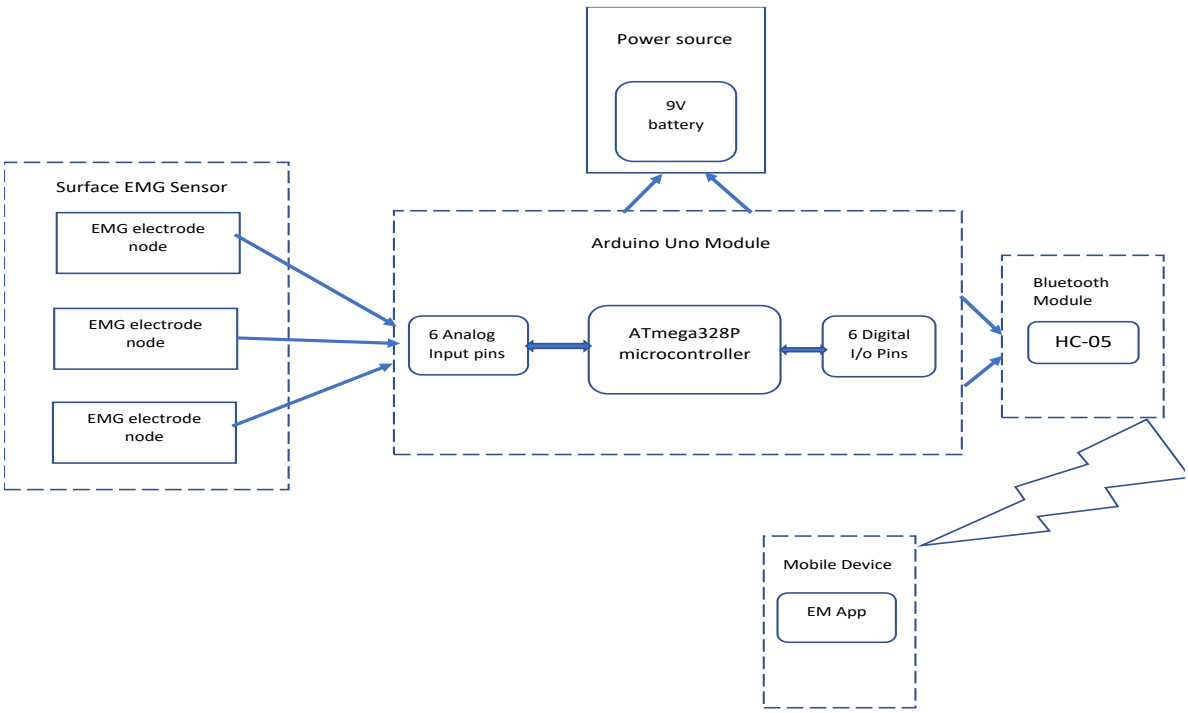

Figure 3. 1 MyoTracker System Architecture

3.3.2 Myoware Sensor

The Myoware sensor module is an all-in-one electrical device designed to measure muscle activity by detecting electrical potentials generated by muscle cells. It is compatible with Arduino and can be used in applications such as prosthetics and rehabilitation. The Myoware sensor board has three electrode

nodes fabricated with two output modes: the raw mode and the enveloped EMG signal mode for measuring electric muscle signals. The sensor board has an adjustable gain, which is purposely designed for microcontrollers [51]. The EMG signals measured by the electrode are then fed into a differential amplifier, allowing the signals to amplify. [Fig 3.2]

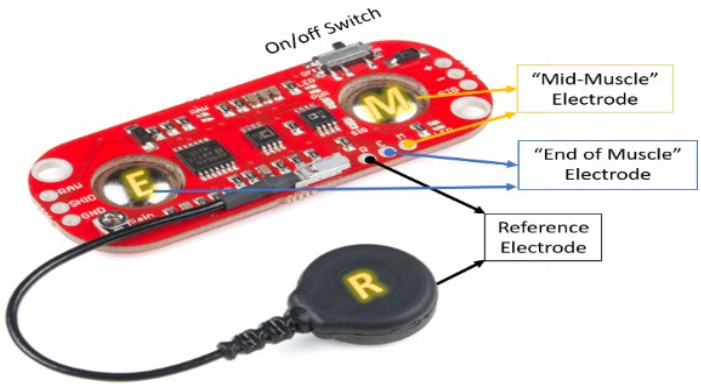

Figure 3. 2 Myoware Sensor board

Table 3. 1 Myoware parameters

Parameters	Values/Range
Operating Voltage	3.3v ~ 5v
Operating Current	9mA
Operating frequency	0-500Hz
Input Impedance	110 Ω
Weight	3.5g
Price	< £5

3.3.3 Bluetooth Module

The HC-05 Bluetooth version 2.0 module is a wireless serial communication module that adds Bluetooth functionality to a system. It can be used with microcontrollers such as Arduino, which can be easily interfaced with laptops or mobile phones with Bluetooth capabilities. The HC-05 Bluetooth module in [Fig 3.3] provides wireless transmission of the muscle signal from the EMG system via the

Android app on the mobile device. The HC-05 module is a master-slave mode device commonly used for wireless Bluetooth data transmission [52] with its parameters in Table 3.2 below. It was used for data transmission with Arduino microcontroller device.

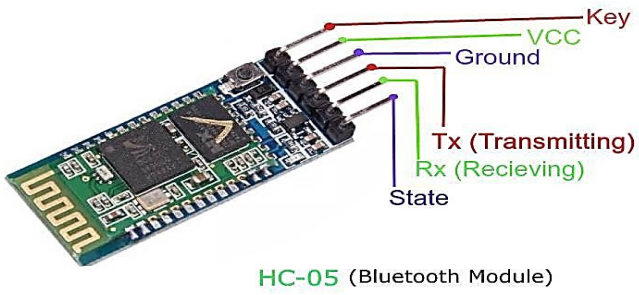

Figure 3. 3 Bluetooth Module board

Table 3. 2 Bluetooth parameters

Parameters	Values/Range
Operating Voltage	4v to 6v
Operating Current	30mA
Range	< 100m
Standardisation	IEEE 802.15.1
Supported baud rate	9600, 19200,38400 bps.
Weight	3.5g
Price	< £5

The HC-05 Bluetooth module uses a serial port protocol for the 2.4GHz frequency band. The Bluetooth technology belongs to the personal area network (PAN), which uses frequency hopping (FH) for data transmission. The sending of data packets between the master and slave mode is encrypted during transmission. An Ad hoc wireless network topology is used by the HC-05 Bluetooth module to connect with neighbouring devices. The transfer of data packets via the HC-05 Bluetooth module depends on the distance and environment. The Bluetooth module can transmit with a distance of 30 metres in a free environment. The HC-05 Bluetooth transmission mechanism can be expressed using the Markov Chain (MC) with two states: N represents the normal state, and D is the duplicated state. In the N-state, the master transmits new downlink frames, or it retransmits the frame to the slave that did not correctly

receive it [53]. The Bluetooth system enters from the N state to the D state when it does not recognise the slave mode, giving a positive acknowledgment. The transition probability from the N state to the D state can be expressed in the equation below.

$$P_{ND} = P_{D_S}^{(M)}(1 - P_{H_S}^{(S)}) \tag{3.1}$$

In the D state, the masters keep transmitting duplicates packets where the transition probability P_{DN} from D to N state.

3.3.4 Arduino Uno

Arduino Uno is a board based on the ATmega328P microcontroller which has 14 digital input/output pins, 6 of which can be used as electrical pulse outputs, and six analog input pins [54]. It also has a 16 MHz ceramic resonator, USB connection, power jack, ICSP connector, and reset button. The Arduino Uno is known for its simplicity and ease of use, making it an excellent choice for programming in designing the low-cost MyoTracker system. It allows users to write programs using the Arduino integrated development environment (IDE), based on the C/C++ programming language. The image of Arduino Uno module board [54] used for the system is illustrated in [Fig 3.4] with its parameters in Table 3.3 below.

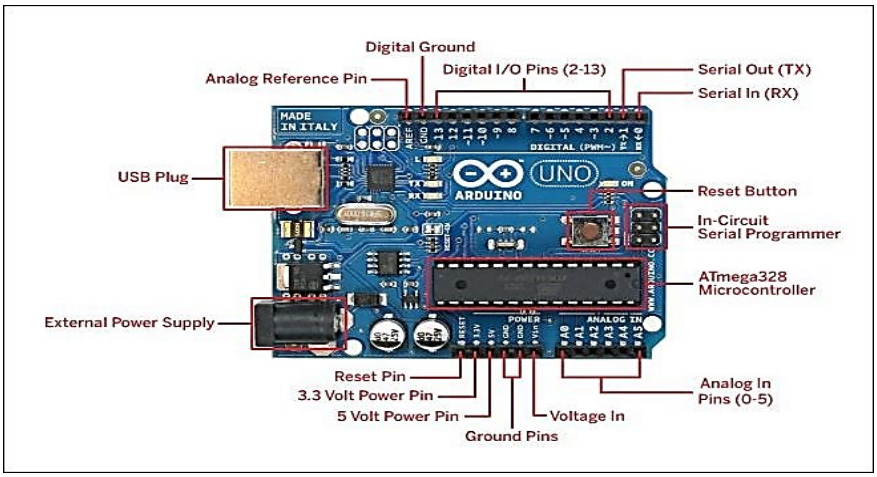

Figure 3. 4 Arduino Uno board

Table 3. 3 Arduino Uno parameters

Parameters	Values/Range
Microcontroller	ATmega328P
Operating Voltage	5V
Input Voltage	7~12V
DC Current per 3.3v	50mA
Clock speed	16MHz
Weight	25g
Price	< £12

3.4 Implementation of MyoTracker System

In this section, the implementation process of the low-cost MyoTracker system is described. Implementing the system involves some key steps in designing the hardware and software. Firstly, the hardware architecture of the MyoTracker system was developed. The system hardware was built from scratch using inexpensive equipment. In the second step, an application was designed to operate the MyoTracker on a mobile device. The MyoTracker was designed to be capable of measuring muscle activity and detecting muscle fatigue. The following sections describe the hardware and software design process of the low-cost MyoTracker system.

3.4.1 Hardware Design of MyoTracker System

The prototype of the designed MyoTracker sensor is illustrated in [Fig 3.5] In the hardware design, jump wires are used to connect the Myoware sensor module, microcontroller, and Bluetooth. The Arduino Uno microcontroller is programmed to connect to the Myoware module and connect wirelessly via Bluetooth to read muscle signals. The amplitude range of the Myoware module is designed to record signals from 0.1-5mV with a digital filter is used to remove noise from the EMG signal. This is achieved by using an inbuilt filter, such as a moving average filter, to smooth the EMG signal and minimise noise. The filtered feature is implemented in Arduino Uno using the analogRead () function and

software algorithms. The Arduino Uno board converts the signals recorded from the Myoware module from analog to digital, which can be transmitted via Bluetooth.

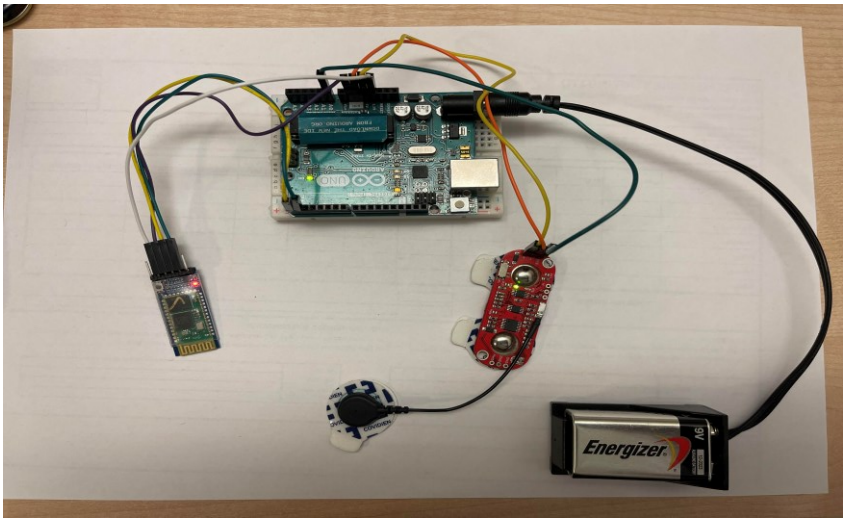

Figure 3. 5 Hardware of the MyoTracker system

When the EMG system is switched on, the Bluetooth module and Myoware sensor lights blinks to show availability. On a mobile device, a user can launch the Myoware app to connect to the MyoTracker system. The user can operate the MyoTracker on the mobile app to record and interpret muscle signals in real-time.

3.4.2 Software Design of MyoTracker System

The Myoware application is designed entirely from the beginning using Android Studio with Java programming language. The user interface application is shown in [Fig 3.6] and [Fig 3.7] has a navigation button and a graph display area. The navigation text area has three main buttons: the start button to commence the MyoTracker sensor reading. It has a stop button to truncate the sensor reading and a clear button to delete the EMG graph display. In the navigation text area has the following features in a drop-down menu:

List Device: This feature shows the HC-05 Bluetooth device available for connection.

View Report: This button allows the user to view the EMG data recorded.

Export Database: This button allows for database of muscle signals recorded in a csv file to exported.

Interpret EMG Recorded: This button does the computation to determine the strength of the muscles recorded in real time.

Clear Database: This button clear the EMG data recorded on the database system.

Exit Application: This closes the entire application and discount from the MyoTracker via the Bluetooth module.

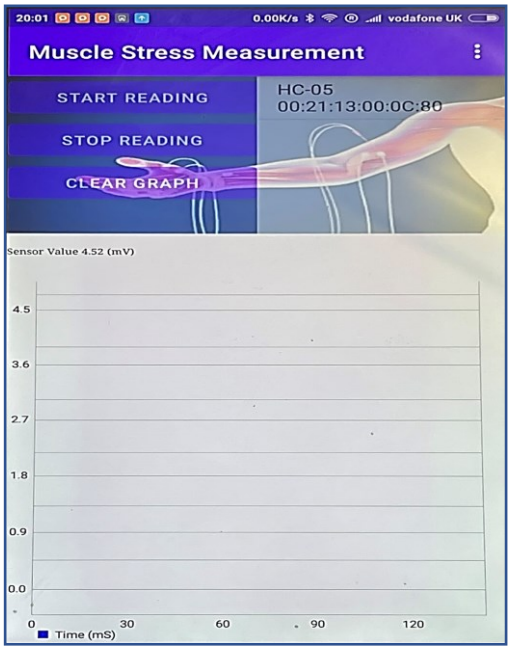

Figure 3. 6 Mobile Application Interface

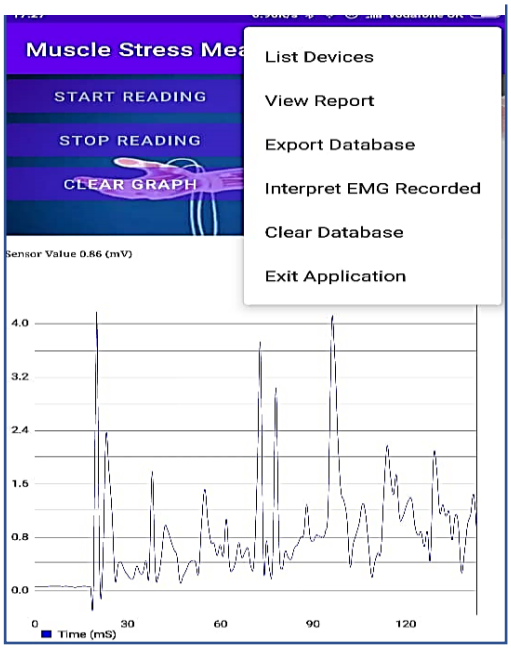

Figure 3. 7 Home View with EMG signal

A user can view reports of EMG signals recorded via the designed Myoware App. EMG signals recorded from a muscle are made up of motor unit action potential (MUAP) [55]. The MUAP is a fundamental feature of muscles contraction activity which can be used to determine the strength of a muscles. The contraction of muscles is key in determine the strength of muscles being measured. The combination of muscle fibers of the single motor unit makes up the MUAP, which can be detected by a surface electrode. This can be expressed in equation 3.2 below.

$$x(n) = \sum_{r=0}^{N=1} h(r)e(n-r) + w(n) \tag{3.2}$$

Where *x(n)* represents the EMG signal, *e(n)* represents the impulse firing, *w(n)* represents the zero means addictive Gaussian noise, and *h(r)* represents the MUAP. RMS can be used to quantify the electric muscle signals that reflect the physiological activity during a muscle contraction process [56]. In the time domain, the EMG signal's amplitude is measured as a time series function. In developing the Android application, the root mean square was implemented to determine muscle strength. The RMS of a signal is given by equation (3.3).

$$X_{RMS} = \sqrt{\frac{1}{N}\sum_{n=1}^{N}|x_n|^2} \tag{3.3}$$

Where *N* is the number of measurements of the signal, and *Xn* represents the value in the measurement. There is a correlation between the root mean square values and the strength of a muscle based on EMG signals. In the algorithm implementation in Java, it is illustrated that the higher the amplitude of the EMG signal, the stronger the muscle contraction activities, and the weaker the muscle, the lower the muscle signal is to the baseline. To determine the strength of a muscle, a threshold is set in categorising muscle strength into two parts, namely weak and strong. For weak muscles, the cumulative average amplitude range of RMS is between (0.1mV to 2.5mV); for strong muscles, the amplitude range of RMS is between (2.6mV to 5.0mV). This is used to interpret the recorded signal in determining muscle strength. The designed microcontroller base Myoware sensor is susceptible to noise, potentially affecting muscle signal fidelity. This is because as the electrical signal travels through the tissues of the muscle fiber, there is some distortion of the muscle signals. In order to take care of the distortion of

signals while testing the designed MyoTracker, the following measures are applied to mitigate the effects of signal distortion.

Ambient Noise: This noise results from electromagnetic radiation, potentially affecting the quality of the EMG signal captured. This is because the human skin surface is inundated with electromagnetic radiation, which is impossible to avoid. The noise in the electronic components can be minimised by using silver chloride electrodes. This technique minimised the noise but increases the signal-to-noise ratio in the designed MyoTracker. The amplitude of the EMG signals is affected by the firing rate of the muscle. The noise can be reduced by filtering out high amplitude outside the normal range of muscle signals.

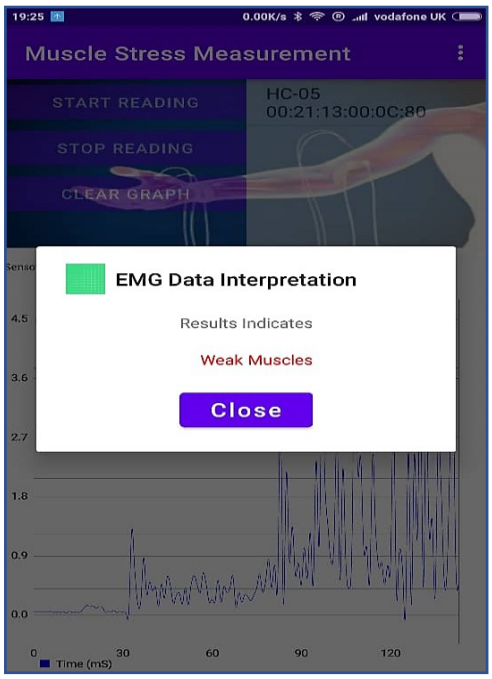

Figure 3. 8 Weak muscles detected.

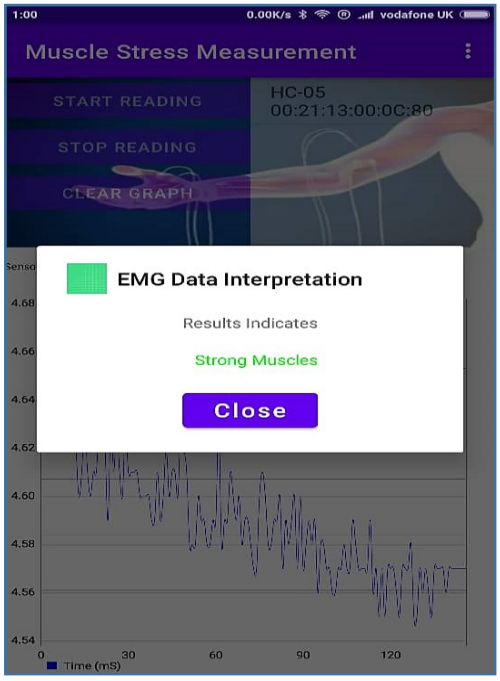

Figure 3. 9 Strong Muscles detected.

The designed Myoware app allows users to visualise the data received from the microcontroller-based EMG sensor via Bluetooth connection. MPAndroidChart library in Java to used display the EMG graph in real-time for users. The recorded EMG signals can be stored in a centralised data source, which can also be exported in a CSV file. In order to take care of the data transmission loss, the Myoware sensor is programmed to synchronise with the HC-05 Bluetooth module with a delay of 200ms. Thus, the designed MyoTracker is able to categorisation of muscles as weak muscles or strong muscles in real time. The Myoware app in [Fig 3.8] and [Fig 3.9] determined the status of the muscle recorded indicating weak and strong muscles respectively.

3.5 Calibration of Low-Cost MyoTracker System

Some studies have validated the design of low-cost electromyography sensors for a variety of applications. Heywood et al [57] presented the validity of a fabricated low-cost EMG sensor on a microchip. A commercial device and the designed low-cost sensor were placed on the vastus lateralis muscle of volunteers performing different exercises. The signals recorded were evaluated by means of a Teager–Kaiser energy operator (TKEO) and maximal voluntary contraction (MVC) of the muscle. The results indicated a good agreement between the two systems and therefore the reliability of the low-

cost sensor in measuring muscle activity. Fuentes et al [58] presented the validation of a designed low-cost EMG sensor against a commercial Delsys system. The authors used four validation indicators to estimate the similarity between the output signals of the two systems: Spearman's correlation, linear correlation coefficient (LCC), cross-correlation coefficient (CCC), and signal energy ratio. The result showed an excellent agreement between the designed low-cost system and commercial systems. However, the limitation of this design had to do with the noise of the hardware components and the delay of the signal output. Another study by Fuentes et al [59], demonstrated the validation of a low-cost surface EMG device for measuring muscle fatigue. In the study, 28 volunteers were prepared for a palpation test, where the designed low-cost sensor and commercial system were placed on the rectus femoris muscle. The mean absolute value (MAV), root mean square (RMS), and mean frequency (MNF) were used to evaluate muscle fatigue. The results indicated that the low-cost EMG sensor can be used to determine muscle fatigue. The only challenge is that this was done in offline classification and not in real time. Alejandro et al [60] illustrated mDurance system's validity for measuring muscle activities by comparing it with a commercial sensor. Volunteers were tested during an isokinetic exercise at different speeds to determine the maximum voluntary contraction. The results indicated an excellent correlation between the vastus lateralis at (ICC > 0.81) and rectus femoris at (ICC > 0.76). This proved that mDurance is a valid tool for measuring muscle activity during dynamic contraction at different speeds. Even though some works have attempted to validate low-cost EMG system, the reliability of these sensors have some challenges to be resolved. In this work, the reliability of the designed low-cost MyoTracker is evaluated to determine muscular fatigue. The design low-cost MyoTracker incorporate some measures to mitigate the noise and allow for muscle fatigue assessment in real-time.

3.5.1 Procedure for MyoTracker Calibration

The experimental procedure involved collecting muscle signals from the newly designed low-cost MyoTracker and the commercial Delsys Trigno Avanti sensor. A total of seven participants were recruited for the MyoTracker validation which included five male and two female. The participants had no known injuries or physical deformities. The exclusion criteria were participants who have walking

deformity. Brunel University granted ethical approval for this work and the participants were given a consent form to sign before partaking in the exercise. The participants were asked to conduct the following exercises,

Frankenstein Walk: A participant stands with his legs together, and one arm straightens, step and kick straight to the opposite leg, then straighten the other arm.

Sidewalk: An elastic band is placed between the ankles of a participant. The participant stands up and slightly bends the knees to a 60-degree angle while holding their waist and walking sideways.

Wall sit: A participants leaned against a wall with the feet firmly planted on the floor, 10 inches apart. The participants are asked to slowly slide down and then up.

Squat: The participant stands lowers the hips from the standing position and returns to the standing position at a comfortable pace.

In testing the low-cost MyoTracker EMG system, exercises like the Frankenstein Walk, sidewalk, Wall sit, and squat provided valuable insights into the system's performance and accuracy. These exercises target different muscle groups and movement patterns, allowing us to assess the EMG system's ability to capture and differentiate signals from various muscles effectively. The Frankenstein Walk, which involves lifting the legs straight out in front with each step, challenges the EMG system to accurately detect and measure activity in the hip flexor muscles. Similarly, the sidewalk exercise, which involves lateral leg movements, can assess the system's capability to capture signals from the abductor and adductor muscles of the hips and thighs. Furthermore, the Wall sit, and squat exercises offer opportunities to evaluate the EMG system's performance during dynamic movements and sustained muscle contractions. During a Wall sit, where the participant maintains a seated position against a wall with knees bent at a 90-degree angle, the EMG system is tested for its ability to track changes in muscle activity over time as fatigue sets in. Squats, on the other hand, involve a combination of knee and hip flexion and extension, engaging major lower body muscles such as the quadriceps, hamstrings, and glutes. Testing the EMG system during squats allows for the assessment of its accuracy in capturing nuanced muscle activation patterns during functional movements. The exclusion criteria were participants with no physical injury and known deformity. The inclusion criteria were healthy participants with age above 25years.

3.5.2 Specification of the MyoTracker and Commercial Delsys System

The designed low-cost MyoTracker system has some specifications and scenarios under which it can be used. The MyoTracker system relies on HC-05 Bluetooth connectivity between the EMG sensor and the Android app. While Bluetooth technology is widely available, its reliability in real-world scenarios, especially in environments with multiple wireless devices. This provides wireless technology for data transmission, allowing for greater freedom of movement during measurement. The sampling rate determines how frequently the sensor samples data. The sample rate of the MyoTracker system is 333Hz. The signal bandwidth of the MyoTracker system ranges between 10-400 hertz. It has a single channel 1 in operating to measure muscle signals. Other specification of the MyoTracker system is illustrated in Table 3.6 specifications of the low-cost MyoTracker System and the Delsys system.

Table 3.6 Specifications of the Two System

Parameters	Low-Cost Sensor (MyoTracker)	Commercial Trigno Avanti Sensor
Image		
Price	$150	$12,000
Dimensions (mm)	MyoWare 52.9 × 20.7 × 5.1	27 × 37 × 13
Weight (g)	Built EMG System 56.5	14.0
Channels	1 channel	1× EMG, up to 6× IMU
Bandwidth (Hz)	10–400	10–850 or 20–450
Gain (V/V)	201Rgain/1 kOhm	300
Sampling rate (Hz)	333	1111 up to 2000
Common Mode Rection Ratio (dB)	110	>80
Operating Voltage (mV)	3.3–5	11
Contact electrode	Silver/Silver-chloride	99.9 silver
Output mode	EMG Enveloped/Raw EMG	Raw EMG

The above table shows the specification of the low-cost MyoTracker system and the Delsys system.

3.5.2 Signal Processing

The signals from the two devices are denoised separately by performing different signal filtering for each. The first signal filtering with the commercial system uses the Butterworth bandpass at 20-450 Hz, with the 4th order. On the other hand, the designed low-cost EMG sensor was filtered with a Butterworth bandpass at 45-55 Hz because the Low-cost systems can handle noise concentrated at 50 Hz. The signals from the two systems were recorded for exercises performed by each participant. The maximum voluntary contraction (MVC) was computed for the two systems in the exercises conducted.

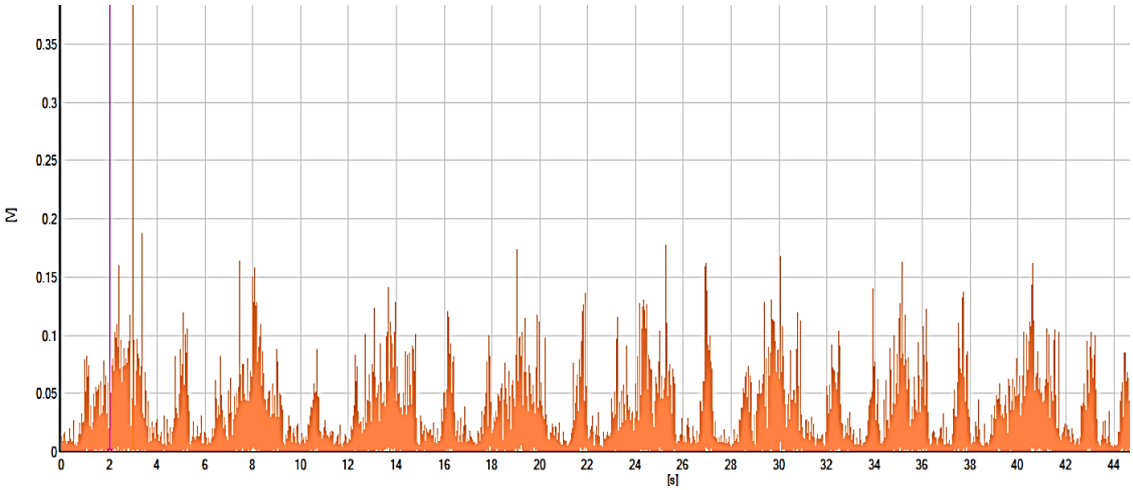

Figure 3. 10 Commercial Delsys EMG System

The root mean square (RMS) at peak and mean levels were recorded. The raw EMG signal is shown in [Fig 3.10] for commercial systems and [Fig 3.11] for the designed MyoTracker system.

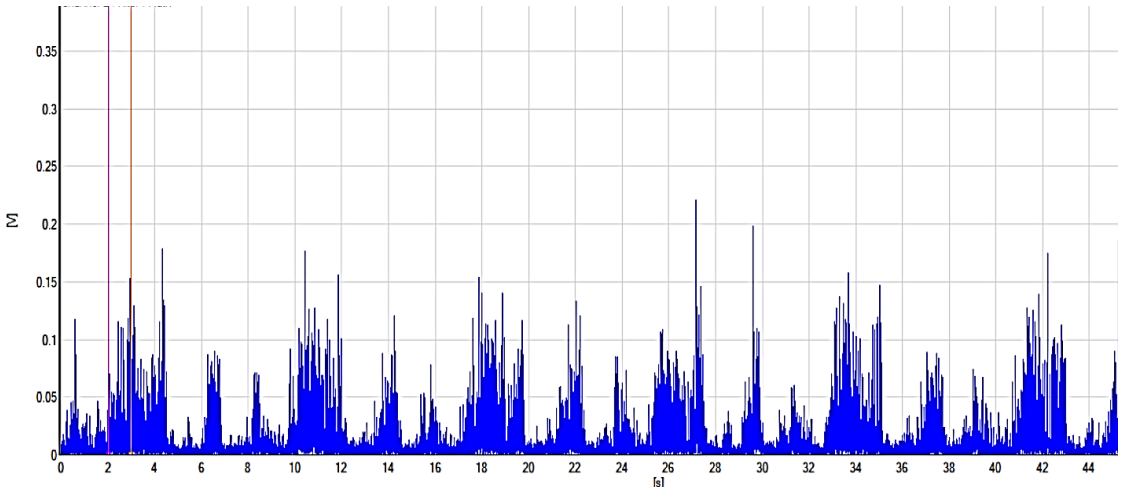

Figure 3. 11 MyoTracker EMG System

3.5.3 Statistical Analysis to Compare the Two Systems

IBM SPSS statistics V.26 was used in the statistical analysis to calculate the intra-class correlation coefficient (ICC) and Spearman's correlation. The reliability of the two systems is calculated using a single measure of a two-way random model. According to Munro's descriptor [61], the reliability coefficients used in indexing the degree of reliability are (0.90–1.00) very high correlation, (0.70–0.89) high correlation, (0.50–0.69) moderate correlation, (0.26–0.49) low correlation, and (0.00–0.25) little or no correlation.

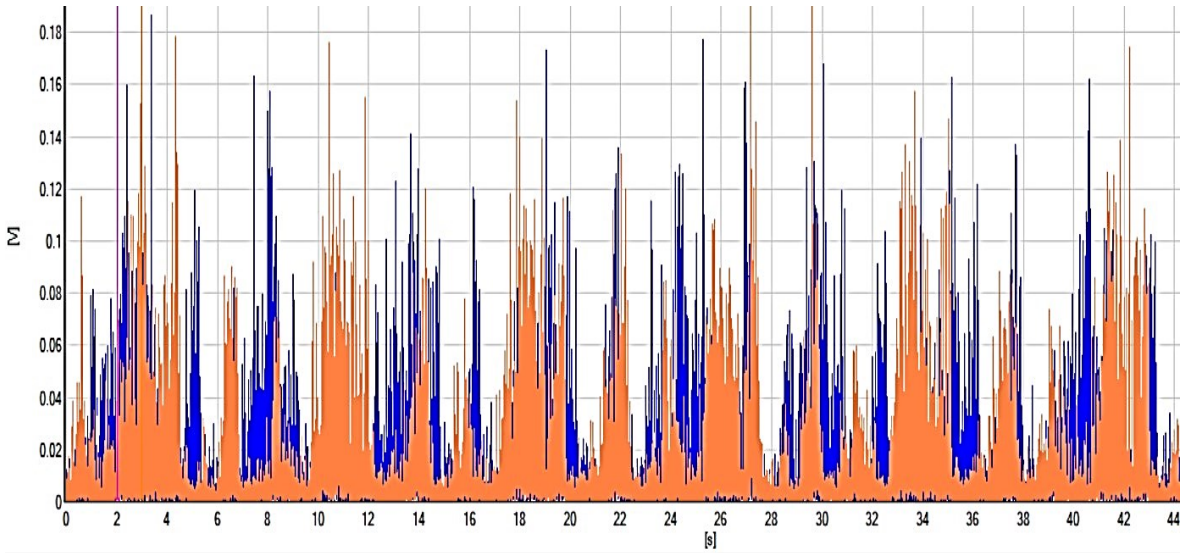

Figure 3. 12 Synchronisation of Systems

The level of agreement between the two systems were examined for each exercise conducted. Other parameters, such as the mean and standard deviation of signal output for the two systems, are computed. Table 3.4 shows the maximum voluntary contraction at peak level for both systems. The absolute agreement (ICC) was found between the range (0.74–0.92) with an average of 0.83 for the two systems. The minimum ICC was 0.74, and the maximum ICC is 0.92 at peak level. The Spearman's correlation coefficient at the peak level is in the range (0.71–0.85). The average is recorded to be 0.76 for the two systems. At peak level, the minimum value for Spearman's correlation is 0.71, and the maximum was 0.85 for the two systems. They were little discrepancies between the two systems because the golden standard had better sensor conductivity with reduced signal to noise ratio. Nevertheless, the results recorded from MyoTracker shows promising results. For the mean level in Table 3.5 the absolute

agreement range is (0.65–0.86). The average ICC is recorded to be 0.74, with the minimum at 0.65 and the maximum at 0.86 for the two systems. The Spearman's correlation coefficient at the mean level is between the range of (0.62–0.81). The average Spearman's correlation is calculated to be 0.71, with the minimum correlation at 0.62 and the maximum correlation recorded at 0.81. The absolute agreement (ICC), Spearman's correlation, and the mean and standard deviation of the two systems at peak level are shown in Table 3.4 below.

Table 3. 4 Dynamic exercise at peak level

Exercise	Commercial Peak (%MVC)	Low-Cost EMG Peak (%MVC)	Relative Agreement (ICC)	Spearman correlation	Mean	SD
Frankenstein Walk	79 ± 28%	68 ± 31%	0.870	0.740	0.203	0.320
Sidewalk	82 ± 17%	59 ± 40 %	0.740	0.720	0.519	0.314
Wall Sit	83 ± 20 %	80 ± 16 %	0.920	0.850	0.032	0.061
Squats	69 ± 31%	54 ± 36 %	0.780	0.710	0.014	0.013

Table 3. 5 Dynamic exercise at mean level

Exercise	Commercial Mean (%MVC)	Low-Cost EMG Mean (%MVC)	Relative Agreement (ICC)	Spearman correlation	Mean	SD
Frankenstein Walk	63 ± 37%	57 ± 42%	0.860	0.740	0.015	0.011
Sidewalk	74 ± 25%	51 ± 36%	0.670	0.620	0.334	0.336
Wall Sit	76 ± 24%	82 ± 18%	0.780	0.810	0.064	0.063
Squats	84 ± 17%	59 ± 40%	0.650	0.670	0.025	0.031

There was significant correlation between the designed EMG sensor and the commercial Delsys system. The Spearman correlation range was between (0.71 and 0.85), with an average of 0.76, indicating good correlation between the two systems. The average Spearman correlation coefficient was 0.76, showing

excellent agreement between the two systems. The average correlation of the two systems was found to be 0.74, which indicates a good agreement. The validation indicators show a good to excellent reliability of the low-cost EMG sensor for measuring muscle activity. The are little discrepancies between the two systems because the golden standard had better sensor conductivity with reduced signal to noise ratio. Nevertheless, the results recorded from MyoTracker shows promising results. Comparing this validation with previous work in [57] the developed low-cost MyoTracker sensor has enhanced features to allow users to connect via mobile device to the sensor. Additionally, the work done in [58] did not adequately put in measures to minimise the distortion of signals from the sensor. In this work, different techniques were applied to reduce noise in the MyoTracker sensor to achieve a better signal-to-noise ratio during validation. In general, comparing this design to previous work, this portable, low-cost EMG sensor is suitable for measuring muscle signals compared to past works.

3.5.4 Muscle Fatigue Assessment

Muscle fatigue can be determined by the extracted signal features in the time and frequency domains. Muscular fatigue detection is estimated with features such as root mean square (RMS) and mean absolute value (MAV) and mean frequency (MEF). Fuentes et al [59] demonstrated that an increase in the amplitude of the signal indicates muscle fatigue. An increase in the RMS and MAV in the time domain suggests the presence of muscle fatigue, while in the frequency domain, a decrease in mean frequency signifies the presence of fatigue muscle. The RMS, MAV and MEF in [Figures 3.13,3.14 and 3.15] respectively were recorded for the two systems.

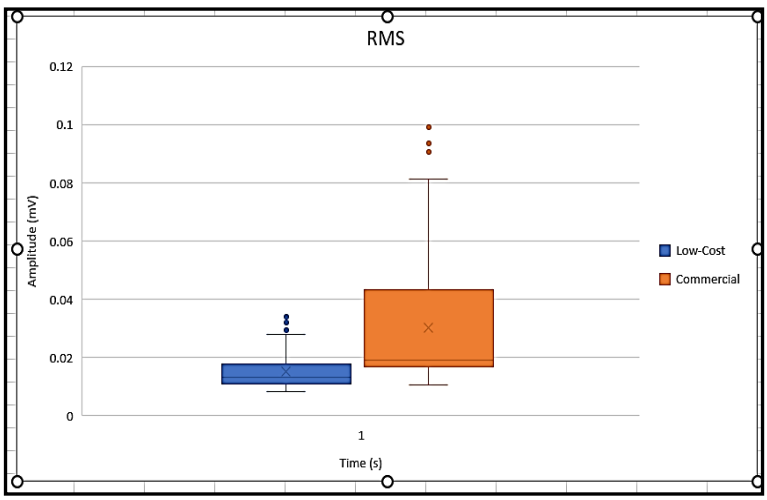

Figure 3. 13 Box plot for RMS

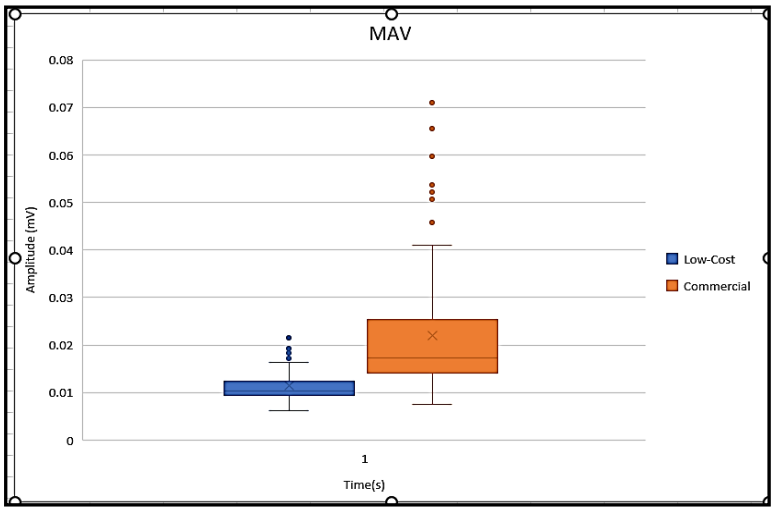

Figure 3. 14 Box plot for MAV

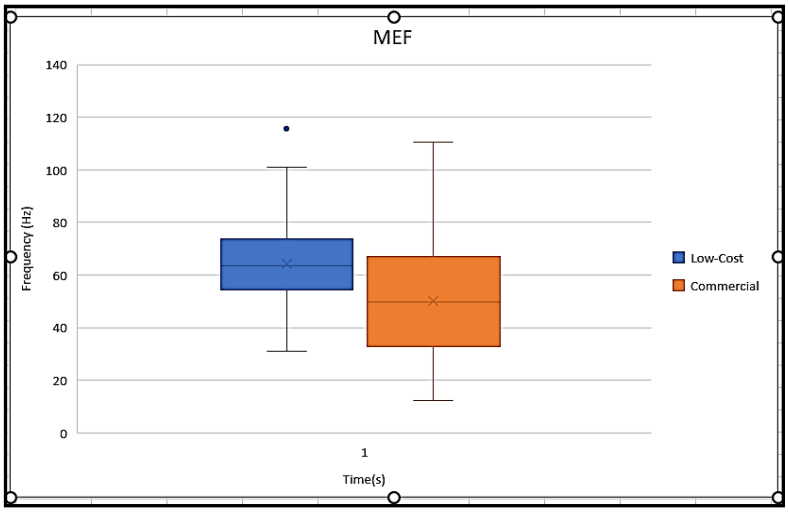

Figure 3. 15 Box plot for MAV

The developed system provides a reliable method for measuring muscle signal activity and is also suitable for determining muscle fatigue. Validation metrics indicate good to excellent reliability of the low-cost EMG sensor for measuring muscle activity. The design system is also ideal for fatigue muscle assessment in a maximum voluntary contraction. The MyoTracker system is also suitable for assessing muscle fatigue in maximal voluntary contraction. Regarding the practical implication of the design system, the designed low-cost EMG sensor is quite promising for clinical implementation.

The low-cost MyoTracker system can be used in various scenarios where muscle activity monitoring is needed but budget constraints or simplicity are factors. In physical therapy settings, monitoring muscle activity is essential for assessing progress and ensuring exercises are performed correctly. Low-cost MyoTracker EMG systems can be used to monitor muscle activation patterns during exercises, helping therapists tailor rehabilitation programs to individual needs while staying within budget constraints. Furthermore, coaches and athletes can use low-cost EMG systems to analyze muscle activation patterns during training sessions and competitions. By understanding how muscles are recruited during specific movements, athletes can optimize their training techniques and prevent injuries. Finally, the Low-cost EMG systems can be integrated into assistive devices such as prosthetics or exoskeletons to enable intuitive control based on muscle signals. These devices can enhance mobility and independence for individuals with disabilities while remaining affordable and accessible.

3.5.5 Limitation of the Low-Cost MyoTracker of System

There are some limitations of the MyoTracker system being used as an alternative to commercial systems. The MyoTracker system relies on Bluetooth connectivity between the EMG sensor and the Android app. While Bluetooth technology is widely available, its reliability in real-world scenarios, especially in environments with multiple wireless devices or interference, could affect the system's performance and user experience. Furthermore, the proposed MyoTracker system primarily targets individual users such as elderly people in care homes or patients undergoing rehabilitation. However, its suitability for broader clinical applications or integration into existing healthcare systems is not explored. In addition, the proposed low-cost MyoTracker system transmits sensitive physiological data wirelessly where robust data privacy and security measures are critical. Some specific protocols or encryption methods need to be employed to protect user data, which could raise concerns regarding privacy breaches or unauthorized access to personal health information. In conclusion, while the MyoTracker system presents an innovative approach to monitoring muscle strength using wearable sensors and mobile technology, it's essential to address the aforementioned limitations to ensure its clinical efficacy, usability, and data security in real-world healthcare settings. Further research and

development efforts should focus improving the system's accuracy, addressing technical challenges, and ensuring regulatory compliance.

Summary 3.6

In this chapter, a low cost MyoTracker system was built from scratch using inexpensive off the selves equipment. The designed MyoTracker was built with the aim to measure and monitor muscle fatigue from strained hip muscles in real time. The MyoTracker was validated with a commercial based EMG sensor using Delsys. The Spearman correlation range was between (0.71 and 0.85), with an average of 0.76, indicating good correlation between the two systems. The designed is very promising and could be used as an alternative the expensive commercial sensors.

CHAPTER FOUR METHDOLOGY: CLINICAL TRIAL AND EMG DATA EXTRACTION

4.1 Overview

This chapter presents the methodology for the clinical trial and features extraction of EMG signal. This section describes the approach used for the clinical trial, which includes participant recruitment, experiment procedure, data collection, and validation of EMG data. This study uses a qualitative design approach in a clinical trial to capture EMG data and observing participants perform different movement activities. This chapter is divided into three parts the first deals with the recruitment of participants, the second part is the clinical experiment in monitoring the movement of participants, and the third part is the EMG feature extraction. Different EMG features were extracted for the classification and analysis.

4.2 Participants Recruitment and Design Approach

The study uses a qualitative design approach in the clinical trial where patients and healthy control subjects were recruited to conduct a movement assessment. The clinical trial was done by observing different movements such as gait, knee extension, and knee lifting exercises undertaken by participants. The intrinsic hip muscle activities were recorded to assess movement patterns for the participants. The setting of the clinical trial was in Ghana, at Komfo Anokye Teaching Hospital (KATH). This was conducted at the rheumatology department of the internal medicine unit in the hospital. Participants were recruited at this unit with advice from a team of medical experts consisting of the resident rheumatologist, medical doctor, nurses, and physiotherapist. The clinical trial was conducted for a duration of two months from August to September 2022.

4.2.1 Ethical Consideration

Ethical approval was obtained from Brunel University London [Appendix A: reference number, 35807-MHR-Apr/2022- 39291-3] and the Komfo Anokye Teaching Hospital in Ghana [Appendix B: reference number, KATH IRB/AP/026/22]. Ethical consideration is essential in the clinical trial to ensure patients' welfare and adhere to required standards for clinical investigations. The risks in conducting the trial

were explained to participants and the precautional measures adopted. Participants were given a consent form to sign before they took part in the movement assessment [Appendix C: Consent form] To ensure data integrity, each participant was assigned ID numbers to safeguard data privacy and anonymity. The participants were given the opportunity to withdraw at any point during the clinical trial without any explanation.

4.2.2 Study Population and Sampling Criteria

The study recruited 25 participants for the clinical data collection, comprised of 18 PMR patients and 7 healthy control subjects. The sample size was justified using Yamane's estimation for sample size calculation [62]. Yamane's formula is given by $n=N/1+N * (e)^2$ (4.1)

where n is the sample size, and N is the selected population. The aim was to have a 95% confidence interval with an acceptable sampling error of 5%. The sample size was sufficient for the population size of N =25 to obtain enough data for the classification. The sample criteria for the clinical data collection considered the following inclusion criteria:

- Male and female patients at the hospital who had been diagnosed with PMR disease.
- Patients with pain and inflammation of the hip muscles who are above 50 years old are known to have a relapse of the disease over period were recruited.
- Patients who met the required criteria and signed the consent form for the clinical trial were included.

The inclusion criteria for healthy controls subjects were individuals with no physical deformity or known walking impairments. Individuals of 50 years and above with no history of musculoskeletal disease or other diseases who signed the consent form were included in the trial. The exclusion criteria for patients were individuals with known physical walking disability. Other exclusion criteria considered in this study were:

- Patients who were suffering from other conditions that impaired their movement.

- Healthy control subjects were people with co-morbidities that affect their movement activity. This also included healthy individuals with known physical disabilities.

4.2.3 Justification of Inclusion and Exclusion Criteria

The inclusion and exclusion criteria outlined are to ensure that the sample populations selected for the clinical data collection are appropriate for the study's objectives and minimize confounding factors. The justification for these criteria is as follows for the inclusion criteria. By including patients diagnosed with PMR disease, the study ensures that the data collected are relevant to the condition being investigated. This criterion allows for the examination of gait abnormalities specific to PMR. In addition, limiting recruitment to patients above 50 years old with hip muscle pain and inflammation, who are known to experience relapses, helps to ensure homogeneity within the patient group and enhances the clinical relevance of the findings.

For the exclusion criteria, the justification is that fellows, excluding individuals with known physical walking disabilities, ensure that the patient group consists of individuals who are capable of walking and performing the required tasks, minimizing confounding variables. Furthermore, excluding patients suffering from conditions that impair movement other than PMR helps isolate the effects of PMR on gait abnormalities. In addition, for healthy control subjects, excluding individuals with co-morbidities that affect movement activity ensures that the control group represents a healthy population without confounding factors that could influence gait parameters. Excluding healthy individuals with known physical disabilities further ensures that the control group is representative of the general population without significant impairments affecting movement. Overall, these inclusion and exclusion criteria enhance the internal validity of the study by ensuring that the selected sample populations are appropriate for addressing the research questions while minimizing the influence of confounding variables.

4.3 Equipment used in the Clinical Trial

Delsys Trigno EMG sensors shown in [Fig 4.1] were used as the main instrument for data collection. The sensors provide essential information on muscle contraction in movement assessment. These sensors offer a wireless measurement of high-quality EMG signals of the muscle activation pattern. The Delsys sensors work with a Trigno base station and an app with a wireless receiver and data logger that connects to a computer via USB or Bluetooth. It has discovery software that allows a real-time display of EMG signals and storage in a CSV file. Before collecting the data, the sensors were calibrated to ensure accurate measurement. The initial testing phase was performed to verify that the sensors were operating correctly, and the signal quality was satisfactory.

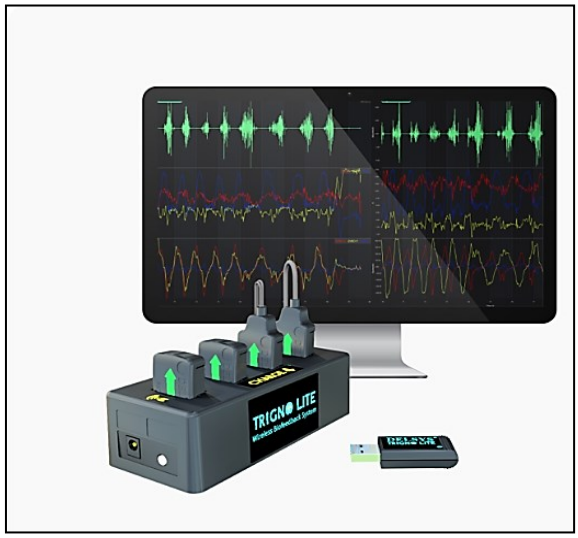

Figure 4. 1 Trigno Lite EMG Sensor

4.3.1 Procedure for Data Collection

EMG data were recorded from the lower limbs of the right and left hip muscles around the pelvic girdle area. The sensors were placed on selected hip muscles to record the muscle activities during movement. This was done because it is the hip muscle area affected by PMR disease. The hip muscles recorded were rectus femoris (RF), vastus lateralis (VL), biceps femoris (BF), and Semitendinosus (SE). These

were the targeted strained hip muscles affected by the disease which was the main focus of the investigation. Instructions were given to participants on how to position themselves for EMG recording while conducting the required activities. Below are the specific hip muscles recorded for participants in the clinical trial in [Figure 4.2] showing the A: rectus femoris, B: vastus lateralis, C: biceps femoris, and D: Semitendinosus muscles respectively. [63]

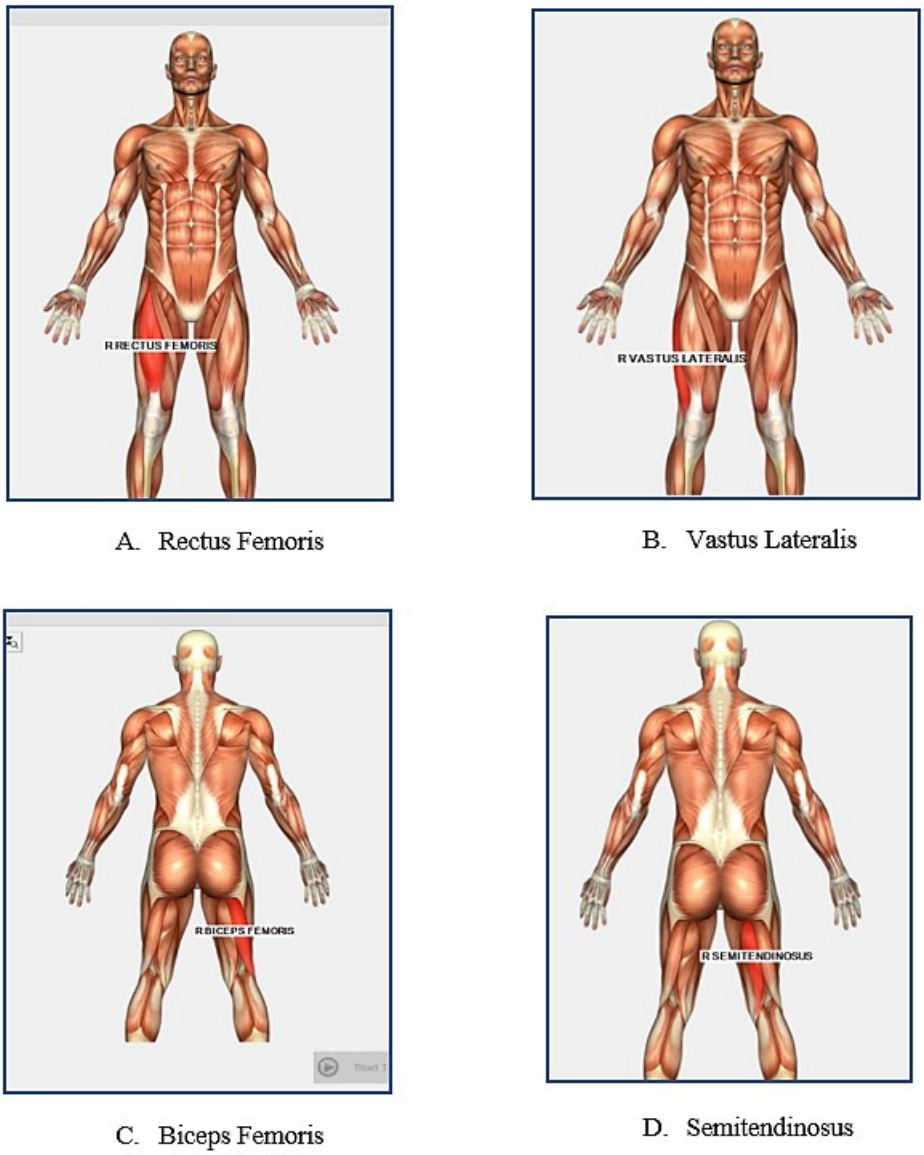

A. Rectus Femoris

B. Vastus Lateralis

C. Biceps Femoris

D. Semitendinosus

Figure 4. 2 Hip muscles recorded for the study.

4.3.2 Clinical Trial Process

The following steps were taken to collect the muscle signals from the hips for investigation.

1: The risks involved in the study were explicitly explained to participants. The participant information sheet, which contains all information on the clinical trial phase, was given to participants.

2: Participants' bio details, such as age, height, and weight, were recorded.

3: The hair on the hip thigh was shaved and cleaned with muslin to give the sensors better conductivity and more accurate readings.

4: Delsys sensors were prepared and placed on the right and left hips concurrently of the participants to record muscle signals.

5: Participants were taken through a pre-trial phase of the gait, knee extension, and knee lifting exercises before conducting the actual exercise.

6: Participants were asked to conduct a gait exercise on a walkway of approximately 12 meters in a simulation room. They also perform knee lifting and knee extension exercises at three trials each. The procedure for the trail lasted for about 20 minutes for each participant.

7: After collecting the data, the sensors were detached and prepared for another participant.

Below were some participants performing the gait, knee lifting, and knee extension exercises in Figures [4.3, 4.4 and 4.5] respectively.

Figure 4. 3 Participant conducting gait exercise.

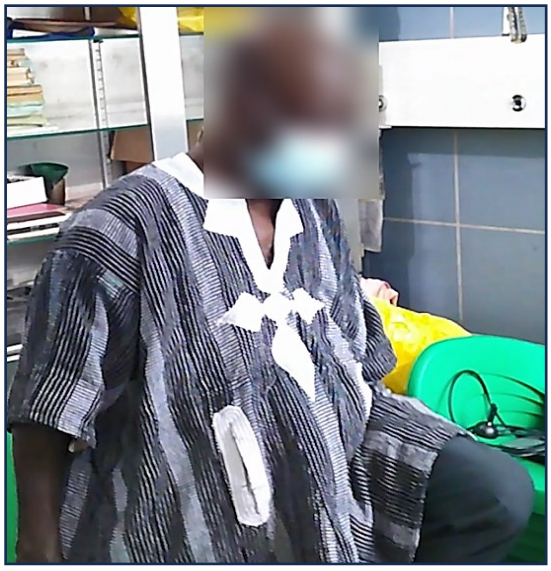

Figure 4. 4 Participant conducting knee lifting exercise.

Figure 4. 5 Participant conducting knee lifting exercise.

4.3.3 Validation of EMG Data Recorded

The recorded EMG signals from the participants needed to be validated to ensure its conforms with similar public dataset available. This was to ensure the integrity and reliability of the EMG signals captured from participants for analysis. They were some challenges in capturing the raw EMG signals from participants. One challenge encountered was the correct positioning of sensor electrodes on individuals hip muscles. Another challenge was the shaving and cleaning of hip muscles for better

conductivity with the sensors. The following measures were taken to address the challenges in recording the EMG data. Firstly, the sensor electrodes had to be correctly placed on the required hip muscles to ensure optimal signals quality were recorded and to minimise signals interference. Secondly, the use of muslin was effective to clean the hip muscles of any artefacts before placing the sensors. The validation process was done using the EMGworks software to inspect the recorded raw EMG signals and remove abnormal signal fluctuation. Finally, the recorded EMG dataset was compared with available public datasets from patients with other musculoskeletal diseases. This was done to ensure correlation of EMG signal and no major discrepancies between EMG dataset and clinically available open-source data.

4.4 EMG Features Extraction

From the data recorded in the clinical trial, there were features extracted from the EMG signals. The extracted features vectors formed the essential components for the classification and analysis. Features extraction of EMG signals is the process of converting raw signals into meaningful data structures. In addition, feature extraction involves selecting and transforming the relevant information for pattern recognition. EMG features were extracted in the time domain and frequency domain for classification and pattern recognition.

Raw EMG signals were produced from the contraction of the hip muscles during movement. EMG signals resulting from motor unit action potentials (MUAPs), indicate a muscle's response to stimulation. The raw EMG signals were recorded in millivolts from a range of 0-10mV. The voltage changes over time, reflecting on the electrical potentials of hip muscles fibers during muscle contraction. Figure 4.6 shows the generation and decomposition of signals a sensor produces. The signals collected in the clinical trial were susceptible to different types of noise, including electrical interference from power lines, motion artifacts, and electrode noise. Below is an example of EMG signal generation and decomposition using surface EMG sensors [64].

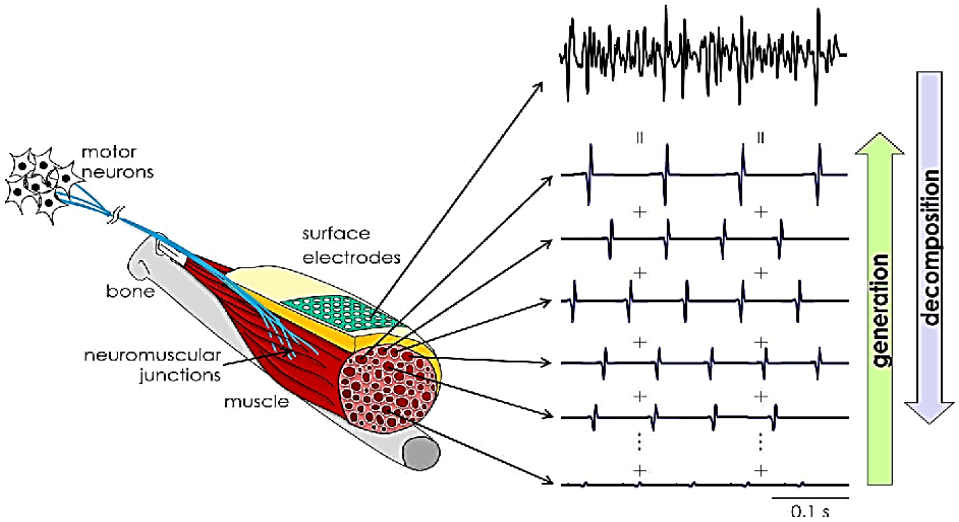

Figure 4. 6 Generation and decomposition of EMG signals

A typical EMG graph has the horizontal axis representing time and the vertical axis representing the magnitude or intensity of the electrical signal. Raw EMG signals are characterised by fluctuating waveforms that change in response to muscle activity which produces the spikes. The spikes are the sharp increase in the amplitude where the (+) are those values above zero in [Fig 4.9] and when the spikes are below zero (-) negative. When muscles are at rest, the EMG signal typically appears as a relatively flat line with low amplitude and occasional small fluctuations that indicate the baseline noise.

4.4.1 EMG Signal Filtering

The EMG data recorded from participants contained different kinds of noise, which were taken care off. This was done by removing the noise and highlighting the essential signal features for classification. By removing the noise from motion artifacts and electrode noise is essential to improve the quality of the EMG signals. Filtering was done to remove unwanted noise sources and thereby improve the quality and reliability of the EMG signal for analysis. To minimise the noise, a Butterworth bandpass filter was used with a cutoff frequency between 20 Hz and 450 Hz. This frequency range gives the most effective functions of EMG signals for analysis [65]. To eliminate noise floors and further suppress motion artifacts, a high-pass filter is integrated into the Delsys system to reduce baseline noise

and motion artifacts [66]. This helps to improve the visibility and clarity of MUAP of signals recorded for analysis.

EMGworks software platform from Delsys was used for the signal processing. Firstly, the raw EMG signals from the rectus femoris, vastus lateralis, biceps femoris, and semitendinosus were filtered. Secondly, the integrated EMG signals for each muscle for each muscle were also computed. A composite plot indicates the filtered EMG signals in blue containing the root mean square signal in red in a window frame in a time of 50 seconds. The graphs below in [Figures 4.7,4.8,4.9 and 4.10] show the filtered EMG signals of the hip muscles recorded for the rectus femoris, vastus lateralis, biceps femoris, and semitendinosus respectively. The x-axis represents the time (s) indicating the duration of recording the muscle signals, while the y-axis represents the amplitude (mV) of the filtered EMG signals.

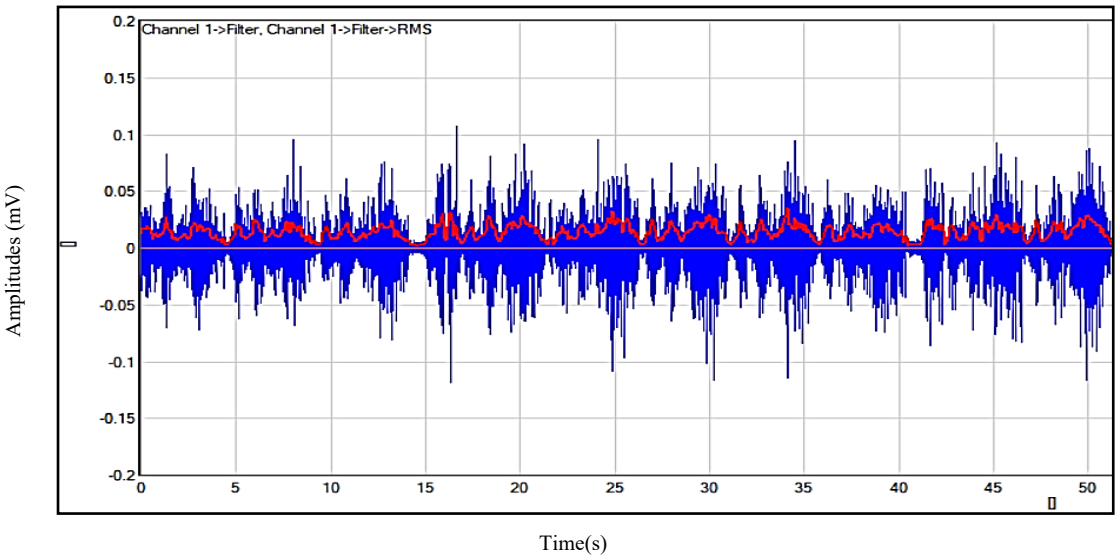

Figure 4. 7 Filtered signal from rectus femoris.

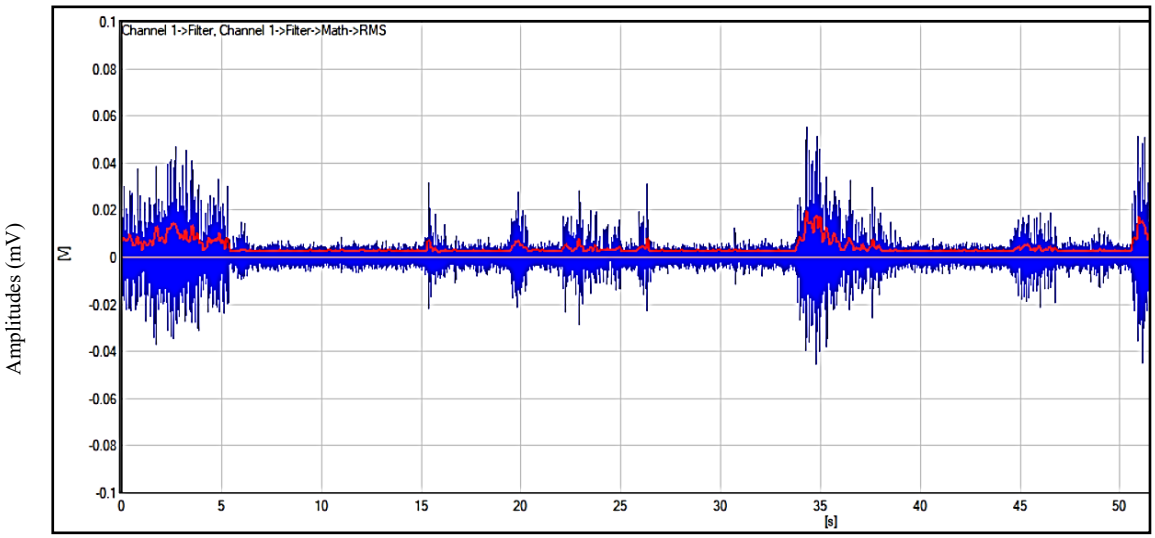

Figure 4. 8 Filtered signal from vastus lateralis.

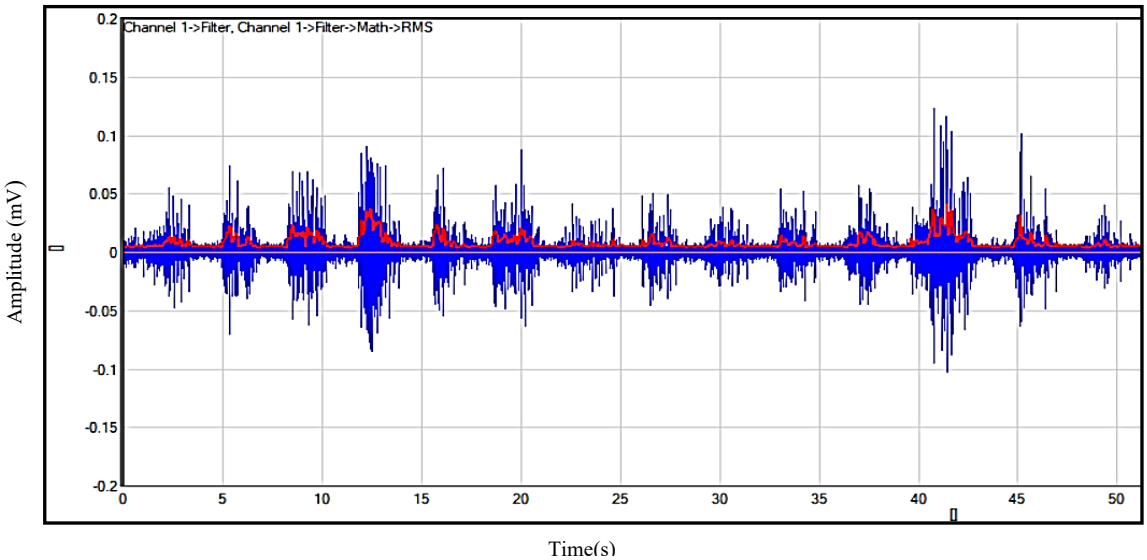

Figure 4. 9 Filtered signa from biceps femoris.

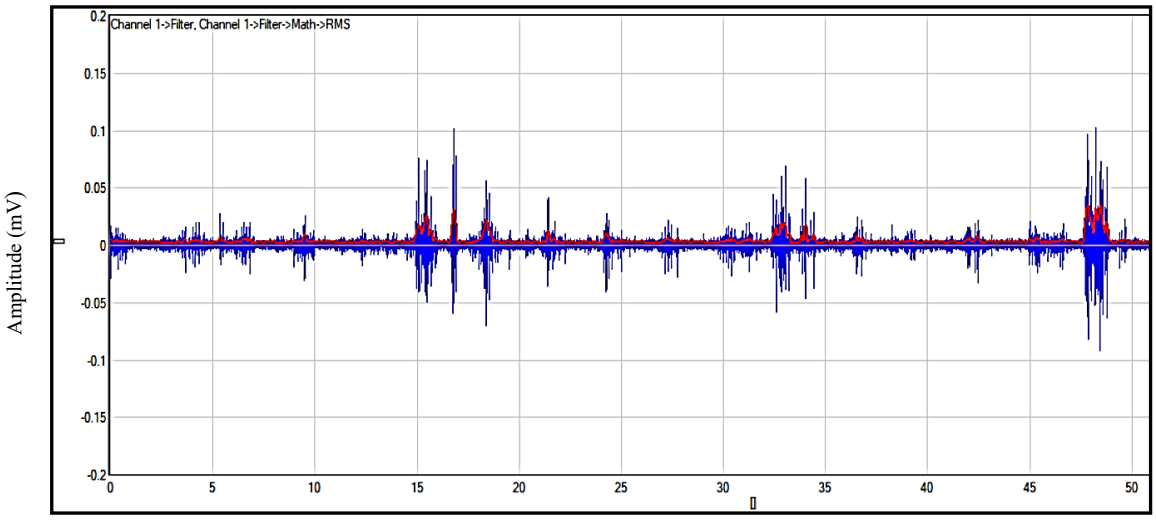

Figure 4. 10 Filtered signal from semitendinosus.

The red line represents the root mean square values which provides an indication of the muscles intensity recorded. This is useful to determine the patterns of muscles contraction in the movement classification.

4.4.2 Absolute Value of EMG Signal

The absolute values of the EMG signals recorded from participants were computed for the hip muscles recorded. The absolute values are used in a full-wave rectification of the signal processing technique. The full-wave rectification converts the negative values of an EMG signal to positive values by taking the absolute value of each data point. The purpose of signal rectification is to prevent it from averaging to zero since raw EMG signals have positive and negative components. By taking the absolute values of an EMG signal, the resulting signals consist of positive values, which are used to assess the muscle activation strength and analyse muscle fatigue. The mean absolute value (MAV) measures the level of muscle contraction within the EMG signals, which can be expressed as a moving average of full-wave rectification. When the muscles are rested, the MAV of the recorded signal is low, and the graphs show relatively low and stable baseline values. Figures 4.11, 4.12, 4.13 and 4.14 show the mean absolute values of the signals recorded from the hip muscles for the rectus femoris, vastus lateralis, biceps femoris, and semitendinosus respectively. The figure indicates that as the muscle contracts, the signals increase, reflecting the average amount of electrical activity produced by the muscle fibers during a particular window time frame for each muscle recorded. The signals plots illustrate the magnitude of the hip muscle contraction recorded over time. The different signal plots of the specific muscles recorded show the magnitude of the muscle contraction levels during the exercises conducted in the clinical trial. The amplitude analysis allows for various signal characteristics to be extracted for classification, such as the interference pattern of the EMG signal, which contains information on the number of motor units, firing rate, and recruitment properties [67].

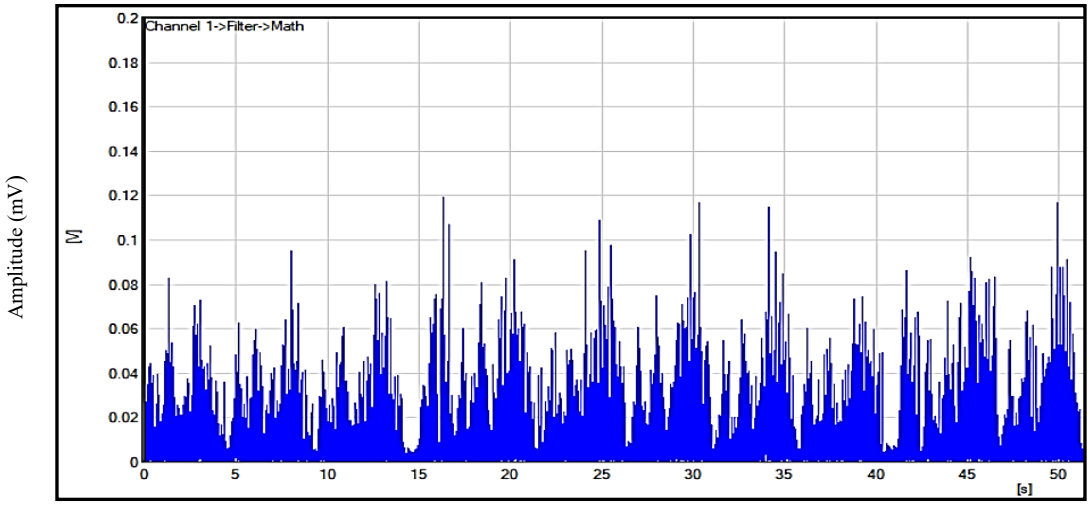

Figure 4. 11 Absolute values of EMG signal for rectus femoris

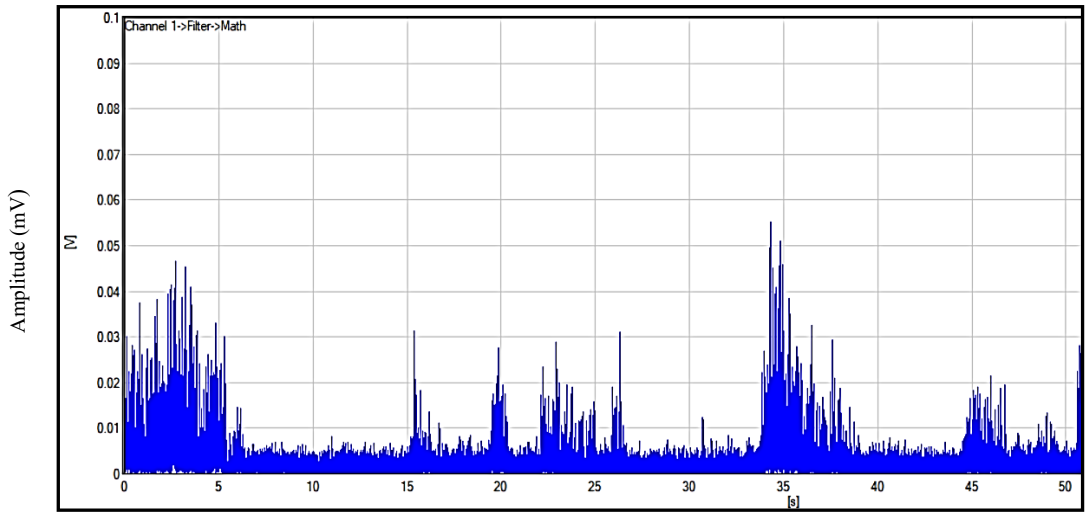

Figure 4. 12 Absolute values of EMG signal for vastus lateralis

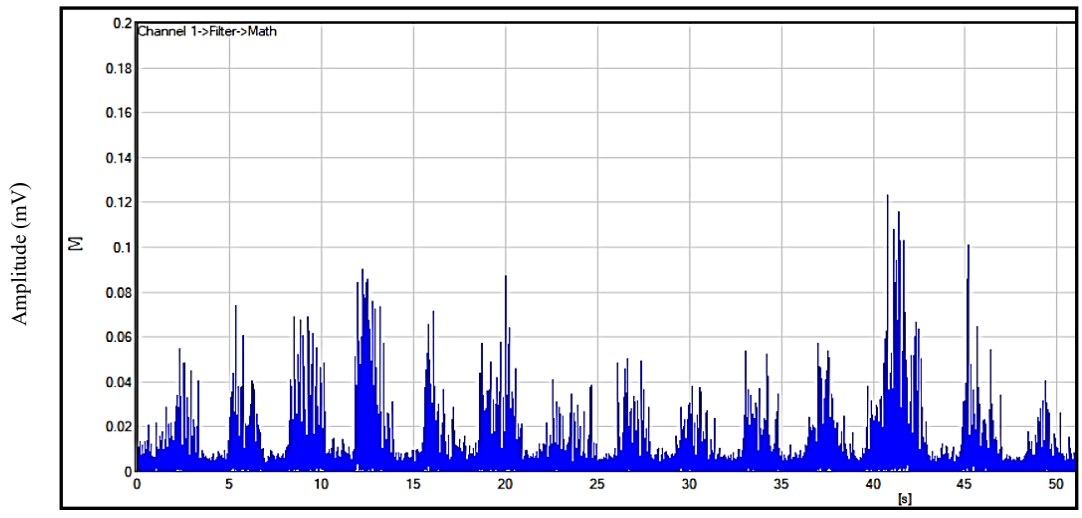

Figure 4. 13 Absolute values of EMG signal for biceps femoris

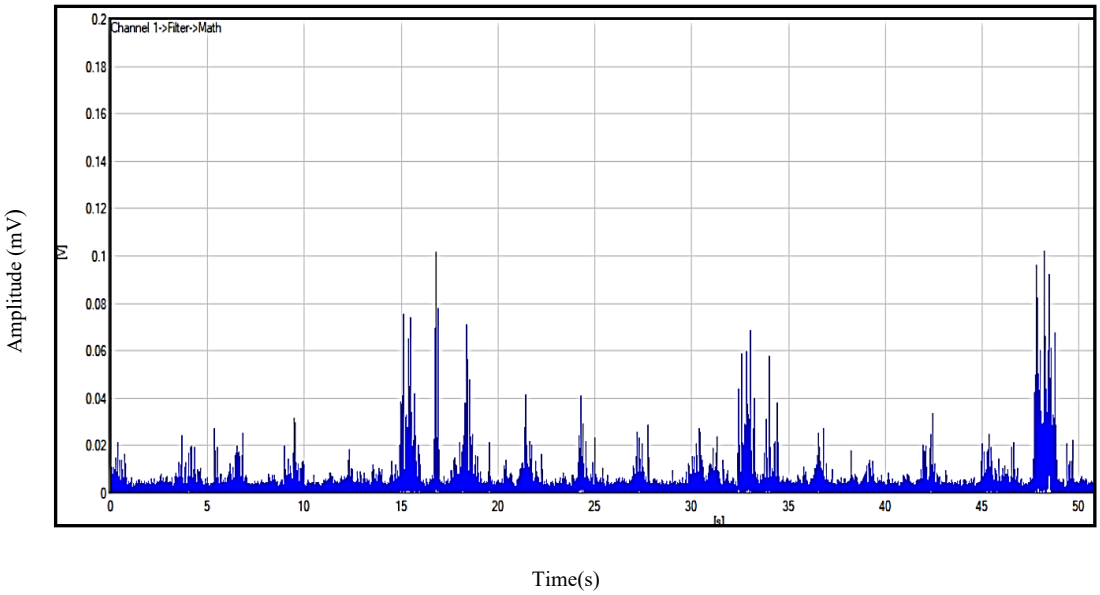

Figure 4. 14 Absolute values of EMG signal for semitendinosus

4.4.3 Mean Frequency of EMG signal

The next feature extracted from the recorded EMG signal was the mean frequency using a Fast Fourier Transform (FFT). The mean frequency (MNF) of the EMG signals refers to the average frequency content and dominant frequency within the signals. MNF measures the central frequency of the power spectrum of the EMG signal, which provides an indication of the firing rate of motor units [68]. The FFT transforms EMG signals from the time domain to the frequency. Furthermore, the FFT also allows for the decomposition of the EMG signals from high and low-frequency spectral components [69]. The mean frequency graphs of the hip muscles were recorded to provide information on the frequency distribution of the signals recorded at a specific window time of 50 seconds. The x-axis represents the duration of the recorded EMG signals in time (s), while the y-axis represents the mean frequency values of the signals at each time point. The graphs in [Figures 4.15, 4.16, 4.17,4.18] show an increase and decrease signals frequency for the rectus femoris, vastus lateralis, biceps femoris, and semitendinosus respectively. This is an indication of the changes in the recruitment of the motor units in the hip muscle contraction. Normally, the frequency content between 0 and 20 Hz is affected by the firing rate of the

motor unit and therefore primarily unstable [69]. In this work, the MNF frequency extraction ranged between 20 to 200 Hz which was more stable for analysis. The MNF plots show the recorded EMG signals for each of the hip muscles within a fixed window below.

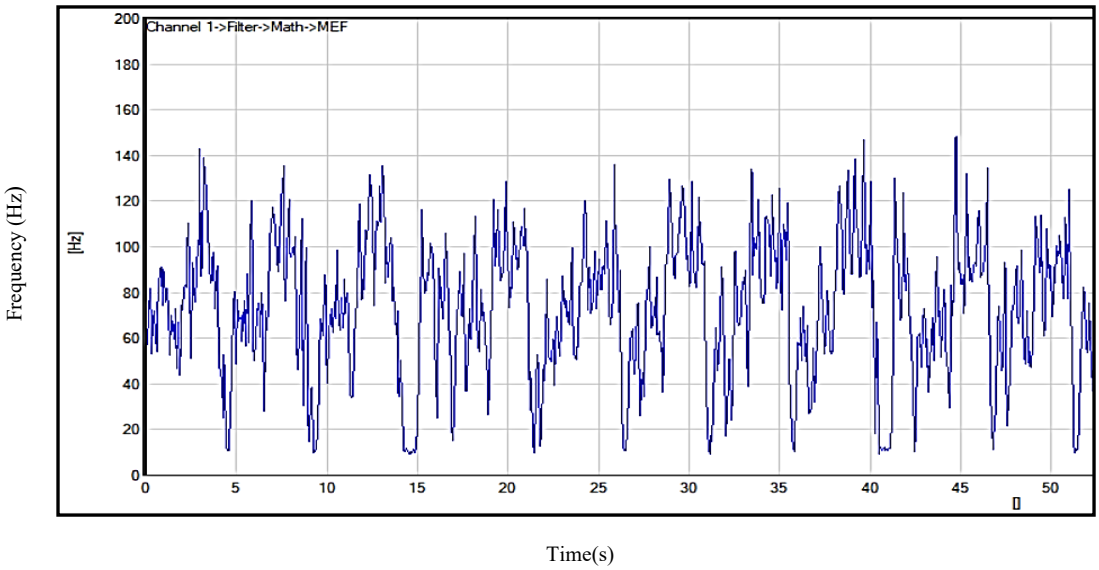

Figure 4. 15 Mean frequency signals for rectus femoris

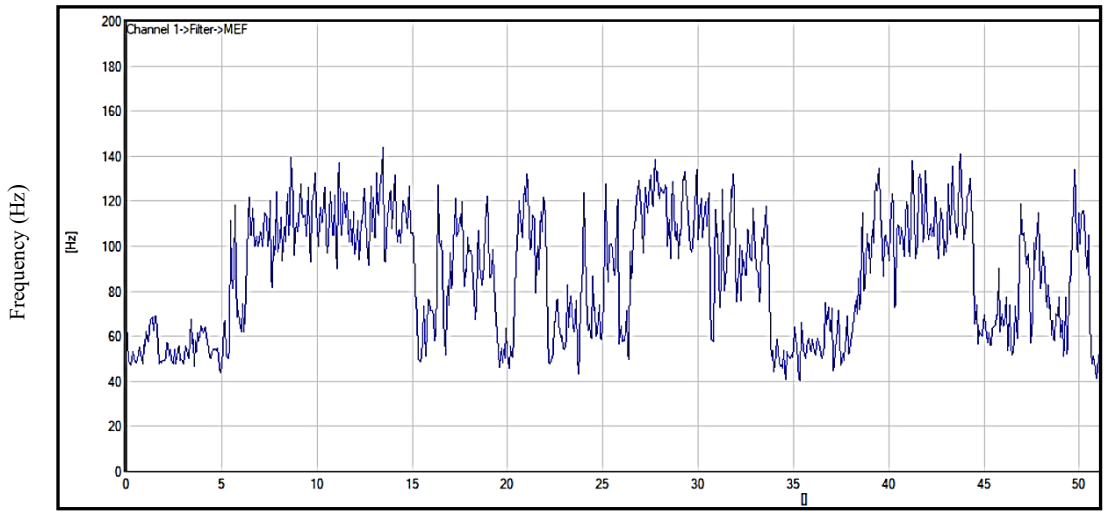

Figure 4. 16 Mean frequency signals for vastus femoris.

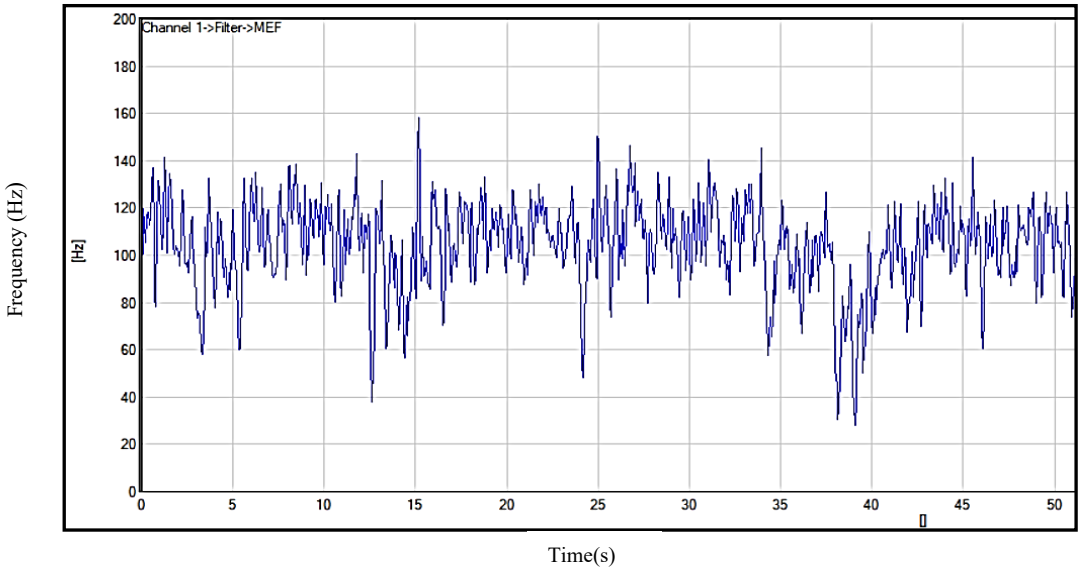

Figure 4. 17 Mean frequency signals for biceps femoris.

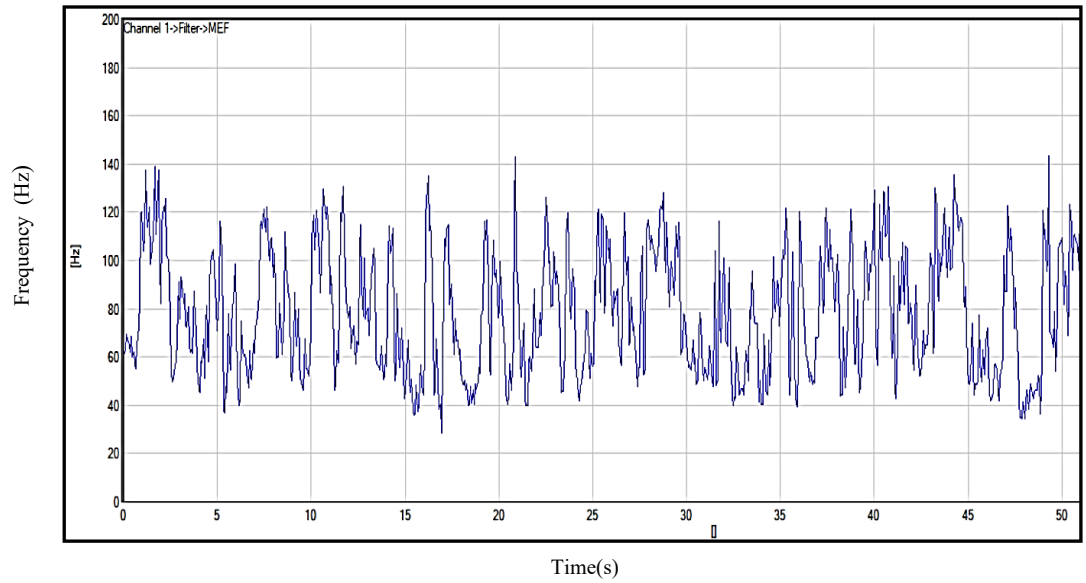

Figure 4. 18 Mean frequency signals for semitendinosus.

4.4.4 Root Mean Square

Another feature extracted that essential for pattern recognition was the root mean square (RMS). The RMS is a method of quantifying the electrical signal of an EMG signal, which reflects the physiological activity during muscle contraction [70]. It measures muscle activity's strength or magnitude over the analysed window frame. In addition, the RMS values can be used to determine a linear relationship between the signals and the force of muscle contraction [71]. In Figures 4.19, 4.20,4.21,4.22, the RMS values of the hip muscles recorded for the rectus femoris, vastus lateralis, biceps femoris, and

semitendinosus respectively within a specific time window. The peak spike in the graphs shows the period of increased muscle intensity with a stronger contraction, while the tough indicates when the muscles were at rest. The RMS is suitable for movement classification as it highlights the changes in the muscle contraction levels at different times, which are used to identify distinct muscle patterns. By analysing the overall trend of the RMS values can provide information on the activation patterns of the hip muscles recorded over a specific period. From the RMS plots, when the muscle is at rest, the RMS values of the signal have lower amplitude. As the muscle contracts, the RMS values of the EMG signal increase, reflecting an increase in the average amount of electrical activity produced by the muscle fibers in a window time frame. RMS is an important feature used to classify muscle signals which depicts the muscle valuable contraction for diagnostic purposes.

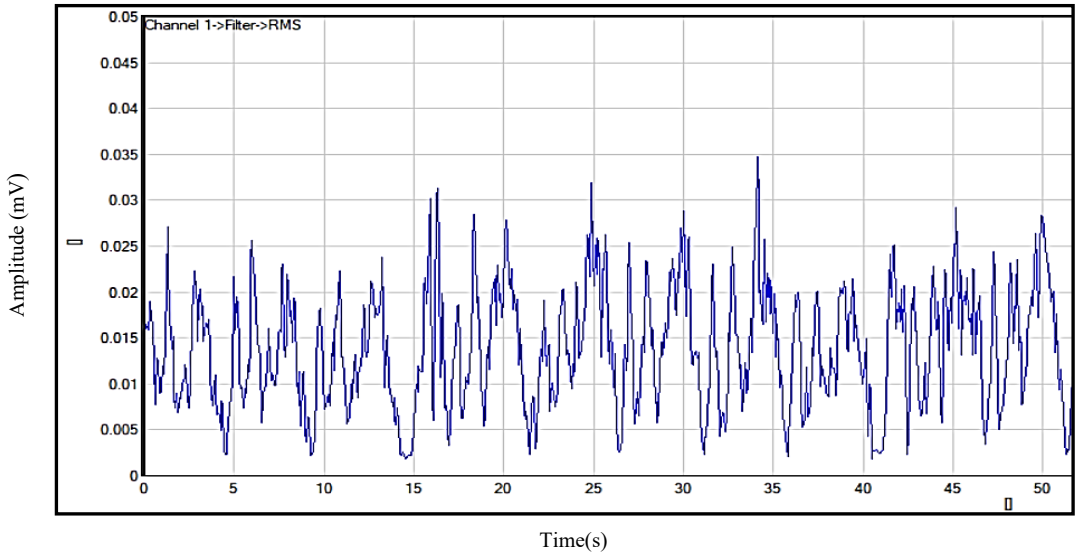

Figure 4. 19 RMS signal for the rectus femoris

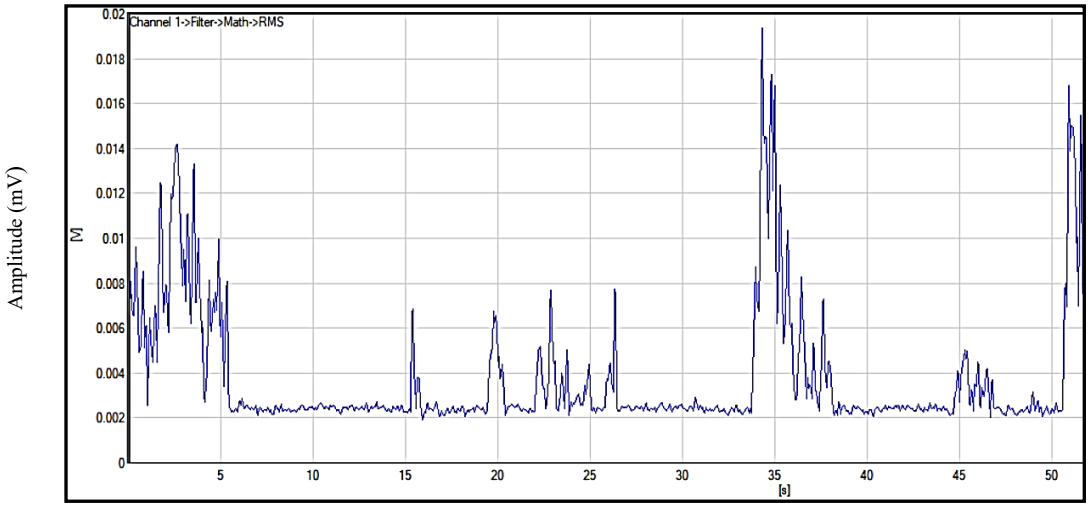

Figure 4. 20 RMS signal for the vastus lateralis

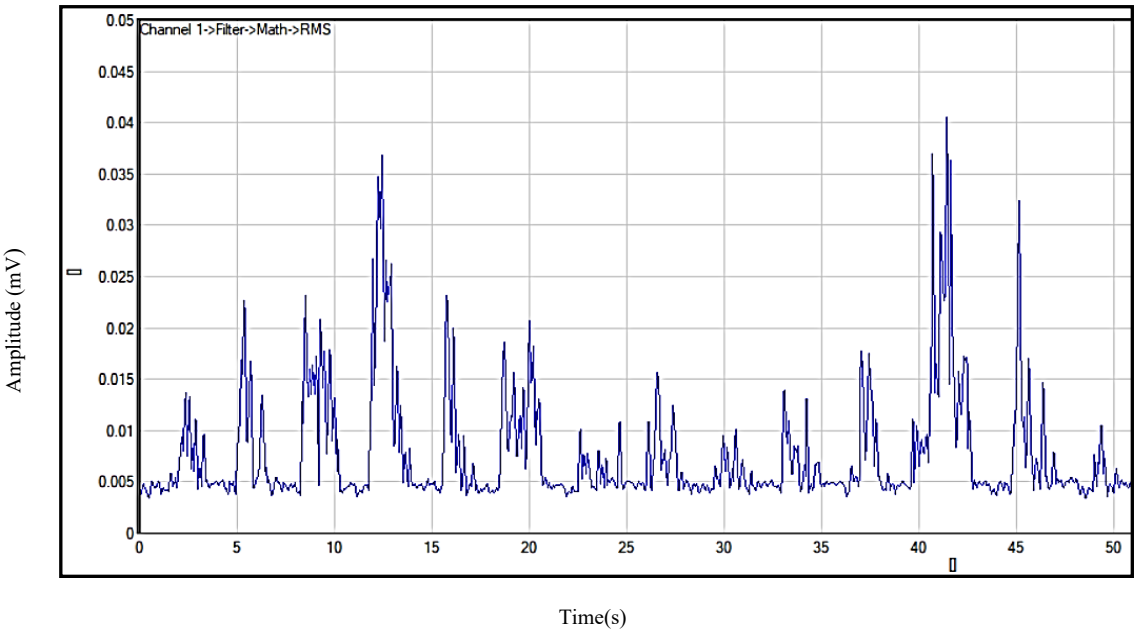

Figure 4. 21 RMS signal for the biceps femoris

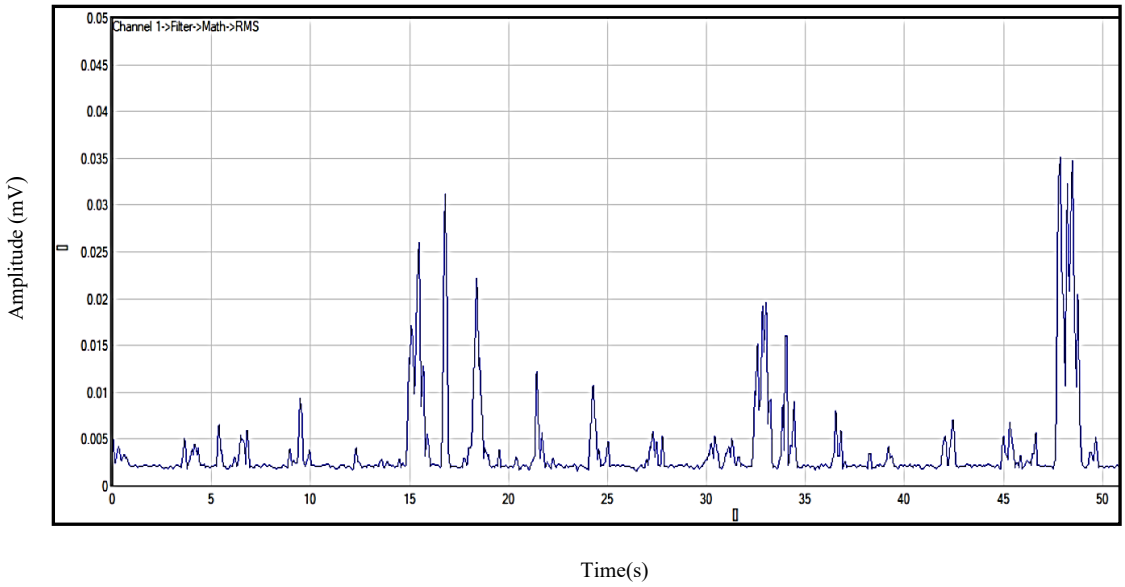

Figure 4. 22 RMS signal for semitendinosus

4.4.5 Integrated EMG Signal

The Integrated EMG signal (iEMG) feature was extracted which allows for the analysis of the motor unit of the signals. The iEMG is a measure that quantifies the total electrical muscle activity over a period in a window frame. It provides an estimate of the cumulative muscle activity during contractions of the hip muscles. iEMG represents the motor unit recruitment and strength of muscle contraction,

which are widely used in assessing muscle activity patterns. The figure shows each muscle recorded, had different intensities during the contraction process. The integrated EMG signal provides information about the recruitment pattern of motor units within the muscle. From [Figures 4.23,4.24,4.25,4.26] show the integrated EMG signal of the hip muscles recorded in the clinical trial for the rectus femoris, vastus lateralis, biceps femoris, and semitendinosus respectively. The integrated information on the total electric activity generated by the muscles within a specific time of 50 seconds. The y-axis represents this as the amplitude (mV), and the x-axis indicates the time in seconds. The integrated EMG signals can used to determine the motor unit action potential and the recruitment patterns of the hip muscles. In general, the integrated EMG signal can provide information on the performance of the muscles in the specific exercises conducted in the clinical trial.

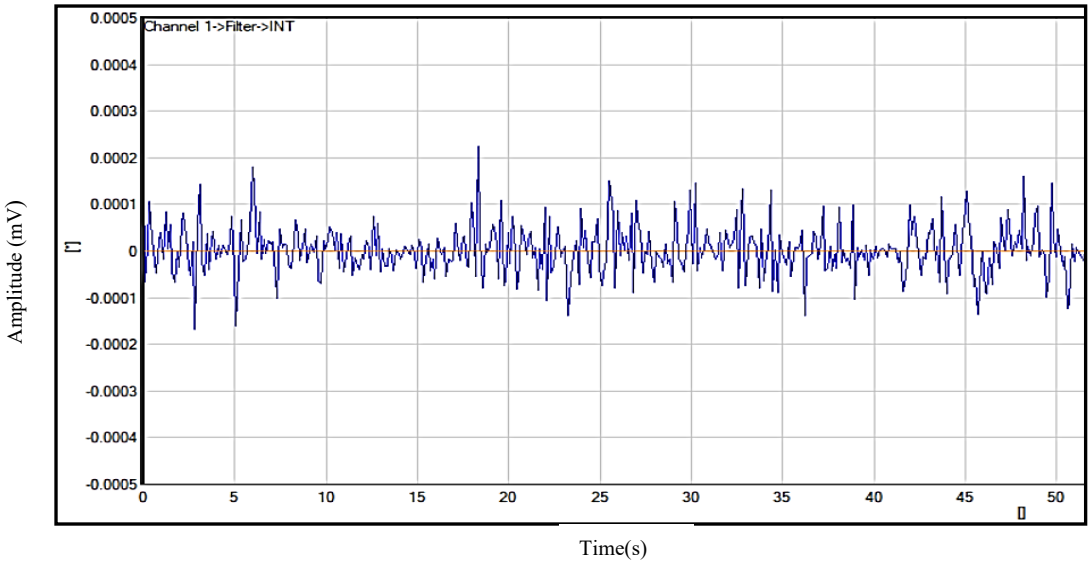

Figure 4. 23 Integrated EMG signal for rectus femoris

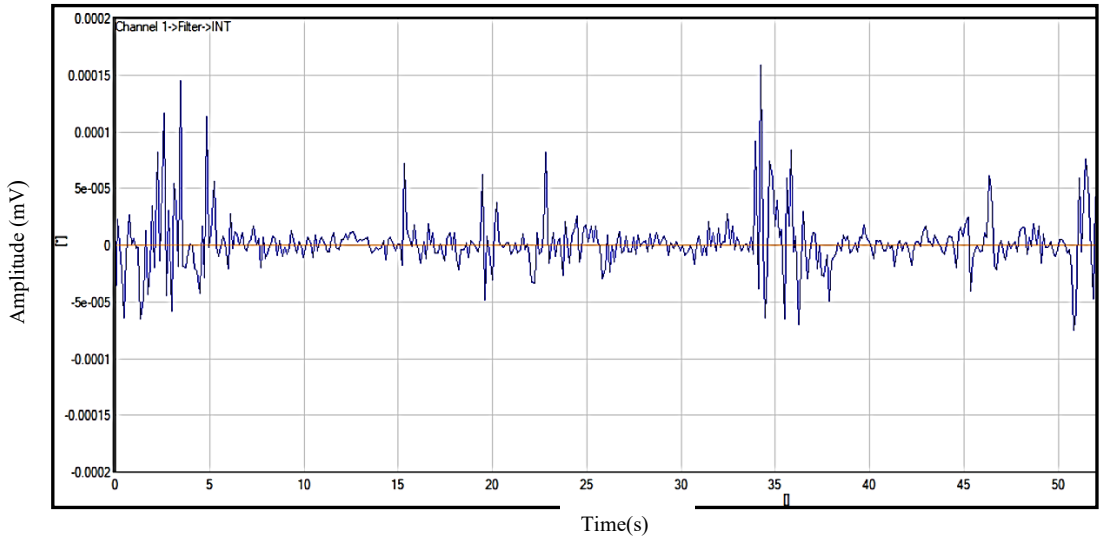

Figure 4. 24 Integrated EMG signal for vastus lateralis

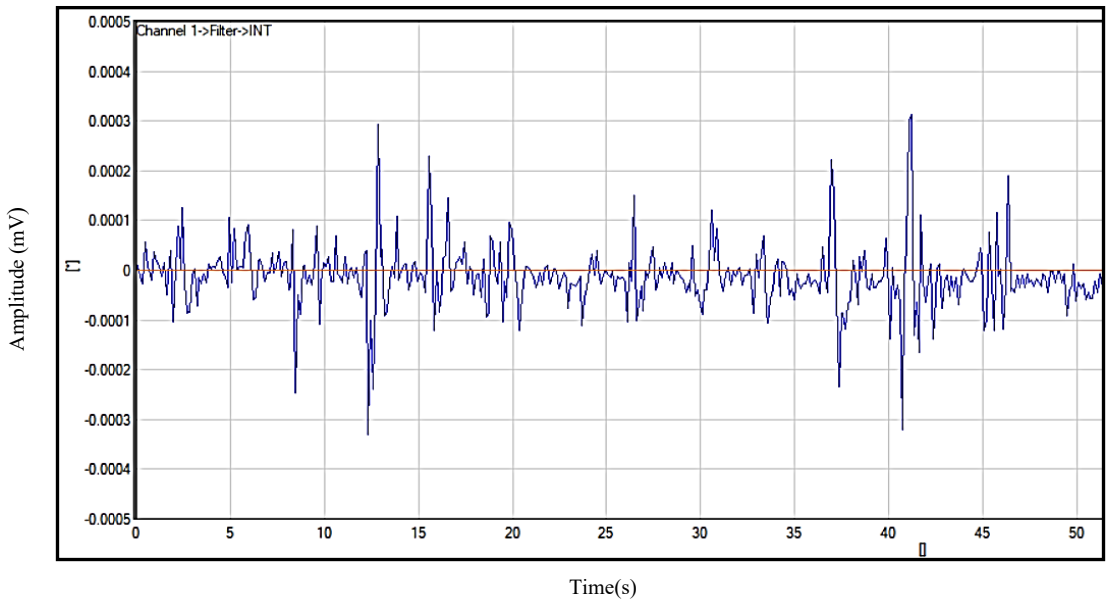

Figure 4. 25 Integrated EMG signal for biceps femoris

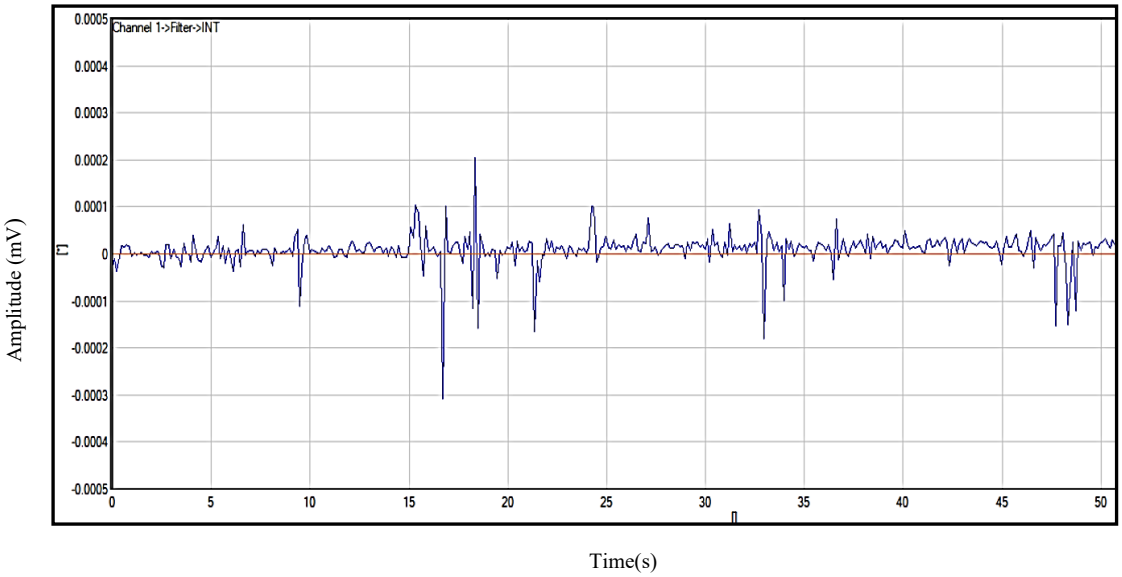

Figure 4. 26 Integrated EMG signal for semitendinosus

4.4.6 Statistical Analysis of EMG

The statistical analysis of the extracted EMG features used in the analysis are indicated in Table 4.1 below [72]. These features were extracted in the time and frequency domain to harness the efficacy of the machine learning models for pattern recognition by formulating the right features. This is useful to identify the most suitable features to evaluate the accuracy of the classification algorithm. Furthermore, the statistical features can be used to compare the effectiveness of different features in pattern

recognition. The statistical Table 4.1 shows the formula definition for the features extracted in the time and frequency domain.

Table 4. 1 Extracted EMG Features

Time Domain	Formular Definitions
Root Mean Square (RMS)	$\sqrt{\frac{1}{N}\sum_{i=1}^{N} EMG^2}$
Mean absolute value (MAV)	$\frac{1}{N}\sum_{i=1}^{N}\lvert nEMG_i\rvert$
Integrated EMG (IEMG)	$\sum_{n=1}^{N}\lvert EMG_i\rvert$
Simple square Integral (SSI)	$\sum_{n=1}^{N} nEMG_i^2$
Variance of EMG (VAR)	$\frac{1}{N-1}\sum_{i=1}^{N} nEMG_i^2$
Modified Mean Absolute Value (MMAV)	$\frac{1}{N}\sum_{i=1}^{N}\omega_i\lvert nEMG_i\rvert$
Average Amplitude Change (AAC)	$\frac{1}{N}\sum_{i=1}^{N-1}\lvert nEMG_{i+1}-nEMG_i\rvert$
Frequency domain	Formular Definitions
Mean Frequency (MNF)	$\frac{\sum_{j=1}^{M} f_j W_j}{\sum_{j=1}^{M} W_j}$
Median Frequency (MDF)	$\sum_{j=1}^{medFreq} W_j = \sum_{j=medFreq}^{M} W_j = 0.5*\sum_{j=1}^{M} W_j$
Mean Power (MNP)	$MNP = \frac{\sum_{j=1}^{M} W_j}{M}$
Total Power (TP)	$\sum_{j=1}^{M} W_j = sm0$

4.6.7 Relevance of Extracted Features for Muscle Analysis

The key features extracted for classification, as listed in the provided in Table 4.1 encompass both time domain and frequency domain parameters derived from electromyography (EMG) signals. These features are relevant for characterizing muscle activity patterns and dynamics, thereby facilitating the

classification of different movement patterns or abnormalities. The relevance of each feature category in the time and frequency domain.

Time Domain Features:

- *Root Mean Square (RMS):* Provides information about the overall magnitude of the EMG signal, reflecting the intensity or amplitude of muscle contractions.
- *Mean Absolute Value (MAV):* This represents the average absolute amplitude of the EMG signal, indicating the overall muscle activity level.
- *Integrated EMG (IEMG):* Summation of EMG signal amplitude over a specific time interval, reflecting the total muscle activation during that period.
- *Simple Square Integral (SSI):* Similar to IEMG but with squared EMG values, enhancing sensitivity to signal changes.
- *Variance of EMG (VAR):* Measures the variability or fluctuations in the EMG signal amplitude, providing insights into muscle activation patterns and coordination.
- *Modified Mean Absolute Value (MMAV):* A variation of MAV that may enhance sensitivity to certain types of muscle activity patterns.
- *Average Amplitude Change (AAC):* Reflects the average rate of change in EMG signal amplitude over time, indicating muscle activity dynamics.

Frequency Domain Features:

- *Mean Frequency (MNF):* This represents the average frequency content of the EMG signal, providing insights into muscle fatigue or activation patterns.
- *Median Frequency (MDF):* Reflects the central tendency of frequency distribution in the EMG signal, which can change with fatigue or neuromuscular alterations.
- *Mean Power (MNP):* This represents the average power of the EMG signal across different frequency bands, reflecting overall muscle activity.
- *Total Power (TP):* Reflects the total energy or power contained within the EMG signal across all frequencies, providing a comprehensive measure of muscle activity intensity.

These features are relevant for classification tasks as they capture different aspects of EMG signal characteristics related to muscle activation, fatigue, coordination, and dynamics. By analyzing these

features, machine learning or classification algorithms can discriminate between different movement patterns, detect abnormalities, or assess muscle function in various applications such as rehabilitation, sports science, and clinical diagnostics. The combination of time and frequency domain features offers a comprehensive representation of EMG signal properties, enabling more accurate classification and interpretation of muscle activity patterns.

4.6.8 Using the Extracted EMG Features to Address Research Problem

In the context of clinical gait analysis and movement classification of Polymyalgia Rheumatica (PMR) disease, the extraction of EMG features plays a crucial role in addressing the main research problem. By extracting EMG features such as Root Mean Square (RMS), Mean Absolute Value (MAV), Integrated EMG (IEMG)..etc help to characterise the hip muscle activity patterns during gait cycles in PMR patients. These features provide quantitative measures of muscle activation intensity, duration, and coordination, allowing for the identification of abnormalities from healthy gait patterns. In addition, the extracted EMG features enable the detection of subtle deviations from normal gait dynamics. EMG features like Variance of EMG (VAR), Median Frequency (MDF), and Average Amplitude Change (AAC) highlight the differences in muscle activity variability, fatigue patterns, or muscle recruitment strategies between PMR patients and healthy controls. By applying machine and deep algorithms to EMG features, researchers can differentiate between various gait abnormalities or disease severity levels. For instance, features like Modified Mean Absolute Value (MMAV) or Simple Square Integral (SSI) can capture specific muscle activation patterns characteristic of PMR-related gait disturbances. Classification algorithms trained on these features can then classify gait patterns into distinct categories, providing insights into disease progression and severity. Furthermore, EMG features can also be used to evaluate the effectiveness of interventions or treatments aimed at improving gait abnormalities in PMR patients. By monitoring changes in EMG features before and after treatment, researchers can assess improvements in muscle activation patterns or coordination. These feature analyses provide valuable insights into the underlying impairments associated with PMR disease.

4.7 Summary

In this chapter, the first part considers the clinical trial for the EMG data collection which involves the recruitment of participants and instrument for data collection. The main instrument for the data collection was the Trigno Avanti EMG sensor from Delsys. In the second part, the features extraction of the recorded EMG data collected from the hip muscles of two clinical groups discussed.

CHAPTER FIVE: MUSCULAR IMBALANCE ASSESSMENT AND MOVEMEMENT CLASSIFICATION

5.1 Overview

This chapter presents the hip muscular imbalance assessment and movement classification using traditional machine learning algorithms. The chapter is divided into two parts, the first part is the muscular imbalance assessment, which forms the first iteration of this study. The chapter investigates the muscular imbalance between patients' right and left hip muscles against healthy control subjects. The objective of muscular imbalances is to determine the difference in the strength between the right and left hip muscles, which may exacerbate the PMR conditions and impair patient movement. It was essential to identify imbalances which will help in designing rehabilitation protocols to improve pain management, leading to better patient outcomes. The metrics used in the muscular imbalance analysis was the maximum voluntary contraction. The second part of this chapter is the movement classification using traditional machine learning algorithms, which forms the second iteration of the study. It discusses the machine learning algorithm used to classify the movement patterns based on the intrinsic muscle activation signals and the dataset used. The machine learning algorithms used were Support Vector Machine (SVM), Decision Tree (DT), Rotation Forest (RF), and K-Nearest Neighbour algorithm. The imbalance assessment and the movement classification provide a clearer understanding of the effects of imbalances and the link with patients' specific movement patterns.

5.2 Muscular Imbalances Analysis

Muscle imbalance occurs when one or more muscles on one side of the human body are stronger or weaker than the corresponding muscle on the other opposing side [73]. Muscle imbalances may also occur when muscle force is uneven between opposing muscle groups. Usually, the muscle on each side of the human body is symmetrical in strength and size. It is important to investigate the hip muscular balance of PMR patients, which provides insight into the muscle activation pattern around the pelvic girdle. Furthermore, imbalance assessment provides valuable information on patients' progression as

they undergo treatment. This allows for a determination of hip muscle weakness in designing rehabilitation exercises for patients.

Some studies investigated muscle activity to determine muscle imbalance among patients and athletes. Wojdala et al [74] compared muscle activity between control (CONT) and sling shout assisted (SS) in a barbell bench press exercise to determine muscle imbalances. A post hoc analysis indicated a decrease in the maximum voluntary contraction (%MVC) for the SS compared to the control. Jorge et al [75] investigated the existence of isokinetic muscle imbalance in professional athletes in various modalities. The results from a comparative analysis indicated that the bilateral difference of the lower limbs was within average values (<10%) among the athletes. Arab et al [76] investigated the hip abductor weakness for people with low back pain. In that study, the hip abductors muscle strength was compared for participants with and without lower back pain (LBP). A post hoc analysis of muscle indicated that the hip abductor muscle strength is significantly lower among people with lower back pain than those without. Nadler et al [77] examined the hip muscle imbalance of lower back pain among athletes. The results validated previous claims that hip muscle imbalance is associated with athletes with lower back pain. In investigating the hip muscular imbalances, the metrics used were the maximum voluntary contraction (MVC%) and the signal amplitude which indicates the force produced by a muscle [78]. The muscle signals recorded from the hip muscles of participants were compared in the exercises conducted. This enables a determination of the bilateral differences of the right and left hip muscles.

5.2.1 Metrics for Hip Muscular Imbalance Assessment

From previous study by Wojdala [74] the maximum voluntary contraction was used as an indicator to determine muscular imbalances. MVC is commonly used in muscle biomechanics to represent the full force produced during voluntary contraction. Furthermore, the MVC evaluates the strength of a muscle, and it provides valuable information about the strength capabilities of a specific muscle or group of muscles. The significant bilateral difference in the MVC between opposing muscles suggests the

presence of muscular imbalance. The MVC was computed for the left and right hips muscles of PMR patients and healthy control subjects.

In the first step, the signal amplitude for each specific muscle was recorded in the voluntary contraction for the gait, knee lifting, and knee extension exercise. EMG signal amplitude indicates muscle contraction intensity which can be used to analyse muscle strength The second step considered the bilateral difference between the MVC (%) of a specific muscle on the right hip and a corresponding opposing muscle on the right. For instance, the difference between the right hip's rectus femoris (RF) and that of the corresponding opposing muscles of the left hip muscle of the rectus femoris is computed. Therefore, the amplitude of each muscle and the maximum voluntary contraction for each muscle is computed for 18 patients and 7 healthy control subjects. From Table 5.1, the amplitude of the muscle activation signals for each muscle is recorded in the gait, knee lifting, and knee extension exercise. This indicates the force produced by a muscle in each of the exercises conducted. The MVC (%) is computed as a muscle's force divided by the total maximum force produced multiplied by 100%. The MVC is given by the formula in equation (5.1) below [74].

$$MCV(\%) = \frac{force\ measure}{Maximum\ force}\ x\ 100 \tag{5.1}$$

The MVC (%) bilateral difference (BD) was calculated as the side-to-side difference between the muscle on the right hip and its corresponding muscle on the left hip [74].

This is given by $BD = MVC_{right\_hip} - MVC_{left\_hip}$ (5.2)

Table 5. 1 Summary of Maximum Voluntary Contraction of Hip muscles

Part.	Exercise	Right Hip RF		Left Hip RF		Right Hip VL		Left Hip VL		Right Hip BF		Left Hip BF		Right Hip SE		Left Hip SE		BD MVC%		BD MVC%	
		Amp	MVC (%)	Amp	MVC(%)	Amp	MVC(%)	Amp	MVC(%)	Amp	MVC(%)	Amp	MVC(%)	Amp	MVC(%)	Amp	MVC(%)	RF	VL	BF	SE
P001	Gait	0.0052	24.89	0.0018	12.72	0.0084	38.32	0.0058	25.28	0.0048	24.42	0.0019	12.49	0.0040	22.42	0.0015	10.83	+12.17	+13.04	+11.93	+11.59
	Knee Lifting	0.0064	32.71	0.0025	12.92	0.0078	35.98	0.0035	20.56	0.0084	38.32	0.0051	24.36	0.0108	61.26	0.0092	45.82	+19.79	+15.42	+13.96	+15.44
	Knee Ext.	0.0058	25.76	0.0027	13.24	0.0087	39.21	0.0056	25.42	0.0096	46.12	0.0060	25.82	0.0074	35.81	0.0054	25.12	+12.52	+13.79	+20.30	+10.69
P002	Gait	0.0128	63.60	0.0084	38.32	0.0184	86.78	0.0112	61.28	0.0142	65.42	0.0087	39.21	0.0136	64.21	0.0095	46.24	+25.28	+25.50	+26.21	+17.97
	Knee Lifting	0.0186	87.32	0.0102	60.28	0.0105	61.96	0.0062	31.98	0.0112	62.12	0.0056	25.72	0.0145	65.72	0.0090	45.16	+27.04	+29.98	+36.21	+20.56
	Knee Ext.	0.0121	62.82	0.0064	32.12	0.0084	38.32	0.0058	25.28	0.0086	38.46	0.0048	25.12	0.0042	23.46	0.0025	13.14	+30.70	+13.04	+13.34	+10.32
P003	Gait	0.0107	63.28	0.0157	74.10	0.0043	23.79	0.0065	32.12	0.0058	25.76	0.0125	63.31	0.0108	61.26	0.0154	74.48	-10.82	-8.33	-37.55	-13.22
	Knee Lifting	0.0124	64.85	0.0189	86.79	0.0096	58.10	0.0154	74.12	0.0073	34.82	0.0114	61.87	0.0112	62.77	0.0156	74.18	-21.94	-10.02	-27.05	-11.41
	Knee Ext.	0.0028	13.42	0.0085	42.72	0.0104	60.28	0.0142	72.63	0.0042	23.94	0.0118	61.96	0.0033	21.24	0.0068	32.54	-29.30	-12.35	-38.02	-11.30
P004	Gait	0.0043	23.49	0.0104	60.28	0.0087	38.35	0.0147	65.86	0.0038	21.34	0.0101	60.28	0.0096	45.76	0.0152	74.62	-36.79	-27.51	-38.94	-28.86
	Knee Lifting	0.0041	23.12	0.0063	32.14	0.0068	32.18	0.0136	64.48	0.0021	12.52	0.0056	24.83	0.0014	10.28	0.0062	26.87	-9.02	-32.30	-12.31	-16.59
	Knee Ext.	0.0052	24.89	0.0074	34.95	0.0021	12.54	0.0046	23.98	0.0028	13.60	0.0078	35.98	0.0125	64.15	0.0075	34.86	-10.06	-11.44	-22.38	-22.04
P005	Gait	0.0057	28.46	0.0026	13.92	0.0115	63.14	0.0090	45.23	0.0148	66.72	0.0046	24.96	0.0106	60.82	0.0086	42.70	+14.54	+17.91	+41.76	+18.12
	Knee Lifting	0.0058	25.28	0.0023	13.19	0.0068	32.54	0.0036	20.58	0.0072	34.77	0.0042	23.42	0.0092	46.35	0.0077	35.12	+12.09	+11.96	+11.35	+11.23
	Knee Ext.	0.0065	32.12	0.0036	20.58	0.0072	34.93	0.0018	12.42	0.0080	37.78	0.0035	20.52	0.0103	60.46	0.0070	34.38	+ 11.54	+22.51	+17.26	+26.08
P006	Gait	0.0160	74.25	0.0084	38.16	0.0095	46.86	0.0067	31.98	0.0132	63.86	0.0041	23.12	0.0185	87.46	0.0102	60.68	+36.09	+14.88	+40.74	+26.78
	Knee Lifting	0.0182	87.90	0.0114	61.80	0.0175	83.37	0.0135	64.32	0.0196	90.21	0.0179	75.86	0.0082	38.15	0.0056	25.14	+26.10	+19.05	+14.35	+13.01
	Knee Ext.	0.0141	72.24	0.0110	61.53	0.0076	34.24	0.0050	23.18	0.0158	74.85	0.0138	63.28	0.0142	73.92	0.0108	61.26	+10.71	+11.06	+12.57	+12.66
P007	Gait	0.0019	12.49	0.0042	23.18	0.0091	45.60	0.0122	63.24	0.0125	63.46	0.0159	75.38	0.0104	60.12	0.0145	72.85	-10.68	-17.64	-11.92	-12.73
	Knee Lifting	0.0036	20.58	0.0065	32.12	0.0043	23.79	0.0085	38.39	0.0024	12.23	0.0075	35.18	0.0048	23.79	0.0108	61.18	-11.54	-14.60	-22.95	-37.39
	Knee Ext.	0.0024	12.83	0.0082	38.42	0.0040	21.23	0.0068	32.54	0.0036	20.58	0.0069	32.89	0.0046	23.76	0.0093	45.68	-8.40	-11.31	-12.31	-21.92
P008	Gait	0.0103	60.64	0.0052	24.63	0.0128	64.28	0.0096	46.72	0.0110	61.28	0.0058	25.76	0.0160	74.24	0.0078	35.18	+36.01	+17.56	+35.52	+39.06
	Knee Lifting	0.0118	62.28	0.0064	33.23	0.0156	74.36	0.0108	61.26	0.0134	64.32	0.0078	35.98	0.0136	64.41	0.0060	25.82	+29.05	+13.10	+28.34	+38.59
	Knee Ext.	0.0125	63.45	0.0078	35.98	0.0136	64.21	0.0091	45.28	0.0102	60.24	0.0084	38.32	0.0078	35.46	0.0040	22.48	+27.47	+18.93	+21.92	+12.98
P009	Gait	0.0015	11.08	0.0046	22.10	0.0027	12.83	0.0058	25.38	0.0035	29.47	0.0124	62.28	0.0065	32.40	0.0092	45.82	-11.02	-12.55	-33.81	-13.42
	Knee Lifting	0.0036	20.58	0.0069	34.70	0.0019	12.18	0.0048	24.34	0.0052	24.92	0.0072	34.72	0.0074	34.28	0.0125	62.96	-14.12	-12.16	-9.80	-28.68
	Knee Ext.	0.0042	23.46	0.0084	38.32	0.0014	10.58	0.0038	21.16	0.0068	32.28	0.0115	62.10	0.0036	20.25	0.0087	39.21	-14.86	-10.58	-29.82	-18.96
P010	Gait	0.0058	25.76	0.0019	12.49	0.0108	61.26	0.0065	32.12	0.0078	35.16	0.0051	23.20	0.0092	46.35	0.0056	25.42	+13.27	+29.14	+11.96	+20.93
	Knee Lifting	0.0102	60.64	0.0051	24.36	0.0072	34.77	0.0043	23.24	0.0075	35.18	0.0036	20.58	0.0084	38.32	0.0052	24.82	+36.28	+11.53	+ 14.60	+13.50
	Knee Ext.	0.0074	34.96	0.0036	20.58	0.0098	46.35	0.0046	24.20	0.0122	63.24	0.0052	24.89	0.0125	64.15	0.0087	39.21	+14.38	+22.15	+ 38.35	+25.27
P011	Gait	0.0098	46.87	0.0052	24.92	0.0184	87.90	0.0112	61.82	0.0125	63.31	0.0078	35.12	0.0136	64.48	0.0077	35.12	+21.95	+26.08	+28.19	+29.36
	Knee Lifting	0.0152	74.28	0.0102	60.64	0.0158	74.46	0.0114	61.87	0.0116	61.85	0.0086	38.24	0.0154	74.10	0.0118	63.16	+13.64	+12.59	+23.61	+10.94
	Knee Ext.	0.0163	75.80	0.0114	62.84	0.0115	63.14	0.0077	35.12	0.0135	64.32	0.0088	39.32	0.0157	75.12	0.0110	62.79	+12.96	+28.02	+25.00	+12.33
	Gait	0.0108	61.26	0.0160	74.18	0.0097	46.26	0.0136	64.25	0.0077	36.77	0.0136	64.21	0.0102	60.28	0.0159	75.48	-12.92	-17.99	-27.44	-15.20

P012	Knee Lifting	0.0118	61.28	0.0158	74.12	0.0098	46.25	0.0154	74.24	0.0140	72.80	0.0186	87.13	0.0110	61.28	0.0176	77.24	-12.84	-27.99	-14.33	-15.96
	Knee Ext.	0.0113	61.35	0.0142	72.63	0.0108	61.26	0.0176	85.43	0.0156	74.18	0.0188	89.74	0.0105	60.17	0.0158	74.18	-11.28	-24.17	-15.56	-14.01
P013	Gait	0.0102	60.28	0.0158	74.25	0.0084	34.82	0.0116	61.85	0.0114	61.14	0.0168	75.29	0.0178	85.56	0.0128	63.45	-13.97	-27.03	-14.15	-10.27
	Knee Lifting	0.0118	63.14	0.0189	90.12	0.0092	45.82	0.0162	72.14	0.0102	60.28	0.0158	74.16	0.0108	61.26	0.0182	87.16	-26.98	-26.32	-26.88	-25.90
	Knee Ext.	0.0130	63.12	0.0182	87.18	0.0074	35.12	0.0112	61.76	0.0108	61.26	0.0140	72.80	0.0152	74.24	0.0186	87.79	-24.06	-26.67	-11.54	-13.55
P014	Gait	0.0140	72.80	0.0102	60.28	0.0184	87.70	0.0130	63.81	0.0128	63.07	0.0068	32.54	0.0134	64.28	0.0075	35.89	+12.52	+23.89	+30.53	+29.83
	Knee Lifting	0.0097	46.24	0.0046	24.89	0.0140	72.50	0.0078	35.24	0.0138	64.82	0.0087	38.35	0.0142	72.63	0.0112	61.26	+21.35	+37.26	+26.47	+11.37
	Knee Ext.	0.0152	74.26	0.0087	38.65	0.0142	72.38	0.0085	38.39	0.0102	60.18	0.0065	32.12	0.0174	85.26	0.0106	61.26	+35.61	+33.99	+28.06	+21.12
P015	Gait	0.0087	39.12	0.0112	61.28	0.0078	35.96	0.0139	64.82	0.0113	61.35	0.0174	82.38	0.0078	35.94	0.0102	60.28	-22.16	-28.86	-21.12	-24.34
	Knee Lifting	0.0098	46.92	0.0135	64.28	0.0086	42.70	0.0163	74.84	0.0068	32.54	0.0118	61.92	0.0090	45.80	0.0142	72.63	-17.36	-21.58	-29.38	-26.83
	Knee Ext.	0.0077	36.21	0.0140	72.80	0.0090	45.16	0.0102	60.93	0.0085	42.71	0.0138	63.40	0.0108	61.26	0.00158	74.25	-36.59	-15.77	-20.69	-12.99
P016	Gait	0.0187	89.24	0.0108	61.26	0.00152	74.24	0.0132	63.10	0.0072	34.82	0.0043	23.49	0.0118	61.28	0.0064	32.12	+27.98	+11.14	+11.33	+29.16
	Knee Lifting	0.0159	74.35	0.0118	61.97	0.00180	85.93	0.0156	74.62	0.0116	62.12	0.0052	24.89	0.0132	63.48	0.0096	46.24	+12.38	+11.31	+37.23	+17.24
	Knee Ext.	0.0143	73.10	0.0098	46.24	0.0142	72.83	0.0083	36.18	0.0082	36.15	0.0036	20.58	0.0125	63.31	0.0092	45.12	+26.86	+36.65	+15.57	+18.19
P017	Gait	0.0041	23.12	0.0075	35.18	0.0114	60.14	0.0186	87.79	0.0098	48.32	0.0152	74.18	0.0121	62.18	0.0156	73.48	-12.06	-27.65	-25.86	-11.30
	Knee Lifting	0.0018	12.42	0.0069	32.89	0.0122	62.83	0.0158	74.18	0.0108	61.26	0.0184	87.42	0.0115	63.14	0.0185	87.10	-20.47	-11.35	-26.16	-23.96
	Knee Ext.	0.0024	12.83	0.0083	36.18	0.0125	62.38	0.0163	75.24	0.0102	60.28	0.0145	73.14	0.0108	61.26	0.0154	73.18	-23.35	-12.86	-12.86	-11.92
P018	Gait	0.0135	63.84	0.0065	32.12	0.0187	89.79	0.0118	61.28	0.0184	87.40	0.0106	61.28	0.0158	74.16	0.0097	46.24	+31.72	+28.51	+26.12	+27.92
	Knee Lifting	0.0152	74.26	0.0102	60.28	0.0174	85.26	0.0112	61.14	0.0165	78.16	0.0092	45.82	0.0118	62.16	0.0084	39.18	+13.98	+24.12	+32.34	+22.98
	Knee Ext.	0.0142	72.80	0.0118	61.18	0.0182	87.67	0.0148	72.83	0.0154	74.16	0.0124	63.60	0.0146	73.28	0.0113	61.35	+11.62	+14.84	+10.56	+11.93
CONT 1	Gait	0.0056	25.14	0.0042	23.46	0.0079	35.81	0.0072	34.92	0.0102	60.64	0.0098	56.35	0.0158	74.12	0.0138	65.28	+1.68	+2.89	+4.29	+8.84
	Knee Lifting	0.0045	23.98	0.0037	21.40	0.0085	36.82	0.0074	35.72	0.0082	35.15	0.0065	32.12	0.0146	71.16	0.0132	64.28	+2.58	+ 1.10	+ 3.03	+6.88
	Knee Ext.	0.0048	25.03	0.0034	21.16	0.0062	26.87	0.0058	25.28	0.0087	37.81	0.0080	35.14	0.0158	74.12	0.0142	70.48	+3.87	+1.59	+2.67	+3.64
CONT 2	Gait	0.0112	61.82	0.0103	60.64	0.0098	47.25	0.0092	45.82	0.0085	38.38	0.0076	34.24	0.0093	46.10	0.0076	35.14	+1.18	+1.43	+4.14	+10.96
	Knee Lifting	0.0126	63.48	0.0114	61.87	0.0078	35.98	0.0072	34.18	0.0088	40.26	0.0081	37.34	0.0092	45.84	0.0088	43.56	+1.61	+1.80	+2.92	+2.28
	Knee Ext.	0.0154	74.32	0.0148	72.12	0.0091	45.80	0.0084	38.32	0.0075	34.20	0.0065	33.12	0.0085	38.98	0.0082	37.10	+2.20	+1.08	+1.10	+1.88
CONT 3	Gait	0.0087	39.21	0.0092	45.82	0.0118	63.14	0.0136	64.41	0.0106	60.82	0.0112	62.77	0.0124	62.28	0.0148	66.72	-6.61	-1.27	-1.95	-4.43
	Knee Lifting	0.0054	25.76	0.0065	32.12	0.0102	60.64	0.0124	63.28	0.0118	62.28	0.0140	64.12	0.0126	65.72	0.0150	68.38	-6.36	-2.64	-1.84	-2.66
	Knee Ext.	0.0048	24.96	0.0064	32.10	0.0072	34.93	0.0085	38.35	0.0127	63.21	0.0136	63.46	0.0142	65.70	0.0152	68.45	-7.14	-3.42	-2.24	-2.75
CONT 4	Gait	0.0046	23.46	0.0019	12.19	0.0091	45.16	0.0084	38.32	0.0068	34.10	0.0062	32.07	0.0077	35.24	0.0068	32.67	+11.27	+6.84	+2.03	+2.57
	Knee Lifting	0.0034	22.41	0.0021	12.83	0.0062	31.54	0.0056	28.24	0.0070	34.08	0.0058	30.34	0.0087	39.21	0.0071	34.12	+9.58	+3.30	+3.74	+5.09
	Knee Ext.	0.0085	38.45	0.0072	34.18	0.0056	25.16	0.0035	20.52	0.0098	48.35	0.0092	46.25	0.0126	63.97	0.0102	60.62	+4.27	+4.64	+2.10	+3.35
CONT 5	Gait	0.0035	22.56	0.0058	25.28	0.0054	25.10	0.0065	32.12	0.0056	25.62	0.0064	32.10	0.0076	34.24	0.0094	46.16	-2.72	-7.02	-6.48	-11.92
	Knee Lifting	0.0058	25.86	0.0074	35.72	0.0068	27.34	0.0071	34.85	0.0062	32.82	0.0077	35.48	0.0080	35.25	0.0085	38.64	- 9.86	-7.51	-2.66	-3.39
	Knee Ext.	0.0078	35.98	0.0079	37.26	0.0062	31.82	0.0076	34.24	0.0087	39.21	0.0094	46.07	0.0085	36.26	0.0092	45.82	-1.28	-2.42	-6.86	-9.56
CONT 6	Gait	0.0126	63.48	0.0098	56.35	0.0124	62.28	0.0103	60.76	0.0072	34.92	0.0054	25.76	0.0136	64.41	0.0128	62.12	+7.13	+1.52	+9.16	+2.29
	Knee Lifting	0.0114	62.96	0.0092	54.82	0.0142	65.72	0.0106	61.26	0.0079	35.81	0.0065	32.12	0.0121	63.28	0.0108	61.37	+8.14	+4.46	+3.69	+1.92
	Knee Ext.	0.0102	60.64	0.0097	56.21	0.0140	65.60	0.0118	63.14	0.0064	32.18	0.0058	25.76	0.0085	38.32	0.0078	35.12	+4.43	+2.46	+6.42	+3.20

CONT 7	Gait	0.0019	12.49	0.0041	23.12	0.0029	14.12	0.0047	24.98	0.0026	13.46	0.0036	22.58	0.0018	12.42	0.0046	23.46	-10.63	-10.86	-9.12	-11.04
	Knee Lifting	0.0023	12.83	0.0040	22.96	0.0027	13.96	0.0035	22.56	0.0028	14.08	0.0046	23.46	0.0035	22.56	0.0058	30.34	-10.13	-8.60	-9.38	-7.78
	Knee Ext.	0.0025	12.98	0.0038	21.28	0.0017	12.35	0.0030	20.58	0.0031	20.12	0.0058	25.76	0.0038	23.46	0.0072	34.92	-8.30	-8.23	-5.64	-11.46

5.2.2 Description of Muscular Imbalance Table

Table 5.1 contains data related to the electromyography (EMG) activity of various muscles during different exercises for participants.

Column 1-Participant: Indicates the participant ID (P001 - P018) for patients and healthy control participant ID (CONT1- CONT7)

***Column 2-Exercise*:** This describes the type of exercise performed by the participant, such as Gait, Knee Lifting, and Knee Extension These exercises likely involve different movements or tasks that elicit specific muscle activation patterns.

Column 3-10 Peak Muscle Activity: The table lists the amplitude (Amp) of EMG signals recorded from the hip muscles during each exercise. The muscles monitored include the right and left Rectus Femoris (RF), Vastus Lateralis (VL), Biceps Femoris (BF), and Semitendinosus (SE). This was done for the right and left hip muscles of participants engaged in the exercise. The amplitude values are typically expressed in arbitrary units which indicate the level of muscle activation during the exercise. The Maximum Voluntary Contraction (MVC%) column provides a percentage of (MVC) achieved by each muscle during the exercise. The MVC represents the maximum force or contraction that the muscle can generate voluntarily and is often used as a reference for normalizing EMG signals.

Columns 11-12: Changes in Muscle Activity based on MVC (%): The last four columns show the percentage change in muscle activity compared to a baseline measurement. These changes indicate how much the EMG amplitude deviates from the baseline, reflecting alterations in muscle activation levels during the exercise based on the MVC (%). The bilateral differences compute the change in the MVC between the right and left hip for each specific muscle recorded. Overall, the table presents quantitative data on EMG activity and MVC percentages for various hip and thigh muscles during different exercises, providing insights into muscle activation patterns and responses to specific movement tasks for each participant.

5.2.3 Analysis of Muscular Imbalances

A positive (+) value indicates the right hip MVC (%) in a specific muscle is stronger than the opposing corresponding muscle on the left hip. On the other hand, a negative (-) value illustrates that the MCV (%) of the left hip in a specific muscle is stronger than its opposing corresponding muscle on the right hip. A threshold of 10% bilateral difference of the MVC between the right hip and the corresponding muscle on the left hip is thought to be significant. This is evident from the previous work by Jorge et al [75], where the MVC was set to 10% threshold of bilateral difference. From Table 5.1, patients had the MVC (%) difference between the right and left hip to be above 10% for the exercise. However, there were some exceptions where the MVC was below 10%. In the knee lifting exercises, some patients with P007 and P009 had the MVC below the threshold of 10%. Furthermore, in the knee extension exercise, a patient with ID P004 had MVC value lower than the threshold difference of 10%. Cumulatively, there was a significant difference in the MVC (%) values compared for each muscle recorded among patients. Regarding the healthy control subjects, the MVC (%) differences between the right and left were lower than the threshold of 10%. It is also noted that in some cases, healthy controls had MVC higher than 10% for some muscles. This is evident for control subjects with ID CONT4 and CONT7 in Table 5.1 of the summary MVC recorded. Figure 5.1 shows the graphical plot of the MVC (%) for the rectus femoris (RF), vastus lateralis (VL) and biceps femoris (BF) and semitendinosus (SE). The plot illustrates that some patients had MVC above 20% for the right hip compared to the corresponding opposing muscle on the left. The plot also indicates healthy control subjects had MVC values below 10% except for some patients with ID CONT2 and CONT4, where the SE and RF muscles are above 10%, respectively. The plot illustrates imbalances between the right hip, which are stronger than the left hip. For the left hip, [Fig 5.1] also indicates cases where the MVC is above 20% for some muscles in some patients, and the remaining MVC is recorded above 10%. This shows the muscles on the left hip to be stronger than the right hip.

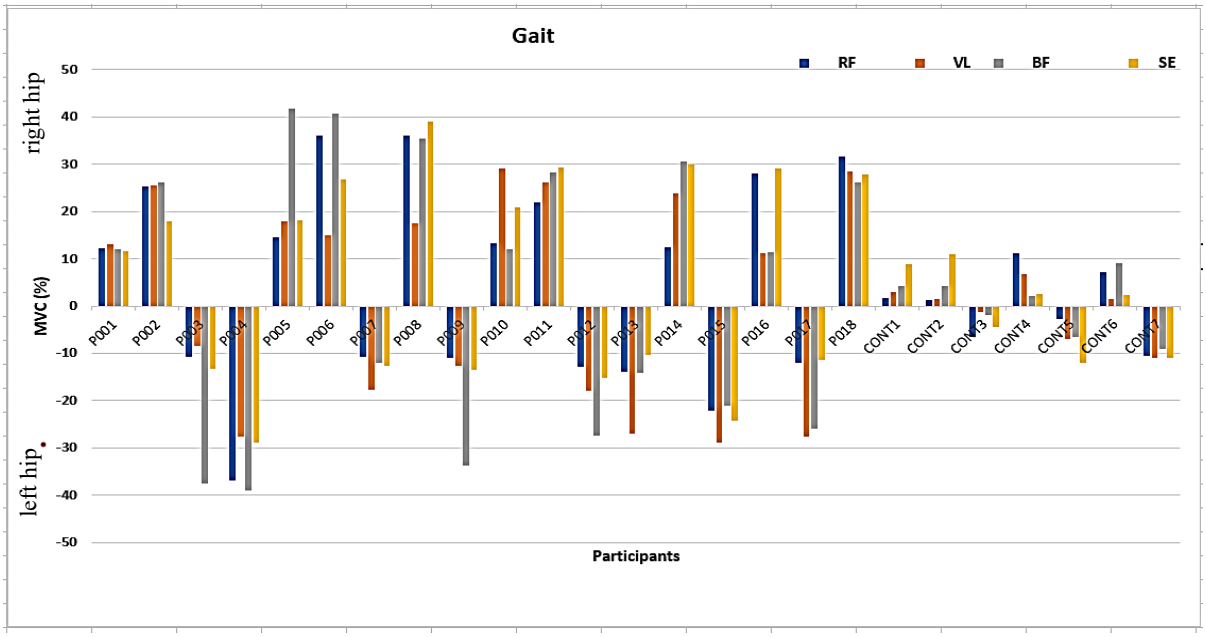

Figure 5. 1 Muscular imbalance plot for gait exercise

The MVC% values for each muscle were recorded considering bilateral differences between the specific muscles. For instance, in [Figure 5.2] a patient with identity P001 had a stronger right hip than a stronger left hip. The plots show that the RF, VL, BF, and SE muscles were above the 10% MVC threshold, indicating the difference between the right hip muscles compared to the corresponding muscle on the left hip. In another instance, a patient with identified P003 in [Figure 5.2], the MVC% bilateral difference indicates that the left hip was stronger than the right hip. The RF and BF were above 30%, which was higher than the 10% threshold set. This indicates a case of muscular imbalances in the hip, with the left hip stronger than the right hip based on the bilateral difference. The plot is an indication that the MVC % was above VL, and SE was noted to be above for each muscle recorded. In the case of healthy control, there were minimal imbalances based on the bilateral differences between the right and left hip. For instance, a healthy control subject with identity CONT1 indicates the right hip was slightly stronger than the left hip. The bilateral difference between the RF, VL, and BF was approximately 4% MVC values. This means that the difference between the muscles is negligible and below the 10% threshold set to be significant. In another instance, for healthy control subjects with ID CONT5, the RF, VL, and BF were approximately 6%. This indicates the left muscles were slightly stronger than the right

hip muscles. However, the exceptional case where the SE muscle was above the 10% threshold set. The imbalances between the hip muscles were recorded to be very minimal for healthy control subjects.

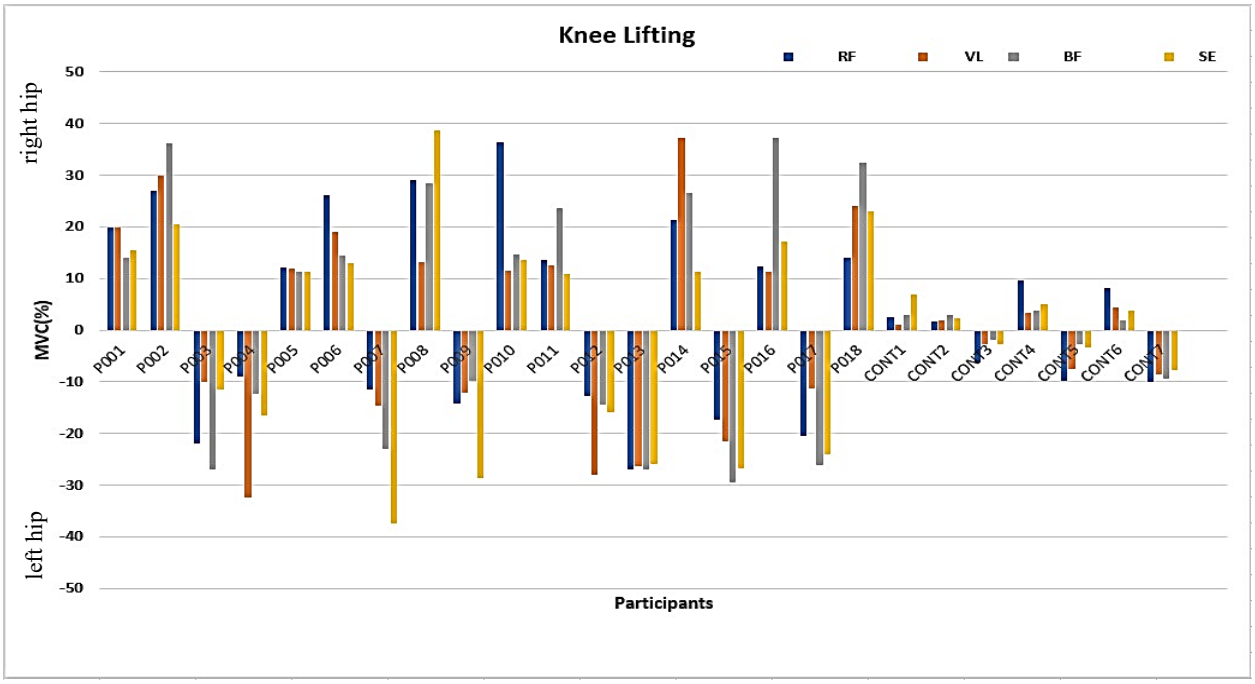

Figure 5. 2 Muscular imbalance plot for knee lifting exercise.

For the knee lifting in [Fig 5.2] patients with the right hip with positive values (+) had the MVC above 10%, while other patients had some specific muscles recorded above 20%. This indicates the presence of muscular imbalance between the right and left hip. Regarding the left hip with negative values (-), some patients had MVC for some muscles above 20%, while the rest of the muscles were above 10% in the knee lifting exercise. For the healthy control subjects, both the left and right hip illustrate the MVC values to be below 10% except in CONT5 and CONT7 where the rectus femoris was above 10%.

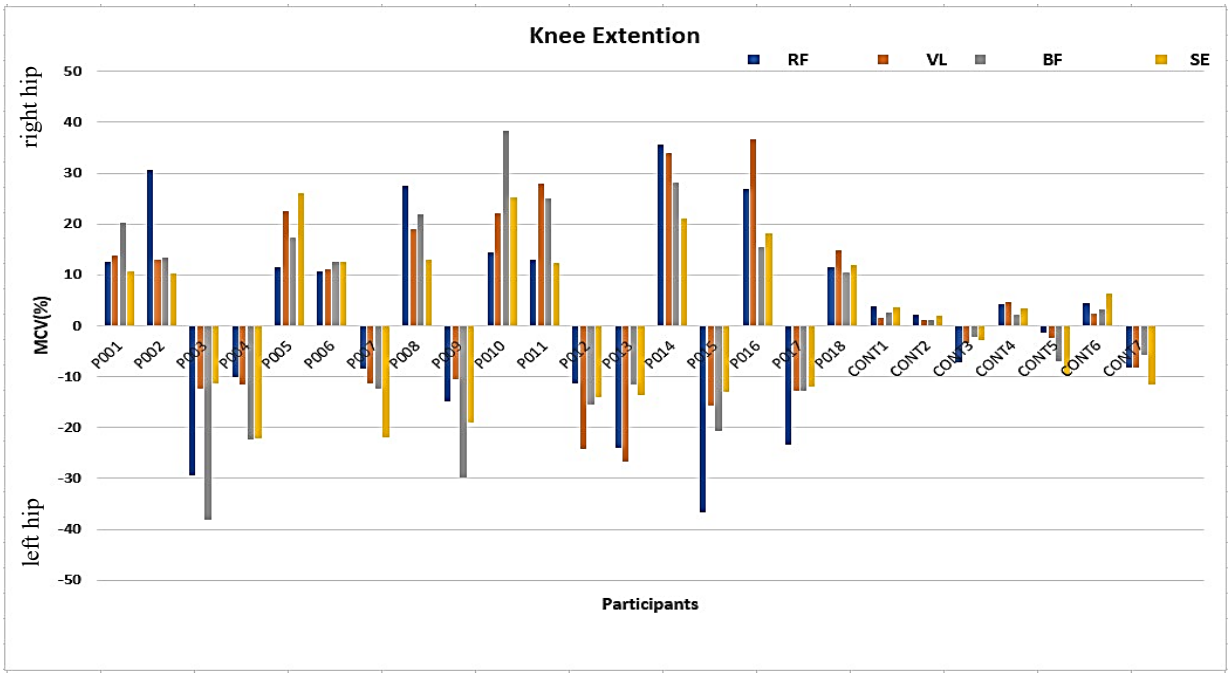

Figure 5. 3 Muscular imbalance plot for knee extension exercise

The knee extension in figure 5.3 shows that the right hip MVC values were above 10% and this was similar for left hip MVC% with some patients having muscles higher than the 20%. On the average patients had 15% in the MVC signifying imbalances in hip muscles. Comparing the MVC for patients and healthy control subjects, significant muscular imbalances were recorded among patients versus healthy control subjects for each exercise. For instance, in a patient identified as P008 in [Figure 5.3], the MVC% bilateral difference indicates that the right hip was stronger than the left hip. The RF, VL, and BF were seen to be above 30%, which was higher than the 10% threshold while the other hip muscle SE was approximately 12%. This indicates a case of hip muscular imbalances with the right hip stronger than the left hip based on the bilateral difference. The plot is an indication that the MVC % was above VL, and SE was noted to be above for each muscle recorded. In another instance, a patient with identified as P012 in [Figure 5.3], the MVC% bilateral difference indicates that the left hip was stronger than the right hip. The RF, VL, BF, and SE muscles were seen to be above 10%, which was approximately 14% and therefore higher than the threshold of 10%. In the case of healthy control subjects, there were minimal imbalances based on the bilateral differences between the right and left

hip. For example, a healthy control subject identified as CONT4 indicates the right hip was slightly stronger than the left but fell below the threshold of 10%. The bilateral difference of the MVC indicated the right hip muscles were approximately 4% and not significant to determine imbalance. In another instance for a healthy control identified as CONT7, the left hip was slightly stronger but lower than the 10% threshold. The MVC of the muscles was approximately 5% for the hip muscles recorded. In general, on average patients had 15% MVC bilateral difference compared to an average 6% MVC for healthy control individuals. Therefore, patients exhibited significant muscular imbalances between the hip muscles in patients as opposed to healthy control individuals.

5.3 Machine Learning Techniques

In the second part of this chapter, traditional machine-learning models are used for movement classification. This forms the second iteration of the study using conventional models for movement classification. This is particularly useful in classifying the movement patterns and having a clearer picture of the hip muscular imbalances identified in patients and their effects on movement. Currently, it is unclear the link between hip muscular imbalances and the movement patterns of patients to provide a better understanding of the pathophysiology of patients. In line with addressing this problem, this section investigated the movement pattern of patients based on the hip muscles, which forms the study's main aim. In the classification, the movement part of patients is compared to healthy control subjects to determine the differences between the two groups. Traditional machine learning algorithms used in this study are models that can learn from a given data and make predictions based on the input EMG data. These algorithms are often called "traditional" machine learning algorithms and are widely used. They are used to model the relationship between the output of the target prediction and the input features. These traditional algorithms can be interpreted by humans, which is essential for analysing errors, improving models, and discovering statistical information. Several standard machine-learning algorithms are used to analyse the movement patterns between patients and healthy control subjects. Traditional machine learning models are essential in EMG classification for the simplicity and speed of

prediction. Furthermore, traditional models typically require less computation compared to deep learning models. This makes the traditional models suitable for resource-constrained situations, requiring real-time processing, or when dealing with large data sets where deep learning can be computationally expensive. The traditional models can perform well with relatively small datasets compared to deep learning models that often require large amounts of labelled data for training, which may only sometimes be available. The four classification models are, support vector machine (SVM), decision tree (DT), rotation forest (RF), and k-nearest neighbour (KNN).

5.3.1 Data Modelling

The data modelling in this study describes the feature vectors extracted from the EMG signals for the classification. The EMG signals recorded from patients and control subjects are represented in a CSV file for classification. The four hips muscles (rectus femoris, vastus lateralis, biceps femoris and semitendinosus) were used in the classification from 18 PMR patients and 7 healthy control subjects. Therefore, in this classification, 100 movement segments were recorded for analysis, which comprised of patients (18x4) and controls (7x4) for the participants. The raw EMG data recorded is represented as Yz (r), where r € [1, R] with R representing the total frames of the EMG data sequences, z € [1, Ƶ] with Ƶ indicating the number of sensor channels in a repetitive gait cycle. This repetitive gait cycle moves between the stance and swing phases during walking. In a gait cycle, the sequence Yz (r) is first segmented into a single K gait cycle {w1 (r) … wk (r) …wK(r) }. The signals were extracted in the time and frequency domain to harness the efficacy of the machine learning models for classification by formulating the right features for classification. This is done for the knee lifting and knee extension exercises. The sample processed data recorded from the muscle signals of patients and control subjects in the CSV file.

5.3.2 Dataset Description for Classification

The datasets used for the classification for participants in the gait activity is illustrated in [Table 5.2] based on the signals recorded in the session. The columns represent the specific time point during which

the signals are recorded. The rows represent the EMG channels that record the EMG values at each time point. Four each participant had four separate channels representing each specific hip muscles recorded. The label in the column contains the class category where patients are indexed "1" and the healthy control subjects were indexed as "0". There were 100 rows in the EMG dataset where patients were 72 rows and healthy control subjects were 28 rows. The values in Table 5.2 represent the data points of EMG signals in timestamp. The primary component of the dataset is the EMG signal recordings recorded represented as a matrix where each row corresponds to a time point and each column corresponds to a channel (electrode).

Timestamps: Time stamps indicating when each sample of EMG data was recorded. This allows for the temporal analysis of muscle activity.

Class Labels: Each sample of EMG data would be labelled with a class indicating whether the corresponding subject is a PMR patient (1) or a healthy control (0).

Each row in the dataset represents a single observation, consisting of the EMG signal data, associated features, class labels, and any additional information relevant to the study. This structured dataset can then be used to train machine learning models for binary classification tasks, in distinguishing between patients with a specific PMR condition and healthy controls based on their EMG signals.

Table 5. 2 Sample EMG dataset

	A	B	C	D	E	F	G	H	I	J	K	L	M	N	O	P	Q	R
60	322.4726	-48.2082	-7.91403	0.752974	0.244447	-1.72107	-0.6238	-0.41492	-0.6508	0.11743	-0.05172	0.152229	0.077355	-0.01116	0.113128	-0.02695	1	
61	-17.1715	-8.25747	-4.33411	-1.31302	-0.68491	-1.08112	-2.82048	-0.67307	-2.9204	-0.1141	-0.19672	-0.11819	0.000449	-1.96664	-0.72902	-0.60098	1	
62	-10.4411	-3.11287	-2.07515	-1.15505	-0.60153	-0.7598	-0.51844	-0.7387	-1.2046	0.290921	2.05123	-0.77489	0.466142	-0.37528	-0.56273	0.771897	1	
63	-15.9302	-7.57211	-3.9302	-0.79589	-0.53202	-1.10669	-1.75782	-0.52549	-2.19648	-0.21451	-0.71151	-0.38245	-0.3781	-1.66047	-0.66611	-0.28979	1	
64	-7.02568	0.110242	2.587018	2.377989	0.251978	0.954253	4.241504	3.490909	-0.46784	0.722087	6.587987	3.243288	-7.52737	1.407498	14.50178	-8.66868	1	
65	-8.52388	-7.00766	8.336861	-4.89189	-2.81835	-1.78285	-18.412	23.07592	18.00826	3.322009	-3.59344	1.314811	0.271235	-0.09467	0.506805	0.311151	1	
66	-6.61744	-3.25832	0.690993	-0.41921	-2.88021	-0.7847	8.805352	-10.6608	16.3102	-13.4887	-11.7312	0.762958	-3.95878	0.165617	3.688911	2.629125	1	
67	-12.3988	-5.57596	0.306447	-0.0889	-0.36353	0.514298	0.667883	-1.28687	0.517276	-2.31144	1.636385	-0.78479	-0.34316	-1.86165	0.29755	0.57567	1	
68	-14.578	-7.29671	-3.03794	-0.49236	-0.39016	-0.67495	-0.33633	-0.04607	-1.90726	1.402028	0.813562	0.202434	-0.76013	-1.14593	-0.72174	0.853118	1	
69	-16.2024	-7.40607	-4.2901	-1.51899	-0.43084	-0.74139	-2.56054	-0.63634	-2.8145	-0.38495	-0.36416	-0.13606	-0.28348	-1.62616	-0.5232	-0.93575	1	
70	-5.06958	-1.28701	1.263345	-0.17227	-2.11051	1.293402	0.890835	-3.3536	8.477105	-2.18183	8.500609	-7.63274	-3.64709	8.029881	-7.73206	-4.02912	1	
71	40.21145	36.35348	75.27011	-23.5063	-7.28686	-7.41868	-1.35725	-2.52175	-3.40385	-0.02235	-0.91456	-0.71308	-0.21045	-0.7764	-0.29607	-0.17723	1	
72	-5.06958	-1.28701	1.263345	-0.17227	-2.11051	1.293402	0.890835	-3.3536	8.477105	-2.18183	8.500609	-7.63274	-3.64709	8.029881	-7.73206	-4.02912	1	
73	40.21145	36.35348	75.27011	-23.5063	-7.28686	-7.41868	-1.35725	-2.52175	-3.40385	-0.02235	-0.91456	-0.71308	-0.21045	-0.7764	-0.29607	-0.17723	1	
74	71.34437	101.7435	-48.7466	-8.77268	-30.5678	8.108222	-1.37286	-0.22187	0.661957	1.863476	0.40133	0.467972	-0.92437	-1.27738	0.218816	0.773163	0	
75	-5.86683	-0.08793	-1.45777	0.217758	-0.27894	0.18942	2.269845	0.428613	0.572921	1.135969	0.432834	0.047492	-1.26167	0.753055	-1.60296	-0.04777	0	
76	-6.54698	-0.33376	0.256182	0.951193	0.626179	-0.12237	1.561832	-0.14346	-0.0988	-0.53008	2.373899	-0.23257	0.389771	1.14203	1.250506	2.528844	0	
77	-7.9787	-1.40568	1.64471	2.006492	-0.04735	0.176669	3.428328	-0.2938	2.873147	0.486798	2.080559	-1.15581	0.40638	1.794422	3.100979	4.763511	0	
78	-15.8016	-7.70583	-3.64155	-0.64462	-0.54763	-0.84886	-1.53918	-0.82065	-1.75098	-0.12011	-0.52638	-0.43496	-0.42393	-1.62998	-0.75246	-0.00308	0	
79	-15.8555	-7.25304	-3.94133	-1.26961	-0.57668	-1.16723	-1.88558	-1.21411	-1.78589	-0.83065	-0.70642	0.122725	-0.36146	-1.21273	-0.37487	-0.0409	0	
80	20.25329	14.56187	16.52581	-10.3412	32.40716	81.07596	-5.72607	-3.01762	-0.67099	1.243483	-2.88153	-1.54896	0.078415	-0.07584	0.603836	0.072963	0	
81	-9.65461	-3.39308	-7.01298	-3.92337	0.55814	0.194021	0.340453	-0.40189	-0.39683	-1.41828	-3.97971	1.529768	-9.68514	-4.6904	-5.23021	-5.08848	0	
82	-12.8264	-3.46263	-2.65457	1.014161	0.717299	-0.21667	-0.93951	0.516147	-2.86594	1.050379	1.16663	-0.57474	2.345063	-0.9214	-0.84136	1.316092	0	
83	2.039339	7.768409	4.913223	-3.92987	3.665087	4.191735	5.688582	-1.13692	8.187171	-12.3891	11.0211	26.1039	13.06318	-0.76755	-5.71526	-4.02005	0	
84	-15.927	-7.91952	-3.72279	-0.78225	-0.52296	-0.88456	-1.68331	-0.61374	-2.28379	0.368503	-0.32445	-0.37544	-0.33129	-1.5048	-0.67112	0.608929	0	

5.3.3 Principal Component Analysis

Principal component analysis (PCA) is an unsupervised feature extraction and selection technique used to perform dimensionality reduction tasks to avoid overfitting [79]. It is used as an orthogonal transformation in explanatory data analysis and examining relationships between variables. Using PCA, we can find a linear projection of the extracted EMG data into a lower dimensional space by reducing the cumulative error and maximising the cumulative variance. PCA is an essential technique in electromyographic (EMG) signal classification because it can extract relevant information and minimise data dimensionality. It presents the following advantages in EMG signal classification. Firstly, PCA is a powerful technique to identify common temporal patterns in time series data sets, such as EMG signals. By capturing the key sources of variation in EMG data, PCA helps to understand the underlying patterns based on the signal features. Furthermore, PCA can reduce the dimensionality of EMG data in classification problems. EMG signals with high dimensionality are significant in size, making them difficult to properly analyse and classify effectively. When applied, the PCA technique can minimise the dimensionality of EMG data by converting it into a new dataset of orthogonal variables. This dimensionality reduction improves the efficiency and accuracy of classification with machine learning algorithms. Finally, PCA can enhance the speed and accuracy of the EMG shape recognition system. This will be useful in cases where patients' movement patterns must be distinguished from healthy control.

5.4 Classification Results

A cross-validation with stratified sampling was used for the classification problem. For each classifier, 80% of the gait cycle segments were used for training, while 20% was used for testing. A 10-fold cross-validation was applied to estimate the predictive performance of each class. This ensured that the overall performance variance was balanced for some test cases. With stratified cross-validation, each fold containing data is evenly presented. Performing multiple iterations of the cross-validation process of

the models, fits the training dataset well. The accuracy, sensitivity, and specificity are computed to evaluate the classifiers' performance.

Accuracy: Accuracy is an essential and widely used classification metric in measuring the ratio of correctly classified cases versus the total number of predictions made by a model. In classification problems, the accuracy measures a model's performance by calculating the correct prediction from all other predictions made. Accuracy is used as the simplest classification performance, and it is given by the equation (5.3) where TP =True Positive, TN = True Negative, FP= False Positive, and FN = False Negative.

$$Accuracy = \frac{TP+TN}{TP+FP+TN+FN} \quad \text{Eq. (5.3)}$$

Precision: It measures the ratio of true positive predictions to the total number of all positive predictions made by a model in a classification problem. It focuses on the quality of positive predictions, which is useful when the cost of false positive prediction is high. This is given by in equation (5.4),

$$Precision = \frac{TP}{TP+FP} \quad \text{Eq. (5.4)}$$

Recall (sensitivity): Recall measures the ratio of true positive predictions to the total number of true positives. It focuses on the model's ability to identify the positives, which is essential in cases where false negatives are high.

$$Recall = \frac{TP}{TP+FN} \quad \text{Eq. (5.5)}$$

Specificity: In machine learning, specificity is a metric that measures a classification model's performance to identify instances of the negative or true negative class correctly. Specificity helps evaluate the model's ability to accurately identify negative cases, which is essential in medical applications. In the context of EMG classification, it presents the ability of a classification model to identify a particular class accurately.

$$Specificity = \frac{TN}{FP+TN} \qquad \text{Eq. (5.6)}$$

A flow chart of a schematic diagram for the gait classification is illustrated in [Figure 5.5] indicating the various phases in the classification process.

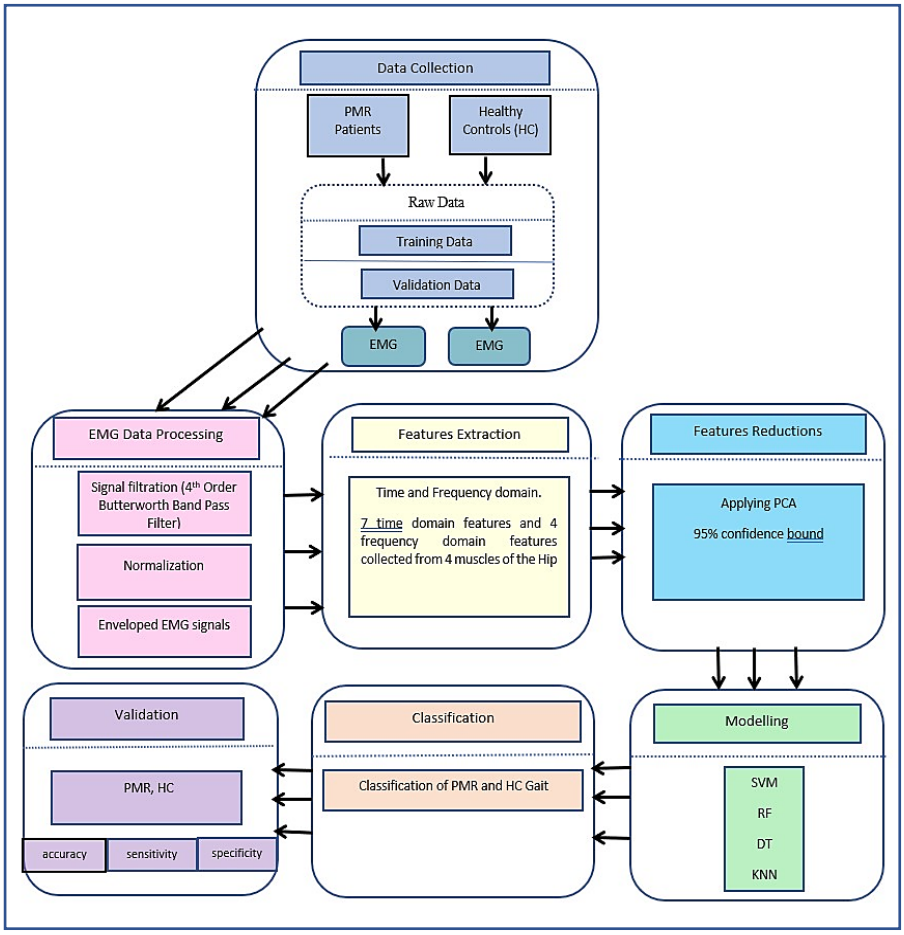

Figure 5. 4 Flowchart for classification process

5.4.1 Support Vector Machine

This first traditional model used for the movement classification is the Support Vector Machine (SVM). It is a non-probabilistic binary linear classifier which uses an optimal hyperplane to splits data points

from one class and those of other classes [80]. The SVM algorithm provides a higher speed and a better performance for classification of EMG signals. The algorithm is used as a multi-pattern recognition of gait segments of the recorded dataset. In SVM, when given a set of instances as mi and its categories as ni and ni ± 1, the splitting plane is given by <p, m> + c =0, where mi Rd and pi Rd are the normal vectors of the hyperplane. The optimal hyperplane ni (<p, mi > + C) > 1 is decided by minimising <p, p>/2. In the case of linear non-separable data, SVM uses soft edges to reduce the additional slack variables wi and penalty parameter D. SVM algorithm is therefore suitable for classifying the movement pattern of PMR patients against healthy control subjects. The classification results obtained for the SVM model are illustrated in Table 5.3 below. The performance of the algorithm for each of the activities is computed using the scikit-learn Python library.

Table 5. 3 SVM classifier results

Exercise	Accuracy	Precision	Recall	Specificity
Gait	85.0%	85.7%	85.7%	67.0%
Knee Lifting	70.0%	85.7%	75.0%	50.0%
Knee Extension	65.0%	64.2%	81.8%	44.4%

The confusion matrix plots help gain insight into the classifier's performance and visualise the results. This is essential for the EMG dataset, where there was a significant class imbalance in the data between PMR patients and healthy controls. The confusion matrices were plotted for each of the exercises performed. The confusion matrix is indexed as 0 for healthy control subjects and 1 for PMR patients. From the confusion matrix plots in [Figures 5.5,5.6 and 5.7] demonstrates the actual predicted class and the misclassified class in the gait, knee lifting, and knee extension exercises respectively.

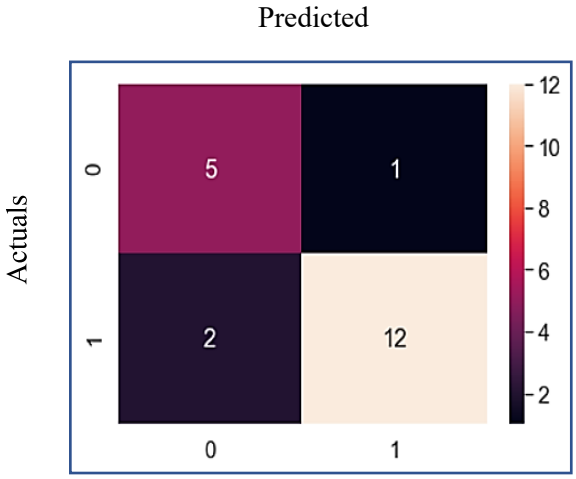

Figure 5. 5 SVM classifier confusion matrix for gait exercise

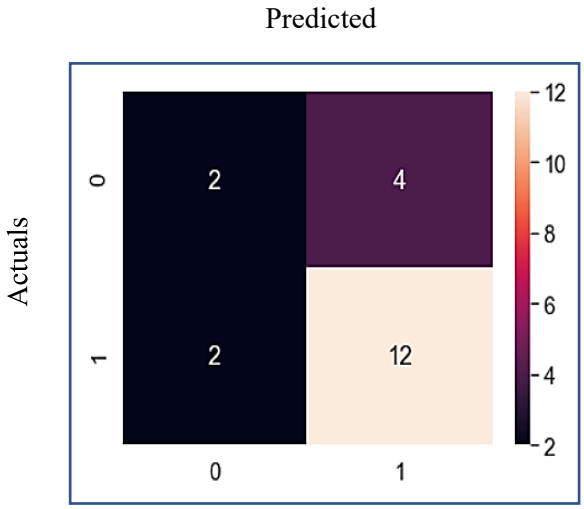

Figure 5. 6 SVM classifier confusion matrix for knee lifting exercise.

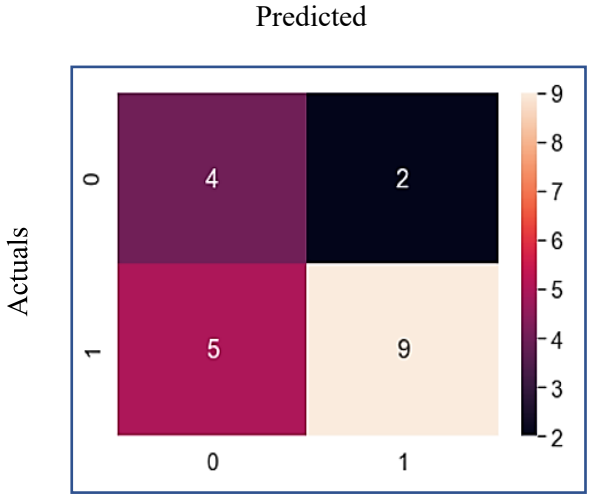

Figure 5. 7 SVM classifier confusion matrix for knee extension exercise.

The classification results in Table 5.4 using the SVM algorithm have an accuracy of 85% for the gait exercise. This indicates the SVM classifier had an accuracy of 85% to discriminate the gait pattern between PMR patients (true positive) and healthy controls (true negative). The precision recorded for the classifier is 85.7%, with a recall of 86%. The precision score of 85.7% indicates the actual positive outcome from all positive predictions for the two groups, which are patients and healthy controls. A recall of 86% recorded by the SVM models indicates the accurate positive prediction from all the actual positive values. In terms of specificity, 67% is recorded using the SVM classifier to correctly predict the true negatives of the two categories: patients and healthy controls. For the knee lifting exercise, an accuracy of 70% is recorded as the true positive correct predictions from all the predictions for the two categories. A precision of 85% is recorded by the SVM model for the true positives correctly predicted out of all positive predictions made. A recall of 75% is recorded for this model in the knee lifting exercise and a specificity of 50%. This means 75% is recorded as a true positive prediction for the movement pattern in the knee lifting exercise for patients and healthy controls out of all the positive values. Regarding specificity, 50% is recorded by the SVM model to predict actual negative values in the two groups. For the knee extension exercise, an accuracy of 65% is recorded with a precision of 64.2%, which shows the advantage of the SVM classifier to correctly predict the true positive and true negative from the two categories out of all predictions made. Regarding recall, 81.8% is recorded as the true positive prediction from all the actual positive values of the two groups. A specificity of 44.4% is recorded with the SVM model in the knee extension exercise.

5.4.2 K-Nearest Neighbour

The second traditional model used for the classification was K-Nearest Neighbour. It is a nonparametric classification algorithm whereby each member of a validation case is given a class label based on the voting power of the ‘K’ nearest neighbours determined by distance measure. The classifier is based on the distance function, such as the Euclidean distance for a given EMG dataset. The Euclidean distance

metric is given by $D(x, y) = \sqrt{(x - y)\, T\, (x - y)}$, which is a selected neighbourhood where a group membership is based on a single closest neighbour. The algorithm finds the distance between a query data point and a specified number of data points most comparable to the query data, then classifies the query based on its popularity class among its K nearest neighbours. The distance between the new data points and each in the training data set is then calculated. This includes applying a chosen distance metric to measure the difference between feature vectors. In determining K nearest neighbours, K case with the smallest distance is selected as the new data point closer to K neighbours. The classification of the movement pattern determines the majority class among the K neighbours. The unique data point is then assigned the most frequent class label among its K nearest neighbours. When predicting outcomes for new data points in KNN, the choice of how many nearest neighbors to consider is crucial. This parameter determines the radius of the neighbourhood surrounding each data point and greatly influences the model's accuracy. Using a smaller value for K results in more adaptable decision boundaries. In this case, K was set to 2, meaning the two closest neighbors were consulted during classification. Adjusting this parameter helps fine-tune the performance of KNN for classification tasks. Hence, the number of nearest neighbors is a critical factor in optimizing the KNN model's effectiveness.

In the training phase, the KNN model learns the data by storing feature vectors and the corresponding labels. The performance of the KNN model in predicting the actual class for the three movement activities is illustrated in Table 5.4 below.

Table 5. 4 KNN classifier results

Exercise	Accuracy	Precision	Recall	Specificity
Gait	75.0%	78.75%	79.0%	67.0%
Knee Lifting	70.0%	85.7%	75.0%	50.0%
Knee Extension	55.0%	50.0%	77.7%	36.4%

The confusion matrix obtained by the KNN model are illustrated in [Fig 5.8, 5.9 and 5.10] indicating the gait, knee lifting and knee extension respectively.

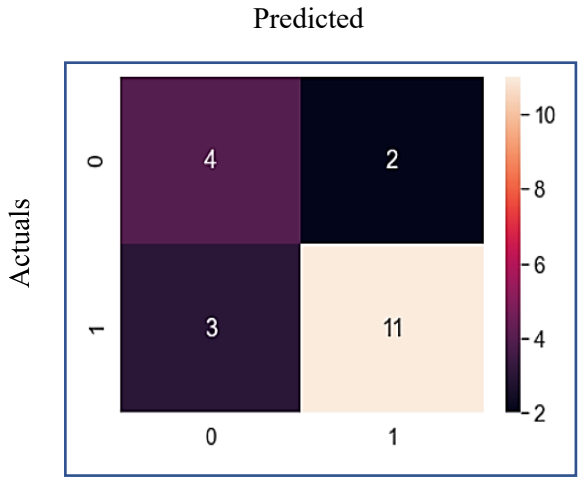

Figure 5. 8 DT classifier confusion matrix for gait exercise

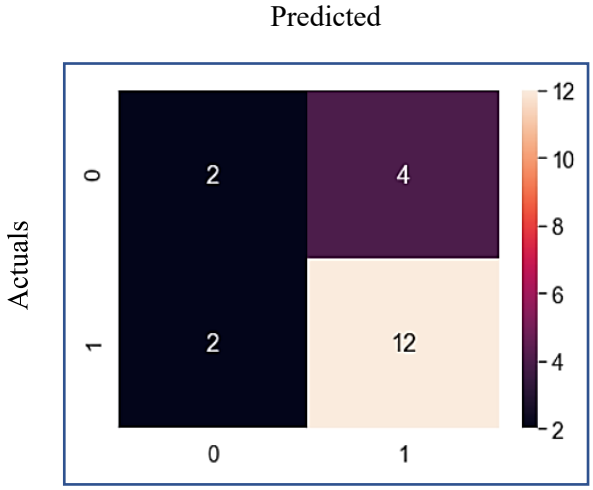

Figure 5. 9 DT classifier confusion matrix for knee lifting exercise.

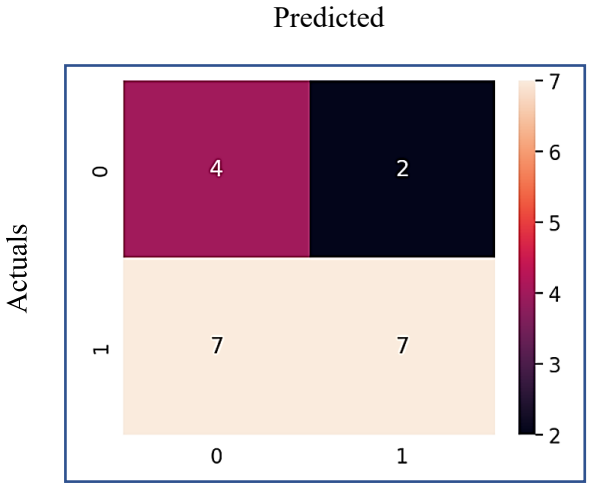

Figure 5. 10 DT classifier confusion matrix for gait exercise

From Table 5.4, the classification results using the KNN model have an accuracy of 75% recorded for gait exercise. A precision of 78.57% is recorded as the accurate positive prediction from all the positive predictions in discriminating the gait pattern between patients and healthy controls. The recall and specificity are 79% and 67% for gait exercises using the KNN model. This indicates 79% is recorded as the true positive predictions, that is, patients and healthy controls from all the actual positive values. Regarding the knee lifting exercise, an accuracy of 70% is recorded with the KNN model. This shows the model scores 70% of true positives (PMR patients) and true negatives (healthy controls) from all the predictions made in the two groups. A precision of 85.7% is recorded with the KNN model for the knee lifting exercise, indicating the correctly predicted movement pattern for patients and healthy controls. The values recorded were 75% and 50% for recall and specificity, respectively. This means the model scores 75% for the true positives out of all the actual positive values recorded with the KNN model. In terms of the knee extension exercise, an accuracy of 55% is recorded in discriminating the movement pattern between PMR patients and healthy controls. A precision of 50.0% is recorded, with a recall of 77.7% with the KNN model for the knee extension exercise. This indicates that the accurate positive prediction is 50.0% out of all the positive predictions made with the model. A specificity of 36.4% is recorded, which indicates the performance of the model to accurately predict the true negatives for each of the two groups.

5.4.3 Decision Tree

The third traditional model used in the classification was the decision tree (DT). The DT is an effective algorithm used in extracted feature classification in the form of a tree structure. It works by recursively partitioning the dataset into smaller subdivisions of branches and nodes. The classier interactively determines the nonlinear relationship between system inputs and outputs, which is used in classifying two different responses. The partitioning from each branch is seen to be identical after the splitting process. The subset belongs to the same class where the algorithm proceeds recursively [81]. This model can be easily implemented, and it is also quite robust to identify and handle outliers.

5.4.3.1 Decision Splitting Process

The decision tree can be used to predict the class of any given dataset from the tree's root node. The algorithm compares the values of the root attribute with the record attribute, and then, based on the comparison, it follows the branch and jumps to the next node. The algorithm starts from the root through to the tree node, where it compares the root values attributed to the records in the dataset. The decision tree classifier is illustrated in the figure below in [Fig 5.11]. The decision tree classifier provides a graphical representation of a model, making predictions based on the likely outcome of an event. The tree structure is made up of decision nodes, chance nodes, and the end node points. This is used to predict the movement pattern based on the two groups. The key parameters used in decision trees for classification include the maximum depth and sample split. DT can consider a subset of features when making a split at each node. This parameter controls the maximum number of features to consider for the best split in the classification. The maximum depth parameter controls the maximum depth of the decision tree and captures the complex relationships in the EMG dataset. A maximum depth helps to prevent overfitting and performance. The minimum samples split parameter specifies the minimum number of samples required to split an internal node.

In the classification process, the dataset is divided into different levels of depth based on these parameters. For example, in this case, the dataset was split into four (4) levels of depth. The depth of the decision tree is a critical hyperparameter that requires careful tuning to achieve optimal performance. By fine-tuning this parameter, we can optimize the model for EMG classification, allowing us to effectively discern the correlation between muscle activity and a specific condition. This splitting process is fundamental to decision tree classifiers, as it determines how the model partitions the data to make accurate predictions.

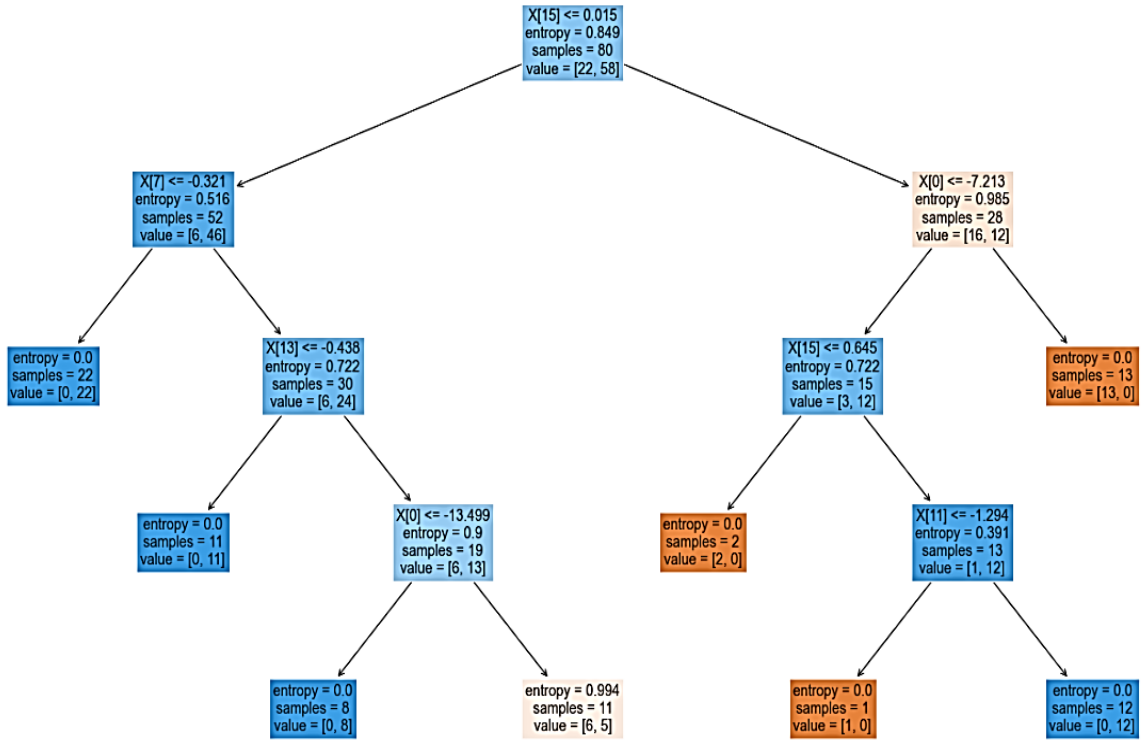

Figure 5. 11 DT classifier tree

The classification results obtained with the decision tree classifier is illustrated in Table 5.5 for the movement classification.

Table 5. 5 DT classifier results

Exercise	Accuracy	Precision	Recall	Specificity
Gait	70.0%	64.3%	90.0%	50.0%
Knee Lifting	60.0%	57.1%	80.0%	40.0%
Knee Extension	55.0%	71.4%	66.7%	20.0%

The confusion matrix obtained using the DT classifier in the predicting the true class for each exercise conducted is illustrated in [Figures 5.12, 5.13 and 5.14] below for the gait, knee lifting and knee extension respectively.

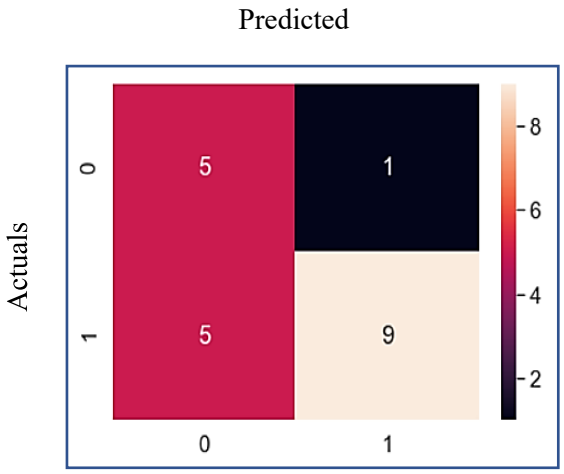

Figure 5. 12 DT classifier confusion matrix for gait exercise

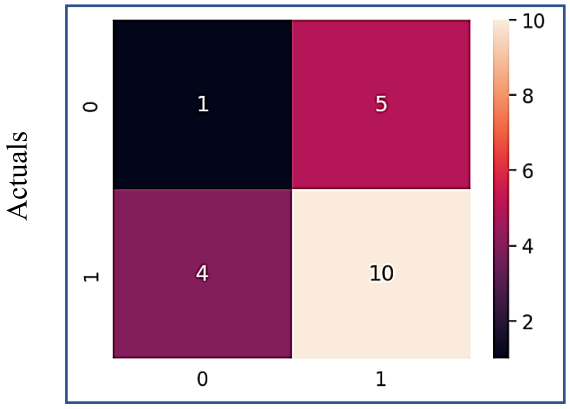

Figure 5. 13 DT classifier confusion matrix for knee lifting exercise.

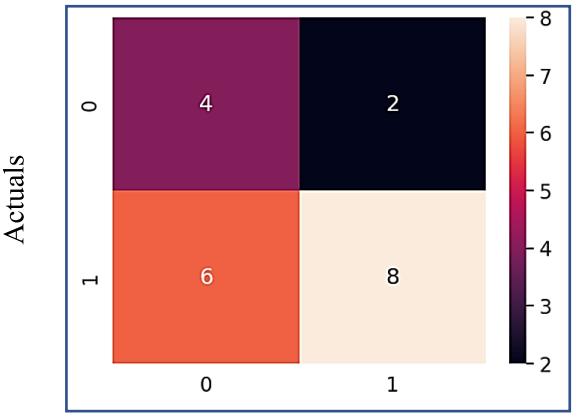

Figure 5. 14 DT classifier confusion matrix for knee extension exercise

For the decision tree algorithm, an accuracy of 70% is recorded in discriminating the gait pattern between patients and healthy controls. The precision and recall scores for the gait exercise are 64.3 and 90%, respectively. This indicates that the DT model scored 64.3% to correctly predict all positive predictions from the two categories. A specificity of 50.0% is recorded, indicating the DT model's ability to predict true positives from the two groups correctly. In terms of the knee lifting exercise, an accuracy of 60% is recorded using the DT model. This indicates that the model correctly predicted most true positives (patients) and true negatives (healthy controls) knee lifting movement patterns from all the predictions by the DT classifier. The precision recorded with the DT model in the knee lifting exercise is 57.1%, indicating the true positive correct prediction out of all positive predictions made in the two groups. The recall and specificity recorded are 80% and 40% for the knee lifting exercise conducted by participants using this classifier. When it comes to the knee extension exercise, the accuracy recorded is 55%, which indicates the true positive (patients) and true negative (healthy control) were correctly predicted from all the predictions made. The precision and recall recorded are 71.4% and 66.0%, respectively, with the DT model. This shows that a precision score of 71.4% of the true positives is correctly predicted out of all the positive predictions made by the model. A recall of 66.0% indicates a measure of the true positives correctly predicted out of all the actual positive values. A specificity of 20.0% is recorded in the knee extension exercise.

5.4.4 Rotation Forest

The Rotation Forest (RF) algorithm is used for generating classifiers ensembles based on feature extraction. It is like the random forest but has an advantage in addressing some challenges of random forest algorithms. RF can achieve better performance in classification problems with a smaller number of trees compared to random forests. With this classier similarly to bagging, bootstrap samples are taken as training sets for individual classification. The Rotation Forest model is an ensemble technique designed to improve the performance of classification tasks. It is particularly effective when dealing with high-dimensional data sets and this can improve of underlying classifiers. The idea behind Rotation

Forest is to introduce diversity into the whole by rotating the featured space. For each base classifier in the ensemble, a random subset of features is selected and the entire dataset. This rotation is performed to remove correlation between base classifiers and introduce variability. After rotating the dataset, the base classifier is usually a decision tree which is modified dataset. The process of feature selection, rotation, and classifier training is then repeated for each base classifier. In making predictions about new cases, each base classifier in the ensemble contributes its prediction is decided through the ensemble method. The confusion matrices obtained from the rotation forest classifier is illustrated in [Figures 5.15,5.16 and 5.15] for the gait, knee lifting and knee extension respectively.

Table 5. 6 RF classifier results

Exercise	Accuracy	Precision	Recall	Specificity
Gait	80.0%	85.7%	85.7%	66.7%
Knee Lifting	65.0%	85.7%	70.6%	33.3%
Knee Extension	70.0%	71.4%	83.3%	66.7%

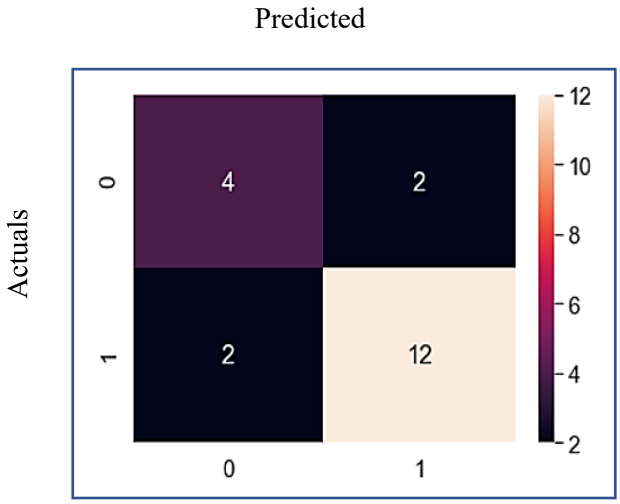

Figure 5. 15 RF classifier confusion matrix for gait exercise

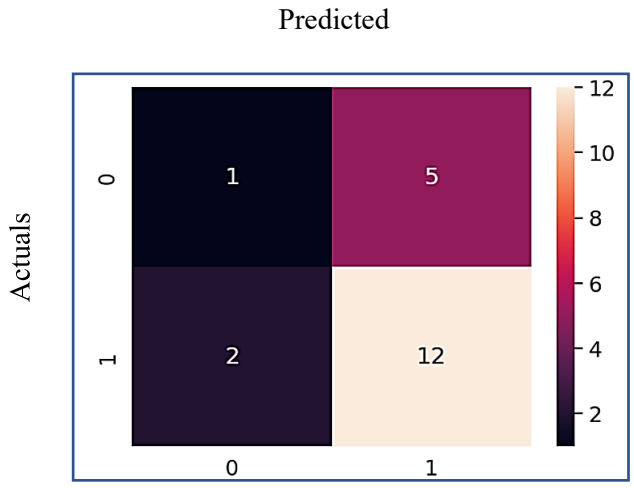

Figure 5. 16 RF classifier confusion matrix for gait exercise

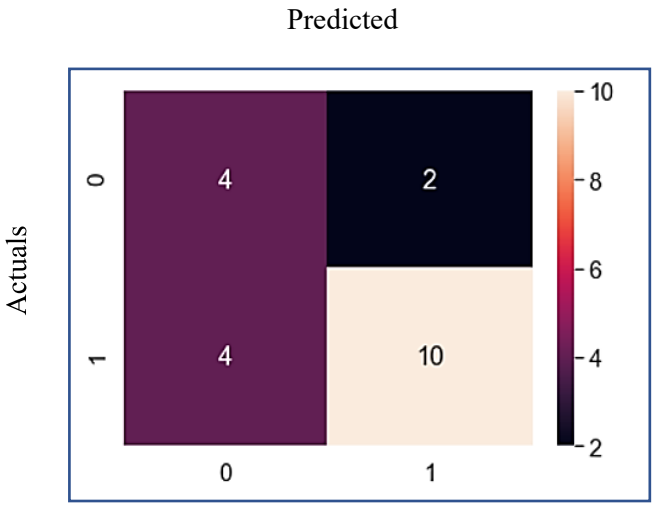

Figure 5. 17 RF classifier confusion matrix for gait exercise

In Table 5.4, the rotation forest classifier has an accuracy of 80% in discriminating the gait pattern between PMR patients and healthy controls. This indicates that the model can correctly predict the gait pattern of PMR patients and healthy controls from all the predictions made. A precision score of 85.7% measures a count of the true positives predicted correctly out of all the positive predictions by the RF model. The recall and specificity measured were 85.7% and 66.7%, respectively. Regarding knee lifting exercises, an accuracy of 65% is recorded with a precision of 85.7%. This shows the performance score of 65% of the model to accurately predict the knee lifting movement pattern for true positives (patients) and true negatives (healthy control). A recall score of 70.6% measures the performance of the rotation forest model to record the true positives from all the actual positives. A specificity of 33.3% is recorded

in knee lifting exercises, indicating the performance of the RF model to predict true negatives from the two categories correctly. For the knee extension exercise, an accuracy of 70% is recorded, which shows the ability of the RF model to correctly predict the movement pattern of patients and healthy control subjects. The precision score of 71.4% shows the model's performance in correctly predicting the true positives from all the positive predictions by the model. The recall and specificity recorded are 83.3% and 66.7%, respectively. This shows that a recall of 83.3% correctly predicts the true positives from the actual positive values recorded.

5.4.5 Overcoming Challenges with Mahine learning Models in Classification

Traditional machine learning models face some challenges when applied to EMG signal classification. These challenges arise due to the unique characteristics of EMG data and the requirements for accurate classification. Here are some common challenges that were encountered in the EMG classification.

High Dimensionality: EMG signals are typically recorded using multiple electrodes, resulting in high-dimensional feature spaces. Traditional models may struggle to handle this high dimensionality efficiently. Techniques such as PCA were used to reduce the dimensionality of the feature space while retaining relevant information for classification. This helps in improving computational efficiency and reducing the risk of overfitting.

Non-linearity and Complex Relationships: EMG signals often exhibit non-linear relationships between features, making it challenging for linear models to capture these complexities effectively. Non-linear models such as decision trees, random forests, support vector machines, and neural networks can better capture the non-linear relationships present in EMG data. EMG signals are inherently time-series data and traditional models. Deep Models specifically designed for time-series analysis, such as recurrent neural networks (RNNs) or Long Short-Term Memory (LSTM) networks, can effectively capture temporal dependencies and improve classification accuracy. Addressing these challenges requires a combination of preprocessing techniques, appropriate model selection, and careful tuning of

hyperparameters. By leveraging these strategies, traditional machine learning models can be effectively applied to EMG signal classification tasks with improved accuracy and robustness.

5.5 Automation of EMG Signal for Movement Pattern

Table 3 presents notable changes in peak muscle activity observed in the EMG signals of patients, which can be attributed to factors such as muscle fatigue and reduced functional capacity. Understanding muscle function throughout the gait cycle largely depends on identifying the beginning and end points of EMG signals. Typically, the muscle activity during the gait cycle follows distinct phases, including a peak (onset) and a trough (offset). The EMG plot in Table 3(a) reveals that patients exhibit delays in both the onset and early offset of muscle activation compared to healthy individuals. This means that patients experience a lag in the activation peak and the subsequent decline of muscle activity relative to the gait cycle. Such deviations in timing can lead to differences in the muscle activation patterns between patients and healthy controls. These timing differences in the EMG signals point to altered hip muscle activation patterns in patients, potentially resulting from factors like muscle weakness, joint stiffness, and disease-related pain. The delayed onset and early offset of muscle activation could be a compensatory mechanism to mitigate muscle weakness or fatigue during movement. Furthermore, Table 3 shows irregularities in the onset and offset patterns of muscle activation in patients compared to healthy controls. These irregularities likely stem from disrupted coordination and sequence of muscle activation during the gait cycle. Such irregular muscle activation patterns, including prolonged activation relative to the gait cycle, may contribute to these discrepancies.

EMG Signal from Muscle	Patients	Healthy Control Subjects
(a) Onset and Offset	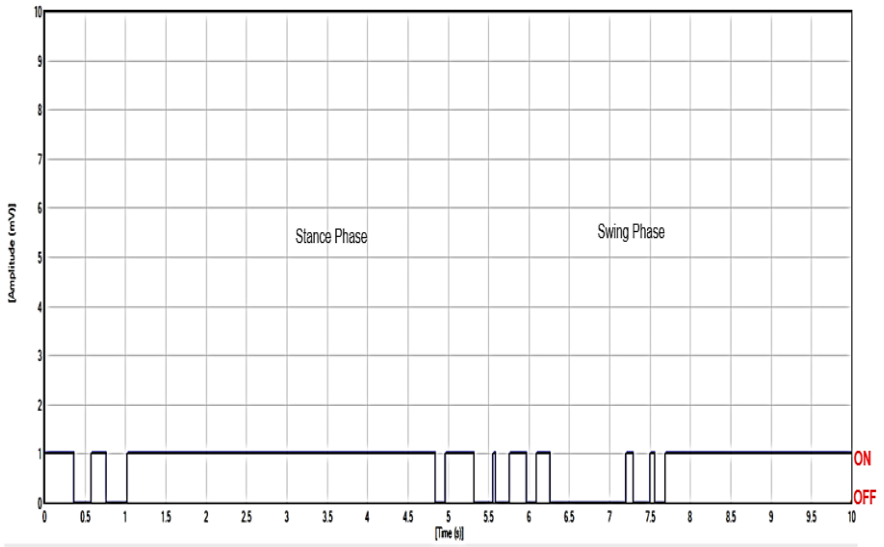	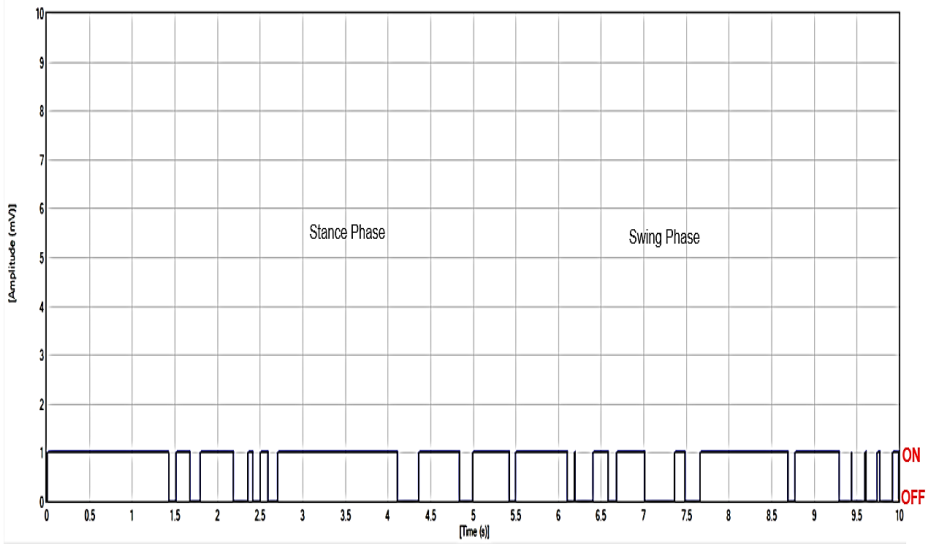

b) RF	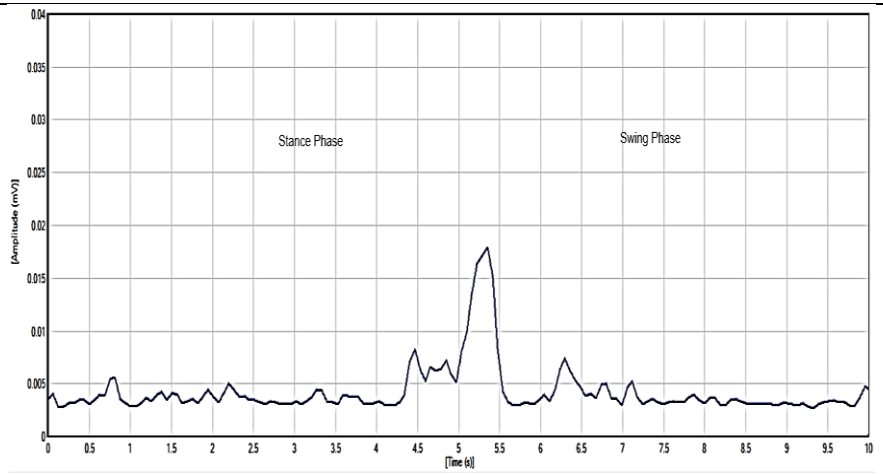 Stance Phase Swing Phase [Amplitude (mV)] [Time (s)]	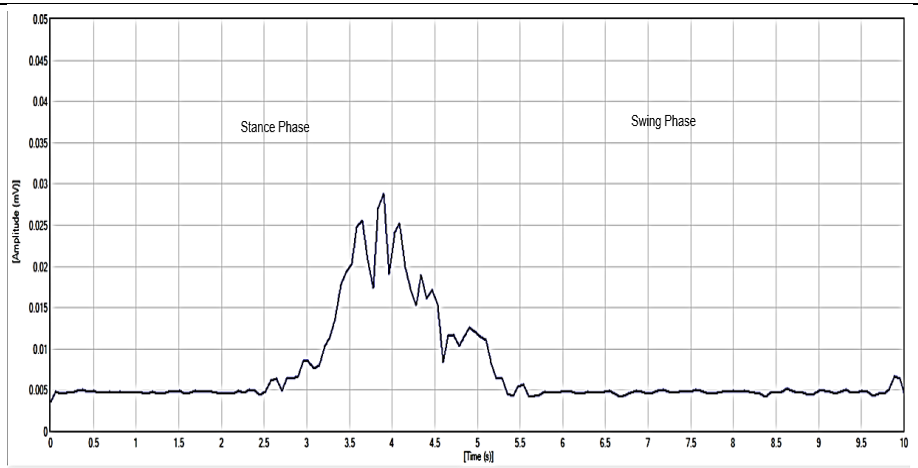 Stance Phase Swing Phase [Amplitude (mV)] [Time (s)]
c) VL	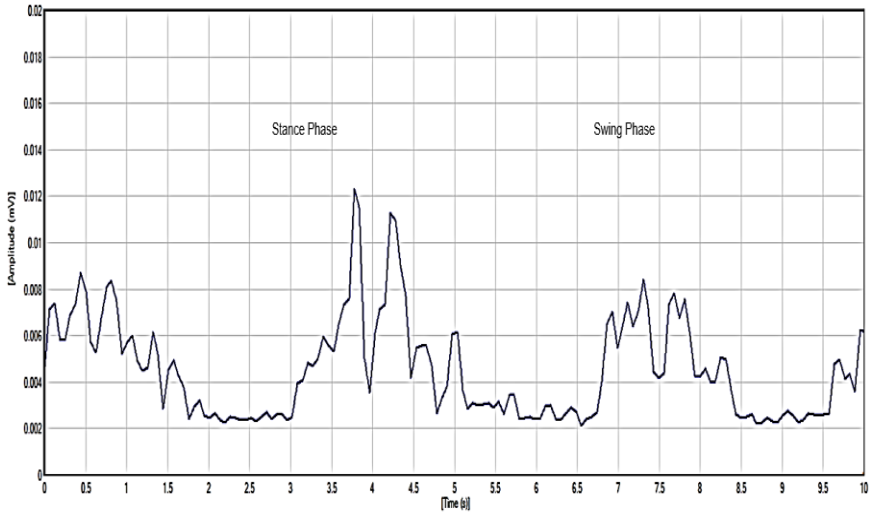 Stance Phase Swing Phase [Amplitude (mV)] [Time (s)]	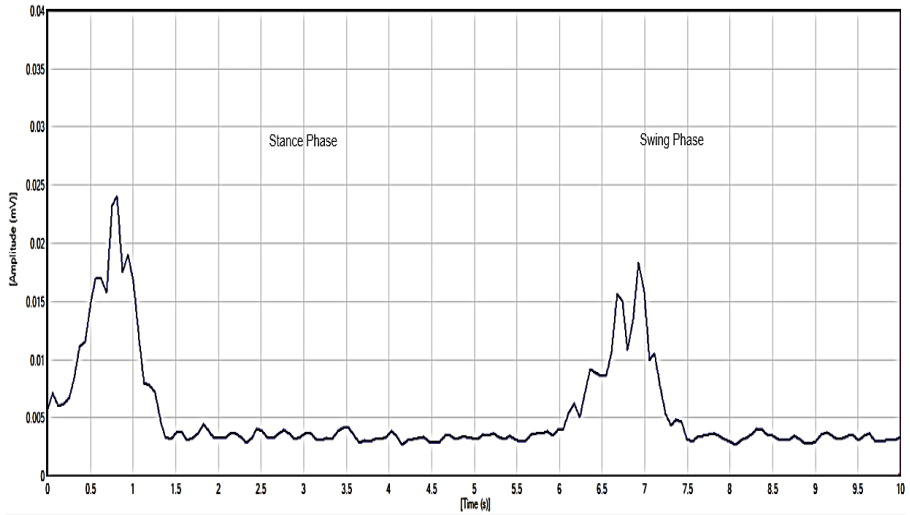 Stance Phase Swing Phase [Amplitude (mV)] [Time (s)]

d) BF	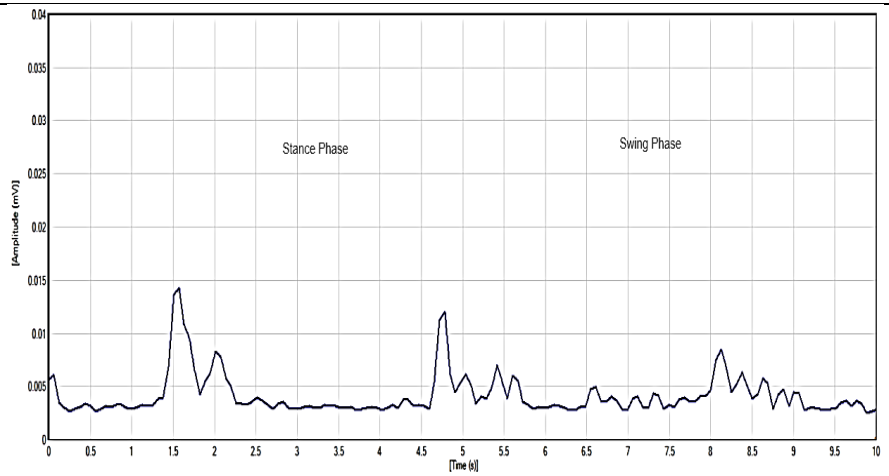 Stance Phase Swing Phase [Amplitude (mV)] [Time (s)]	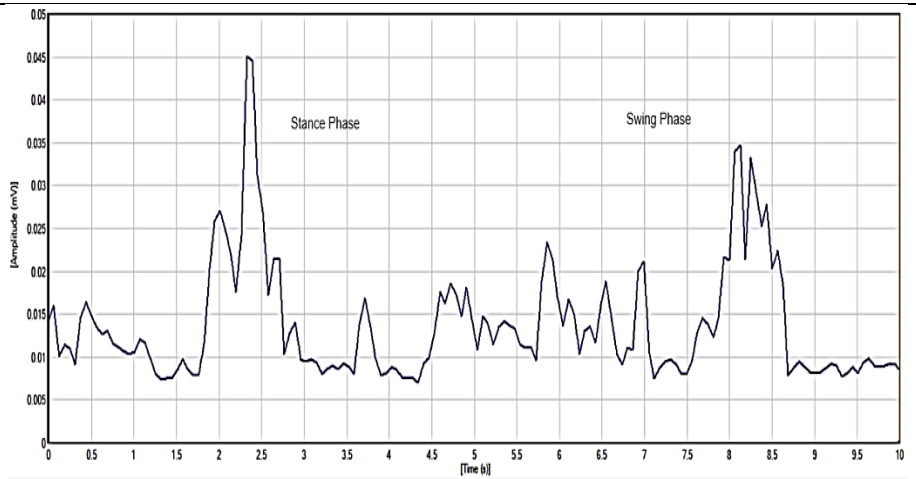 Stance Phase Swing Phase [Amplitude (mV)] [Time (s)]
e) SE	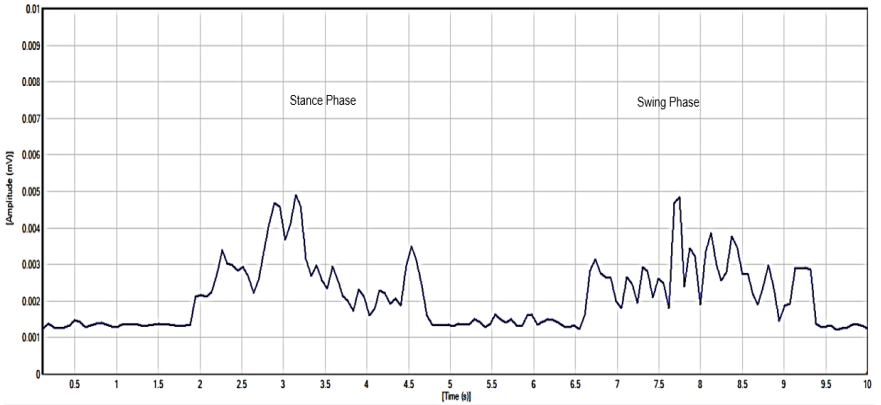 Stance Phase Swing Phase [Amplitude (mV)] [Time (s)]	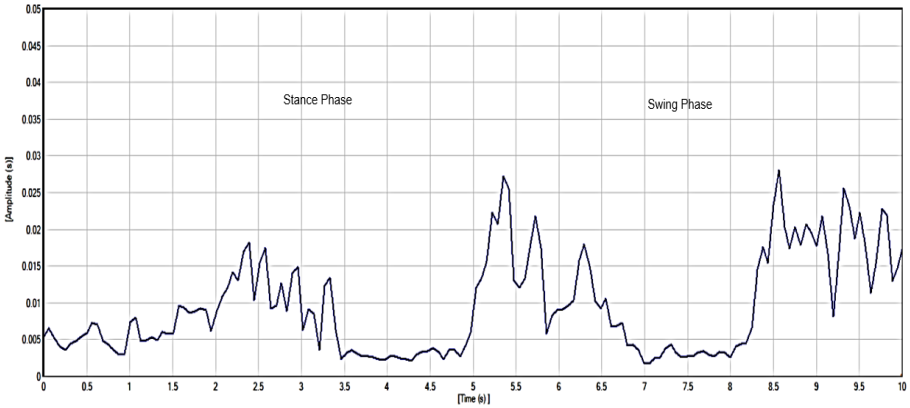 Stance Phase Swing Phase [Amplitude (mV)] [Time (s)]

In this study, a line plot was used to visualize movement patterns by analyzing a DataFrame containing two groups: patients and healthy control subjects. The line plot was generated using matplotlib in Python and represents muscle activation levels based on the DataFrame subsets. Each legend in the plot corresponds to a row in the DataFrame, showing the amplitude of EMG values for each group's movement patterns. For patients' gait patterns, Figure 5.18 displays lower muscle activation amplitudes compared to healthy control subjects. This figure illustrates changes in muscle activation over time for patients. Figure 5.19, on the other hand, represents muscle activation channels characterizing the movement patterns of healthy control subjects. Each legend or channel in the plot represents muscle activation levels from the data frame. For instance, a brown legend indicates hip muscle activation for specific patients with a peak of 250 millivolts that decreases over time. Other legends show activation levels ranging from 10-25 millivolts, fluctuating over timestamps, reflecting patient movement patterns.

Comparing the plots of the two groups reveals that patients exhibit altered muscle activation patterns during the gait cycle compared to healthy control subjects. Due to the challenge of visually distinguishing between normal and impaired movements, this automated approach is crucial for differentiating between the two groups. Figure 5.18 displays the automated EMG gait pattern for patients, while Figure 5.19 shows patterns for healthy control subjects. These visualizations highlight that patients' movement patterns differ from those of healthy individuals, indicating altered movement patterns in patients compared to controls.

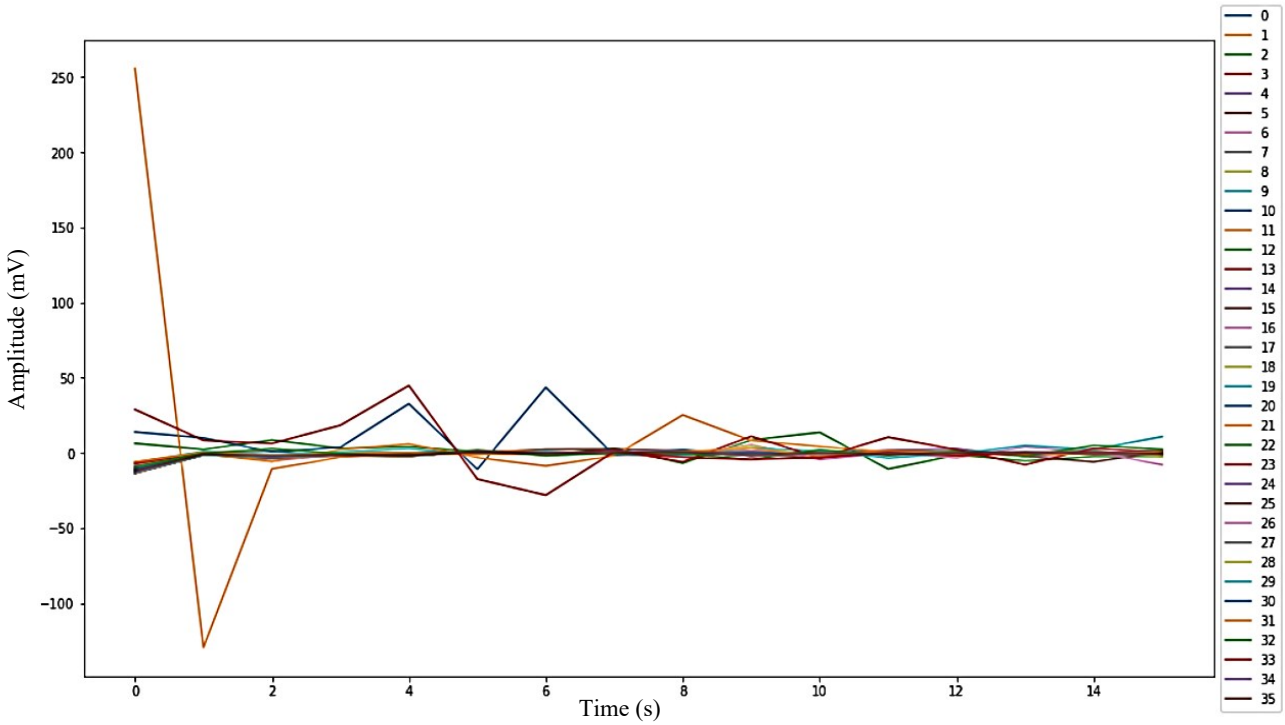

Figure 5. 18 Patients gait pattern.

The plot in Figure 5.18 displays a gait pattern with initially high amplitude values that decrease over time. In this plot, the x-axis represents the time in seconds for the gait cycle, while the y-axis shows the amplitude in millivolts. This plot illustrates how muscle activation patterns change over time for patients. The legends in Figure 5.18 correspond to channels of muscle activation levels that define the movement patterns of individual patients. These legends help automate the movement analysis for healthy control subjects as well. In Figure 5.19, for healthy control subjects, peak muscle activation levels reach up to 240 millivolts before sharply declining. The legends in this figure show a range of 20-50 millivolts, indicating oscillations in hip muscle activation over timestamps. As time passes, the muscle activation patterns change, reflecting the movement patterns of the individuals. The gait pattern for healthy control subjects for the exercise is depicted in Figure 5.19.

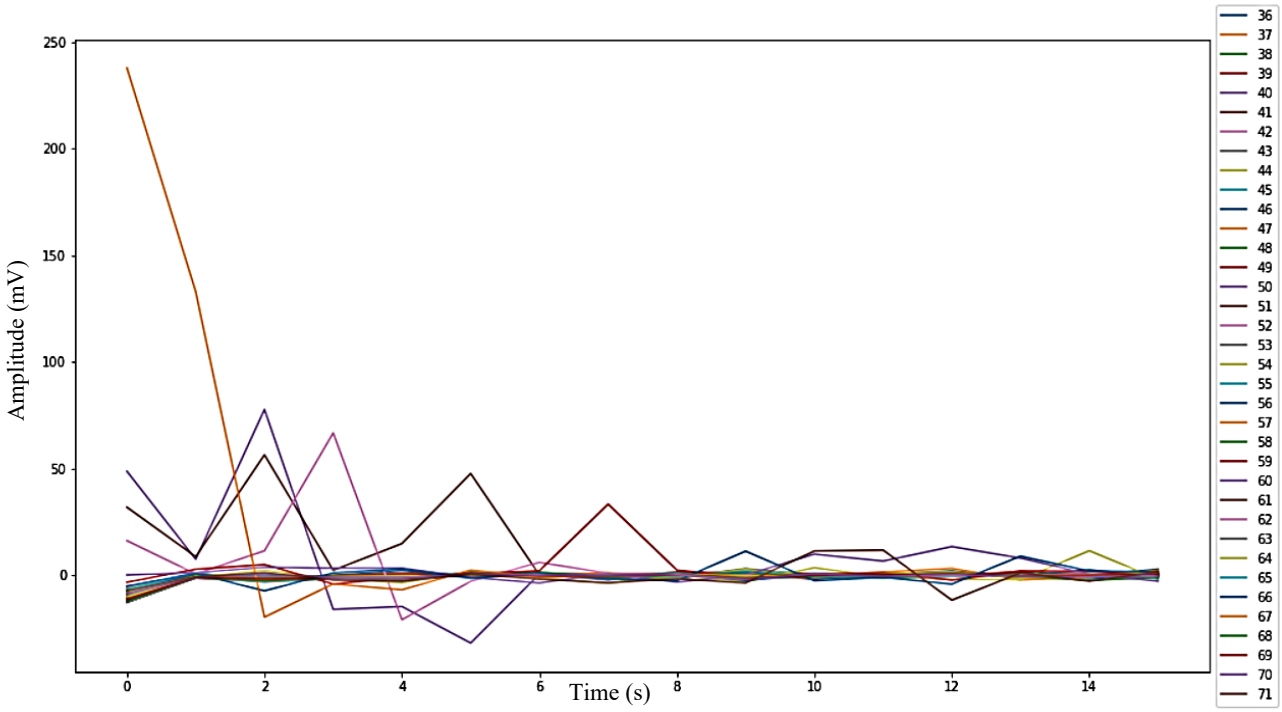

Figure 5. 19 Healthy Control subjects gait pattern.

The plots in Figures 5.20 and 5.21 depict muscle activation patterns during the knee lifting exercise for patients and healthy control subjects, respectively. Each legend in the plots corresponds to a muscle activation level channel from the DataFrame used to automate the movement analysis for the knee lifting exercise in patients.

In Figure 5.20, for patients, the legends show activation levels ranging from 10 to 30 millivolts, indicating oscillations in muscle activation over time. These lower amplitudes suggest weaker muscle contractions in patients compared to healthy control subjects.

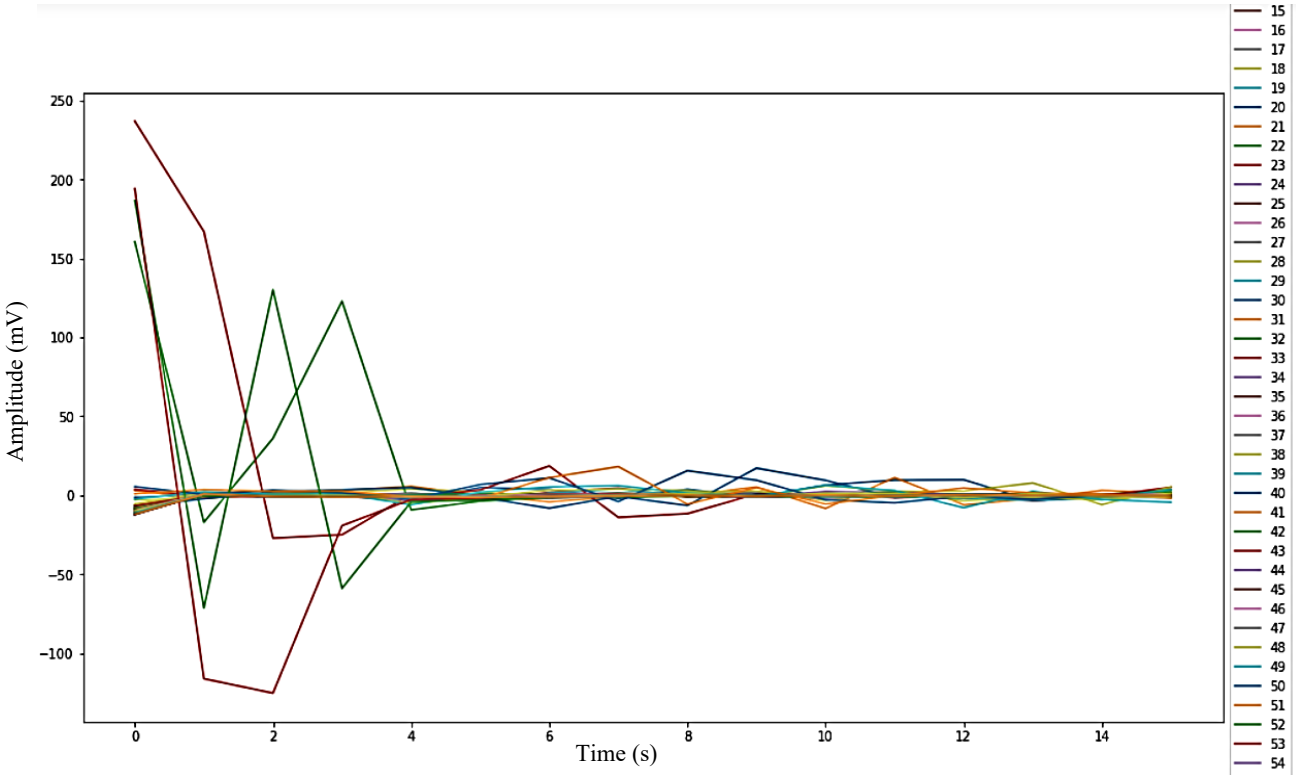

Figure 5. 20 PMR Patients knee lifting pattern.

In Figure 5.21, the brown and green legends represent muscle activation patterns of some healthy control subjects, peaking at 240 and 200 millivolts respectively, followed by a rapid decline over time. Other legends in this figure range from 20 to 50 millivolts, showing oscillations in muscle activation levels over timestamps. The legends indicate that healthy control subjects generally exhibit higher muscle activation amplitudes, which gradually decrease over time during the knee lifting exercise. Some legends for healthy control subjects show higher initial amplitudes that decline over time, indicating stronger muscle contractions with a gradual decrease. Overall, the muscle activation levels in patients shown in Figure 5.20 are lower compared to those in healthy control subjects depicted in Figure 5.21.

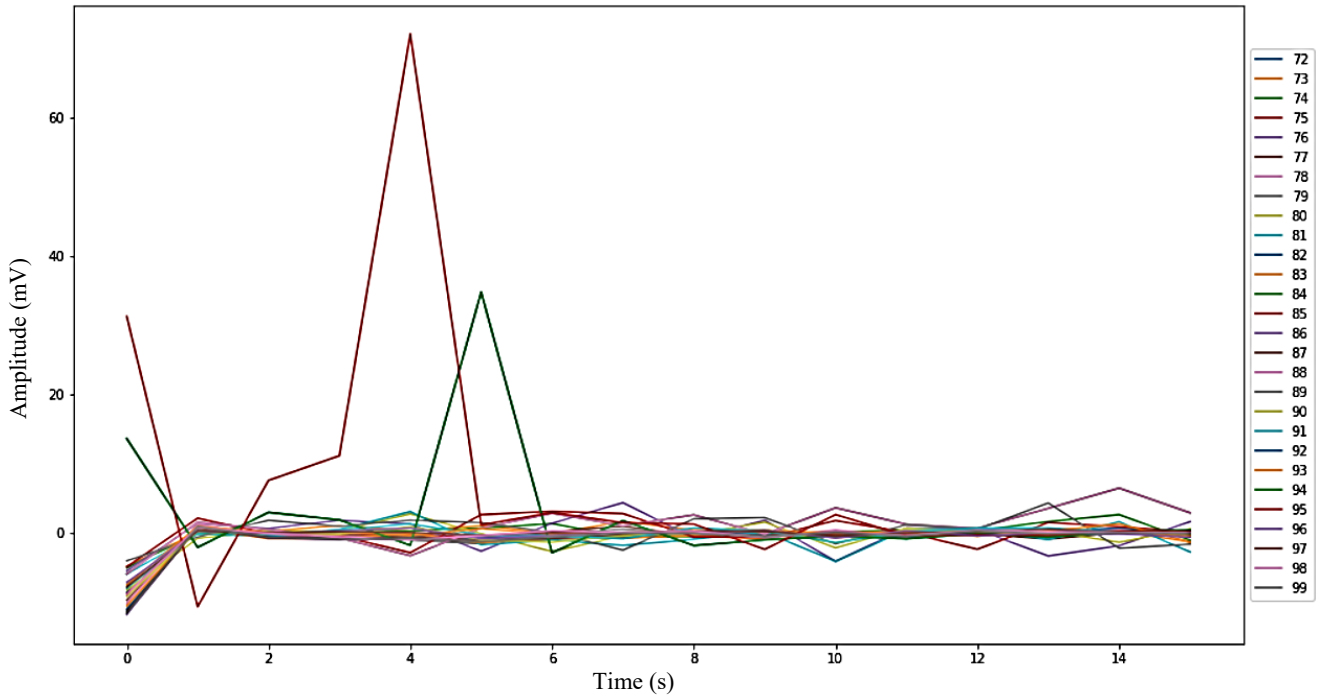

Figure 5. 21 Healthy control subjects lifting pattern.

For the knee extension exercise in [Fig 5.22], the plot in each legend shows the muscle activation levels for patients differ from that of healthy control subjects in [Fig 5.23]. The muscle activation pattern for patients has a lower amplitude, illustrated in the plots, which falls gradually over time in the movement pattern. The different legends on the plots represent the muscle activation channel levels for each muscle recorded in knee extension exercise. For the patients, the knee activation is illustrated in [Fig 5.23] indicating the muscle activation levels.

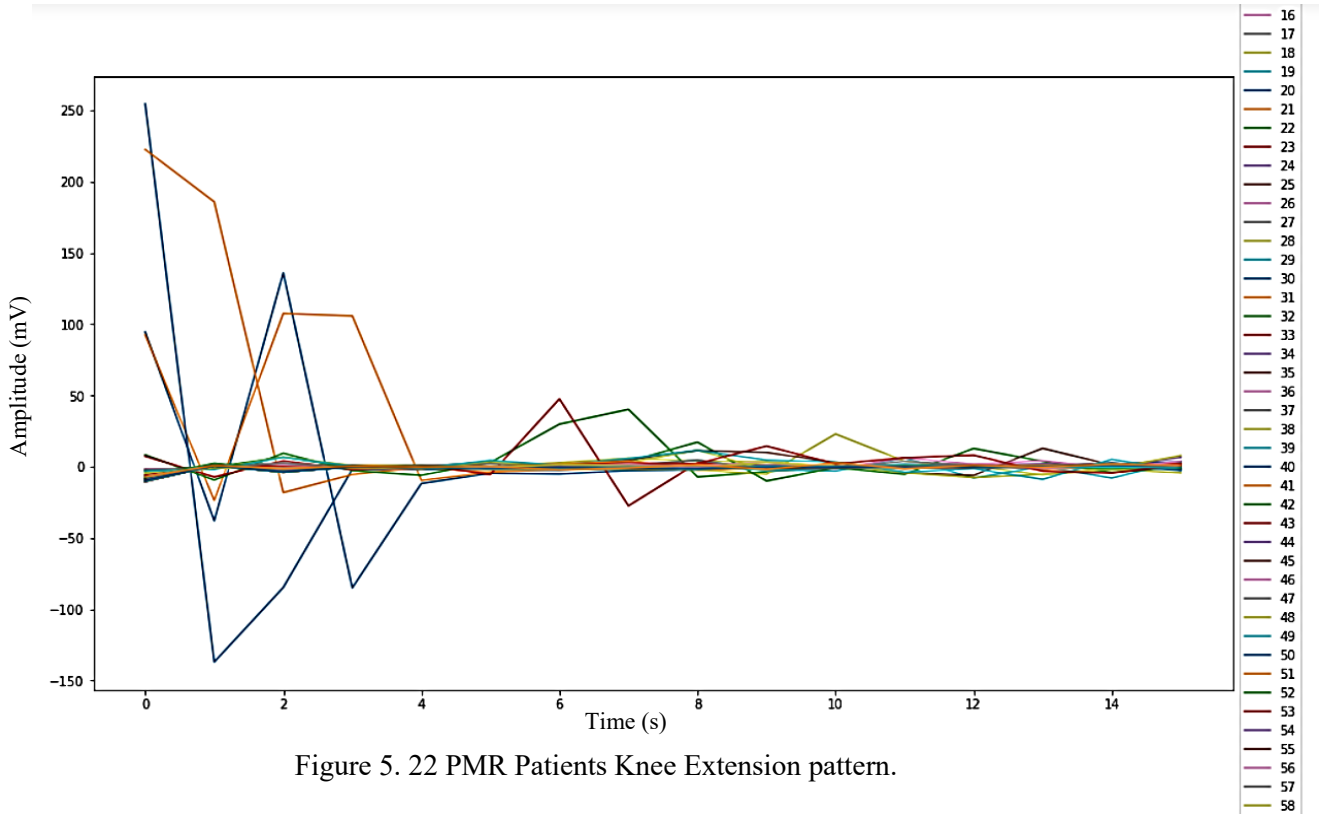

Figure 5. 22 PMR Patients Knee Extension pattern.

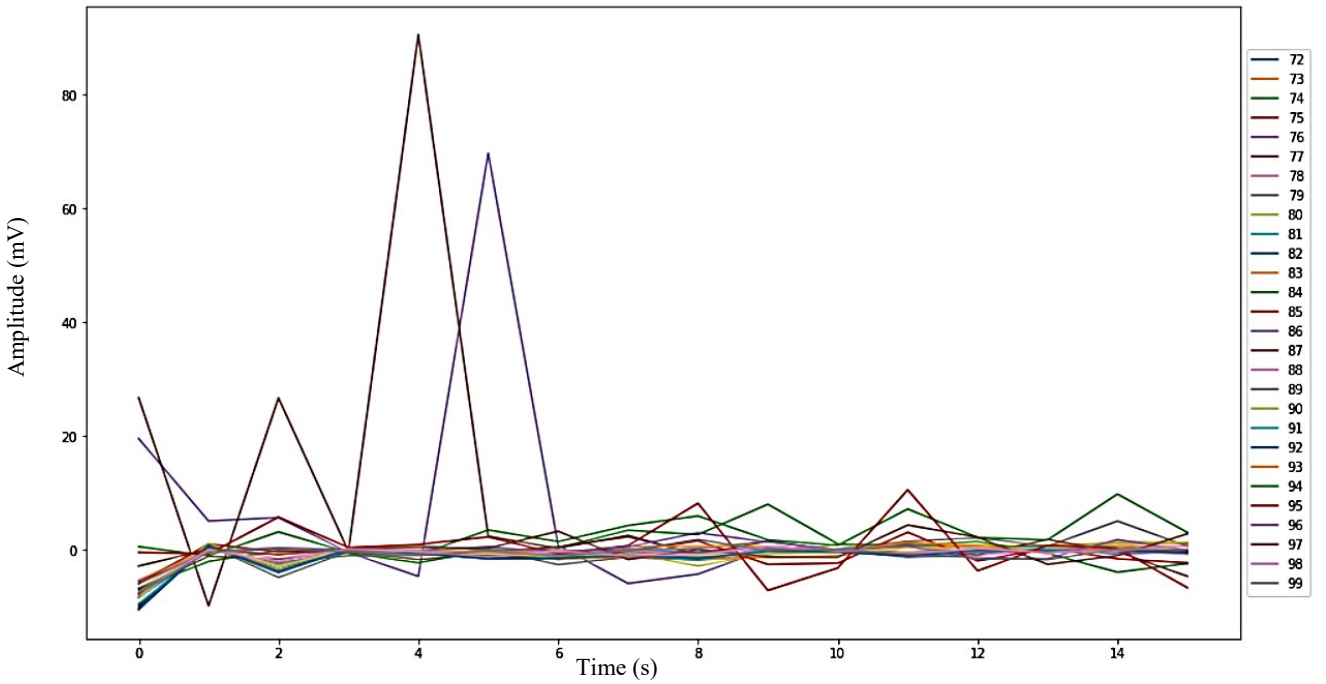

Figure 5. 23 Healthy Control subject knee lifting pattern.

In this chapter, we employed four classification models to automatically analyze EMG signals in clinical movement assessments. A significant focus was on classifying clinical gait patterns in patients diagnosed with polymyalgia rheumatica, comparing them to those of healthy control subjects. Additionally, we classified movement patterns during knee lifting and knee extension exercises for both groups. Our findings indicate that EMG data is effective in examining the intrinsic hip muscle activity of patients. Moreover, the EMG data provides valuable insights into the neurobiological basis of gait characteristics, aiding in the classification of abnormal gait patterns. Table 5.7 below offers a concise comparison of the accuracy and precision achieved by the various machine learning models used for movement classification. This study's comprehensive approach not only helps in understanding the distinct movement patterns between patients and healthy control subjects but also underscores the potential of EMG data in clinical movement analysis and abnormal gait classification.

Table 5. 7 Comparison of classification algorithms

Algorithm	Metrics	Gait	Knee Lifting	Knee Extension
	Accuracy	85.0%	70.0%	65.0%
SVM	Precision	85.7%	85.7%	64.2%
	Accuracy	75.0%	70.0%	55.0%
KNN	Precision	78.7%	85.7%	50.0%
	Accuracy	70.0%	60.0%	55.0%
DT	Precision	64.3%	57.1%	71.4%
	Accuracy	80.0%	65.0%	70.0%
RF	Precision	85.7%	85.7%	71.4%

The results demonstrate that machine learning models could increase the usefulness of clinically available data to classify movement disorders of patients with polymyalgia rheumatica. SVM was

known to be the most suitable machine learning model for the movement classification. It was the most efficient and suitable algorithm that best suits the need for movement classification of the two groups. From the results obtained, the main aim of the study has been achieved which demonstrates that patients have altered movement pattern based on the hip muscles activation compared to healthy control subjects. This also validates the first hypothesis that polymyalgia rheumatica patients will have altered movement pattern compared to healthy control subjects. This Even though the models used in this study yielded an excellent performance, there is a need to explore deep learning techniques for the movement classification.

5.6 Summary

In this chapter, the muscular imbalance of the hip muscles was analysed for patients and control subjects. The muscle load activities around the pelvic girdle were computed to determine imbalances. The results indicated a significant imbalance between patients' right and left hip muscles compared to control subjects. The second section classifies the movement pattern using the traditional machine learning model. The EMG data helps discriminate the movement patterns using various classifiers. The results were significant in distinguishing the movement patterns of the two groups. The classification provides valuable information for clinicians to detect altered movement patterns in patients for immediate interventions.

CHAPTER SIX: DEEP LEARNING TECHNIQUES USING RNN-LSTM AND VISION TRANSFORMER MODEL

6.1 Overview

This chapter presents the results obtained from deep learning techniques using recurrent neural networks with Long-Short Term Memory (RNN-LSTM) and a vision Transformer (ViT) model for the movement classification. In the first phase, a simple RNN algorithm is used to classify the gait pattern from patients and healthy controls. This was to allow for evaluation of the performance of the RNN algorithm on the gait dataset. In the second phase, two EMG metrics were used to segregate between severe and mild conditions among patients with PMR disease. This was particularly useful when researching on patients with PMR to determine severe and mild conditions. The motor unit action potential (MUAP) and the motor unit interference pattern are applied to determine the severity of the condition in patients. In this section, synthetic datasets were generated from the actual datasets for classification based on the design data model. The synthetic EMG datasets were classified using the RNN-LSTM and Transformer algorithms. The goal was to improve the classification performance using deep learning techniques in discriminating the movement patterns and also address the challenge with the unbalanced dataset.

6.2 Deep Learning Techniques

Deep learning (DL) is a sub-component of machine learning that focuses on training neural networks to classify input data into different predefined classes. DL models have been applied in recent works, showing great potential in analysing EMG data and can address some limitations with traditional machine learning algorithms [82]. DL models typically consist of many layers of artificial neurons that are interconnected to a deep neural network (DNN). The input data is usually fed into the neural network, passing through a series of hidden layers. Each layer performs some operations on the input data and extracts data representations for the output layer to generate classification predictions. Some

of the most popular deep neural networks are Multi-Layer Perceptron (MLP), Convolutional Neural Networks (CNNs), Recurrent Neural Networks (RNNs), Long Short-Term Memory Networks (LSTMs), and Generative Adversarial Networks (GANs). The architecture of a deep neural network used in classification problems has three different layers. Figure 6.1 illustrates the architecture of a deep neural network with the three layers.

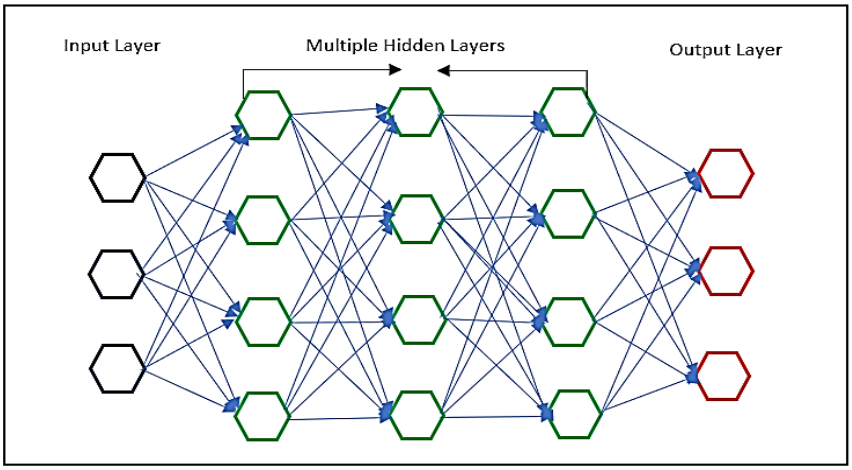

Figure 6. 1 Architecture of Neural Network

DL has proven to be more efficient as it extracts high-level features capable of learning hierarchical representations from low-level input samples [83]. Furthermore, the DL model offers some advantages by reducing background noise-related errors, especially for EMG classification in real-time applications [84]. The Processing of sEMG using a DNN architecture has led to significant improvements in classification problems. One of the most widely used DL models in classification problems is the convolutional neural network (CNN). However, CNN is unsuitable for EMG classification because the target learning features are ineffective in representing temporal properties of EMG data. RNN-LSTM model have been proposed in previous works for sEMG classification with promising results. From previous works in [85][86], RNN-LATM the model was adopted for classification because of the model's advantages in EMG classification.

Before using the RNN-LSTM model, it is essential to understand how neural networks operate as well as the matrix. In a neural network, the ridge regression task is randomly defined as feature map [87]. For a given input data, it is multiplied by a matrix where the function $\sigma: \mathbb{R} \longrightarrow \mathbb{R}$ is applied as input to the vector W_x and providing a set of n random features $\sigma(W_x)\ \epsilon\ \mathbb{R}^n$ in each datum $x\ \epsilon \mathbb{R}^{\mathcal{P}}$. The output $z\ \epsilon \mathbb{R}^d$ from a linear regression is a scalar product $z = \beta^T \sigma(W_x)$ for a matrix $\beta \epsilon \mathbb{R}^{n\ x\ d}$. In a neural network, the n neurons of the network are virtual units that operate using the mapping $W_{\mathrm{i}}.\ x \longmapsto \sigma(W_{\mathrm{i}}.\ x)$, For $1 \leq i \leq$ n. The neural network operates in two phases which are the learning stage in which the regression matrix β is learned based on the input and output dataset pair (X, Y) and the testing stage where the β is fixed. The neural network operates on new input dataset $\hat{X}$ with an unknown corresponding output $\hat{Y}$. The training phase of a neural network is based on a given set of known input $X = [x_1, \ldots\ldots, x_T]\ \epsilon\ \mathbb{R}^{p\ x\ T}$ and output $X = [y_1, \ldots\ldots, y_T]\ \epsilon\ \mathbb{R}^{d\ x\ T}$, the matrix β is chosen in order to reduce the mean square error $\frac{1}{T}\sum_{\mathrm{i}=1}^{T} \|z_i - y_{\mathrm{i}}\|^2 + \gamma\ \|\beta\|_F^2$, where $z_{\mathrm{i}} = \beta^T \sigma(W x_{\mathrm{i}})$ and $\gamma > 0$ is a regularisation factor [87]. In solving for β, the explicit ridge-regressor is given by equation 6.1,

$$\beta = \frac{1}{T}\sum \left(\frac{1}{T}\sum_{\cdot}^{T} \sum \gamma I_T\right)^{-1} Y^T \tag{6.1}$$

Where $\sum \equiv \sigma(WX)$. This is obtained in the differentiation of the mean square error along β to obtain $0 = \gamma\beta + \frac{1}{T}\sum_{\mathrm{i}=1}^{T} \sigma\ (W x_{\mathrm{i}})(\beta^T \sigma(W x_{\mathrm{i}}) - y_{\mathrm{i}})^T$, so that $\left(\frac{1}{T}\sum \sum_{\cdot}^{T} + \gamma I_{n)}\right)\beta = \frac{1}{T}\sum Y^T$ which, along with $\left(\frac{1}{T}\sum \sum_{\cdot}^{T} + \gamma I_n\right)^{-1} \sum = \sum \left(\frac{1}{T}\sum_{\cdot}^{T} + \gamma I_T\right)^{-1}$ This can be donated by the equation 6.2 [87]

$$Q \equiv \left(\frac{1}{T}\sum_{\cdot}^{T} \sum \gamma I_T\right)^{-1} \tag{6.2}$$

The resolvent of $\frac{1}{T}\Sigma^T\Sigma$, where Q matrix naturally appears as a principal quantity in neural network performance. In particular, the mean squared error E_{train} on training dataset X is given by equation 6.3 below [87].

$$E_{train} = \frac{1}{T}\left\| Y^T - \Sigma^T \beta \right\|_F^2 = \frac{\gamma^2}{T} tr Y^T Y Q^2 \tag{6.3}$$

The neural network testing phase reveals the real performance of the network. For a test dataset $\hat{X} \epsilon \mathbb{R}^{p\,x\,\hat{T}}$ of length $\hat{T}$, with an unknown output $\hat{Y} \epsilon \mathbb{R}^{d\,x\,\hat{T}}$ the root mean square error of the trial is determined by equation 6.4 [87].

$$E_{test} = \frac{1}{T} \left\| \hat{Y}^T - \hat{\Sigma}^T \beta \right\|_F^2 \tag{6.4}$$

Multi-Layer Networks: For any given neural network with L, the hidden layer is a function which can be expressed in equation 6.5,

$$f(x) = \sum_{i_L=1}^{m_L} a_{i_L}^{L} \sigma\left(\sum_{i_{L-1}=1}^{m_{L-1}} a_{i_L i_{L-1}}^{L-1} \sigma\left(\ldots \sigma\left(\sum_{i_1=1}^{m_1} a_{i_2 i_1}^{1} \sigma\left(\sum_{i_0=1}^{d+1} a_{i_1 i_0}^{0} x_{i_0} \right) \right) \right) \right) \tag{6.5}$$

where $a_{i_{\ell+1} i_\ell}^{\ell}$ with $i_{\ell+1} \in [m_\ell]$ and $i_\ell \in [m_\ell]$ are the weights of the neural networks. The bias terms within the intermediate layers of the neural network are omitted without a loss in generality.

6.3 Recurrent Neural Networks (RNNs)

The first step was to apply the recurrent neural networks (RNNs) algorithm to evaluate its performance in the movement classification. RNNs are designed for sequential data processing using feedback loops. RNNs have connections that allow information to move from one step to another in a sequence. RNN is an effective EMG signal analysis model by capturing the relationship and pattern of muscle signal recorded in different time steps [88]. In sEMG classification, RNNs capture the temporal dependencies present in EMG signals. In addition, RNNs can handle variable length sequences by automatically adjusting the internal state based on the input at each time step. EMG signals can be in different lengths depending on the activity's duration in single or multiple windows. This flexibility makes RNNs suitable in processing EMG signals for different lengths [88]. The input layer processes the EMG signals as a feature vector and returns an output for classification [89]. The feature vector represents a set of numerical statistics extracted from the EMG signal and used as input in the RNN model. It is essential

to convert the EMG data into a format the model can understand and learn. This transformation extracts necessary features from the signal to represent underlying patterns. Figure 6.2 shows the architecture with a cyclic hidden state for RNN model.

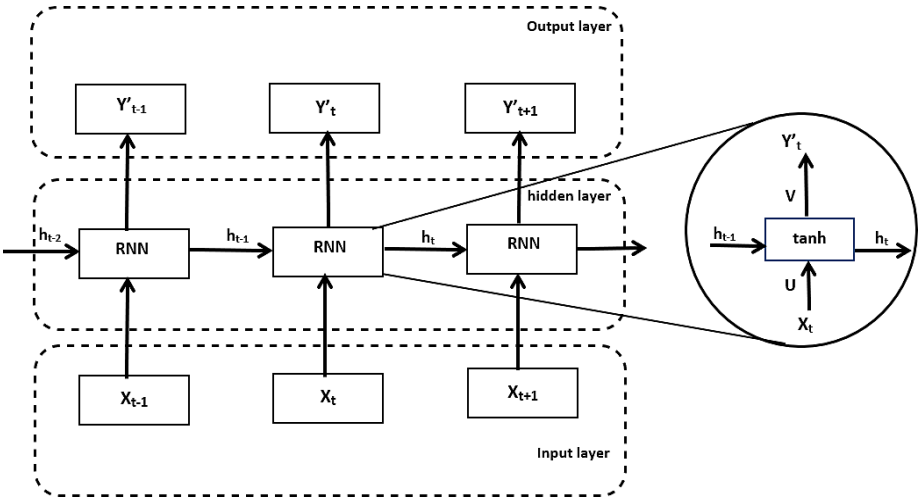

Figure 6. 2 RNN Architecture

- The input layer at time *t-1* is plugged into the RNN hidden layer. The RNN cell then produces an output Y'_{t-1} from a memory state input h_{t-1}. The memory state is a result of input X_{t-1} and a previous value of the memory state h_{t-2} in the RNN cell. In the initial timestep, it assumed that h_0 is a zero vector.
- The resultant input X_{t-1} produces an output Y'_{t-1}. The RNN architecture moves several time steps forward until a final step is reached for prediction.
- In the hidden layer, the data is passed from one timestep which is a memory h_{t-1}, the next memory h_t depends on the previous memory value. For a given matrix, **U** connects the input layer to the hidden layer while **V** connects the hidden layer to the output layer. **W** connects the memory layers together. This is given by the equation $h_t = tanh\ (UX_t + Wh_{t-1})$ (6.6)

As stated earlier, this study first evaluates the performance of using a simple RNN for the EMG signal classification with the gait dataset. In training the RNN model a10-fold cross-validation was used to evaluate the model's performance with different optimisation algorithms. The optimisation algorithms used were Stochastic gradient descent (SDG), Adaptive moment estimation Max (Adamax), Adagrad, and RMSprop.

- *Stochastic Gradient Descent (SGD):* It is one of the simplest and most widely used optimisation algorithms. SGD updates the model parameters at each training iteration by computing the gradient of the loss function concerning the parameters. It performs parameter updates based on a small set of randomly selected training samples to increase computational efficiency.
- *AdaGrad:* This optimisation algorithm adjusts the learning rate of each parameter based on the sum of squares of past slopes. Rare features receive significant updates, and popular features receive minor updates. AdaGrad is well suited for processing sparse data and is commonly used in natural language processing.
- *RMSprop:* This is an optimisation algorithm that adjusts the learning rate of each parameter based on the average of the final quadratic gradients. This reduces variation or fluctuations in the learning rate and allows for rapid convergence, especially in low-slope situations.
- *Adamax:* It is a variation of Adam that replaces the second moment of the gradient with the infinity norm. It is more powerful for steep gradients and suitable for low-slope models.

The above-mentioned optimisation algorithms were evaluated for their performance on the EMG dataset to classify the gait pattern. The choice of an optimisation algorithm is important as it significantly impacts the performance of RNN model for classifying movement based on EMG signals. The optimisation algorithm is responsible for updating the weights of the RNN layer during the training phase to reduce the loss function and thus improve the model's accuracy. The metrics used to evaluate the performance of the RNN model were accuracy, precision, F1-score, and recall which is illustrated with the results in Table 6.1 below.

Table 6. 1 Optimisation performance

Optimiser	**Adamax**			**Adagrad**			**SGD**			**RMSprop**		
Metrics	**Precision**	**Recall**	**F1-Score**	**Precision**	**Recall**	**F1-score**	**Precision**	**Recall**	**F1-Score**	**Precision**	**Recall**	**F1-Score**
0	1.00	0.85	0.92	0.86	0.92	0.89	1.00	0.67	0.80	0.91	0.77	0.83
1	0.71	1.00	0.83	0.75	0.60	0.67	0.78	1.00	0.88	0.57	0.80	0.67
Accuracy	-	-	0.89	-	-	0.83	-	-	0.85	-	-	0.78
Macro avg.	0.86	0.92	0.88	0.80	0.76	0.78	0.89	0.83	0.84	0.74	0.78	0.75
Weighted avg.	0.92	0.89	0.89	0.83	0.83	0.83	0.88	0.85	0.84	0.82	0.78	0.79

Table 6.1 shows the classification score for the optimisation algorithms used in classifying the gait pattern between patients and healthy control subjects. From Table 6.1, Adamax had an accuracy of 0.89, Adagrad was 0.83, SDG recorded 0.85, and RSMprop recorded 0.78. The mean accuracy was 0.84 from the four optimisations which is sufficient to distinguish the gait patterns of the two groups. Precision in deep learning classification focuses on the accuracy of positive predictions, especially in situations that involve high costs associated with class imbalance. Adamax had the best precision among the optimisation algorithms used. The mean macro values in the classification report were used to determine the performance measures in the two classes. Each optimisation algorithm was evaluated by discriminating the gait patterns between the two groups. Regarding sensitivity, Adamax and SDG performed better in predicting the gait patterns of impaired patients, compared to Adagrad and RMSprop. Adagrad was noted to be the least sensitive optimisation algorithm in identifying impaired walking patterns. For the F1-score, the SGD algorithm outperformed Adamax with 0.88, while Adamax scored 0.83 in determining impaired gait. Adagrad and RSMprop performed poorly for the F1-scores in identifying impaired patients gait patterns. Figure 6.3 shows the bar chat plot for the optimisation algorithms illustrated for the various classification metrics.

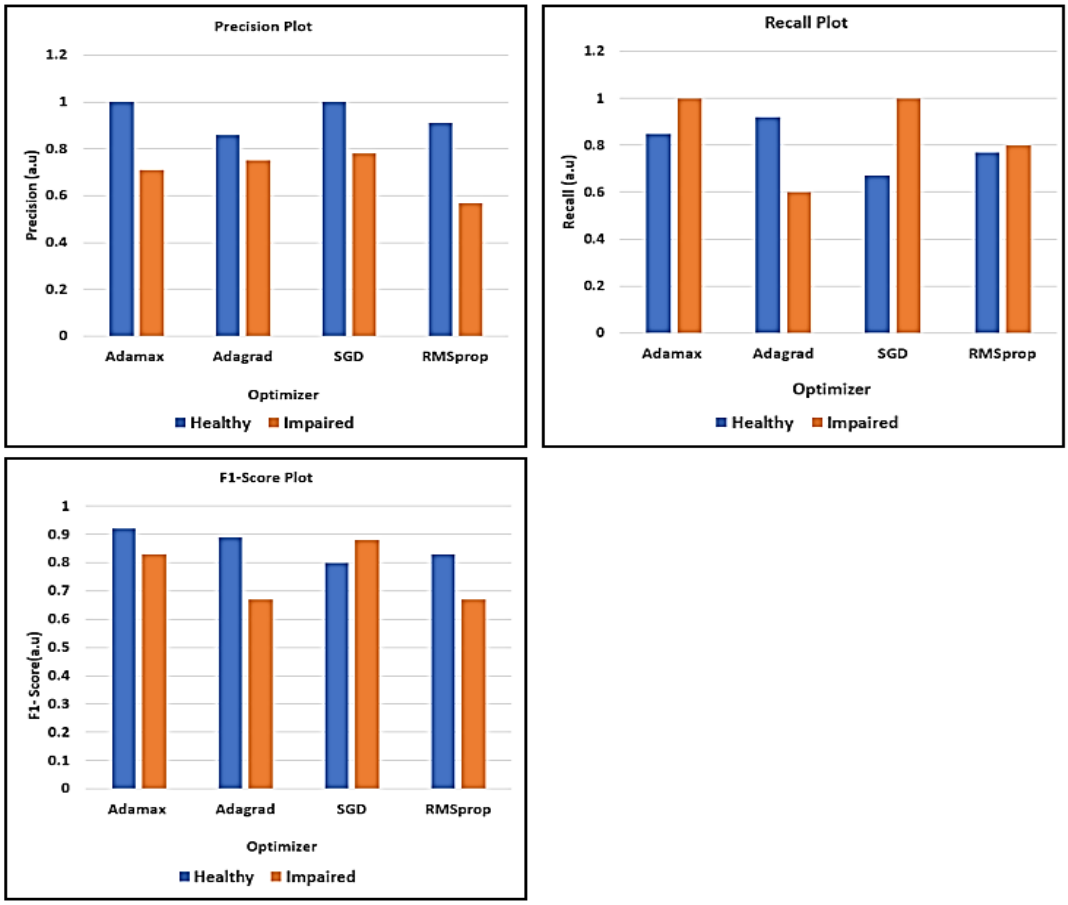

Figure 6. 3 Score metrics for optimisation algorithms using RNN.

The results indicated that the best optimisation algorithm in classifying the gait patterns between patients and the healthy control subjects was Adamax. Figure 6.3 illustrates the receiver operating characteristics (ROC) curve for the different optimisers used in the classification. ROC curves are critical in deep learning classification to evaluate performance and handle unbalanced datasets.

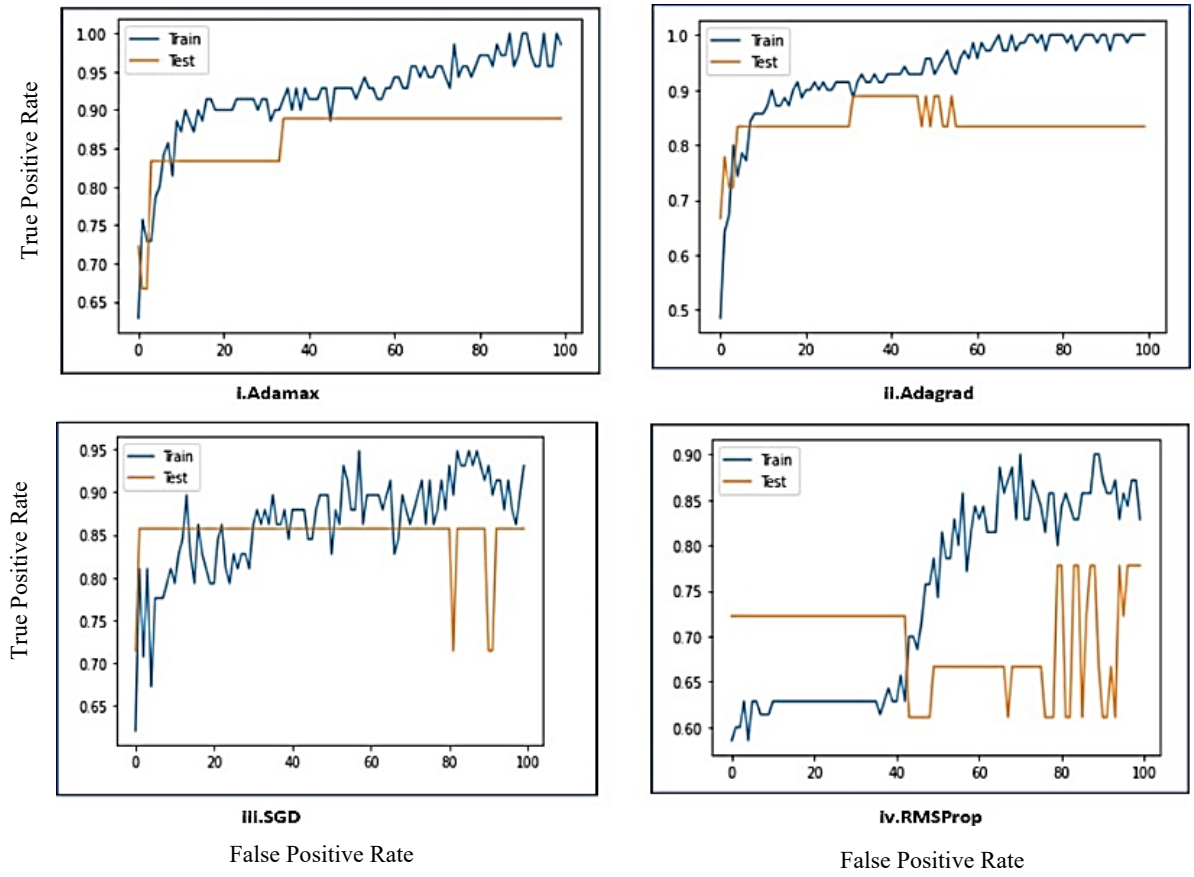

Figure 6. 4 Accuracy plot for optimisation algorithms

The limitation of this classification was the imbalance data between patients and healthy control subjects. Even though the RNN achieved promising results in the classification, the goal was to improve the accuracy and address the issue of imbalance dataset. The LSTM-RNN was introduced to take care of the limitations of the RNN model. Synthetic data was generated from the actual dataset to balance the data in training the LSTM-RNN model. This measure was adopted to mitigate the limitation of the minority class (healthy control subjects) by using the Synthetic Minority Oversampling technique (SMOTE). The SMOTE is a method used to address the issues of imbalance datasets. With this method synthetic data was generated to make the dataset balance for patients and healthy control subjects.

6.4 Segregation of Severe and Mild Conditions of PMR Patients

The next phase in this section was to determine the severity of the PMR condition based on the strained hip muscle signals. This ties in with the second objective of this study to determine the severity of the condition among patients. EMG signals have been introduced in previous work to classify the severity of muscle diseases [90]. EMG signals can be used to distinguish between severe and mild conditions of PMR disease based on the hip muscles activation. This is important because of the lack of cheaper mechanism to distinguish between severe and mild condition of PMR disease. The metrics used to segregate the PMR condition among patients were the motor unit recruitment pattern and the interference pattern. These metrics were computed using EMGworks software to distinguish the two groups in determining severity. The MUAPs represent the electrical activity generated by a group of muscle fibers that a single motor neuron has innervated. The motor unit parameters vary depending on the muscle being examined. MUAP parameters such as the amplitude, duration, and number of phases measured in muscle activation can be used to differentiate between severe and mild cases of muscle disease [90]. The MUAP amplitude and duration can be used to determine the size of the motor unit [91]. Figure 6.5 illustrates the MUAP of an EMG signal which is used to evaluate a muscle signal.

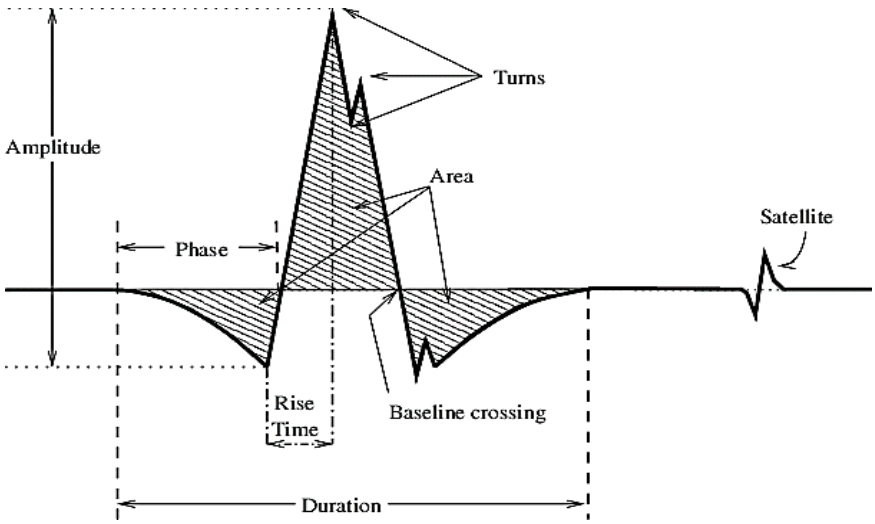

Figure 6. 5 MUAP of EMG signal

The denervation of a muscle leads to the loss of nerve supply to the specific muscle with a decrease in MUAP amplitude and a longer duration. The muscle activation pattern of severe cases of PMR disease would have a lower amplitude with a longer duration compared to mild cases with slightly higher amplitude. In muscle activation patterns, parts of the muscles would have a reduced nerve supply due to the effect of polymyalgia rheumatica disease. Per the rule of thumb, the motor unit potentials are less than 2mV in amplitude, lasting 10-5ms with 3-4 phases of MUAPs [92]. In severe musculoskeletal disease, the motor unit potential would be small with a short duration, where values will be between 0.1-0.5mv with a duration of 5-10ms [92]. This indicates that the MUAP may have several morphological alterations, such as an increased amplitude, decreased duration, or increased polyphasic muscle contraction. The metrics mentioned above were implemented in evaluating strained muscle signals to distinguish the two groups (severe and mild conditions). The muscle activation pattern for healthy control subjects would have higher amplitude and a shorter duration. Mild cases of PMR would have higher amplitude with a long duration while severe condition with lower amplitude and short duration of the MUAP in the strained hip muscle activation.

6.4.2 Motor Unit Action Recruitment Pattern

The recruitment pattern of motor unit refers to the process by which different motor units are activated to produce a level and type of muscle contraction [93]. The motor unit action recruitment pattern can be used to distinguish between severe and mild conditions of polymyalgia rheumatica disease. The early recruitment plan aims to identify recruitment patterns by measuring the firing rate of MUAPs in the first few recruits [94]. In severe condition of PMR disease, there is an excessive firing rate in the early recruitment due to muscle denervation compared to mild condition with less firing. In a severe condition of PMR patients muscle signal shown in [Figure 6.7], the motor unit's early recruitment plan has many firings. The early recruitment plan of the severe conditions shows an excessive firing rate of the first few MUAPs during muscle contraction. Figures 6.7 and 6.8 illustrate the recruitment pattern of mild and severe condition of the MUAP signal respectively. From the two figures, severe conditions of PMR

have excessive firing rate of the signals in the early recruitment compared to the mild condition due to muscle denervation. In musculoskeletal disorders such as polymyalgia rheumatica, muscle denervation leads to a loss in muscle function. The early recruitment pattern indicates a compensatory mechanics due to muscle function loss, which is present in severe condition of PMR disease. Figure 6.6 shows EMG signal of a control subject have minimal firing rates with early recruitment. In Figure 6.7, for the EMG signal for mild condition there is less firing in the early recruitment, while Figure 6.8 shows massive firing of the hip muscle signal of patients with severe conditions. This indicates a reduced firing rate in the muscles of patients with mild conditions compared to excessive firing in severe conditions.

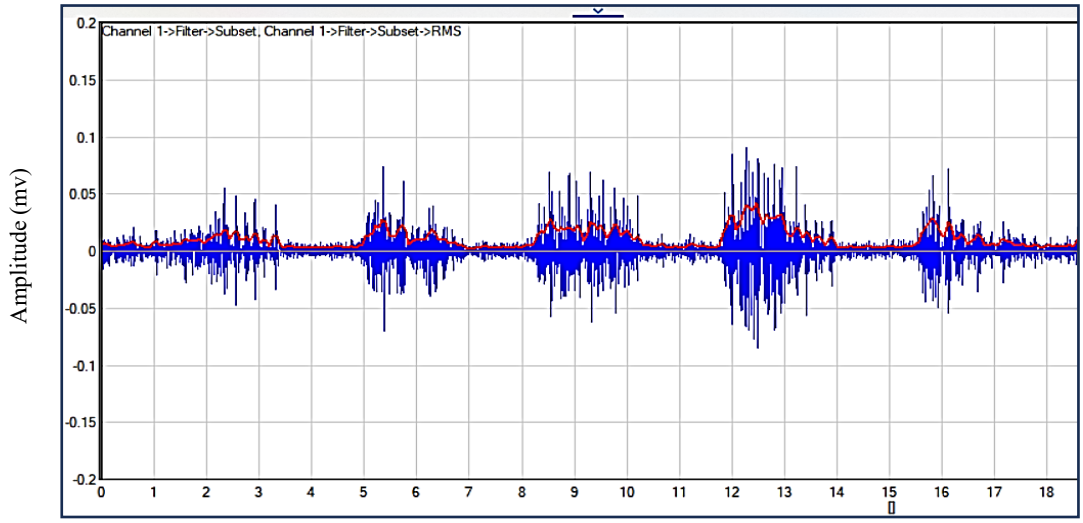

Figure 6. 6 Healthy EMG signal pattern

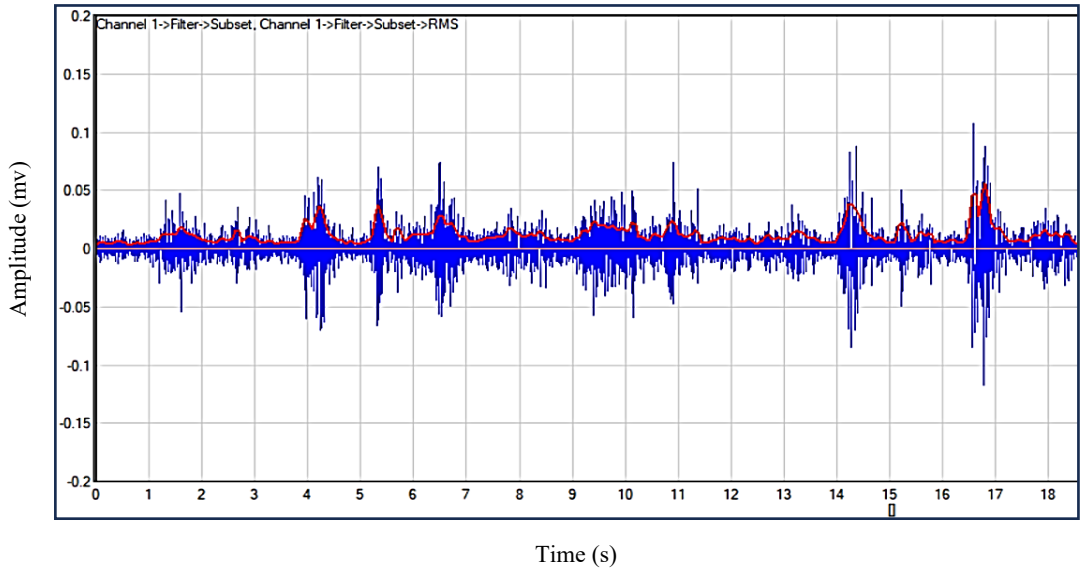

Figure 6. 7 Mild patients EMG signal pattern

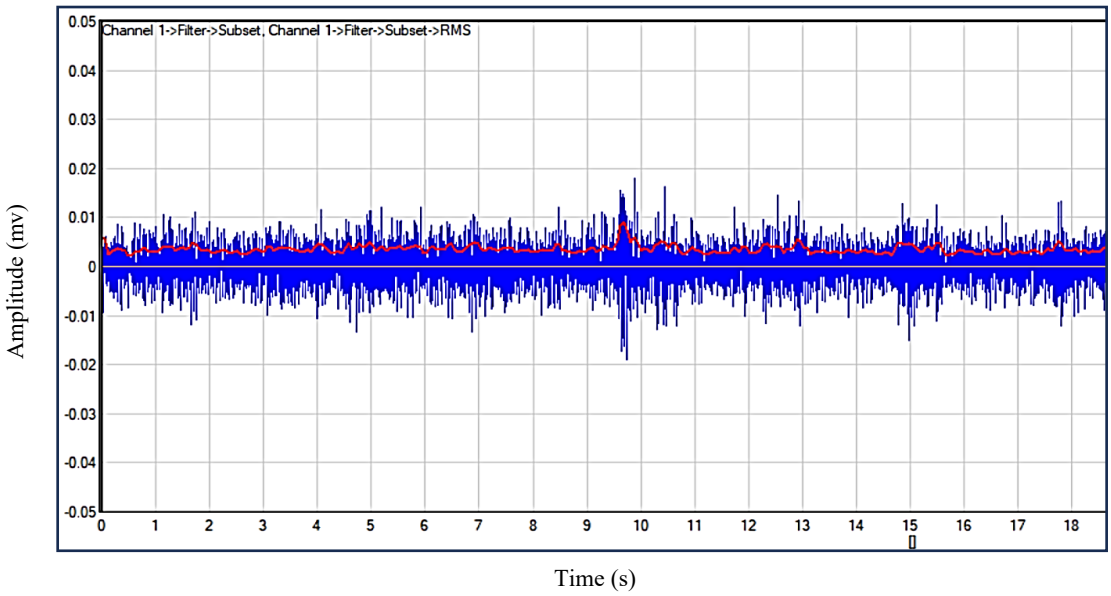

Figure 6. 8 Severe patients EMG signal pattern

6.4.3 Interference Pattern of Motor Units

The interference pattern is built up from a single unit action potential and contains information about the number of MUAPs, firing rate, and recruitment characteristics of motor units. The amplitude of the interference pattern was analysed using EMGworks software to count the spikes, amplitude measurements, and signal integration. The interference pattern of hip muscle signals provides valuable information about the recruitment and firing patterns of the motor units of the hip muscle. In healthy muscles, the interference patterns are stable and consistent, with a regular motor unit recruitment pattern [94]. For muscles affected by PMR disease, motor unit recruitment patterns become irregular, leading to increased variability in the amplitude and duration of the MUAPs. Therefore, in severe cases of PMR disease, the interference is massive with irregular patterns and increased variability of amplitude compared to mild condition with less interference pattern. Figure 6.9 shows that the EMG signal for

healthy control subject with less interference and regular pattern of the motor unit potential. Figure 6.10 shows a mild case of PMR disease with less interference signal, but Figure 6.11 indicates EMG signal severe case of PMR disease with considerable EMG signal interference. The yellow and purple lines in the y-axis were used to indicate the interference pattern of muscle signals to determine the severity of the disease.

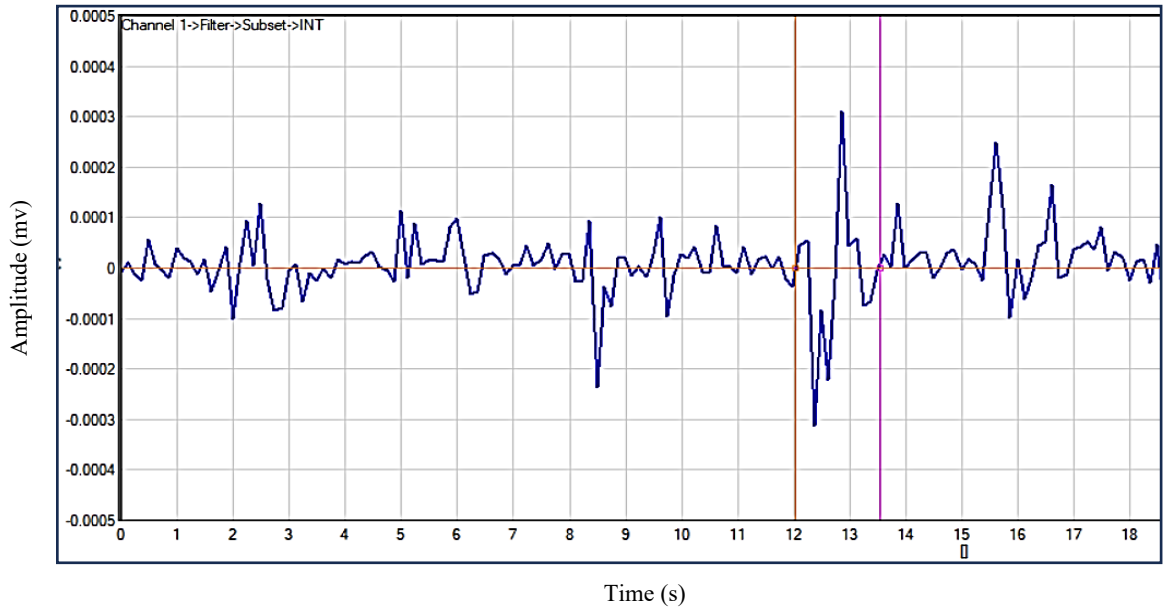

Figure 6. 9 Healthy control integrated EMG signal

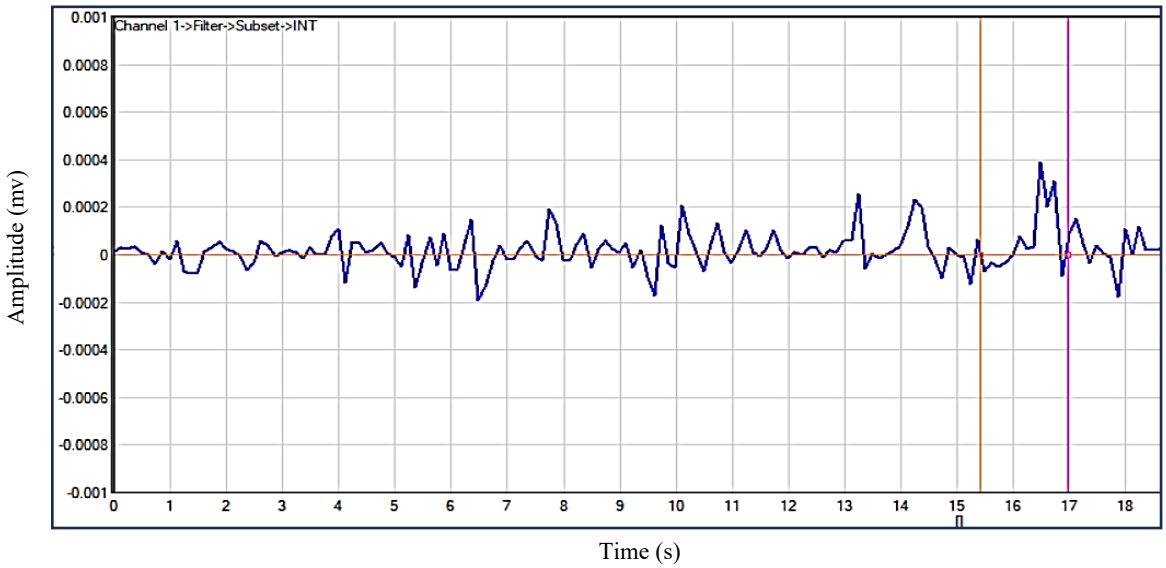

Figure 6. 10 Mild patients integrated EMG signal.

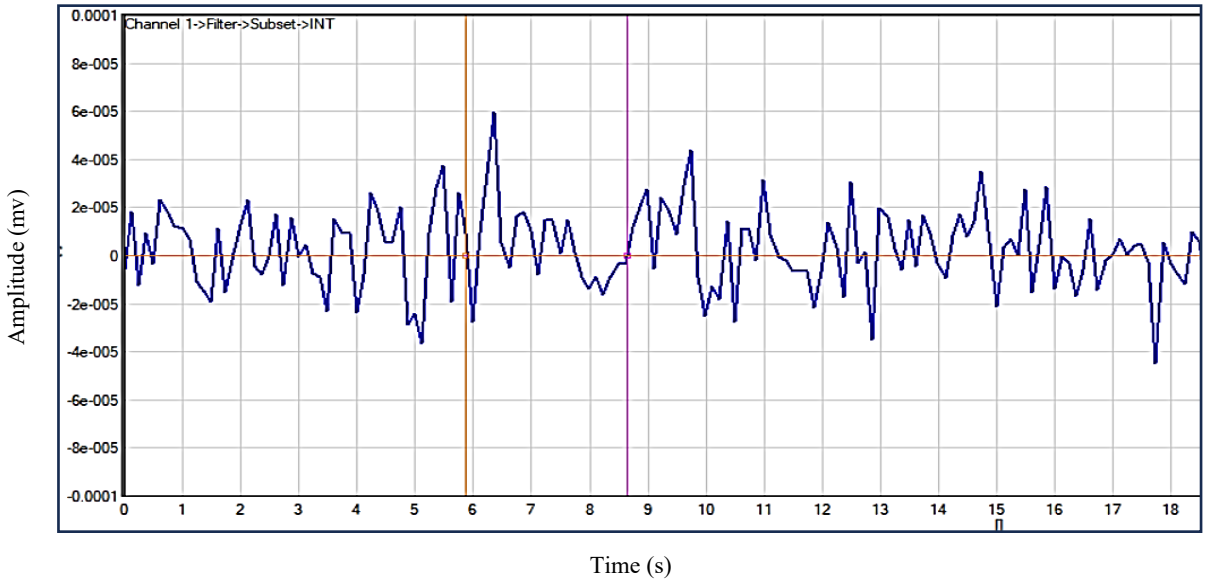

Figure 6. 11 Severe patients integrated EMG signal.

6.5 Generation of Synthetic EMG Dataset

Based on the segregation of the muscle signals to group between severe and mild conditions of PMR disease, this was then used to generate the synthetic dataset using generative adversarial networks (GANs). Synthetic data is the generation of signals that mimic the actual EMG data recorded from the participant. It was important to generate synthetic EMG data for classification. Firstly, it addresses the limitations of an unbalanced dataset. Synthetic data generation addresses the unbalanced dataset between patients and healthy control subjects used in the previous chapter with machine learning algorithms. Secondly, synthetic data generated from the original EMG dataset also allows for faster iteration and testing of the RNN-LSTM model. Therefore, the synthetic EMG dataset generated was able to address the challenges with the actual dataset from participants. The following steps were taken to generate the synthetic dataset for the movement classification.

Step 1: The first step was to analyse the statistical properties of the actual EMG data recorded. This includes the critical feature vectors used to analyse the distribution of features, temporal patterns, and any observed variability of the EMG dataset.

Step 2: In the second step, a computational model is designed in Python using *skylit* library to capture the essential features of the actual EMG signal. The developed model is based on the known physiological features such as the motor unit and the muscle contraction. The model parameter estimation is based on statistical attributes and features of the EMG, extracted from the actual dataset. This process involves fitting the model to the actual dataset to determine the relevant parameters.

Step 3: In the third step, the designed model is randomised to simulate the natural variability extracted from the real and noise found in real EMG signals. This includes variations in motor unit recruitment, firing rates, and muscle activation patterns.

Step 4: In the fourth step, the developed model and parameter estimates were used to generate the synthetic EMG signal. This was done by simulating the behaviour of motor units and the overall signal. The generated synthetic EMG data was then validated by comparing it with the original dataset. The synthetic EMG dataset was generated for the gait, knee lifting, and knee extension exercises by participants. Overall, 1,605 data samples were generated in the synthetic data, 80% (1284 samples) for training and 20% (321 samples) for testing for each of the dataset exercises conducted.

6.5.1 Challenges of Synthetic Dataset and Addressing these Limitations

The synthetic EMG dataset was using the Generative Adversarial Networks (GANs) model. The generated synthetic data presents unique challenges and limitations due to the specific characteristics and requirements of EMG data. The key limitations of generating synthetic EMG datasets using GAN models are.

Signal Variability: EMG signals can vary significantly depending on muscle activity, electrode placement, and individual differences. Capturing this variability accurately with a GAN model can be challenging.

Training: Generative Adversarial Networks can be difficult to train and suffer from issues like non-convergence, vanishing gradients, and mode collapse. This makes it challenging to reliably train a GAN to generate high-quality synthetic EMG data.

Evaluation Metrics: There is no established consensus on the best evaluation metrics for assessing the quality of synthetic time series data generated by GANs, including EMG signals. This makes it difficult to reliably evaluate the fidelity of the generated EMG data. The GAN model is significant for generating synthetic time series data, but there are significant challenges in applying them reliably to EMG datasets due to the inherent instability of GAN training, lack of established evaluation metrics, and limited generalization.

Addressing the challenges in generating synthetic EMG datasets using GANs requires a combination of methodological approaches, domain-specific knowledge, and advanced techniques. The solutions to the limitations of generating synthetic data for the classification,

Signal Variability: Using multi-modal GANs that can capture different modes or variations in the EMG signals due to muscle activity, electrode placement, or individual differences.

Training: Utilizing advanced GAN architectures such as Conditional GANs, or Self-Attention GANs that are more stable and less prone to issues like mode collapse or vanishing gradients.

Optimized Hyperparameters: Systematically tuning hyperparameters such as learning rates, batch sizes, and network architectures through cross-validation or automated hyperparameter optimization methods to improve GAN training reliability.

*Evaluation Metrics**:*** Developing domain-specific evaluation metrics tailored for assessing the quality and fidelity of synthetic EMG signals. This could involve measures of signal similarity, noise level, or physiological relevance. By integrating these solutions, it addresses the challenges associated with the generated synthetic EMG datasets using GANs and thus paving the way for more reliable classification.

6.5.2 Validation of Synthetic EMG dataset

Validating synthetic EMG datasets using real EMG datasets is crucial to ensure that the synthetic data accurately represents the characteristics and variability of real EMG signals. The generated synthetic EMG datasets ensure that the synthetic data covers a similar range of variability as the real EMG data.

Comparative Analysis: Compute statistical measures to compare the distributions of extracted features between real and synthetic EMG datasets, such as mean, standard deviation, and correlation coefficients. A smaller difference indicates better similarity between the datasets.

Domain-Specific Validation: Evaluate the performance of EMG signal processing or analysis algorithms using both real and synthetic EMG datasets. If the algorithm used performs similarly on both datasets, it indicates that the synthetic data is suitable for the intended classification.

The validation process ensures the quality, and utility of synthetic EMG datasets generated using GANs. Validated synthetic EMG datasets can then be confidently used in various applications, including algorithm development with a better understanding of their reliability and applicability of EMG dataset.

6.6 LSTM-RNNs Model

In this section, the synthetic data was used to train the LSTM-RNN to improve the accuracy of the movement classification. Long-Short Term Memory (LSTM) was introduced to solve the missing gradients in RNNs. The RNN model has difficulty in understanding long-term dependencies because of the vanishing gradient problem. One advantage of LSTM is that it can handle long-term dependencies more efficiently than traditional RNNs. This is because LSTM has short-term memory that can last several steps, allowing it to keep past data in memory. Another advantage of LSTM is that they have repeating gates that allow the network to forget information that is no longer relevant selectively. This makes LSTM more efficient in data processing and prediction than traditional RNN. The fundamental difference between the architectures of LSTM and RNN is that the hidden layer of the LSTM is in a closed unit. The architecture of the LSTM-RNN model used in the classification shown in [Figure 6.12] below.

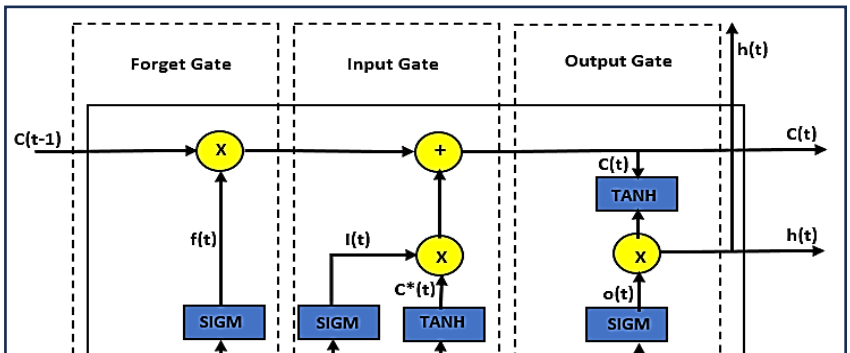

Figure 6. 12 Architecture of LSTM model

The units take the current input vector, which represents X(t), and the layer's previously hidden state vector, a gain denoted by h(t). The cell state vector denoted by C(t) is updated by three main gates, namely the input gate I(t), the forget gate f(t), and the output gate o(t). The forget gate determines the information that should be removed from the cell state. The input gate adjusts the new information that is stored in a cell state, and the output gate controls the output of the LSTM unit, known as the hidden state. At each time step t, the hidden state with vector h(t) and the cell state vector C(t) are propagated to the next time step t + 1. The LSTM at time t represents the short-term memory of the unit, and the cell state C(t) represents the long-term memory. **[95]**

$$f(t) = sigm(W_f\, X(t) + U_f h(t-1) + b_f)$$

$$I(t) = sigm(W_I\, X(t) + U_I h(t-1) + b_I)$$

$$\bar{C}(t) = tanh(W_C\, X(t-1) + U_C h(t-1) + b_C)$$

$$C(t) = f(t).C(t-1) + I(t).\bar{C}(t)$$

$$o(t) = sigm(W_o\, X(t) + U_o h(t-1) + b_o)$$

$$h(t) = o(t)\,.\,tanh(C(t)) \qquad (6.7)$$

From the equations above W, U and b represent the weight matrices for the input, output, hidden layers, and bias vectors. In the same equation, (·) represents element-by-element multiplication. The two activation functions are the sigmoid, denoted by *sigm,* and the hyperbolic tangent, denoted *tanh* [95].

6.6.1 LSTM-RNN Model Training and Classification Results

The LSTM-RNN model was trained with the EMG datasets in the gait, knee extension, and knee lifting exercises. The training consists of feeding the segmented EMG signals into the LSTM layer with one step at a time. The model takes the EMG signals as an input feature vector and generates a probability distribution over the classes. The output from the model is compared with the real label classes and the error is computed using the loss function. The performance of the LSTM-RNN model was evaluated by the accuracy, recall, precision, and F1-score. These metrics allow for the evaluation of the model's ability to accurately classify the different classes, which were patients with either severe or mild conditions and then healthy control subjects. A Principal Component Analysis (PCA) plot illustrated the data points in the distribution for the three classes. The PCA plot for the datasets used in the classification indicates Purple (healthy controls), Green (mild cases), and Yellow (severe cases) in Figures ow the correlation between evere). Figure 6.13 shows t the distribution of points ir

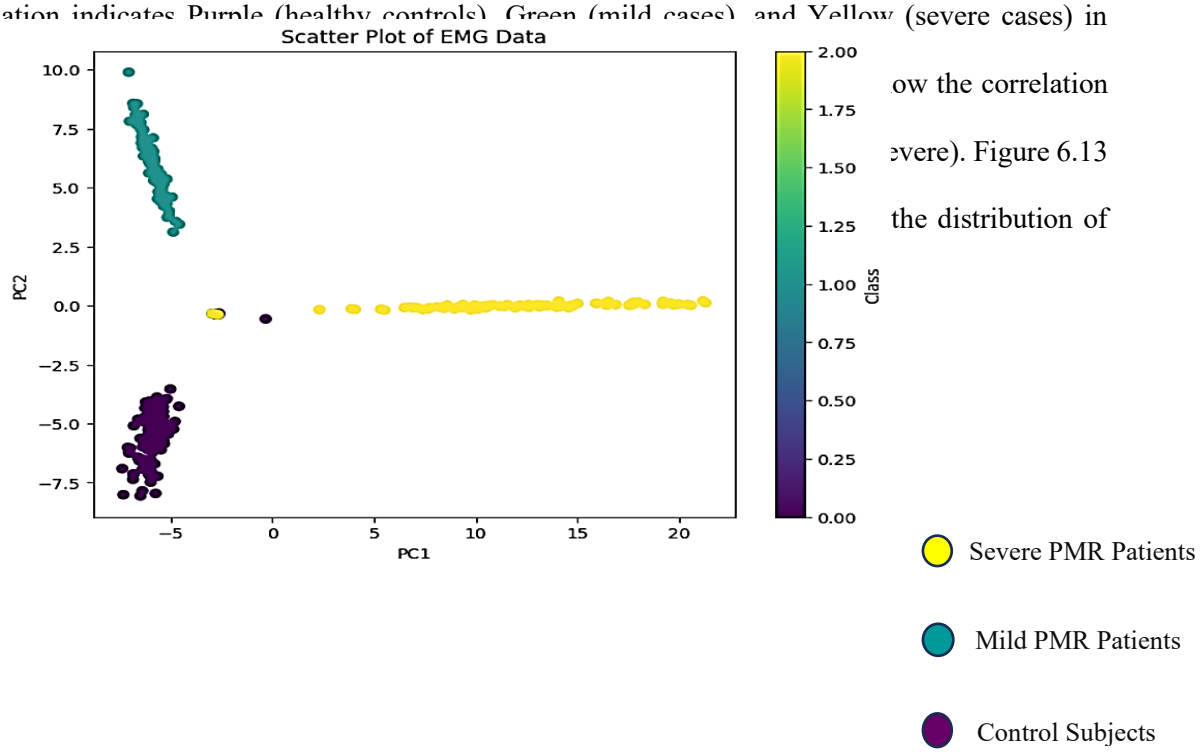

Figure 6. 13 PCA plot for gait exercise

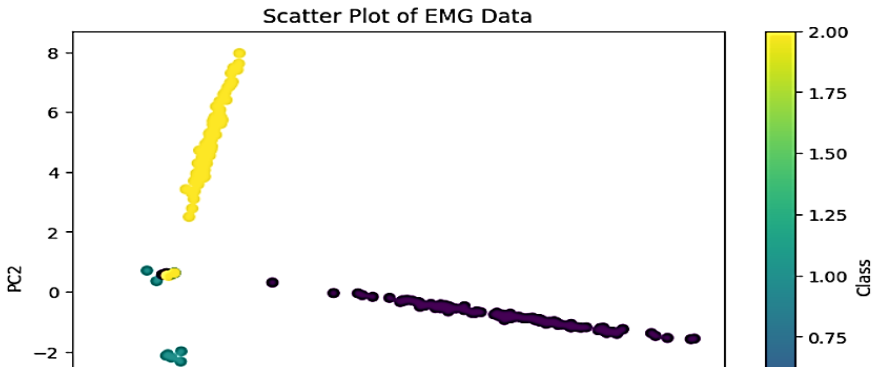

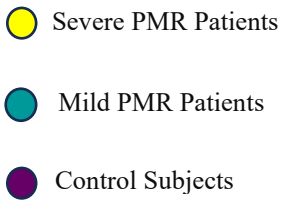

Figure 6. 14 PCA plot for knee lifting exercise.

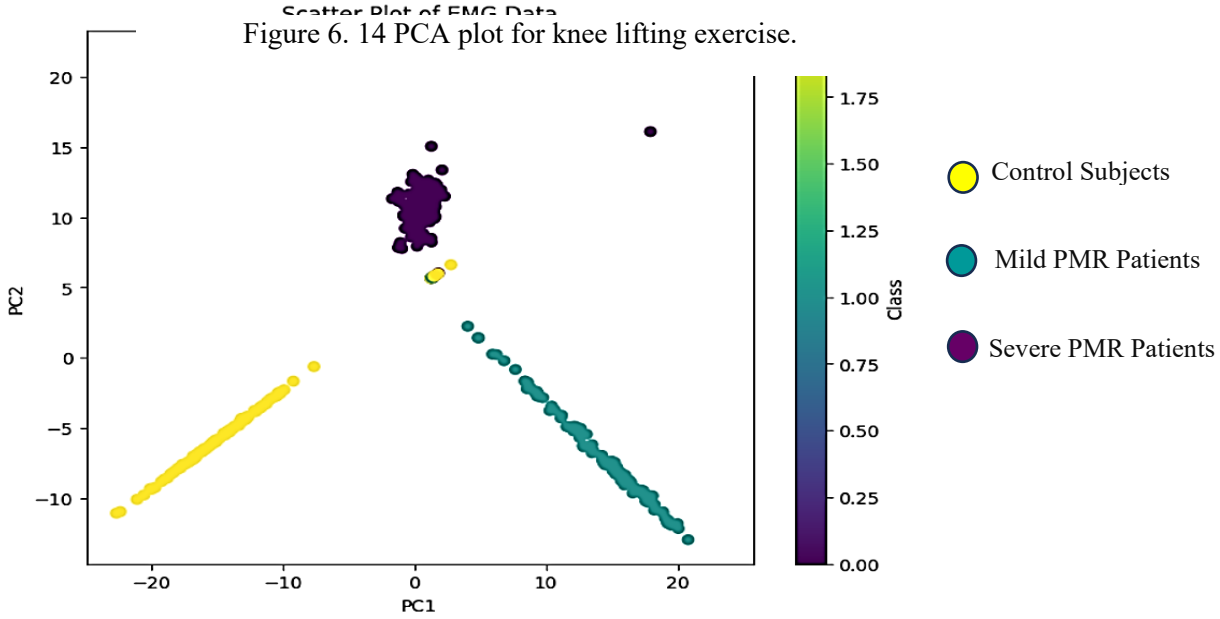

Figure 6. 15 PCA plot for knee extension exercise

The Receiver Operating Characteristics (ROC) curve is a graphical representation that shows the performance of the LSTM-RNN model. It represents the true positive ratio (TPR) versus the false positive rate (FPR) at different classification thresholds of the LSTM-RNN model. The ROC curve is generated by plotting TPR on the y-axis versus FPR on the x-axis to indicate the classification thresholds. Each point on the ROC curve represents the specific threshold and how the performance of the model changes. The ROC curve provides a visual representation of the trade-offs between the actual positive rate and the false positive rate of the LSTM-RNN model. Figure 6.16 illustrates the

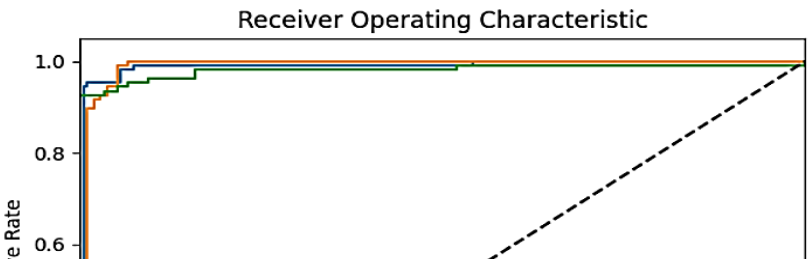

performance of the LSTM-RNN model for the gait exercise, indicating the different class score. Figures 6.17 and 6.18 show the performance of the ROC curve in the knee lifting and knee exercise respectively.

Figure 6. 16 ROC curve for gait classification

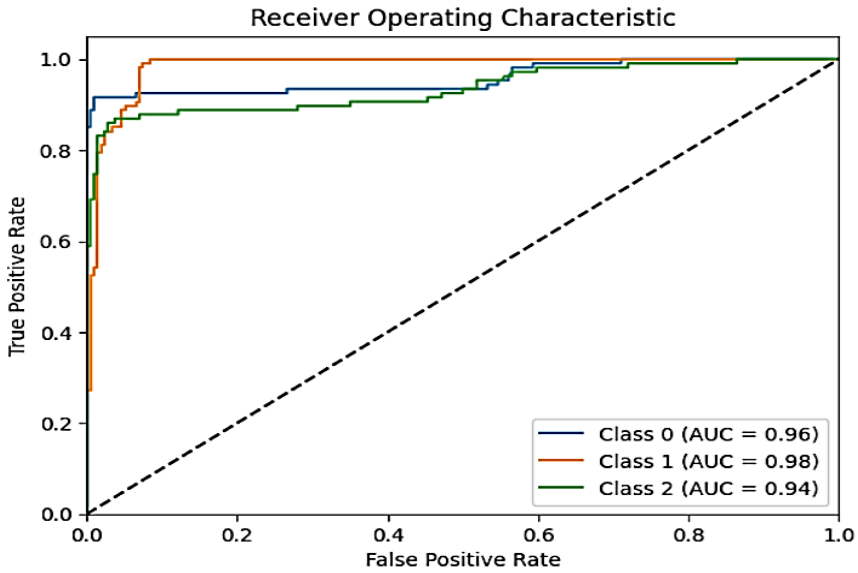

Figure 6. 17 ROC curve for knee lifting exercise.

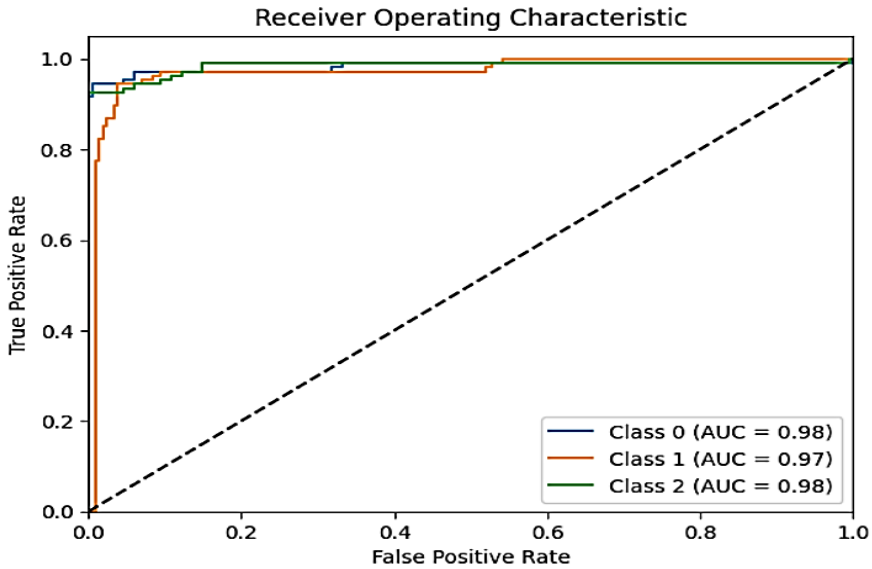

Figure 6. 18 ROC curve for knee extension

The confusion matrix summarises the performance of the LSTM-RNN model by showing the true positives, true negatives, false positives, and false negatives values. It helps evaluate the performance of the LSTM-RNN and identify the types of errors created by the model. The confusion matrix is useful in computing other performance parameters, such as recall and F1-scores. The confusion matrix in Figure 6.19 indicates the model's score in discriminating the gait pattern for the three classes. Figures

6.20 and 6.21 also indicate knee lifting and knee extension, respectively. Examining the confusion matrices show the misclassification, indicating the false positive (FP) and false negative (FN) were minimal in the gait exercise compared to the misclassification in the knee lifting and extension exercises. The true positive (TP) and true negative (TN) values for the gait were higher than the knee lifting and extension exercises

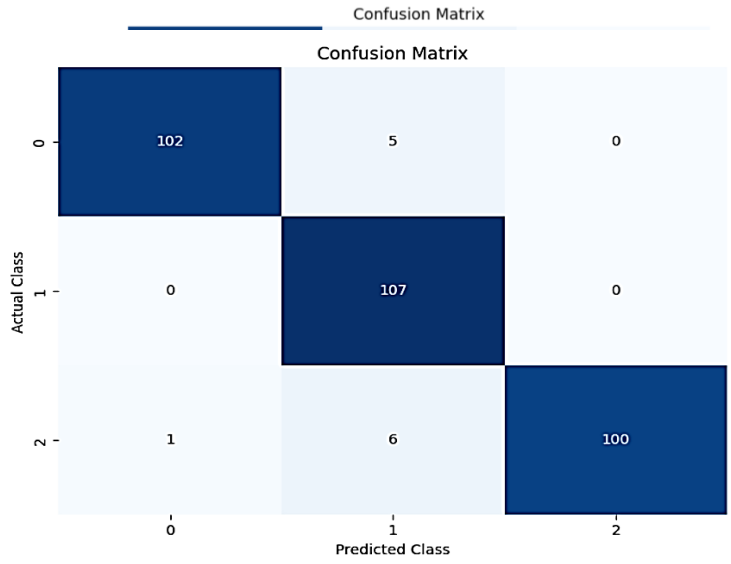

Figure 6. 19 LSTM-RNN classifier confusion matrix for gait exercise

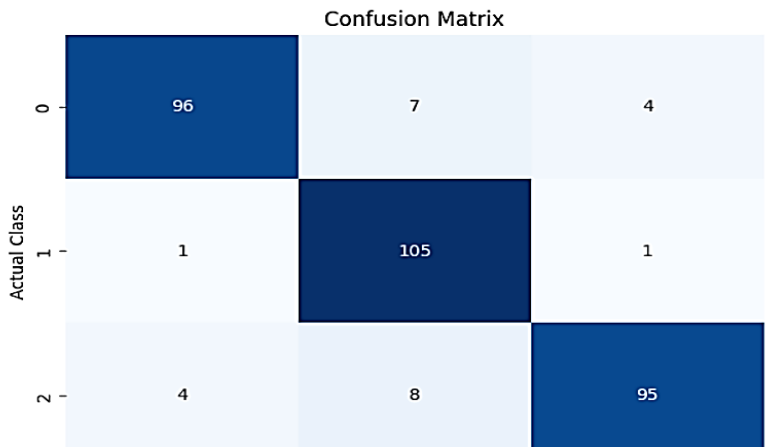

Figure 6. 20 LSTM-RNN classifier confusion matrix knee lifting exercise.

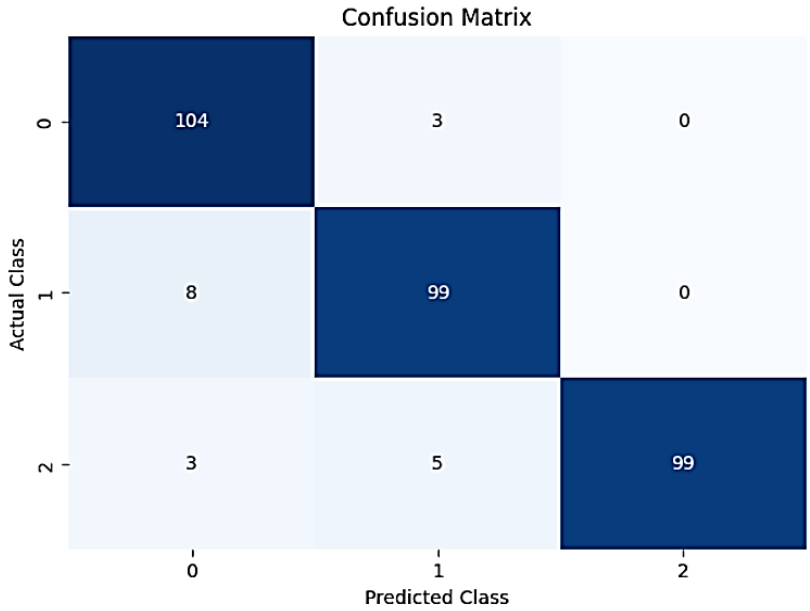

Figure 6. 21 LSTM-RNN classifier confusion matrix for knee extension exercise

Table 6.2 shows the performance of the LSTM-RNN model in the classification, which indicates the score for each class with regard to the precision, recall, and F1-score.

Table 6. 2 Performance of LSTM-RNN model

Metrics		Gait	Knee Lifting	Knee Extension
Accuracy		0.95	0.92	0.94
Precision	Class 0	0.99	0.95	1.00
	Class 1	0.88	0.88	0.86

	Class 2	1.00	0.95	0.99
Recall	Class 0	0.94	0.90	0.92
	Class 1	1.00	0.98	0.99
	Class 2	0.92	0.89	0.93
F1-Score	Class 0	0.97	0.92	0.96
	Class 1	0.94	0.93	0.92
	Class 2	0.96	0.92	0.96

The performance of the model is represented in bar graph indicating the score for each class. Figure 6.21 indicate the bar graph for the gait exercise while Figures 6.22 and 6.23 also indicate the bar graphs for the knee lifting and knee extension respectively.

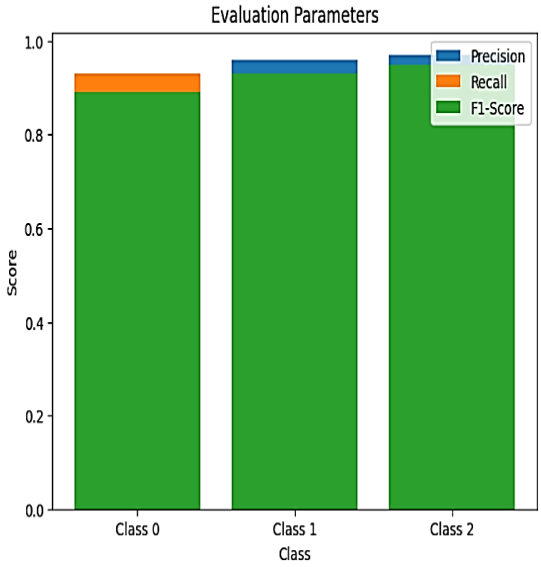

Figure 6. 22 RNN-LSTM score for gait exercise.

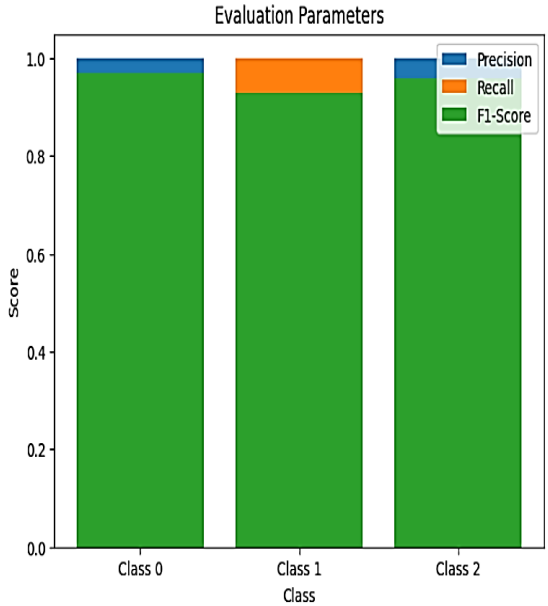

Figure 6. 23 RNN-LSTM score for knee lifting.

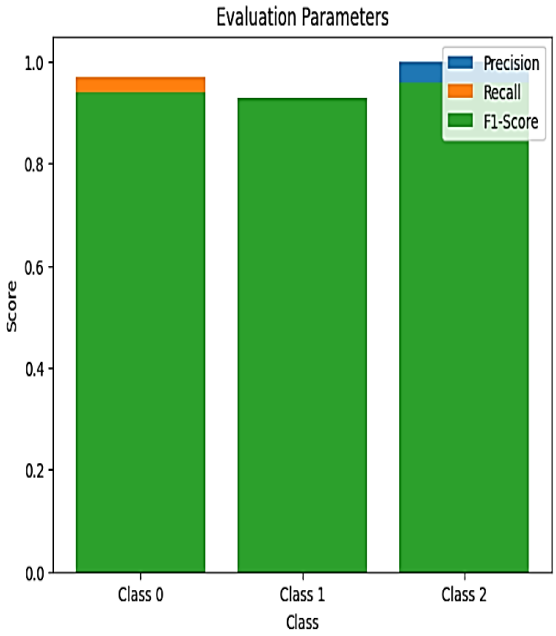

Figure 6. 24 RNN-LSTM score for knee extension.

The performance of the RNN-LSTM is represented in a bar chart indicating the score for each class. Figure 6.22 shows a graph for the gait exercise, while Figures 6.23 and 6.24 also indicate the graph for knee lifting and knee extension respectively for the RNN-LSTM model.

6.7 Transformer Model

In this study, the novel transformer model was applied for the movement classification. The transformer model is a deep learning architecture based on a parallel multi-header attention mechanism. This model was first proposed in 2017 by Vaswani et al [96] in the article "Attention Is All You Need". The model is based on the concept of attention and removes the need for periodic connections and convolution. The transformer model uses the self-attention mechanism to process tokens in sequence simultaneously and calculate attention weights between them in successive layers. The Transformer model has some advantages over traditional and deep learning techniques. The Transformer model is faster in training time, performs better for long sequences, and can process strings in parallel. This is because the transformer model has a self-attention mechanism, which allows the model to focus on the relevant parts of the input sequence. This makes the model more efficient than the current deep-learning techniques. Transformer model has proven to outperform deep learning models, such as RNN and CNN, in several natural language processing (NLP) tasks, including machine translation, text synthesis, and sentiment analysis.

6.7.1 Transformer Model Architecture

The transformer architecture uses the stacked self-attention and connecting point layers for the encoder, and the decoder is illustrated from the left half to the right, as shown in Figure 6.24. The encoder is made up of a stack of N=6 identical layers [97]. Each layer of the model has two sub-layers. The first part of the architecture is the multi-headed self-attention mechanism, and the second part is a simple, fully connected location-based prediction network. The output of each sublayer is given by LayerNorm (x + Subclass(x)), where the Subclass(x) is a function performed by the sublayer. The decoder includes a stack of N=6 identical layers. Further to the two sublayers in each encoder layer, the decoder puts in a third sublayer that performs multi-head attention above the output of the encoder stack. The output is calculated as the weighted sum of the values, in which the weight is assigned to each value computed using the query with a corresponding key. Below is an image of the transformer model shown in [Figure 6.25] below.

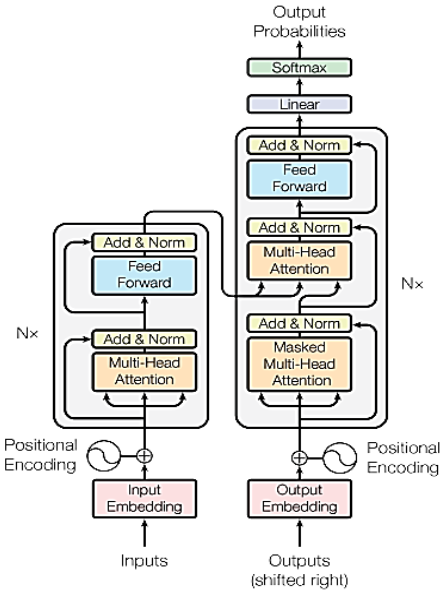

Figure 6. 25 Transformer Architecture model

The mathematical expression of the transformer model can be expressed in the following equations.

The transformer has parameterised function class, $f_\theta : \mathbb{R}^{n\ x\ d} \longrightarrow \mathbb{R}^{n\ x\ d}$. If $x \in \mathbb{R}^{n\ x\ d}$ and then $f_\theta(x) = z$ whereby.

$$Q^{(h)}(\mathrm{x}_i) = W_{h,q}^T x_i, \quad K^{(h)}(\mathrm{x}_i) = W_{h,k}^T x_{i,}\ V^{(h)}(\mathrm{x}_i) = W_{h,v}^T x_i, \quad W_{h,q} W_{h,k} W_{h,v} \ \in \ \mathbb{R}^{d\ x\ k},$$

$$\alpha_{i,j}^{(h)} = softmax_j\left(\frac{\langle Q^{(h)}(x_i), K^{(h)}(\mathrm{x}_j)\rangle}{\sqrt{k}}\right), \tag{6.8}$$

6.7.2 Vision Transformer Model for Movement Classification

The Vision Transformer model (ViT) is used in sEMG-based motion classification by transforming the multi-channel sEMG signal into an image as input to the model [98]. The framework of the proposed motion classification method based on sEMG signals is shown in [Fig 6.26] below. The Vision Transformer model is based on the Transformer encoder. The multi-head attention is a very important block of the transformer encoder, that is used to learn the deep features of the sEMG signal. The proposed vision architecture framework is similar to the model used in [98] for the recognition of hand gesture. In this study a vision transformer framework was applied movement patterns classification.

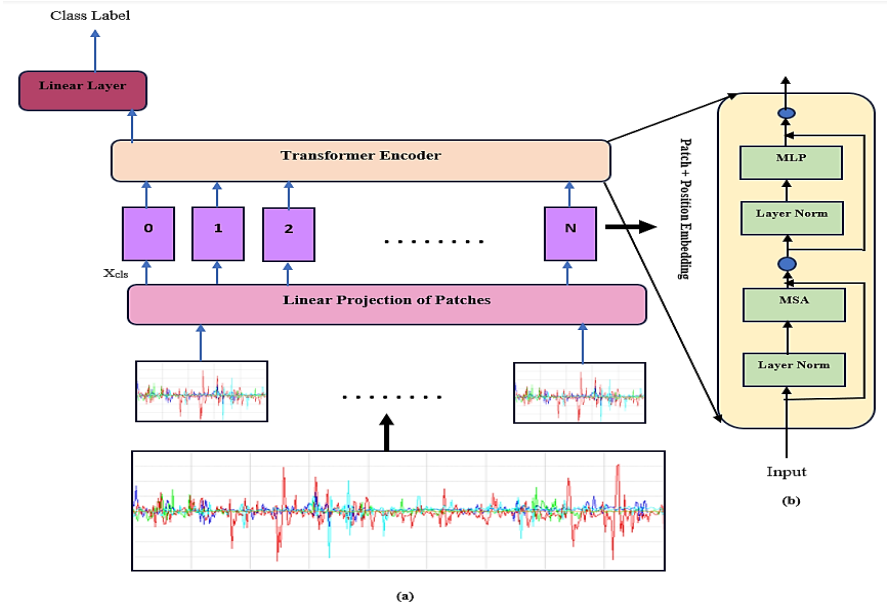

Figure 6. 26 Vision Transformer model for movement classification

Figure 6.26 indicates the graphical representation of the vision transformer model for recognition framework. The EMG signals are fed into the vision transformer model which is converted into small patches. The patches pass through a path plus position embedding layer whereby the class token is prepared. The prepared token of the class is then inputted into the transformer encoder. The transformer model has a combination of multi-head self-attention, multilayer perceptron, layer norms and two add layer. The ViT was trained using the synthetic EMG datasets generated for the gait, knee lifting, and knee extension exercises. This includes splitting the dataset into training and testing as well as setting the hyperparameters to optimise the model's performance. During the training phase of the model, different hyperparameters were tested to optimise the model's performance. This includes model architecture, such as the number of layers, attention heads, hidden dimensions, and batch sizes. In all, 80% (1284 samples) of the synthetic data generated was used for training, and 20% (321 samples) was used for testing the model's performance. In the training process a 10-fold cross validation was used to provide clearer evaluation of the ViT model for the movement classification The accuracy and loss were monitored to avoid overfitting of the model. The performance of the transformer model was then evaluated based on the accuracy, precision, recall, and F1 score.

The area under the curve plot represents the performance of the classification model, where the plot is useful in evaluating the classification models. Area under the curve (AUC) is a metric used to assess the performance of the Transformer model. The AUC curves were generated based on the classification threshold of 80%, which was set in the Transformer model in the testing of the dataset. The AUC in Figure 6.27 indicates the accuracy and loss of the transformer model in the gait exercise. Figures 6.28 and 6.29 show the knee lifting and extension performance of the model respectively.

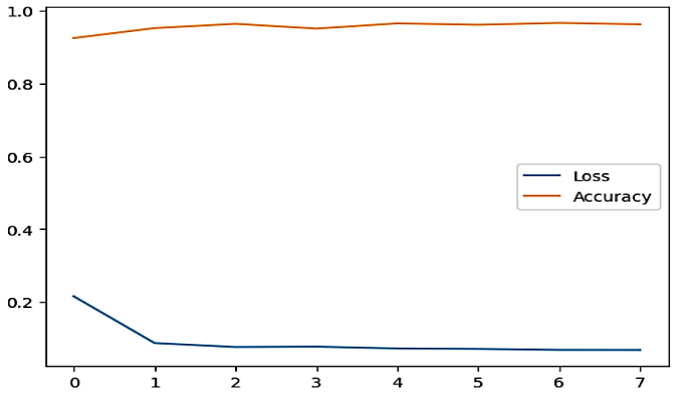

Figure 6. 27 AUC plot for gait classification

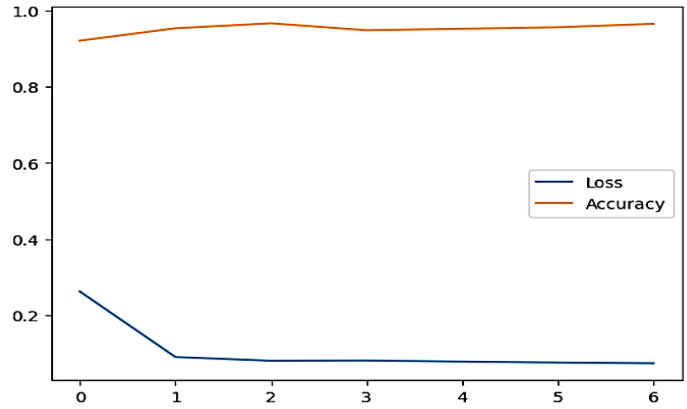

Figure 6. 28 AUC plot for knee lifting

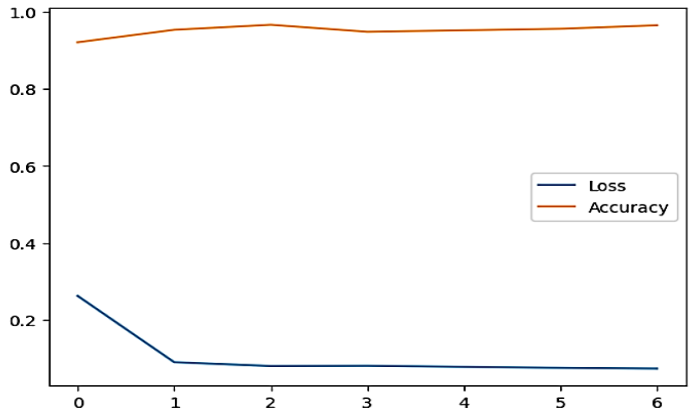

Figure 6. 29 AUC plot for knee extension

The ROC curve indicates the performance of the Transformer classification model for the true positive rate (TPR) versus false positive rate (FPR) for each dataset used. The curves are generated with TPR on the y-axis against FPR on the x-axis, indicating the different classification thresholds. Figure 6.30 shows the ROC plot and the degree separation of the classes in the gait exercise. Figures 6.31 and 6.32 illustrate the ROC for the knee lifting and knee extension exercise.

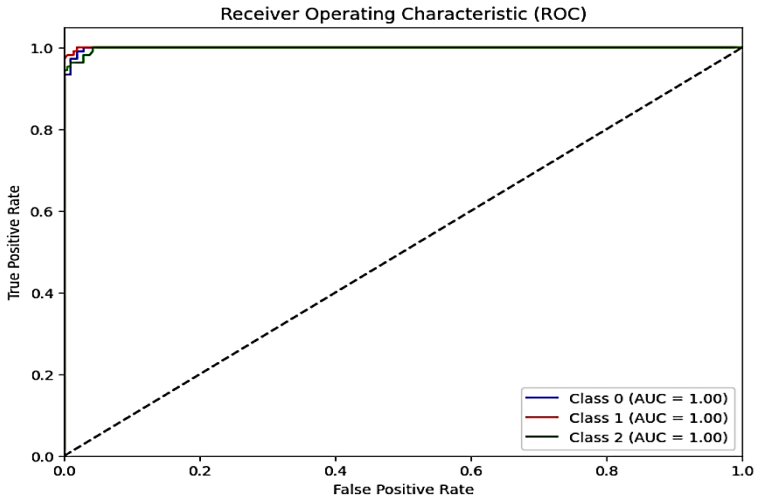

Figure 6. 30 ROC curve for gait using ViT model.

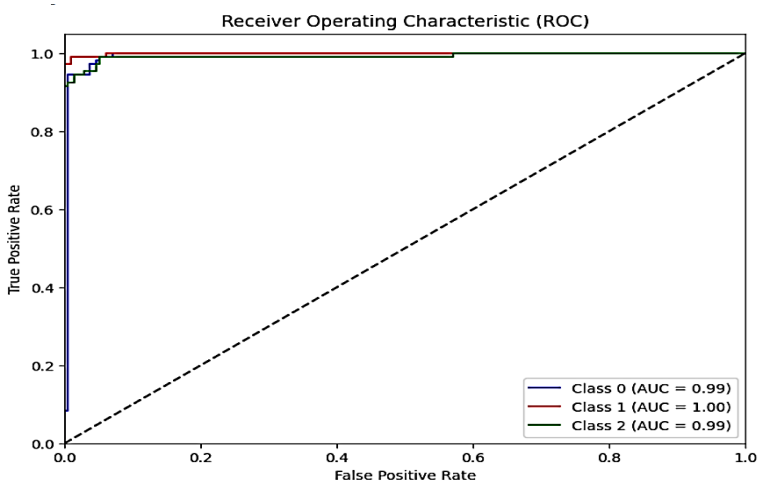

Figure 6. 31 ROC curve for knee lifting using ViT model.

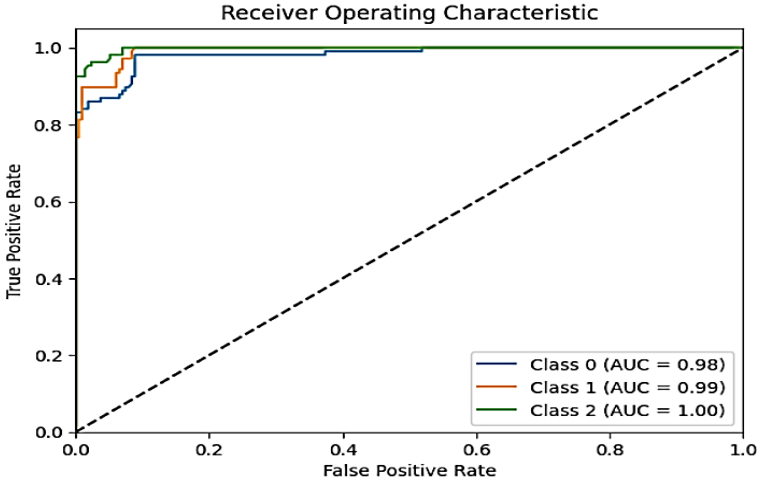

Figure 6. 32 ROC curve for knee lifting using ViT model.

The confusion matrix for the gait in Figure 6.33, indicating the score of the actual class and the predicted class in each category, with the true positive (TP) and true negative class (TN). Figures 6.34 and 6.35 show the confusion matrices for the knee lifting and knee exercise respectively, with some misclassifications indicating the false negative (FN) and false positive (FP) in the model's performance. Table 6.3 presents the classification score for each exercise using the transformer model.

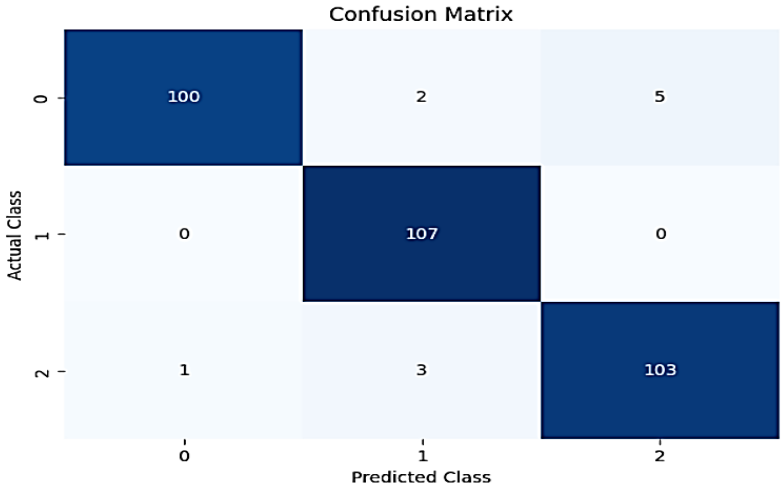

Figure 6. 33 ViT confusion matrix for gait exercise

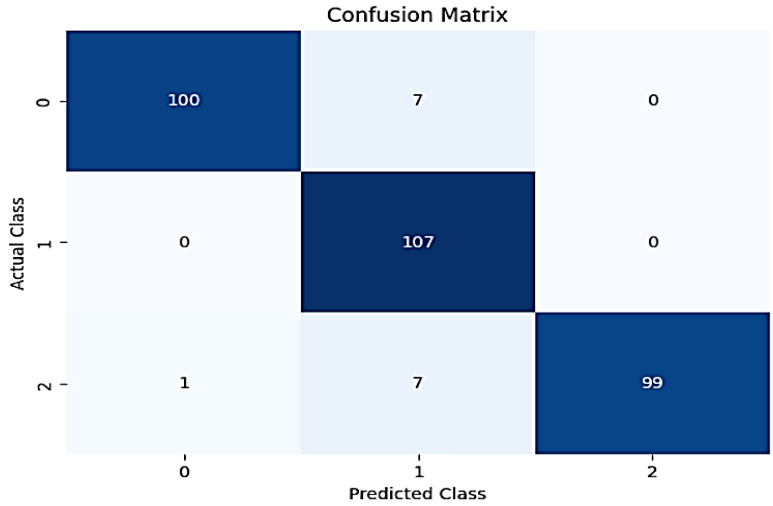

Figure 6. 34 Vit confusion matrix for knee lifting exercise.

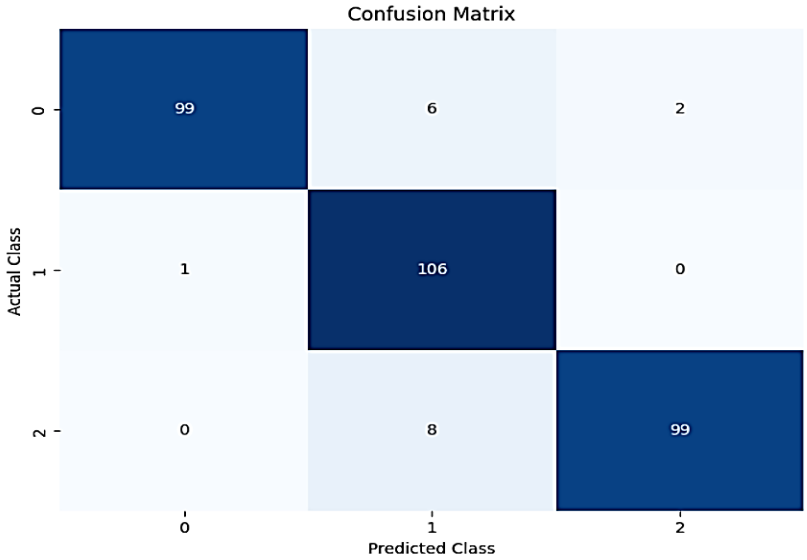

Figure 6. 35 ViT confusion matrix for knee extension exercise.

Table 6. 3 Performance of Vision Transformer model

Metrics		Gait	Knee Lifting	Knee Extension
Accuracy		0.97	0.94	0.96
Precision	Class 0	0.98	1.00	0.91
	Class 1	1.00	0.86	1.00
	Class 2	0.92	0.99	0.99
Recall	Class 0	0.93	0.92	0.99
	Class 1	0.97	0.99	0.97
	Class 2	0.99	0.93	0.93
F1-Score	Class 0	0.96	0.96	0.95
	Class 1	0.99	0.92	0.99
	Class 2	0.95	0.96	0.96

The plot in [Figure 6.36] shows the performance score for the exercises conducted using the ViT model. Figure 6.37 also indicate the performance metric score for precision, recall and F1-score for the different classes in the exercises conducted.

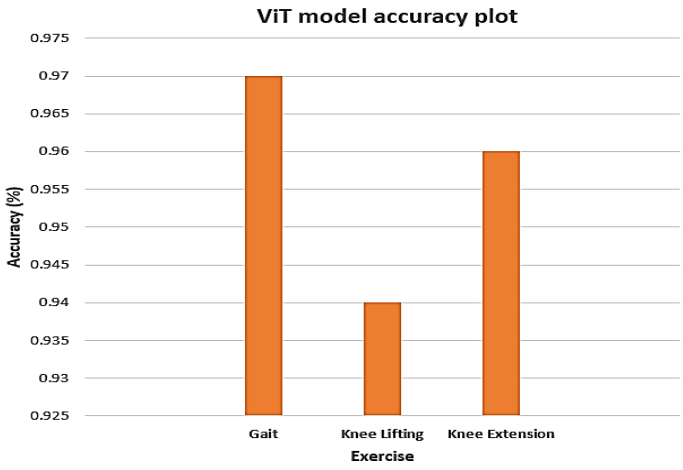

Figure 6. 36 ViT score for gait exercise.

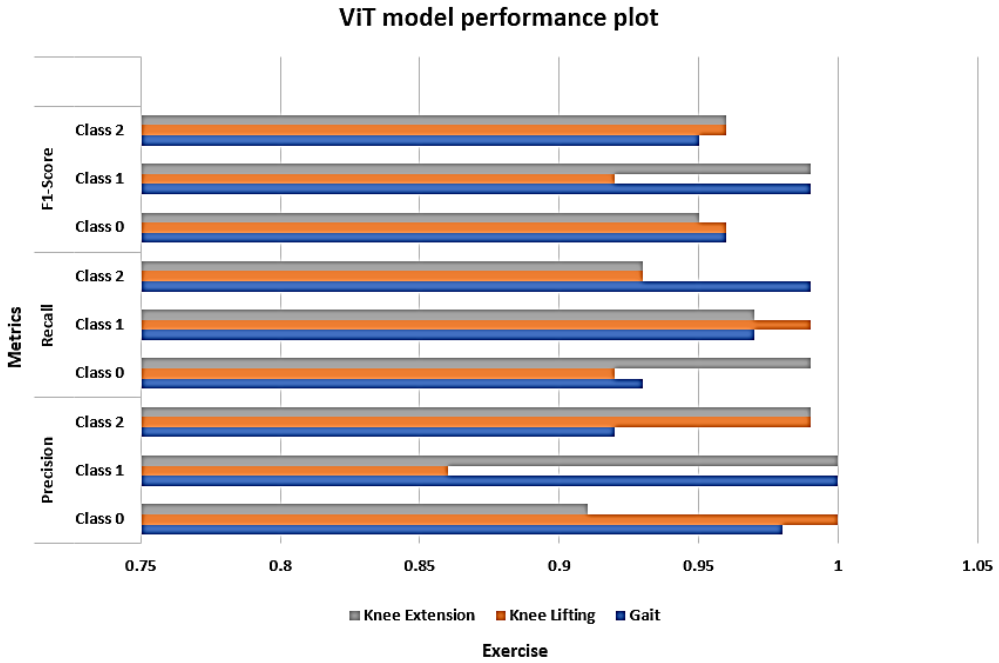

Figure 6. 37 ViT performance score

6.8 Summary

This chapter presents the results from deep learning classification using the simple RNN and LSTM-RNN. The vision Transformer model was also introduced as a new technique for classification in patients with PMR disease. The models used in the chapter were evaluated for their performance in the movement classification between patients and healthy control subjects. In the first phase, the simple RNN model was used for the classification of the gait pattern to observe the performance of the model. This was done with different optimisation algorithms to determine the performance of the RNN model. EMG metrics were also introduced to classify the severity or mild condition based on the EMG dataset recorded. In the second step, synthetic datasets were generated from a model designed using the actual EMG data recorded from patients. The synthetically generated dataset was used to train the LSTM-RNN and the Transformer model to evaluate their performance. The two models heavily depend on data in the classification to improve accuracy. The results indicate that an accuracy of 95% was achieved with LSTM-RNN for the gait exercise, while the vision Transformer model recorded 97%. Regarding the knee lifting exercise, the LSTM-RNN model recorded 92%, while the Transformer model scored

94%. Finally, the Knee extension exercise, the RNN-LSTM model achieved 94%, while the Transformer model scored 96% in the classification. Overall, the Transformer model improved the classification accuracy by a 2%. This was significant, and it helped to improve the accuracy in prediction of the movement patterns. This made some differences using the vision transformer model compared to the LSTM -RNN model. This indicates the significance of using a novel transformer technique in the classification of the movement pattern.

CHAPTER SEVEN: DISCUSSION

7.1 Overview

This chapter presents a discussion of the research findings and the contributions of the study as set in Chapter 1 as well as the clinical implications. The results from previous chapters are highlighted, along with how they meet the research objectives. The research hypotheses are tested to validate the assumptions of this research work based on the findings. The limitations of the results in this study are also outlined. In this chapter, the first section discusses the design of the low-cost MyoTracker's and its significance. The limitations of the designed MyoTracker and its broader implications are highlighted. The second section discusses the muscular imbalance assessment results and the implication of hip imbalances among patients. The third section discusses the offline movement classification results for patients and healthy control subjects. Both traditional machine and deep learning techniques are used in the classification. The section compared the movement patterns of PMR patients and healthy control subjects. In the fourth section, the main contributions of this thesis are presented, and the proposed therapeutic exercises to assist patients in rehabilitation.

7.2 Design of a Low-cost MyoTracker System

In chapter three of this study, a low-cost MyoTracker sensor was designed from scratch to monitor muscle strength in real-time. This meets the study's second objective to create an inexpensive system to record muscle activation signals via a mobile application. The problem was that existing low-cost EMG designs did not make provision to monitor muscle signals via a mobile app. The MyoTracker monitors muscle activities and allows users to view the muscle activation levels on a mobile phone. In the design, an easy-to-use Android application was built with Java Android studio to visualise EMG data received from the MyoTracker via Bluetooth connection. EMG signals were recorded to compute the strength of the muscles, where higher EMG signal amplitudes resulted in stronger muscle

contraction and vice versa. The designed MyoTracker system was calibrated with a commercial-based Delsys sensor to evaluate its performance. The Spearman's rank correlation coefficient and intra-class correlation (ICC) parameters were used to evaluate the designed MyoTracker sensor's reliability. The validation results indicated absolute agreement in the ICC with the range (0.74 to 0.92) for the two systems. The average intraclass correlation was recorded at 0.83, indicating a good to excellent agreement between the designed MyoTracker and the Delsys system. The validated results were compared to the work by Jang et al [99], illustrating the success of the designed MyoTracker system.

Comparing the MyoTracker to previously built low-cost EMG sensors, this was an improvement of previous designs. The works by Wu et al [47] and J. Fu et al [48] developed low-cost EMG sensors which were capable of recognising hand motion and predicting gestures. Even though these designs were significant, the sensors were not coupled to monitor muscle activities via mobile application. Furthermore, previous designs did not incorporated features to determine the strength of muscles in real-time. Considering the low-cost sensor that Supuk et al [49] designed to monitor muscular activities, the developed sensor did not incorporate a mobile app. Dombele et al [50] attempted to address this problem by building a mobile app to monitor muscle activation levels, but this fell short of determining muscle strength in real-time. The designed MyoTracker addressed this issue by enabling muscle strength determination via a mobile app in real-time. This approach was novel and seen as an improvement to previous works in the design of low-cost EMG sensors.

In the design of the MyoTracker, two challenges were encountered in the implementation stage. One challenge was the noise from the designed microcontroller base system. Some measures were implemented to mitigate the noise in the electrical components of the designed MyoTracker. Another limitation was that there are no clinically established range to segregate between weak or strong muscles based on the EMG signal. This study proposed a range to determine weak or strong muscles based on the amplitude of the muscle signals recorded within a specific duration. For weak muscles, the cumulative average amplitude signal range was between (0.1mV to 2.5mV) and for strong muscles, the

amplitude signal range was between (2.6mV to 5.0mV). This range was suitable for determining the strength of muscles.

There are benefits of the designed MyoTracker system, which has the potential for broader clinical application in future development. The system is suitable for assessing muscle fatigue in athletes conducting sports activity. The designed MyoTracker answers the research question on the potential of using this device as an alternative biomarker to monitor patients' progress. Regarding the practical implications, the MyoTracker device is promising for clinical deployment as it would be useful for clinicians to monitor the muscle activation levels of patients undergoing rehabilitation. It would also suit older people living in a care home with other musculoskeletal conditions. The MyoTracker would require further testing to improve its accuracy and reliability before manufacturing.

7.3 Assessment of Hip Muscular Imbalances

In Chapter five, the first iteration of this research was to investigate hip muscular imbalances in PMR patients and healthy control subjects. The maximum voluntary contraction (MVC) was used to evaluate the bilateral asymmetry difference of the hip muscles. The MVC was computed for each muscle on the right and then compared to the corresponding muscle on the left hip. A 10% threshold was set to be significant as the bilateral difference between the right and left hip muscles. The results in Table 5.1 in chapter five, showed that the MVC above 10% indicated muscle imbalances among patients. A few muscles found in patients, had the MVC values above 20% while majority of the muscles were above 10% threshold. For the healthy control subjects, the results indicated minimal imbalances below the 10% threshold. It must be stated that there were some exceptional instances where the healthy control subjects had MVC values above 10%. However, in general, there were massive imbalances among patients compared to health control subjects. The plots in [Figures 5.3, 5.4, and 5.6] from chapter five, indicated the hip muscular imbalance found in the gait, knee lifting, and knee extension, respectively. In general, on average patients had 15% MVC bilateral difference compared to an average 6% MVC for healthy control individuals. Therefore, patients exhibited significant muscular imbalances between

the hip muscles in patients as opposed to healthy control individuals. The factors that accounted for the hip muscular imbalance may be muscle denervation. Another factor that may have precipitated the imbalances can be attributed to the stress in the muscle tendons and hip joints. This results in muscle fatigue and, thus, uneven strength between the hip muscles.

Comparing the findings of this research with previous work showed some resemblance in the results obtained. Nadler et al [77] demonstrated the side-by-side muscle force difference to determine muscular imbalances. The hip muscles were used to determine muscular imbalance, whereby the logistic regression analysis indicated the difference of P=0.05 as significant. In the findings by Hides et al [100], MRI scan was used to conduct imbalance by examining the cross-section area (CSA) of the trunk and pelvic muscles. The variation in the size of the trunk muscles was evidence of muscular imbalance. Even though this technique was good in muscular imbalance assessment, the approach is quite expensive. This study compared the bilateral asymmetry between the right and left hip muscles which is seen as an inexpensive approach to determine imbalances as against MRI scans. The works by Amir et al [76] and Jorge et al [75] illustrated different approaches for imbalance assessment. In analysing the work by Amir, the findings showed that subjects with iliotibial band (ITB) and those without ITB of lower back pain experienced imbalances. The results by Jorge indicated the bilateral difference and the hamstring/quadriceps ratio were sufficient in muscular imbalance assessment among athletes. The MVC values above 10% were significant in identifying muscular imbalance. Similarly, the asymmetry bilateral difference of the MVC above 10% was set to be substantial to identify muscular imbalances.

The results in this thesis indicated that PMR patients had significant muscular imbalances compared to healthy control subjects. These imbalances may further worsen the hip and joint pains that could lead to difficulty in mobility if not addressed. Furthermore, the imbalances could exacerbate the symptoms of the disease with an increase in muscle fatigue. In addition, the hip muscular imbalance may alter patients' knee and hip joints over time. Therefore, patients would try to compensate for the

weak hip muscles by changing their movement pattern, which only leads to further pains in the knee and hip joints. The findings of this study are novel, and it validated the study's second hypothesis which anticipate imbalances among patients. In addition, the third objective of this study is achieved by comparing the hip muscular activities between patients and healthy controls to identify imbalances. The findings proved that patients have higher hip muscular imbalances than healthy control subjects. This results also answers the third research question that there are substantial imbalances in patients' hip muscles. The limitation of this results is that, only MVC was considered but other factors such as the timing and muscle activation patterns were not considered. Nevertheless, the MVC was sufficient to demonstrate muscular imbalance among patients. The findings provide relevant information to clinicians to address the problem of hip muscular imbalances. Muscular imbalance could lead to poor posture and further exacerbation the symptoms in individual patients.

7.4 Movement Classification with Machine Learning Algorithms

This study aimed to investigate if PMR patients have altered movement patterns based on hip muscles activation. A clinical trial was conducted using non-invasive EMG sensors to identify patients' specific movement patterns and compare them to healthy control subjects. This was to provide a better understanding of the pathophysiology of PMR patients. Identifying patients' specific movement patterns gave insight into the muscle's activation and its effect on the knee and hip joints. Other movement patterns, such as knee extension and knee lifting were also examined. Traditional machine learning algorithms and deep learning models were used for the offline movement classification. The machine learning algorithms used in the movement classification were SVM, DT, KNN, and KNN. In the training phase, the EMG datasets were analysed using python language in a 10-fold cross validation. SVM had an accuracy of 85% in classifying the gait patterns between PMR patients and healthy controls. The precision recorded was 85.7% as a measure of the correct predictions for the true positives (patients) and true negatives (healthy control) movement patterns. For the knee lifting exercise, an accuracy of 70% was recorded with a precision of 85% with the SVM algorithm. Regarding the knee

extension exercise, an accuracy of 65% was recorded with a precision of 64.2%. The next algorithm applied in the movement classification was the KNN, which recorded an accuracy of 75% and a precision of 78.57%. For the knee lifting exercise, an accuracy of 70% was recorded with a precision of 85.7%. Regarding the knee extension, an accuracy of 55% was recorded with KNN in classifying the movement patterns of the two groups. A precision of 50.0% recorded was not sufficient in identifying the knee extension patterns for the two groups. The third algorithm used for the movement classification was the rotation forest (RF). This algorithm is a variation of random forest that can accommodate classification using small datasets. The rotation forest algorithm had an accuracy of 80% in classifying the gait patterns between the two groups, with a precision of 85.7% recorded, indicating the true positives and negatives. Regarding the knee lifting, an accuracy of 65% was recorded with a precision of 85.7%. For the knee extension exercise, an accuracy of 70% was recorded with a precision of 71.4%. In terms of the decision tree (DT), an accuracy of 70% was recorded in classifying the gait patterns with a precision of 64.3%. For the knee lifting exercise, an accuracy of 60% was recorded with a precision of 57.1%. Regarding the knee extension, the accuracy recorded was 55%, and a precision of 71.4% in accurately predicting the true positives and negative outcomes.

Comparing the classification results from the traditional algorithms, SVM was the best in predicting the movement patterns between patients and health control subjects. RF performed significantly better ahead of the remaining two algorithms. DT was the least-performing algorithm in classifying the movement patterns. The movement patterns were plotted for each exercise to distinguish between patients specific movement as opposed to healthy control subjects. In chapter five, Figures 5.18 and 5.19 illustrated the gait plots for healthy control subjects and patients respectively. The plots indicate the difference in the movement patterns based on the muscle activation levels over time. From the plots in Figure 5.19, patients specific gait patterns had low amplitude levels signifying weaker muscle contractions. In contrast, in Figure 5.18, the healthy control subjects had higher amplitudes signifying strong muscle contraction. There is a correlation between the amplitude of EMG signal and muscle activation levels. It suggests that higher EMG signal amplitude is associated with higher levels

of muscle activation, indicating strong muscle contraction and better range of movement. On the other hand, lower muscle activation levels lead to weaker muscle contraction and thus reduced mobility. Similarly, in the knee lifting exercise, the movement patterns differed for that of healthy control subjects and patients in Figures 5.20 and 5.21 respectively. The plot for healthy control subjects indicated higher amplitudes with a gradual decline in muscle activation levels over time while patients had lower amplitudes in the muscle activation levels. As a result of the reduced functioning and weaker muscles in patients, the knee lifting movement patterns were modified compared to healthy control subjects. That showed that weaker muscle contraction resulted in altered movement patterns in patients compared to healthy control individuals. Regarding the knee extension exercise, Figures 5.22 and 5.23 plot showed the movement patterns for healthy control subjects and patients respectively. Here again, the movement patterns for healthy control subjects had higher amplitude levels resulting in stronger muscle contraction while patients had lower amplitude levels, which indicated weaker muscle contraction. Based on the muscle activation levels, it can be deduced that patient-specific movement patterns were altered compared to healthy individuals. It therefore be concluded that weaker muscle contraction in patients resulted in movement abnormality.

This results from the classification were compared to previous works which investigated the pathological features in classifying human movement using kinematic data [101]. Although kinematic data has some advantages, there are limitations when investigating the movement patterns of patients with musculoskeletal disease. EMG data is better and more widely used in classifying gait patterns in the clinical setting for patients with muscle disease. Furthermore, EMG data is more desirable in patients with musculoskeletal disease where muscle activation levels are desired. In addition, muscle signals provide a true reflection of the proximal neural control for human movement, which is more reliable. The results in this research were compared with recent works by Guo et al [32] and Fricke et al [102], which demonstrated EMG data for detecting gait abnormality. This study focused on polymyalgia rheumatica disease, where the hip muscle activation levels were considered in investigating movement impairments. There is evidence by Chakraborty et al [37] suggested that a

smaller number of muscle data is sufficient to distinguish between health and impaired gait patterns. Even though the analytical approach used is similar to this study, there were slight variations. In Chakraborty's work, the authors demonstrated gait disorders by analysing intrinsic features of muscle activation patterns. Three classification algorithms were used namely SVM, KNN, and CNN, to automatically classify the EMG patterns in detecting gait disorders between patients and healthy individuals. The automatic classification indicated normal and abnormal, with CNN achieving an accuracy of 91.9%, SVM recorded 67.6%, and KNN had 48.7%. Comparing the previous results with this research where an average accuracy of 77.5% was recorded to automatically classify the gait patterns between two groups. The results by Tenguku et al [104] indicated the classification of EMG signals to determine different tasks performed by patients with musculoskeletal disorders. Four machine learning algorithms KNN, LDA, NB, and SVM were implemented for the classification. The results showed that SVM outperformed other classifiers with more than 80% accuracy, and NB came closer with an accuracy of 73.33%. The results indicated that SVM was the most suitable algorithm for classifying EMG signals. Similarly, in this research, SVM was the best-performing algorithm for classifying movement patterns.

The findings from the offline classification of the movement pattern validated the study's first hypothesis which was patients with PMR disease have altered gait patterns due to the strained hip muscle. The hypothesis was tested against the results obtained in the movement classification using machine learning algorithms. This confirmed that patients have altered movement patterns compared to healthy control subjects. Furthermore, the main aim of this study was achieved based on the findings and therefore gait impairments were identified among patients with polymyalgia rheumatica disease. The second research question was also answered by illustrating that PMR patients have different movement patterns in knee lifting and extension exercises compared to healthy control subjects. This information is very essential to clinicians to identify patients-specific movement pattern in providing a guide to the design of rehabilitation protocols. The limitation of this result is that the hip and knee joints

angles were not considered. The dataset was also limited and imbalanced between the two groups. Nevertheless, the recorded EMG data provided enough granularity in the movement classification.

7.5 Deep Learning Techniques with LSTM-RNN and Vision Transformer

Deep learning models were applied in the movement classification using synthetic data generated from the recorded EMG data. The deep learning models were introduced in this study to mitigate the challenges with the traditional machine learning models. The RNN model was first used with the gait dataset to evaluate the model's performance. An average accuracy of 84.0% was recorded using different optimisers with the RNN model. Even though the performance of the simple RNN was good, in clinical classification, the goal was to further improve the accuracy. There was a need to distinguish patients movement based on the severe and mild conditions of the disease. The metrics used to segregate between severe and mild conditions among patients were the motor unit recruitment pattern and the interference pattern of the motor units. These two EMG features were computed using EMGworks software from Delsys. There was also a need to address the limitation of the small and imbalanced dataset previously. A model was designed to generate synthetic data and manage the limitations of the dataset. The synthetic datasets were generated for the gait, knee lifting, and knee extension exercises.

From the results recorded, the LSTM-RNN model in the gait classification had an accuracy of 95% with a precision of 96%. This indicated that the model was able to accurately predict the true positives and true negatives for each of the classes. Regarding knee lifting, the accuracy recorded was 92%, with a precision of 93%. For the knee extension, the accuracy recorded was 94% in predicting all three groups namely severe patients, mild patients, and healthy controls. The precision recorded was 95% successful in accurately predicting the true positives and true negatives using the model. The classification results recorded with the LSTM-RNN model were significant improvements in the classification compared to the machine learning. Even though the datasets used were different, the synthetic data allowed for an improvement in the accuracy and precision in identifying different groups based on EMG signal. For the vision Transformer (ViT) model, an accuracy of 97% was recorded for

gait with a precision of 96% in predicting for the three groups. This indicates the model correctly predicted the true positives and negatives for each category. When it comes to knee lifting, the accuracy recorded was 94% in predicting all instances. The precision recorded was 95% among the three groups in accurately predicting the true positives and true negatives. For the knee extension, the accuracy was 96%, with a precision of 97% in the classification. The RNN-LSTM and vision Transformer models performance were compared, and it was noted that the vision Transformer was better. The vision Transformer was able to improve the accuracy and precision by 2% when compared with the RNN-LSTM model. This shows the novel vision Transformer model as the best deep model for the movement classification of patients and healthy controls.

Comparing the results using a vision Transformer for surface EMG classification with previous works indicates some improvements in this study. The results by Montazerin at al [104] demonstrate the use of ViT to classify gestures using sEMG signals with an average accuracy of 84.62 ± 3.07% being recorded. In this study, the results with ViT had an accuracy of 94 ± 3% for the different movement classifications. In another study by Shen et al [105], the results from a convolutional vision transformer had an accuracy of 83.47% and 84.09% with a windows length of 200ms and 300ms respectively. Similarly, in this study, the accuracy recorded was above 92% for the different movement classification patterns with a window length of 300ms. The results from Zhang et al [106] demonstrated the use of ViT for lower limbs classification in motion recognition. An accuracy of 94.62% was recorded with signals from multichannel Mechamyography (MMG) and kinematic data. A comparison of the results by Zhang and the results in this study showed an accuracy of up to 97%. Therefore, the ViT model used in this study illustrated significant improvement of the model compared to previous results. The second aim of this study was achieved by using EMG signals to determine the severity of the disease among patients. This research findings demonstrate the efficiency of using a novel vision Transformer for movement classification. Furthermore, the results from deep learning classification validated the third and fourth hypotheses of this study. The third hypothesis was proven that EMG signals can efficiently determine the severity of PMR among patients and are useful for offline

diagnostic of the disease. Therefore, the EMG signals recorded from the hip muscles can determine the severity of PMR disease among patients. The four hypothesis was also validated, demonstrating that hip muscle activation patterns can be used to diagnose polymyalgia rheumatic. The findings also answer the research question and illustrate deep learning models can support the diagnosis of polymyalgia rheumatica disease. Furthermore, the results showed that the most efficient deep learning algorithm for movement classification is the ViT model.

7.6 Main Contributions of the Study and Clinical Implications

The main contributions of the research are outlined in five key points:

- A novel patient-specific gait pattern of polymyalgia rheumatica disease in a clinical trial was established. This indicates patients have impaired gait patterns compared to healthy control subjects. This is the first study to provide empirical evidence of gait impairment among PMR patients, to the best of my knowledge.
- This study established significant hip muscular imbalances among PMR patients compared to healthy control subjects. These imbalances further worsen the conditions among patients and make it difficult to perform routine daily activities.
- This study also proved patients have altered movement patterns in the knee lifting and knee extension exercises compared to healthy control subjects.
- A novel approach using vision Transformer model and EMG signals to determine the severity of PMR disease among patients. This can also be used to segregate between patients with severe conditions and those with mild conditions with high accuracy and precision.
- The designed low-cost MyoTracker system can potentially serve as an alternative biomarker to monitor the progress of patients in rehabilitation. This study introduced a unique component in the development of the MyoTracker, which can be used to determine the status of a muscle in real time.

The movement classification patterns of polymyalgia rheumatica patients using EMG signals provides useful information to clinicians. Firstly, the study established that there is gait impairment based on hip muscle activation which answers the main research problem. This is significant and will help clinicians design specific exercises to assist patients in their recovery process. This allows for intervention to correct the gait impairment and reduce the risks of fall injuries or poor posture. This study also demonstrated that both traditional machine learning and deep learning algorithms can be used in the offline classification to augment the diagnosis of PMR disease. By accurately classifying the movement patterns, this can be used to build a decision support system for diagnosing the disease. The movement patterns classification is also suitable for developing an effective rehabilitation protocol as part of the treatment plan for PMR patients. By accurately classifying patients' specific movement patterns, clinicians and physiotherapists can tailor treatment plans to meet patient-specific needs. Another implication of the findings is that EMG signals are suitable to monitor the progression of the disease in patients. Clinicians can monitor the changes in muscle activity in patients and evaluate the effectiveness of the treatment plans by tracking the muscle activation levels periodically for proper evaluation.

7.7 Proposed rehabilitation protocols

One objective of the study is to propose therapeutic exercises that can augment the existing rehabilitation protocols for clinicians. The proposed rehabilitation protocols below were studied and suggested in collaboration with the clinicians at KATH hospital aiming to improve patient outcome. These exercises proposed would support patients at the physiotherapy along with already existing exercises [107]. These exercises can help strengthen the hip muscles and minimise muscular fatigue that leads to the imbalances among PMR patients. The following exercises were recommended.

Hip bridge: With this type of exercise, patients lie on their back and then with their knees and feet on the floor. Patients then lift their hips gently upwards by squeezing their glutes at the top. This can be done repeatedly for 5-10 times each morning.

Hip Rotation: With this exercise, the patients lie on their side way on the floor. One leg is slightly lifted at approximately an angle of 60 degrees and gently rotates the leg for 2 minutes, turns on the other side, and repeats the process. This can be done for a repetition of 5-10 steps at an individual pace to assist the muscles strengthening.

Single leg Balancing: For this exercise, the patients stand on one leg with hands on their hips. They should hold on to the position for approximately 15 to 30 seconds. After that, a repetition on the other side of the leg for 5-10 different laps.

Adjusted Step-ups: This exercise differs from the usual step-ups exercise. Here, patients stand up from sitting on a chair, take a step forward, and then bring the other format to meet the foot. The patients step backward again with one leg back and the other foot fellows backward. The patient resumes a sitting position on the chair. This exercise can be repeated for 5-10 steps at a comfortable pace for individual patients.

Adaptive squats: For this exercise, patients are required to squat slowly at a 60-degree angle to improve muscle fatigue. Patients should put on knee support bandages before patients attempting the exercise. With the patient's hands on the hip, they can be done gently due to pre-existing muscle pains.

These proposed exercises would argument existing protocols in supporting patients in their rehabilitation. The proposed therapeutic exercises can address muscular imbalances and improve the range of hip joint motion. The combination of existing rehabilitation protocols and the proposed exercises in this study will help improve movement. This would also minimise muscle pain and other limitations during the movement. Clinicians can review the therapeutic exercise periodically and tailor it to individual patients' needs.

7.8 Summary

This chapter presents the discussion based on the study's findings and its clinical implication for patients with polymyalgia rheumatica disease. The chapter also presents the implications of the results and the

limitations based on the findings. The four hypotheses of the study are tested, and the research questions are answered based on the results obtained. The main contribution of this research is outlined together with the wider application for the management of patients. The chapter also proposes therapeutic exercises that can be used to support rehabilitation protocols for patients' treatment process.

CHAPTER EIGHT: CONCLUSION AND FUTURE WORK

8.1 Conclusion

This study conducted a clinical trial on movement assessment for patients with polymyalgia rheumatica disease at Komfo Anokye Teaching Hospital (KATH) in Ghana. The study aimed to investigate the gait and other movement patterns to provide a better understanding on the pathophysiology of PMR patients. The main research problem was the lack of clarity and uncertainty weather PMR disease affects the movement pattern of patients. The early detection of gait abnormality provided clinicians with the needed information to take appropriate measures to address the mobility limitation. The study compared the movement patterns of patients with PMR disease and those of healthy control subjects using EMG data from the hip muscle activation. Another objective was to conduct a hip muscular imbalance assessment between patients in two groups. Furthermore, the research also sought to determine if the EMG signals can be used to determine the severity of the condition in patients. In the first step, an extensive literature review was conducted to identify the gap in research and the focus of the problem to be resolved, forming the study's first objective. A MyoTracker EMG system was designed to monitor muscles using inexpensive electronic equipment. The designed MyoTracker allowed users to monitor muscles strength via a mobile app in real time.

The methodology applied in the clinical trial was a qualitative approach where the movement of patients and healthy control subjects were observed in the gait, knee lifting, and knee extension exercise. Commercial-based EMG sensors were used to record hip muscle signals from patients and healthy control subjects. The clinical trial was conducted for two months between August and September 2022, with ethical approval granted by Brunel University London and KATH Hospital in Ghana. This thesis had three main iterations to achieve the main aims and objectives of the research work. The first iteration was the hip muscular imbalances assessment, where the MVC was computed for right and left hip muscles. The second iteration was the offline movement classification using

traditional machine learning algorithms. The third iteration was the application of deep learning techniques for classification to determine the severity of the disease using synthetic data.

The findings of this study meet the aims and objectives as set in the beginning. In the first objective, an extensive literature review was published on movement disorders. In the second objective, an inexpensive MyoTracker system was designed to monitor and determine muscle strength in real-time. The validation of the designed MyoTracker device indicated its potential to serve as an alternative to a commercial system. The research's first iteration showed significant patient imbalances compared to healthy control subjects. In the second iteration, it was established that patients had gait impairments compared to healthy control individuals. Therefore, the study's main aim was achieved indicating the altered movement patterns based on their hip muscle activation. The third iteration indicated that the RNN-LSTM model and the vision Transformer (ViT) had significant performance in the classification polymyalgia rheumatica disease. The EMG parameters were capable of determining the severity of polymyalgia disease among patients. The second aim of the study was achieved with the deep learning models to demonstrate the offline diagnose of the severity of PMR disease among patients. It was noted that the ViT model performed better compared to the RNN-LSTM in the classification. One key limitation of this work is the limited dataset used in the classification. Another limitation was the hip and knee joints angles were also not considered in this study. Nevertheless, the findings were significant and achieved the overall aims and objectives of the study. These findings are significant for clinicians to design solutions in the form of therapy to assist patients in their recovery process. In addition, the findings allowed for intervention to correct gait impairment and reduce the risks of fall injuries.

8.2 Future Work

This study has the following recommendations for future works in the investigations of the movement of PMR disease. Firstly, the design of the MyoTracker device will need further research to explore the capabilities of using alternative power sources for the device. Further research and testing are required before the device can be manufactured in large quantities for commercial use. The second recommendation for further research is the real-time classification of movement patterns that will assist clinicians in monitoring and determining muscle controls. Researchers can explore the capabilities of a real-time classification of EMG signals of polymyalgia rheumatica disease to assess movement patterns. This will allow for the early detection of gait abnormalities clinicians in real-time. Future research can also explore the development of new technologies that can support the diagnostics of PMR disease in real-time. A decision support system can be designed to provide timely feedback to clinicians to assist patients in their treatment process. The design decision support system would guide patients by keeping track of their progress. Continuous monitoring over sometime during rehabilitation would give the necessary feedback to clinicians. Finally, future work should also evaluate the effectiveness of the proposed therapeutic exercises in this study. This would determine the intensity of the exercises and patients' responses to the treatment plan. This will help improve the symptoms experienced by PMR patients and provide better mobility for individuals.

Bibliography

[1] Jovanov, Emil, et al. "Patient monitoring using personal area networks of wireless intelligent sensors." *Biomedical Sciences Instrumentation* 37 (2001): 373-378.

[2] H. Alabbasi, A. Gradinaru, F. Moldoveanu and A. Moldoveanu, "Human motion tracking & evaluation using Kinect V2 sensor," *2015 E-Health and Bioengineering Conference (EHB)*, Iasi, 2015, pp. 1-4, doi:10.1109/EHB.2015.7391465.

[3] Saljoughian, M. (2012). Polymyalgia rheumatica: A severe, self-limiting disease. U.S. Pharmacist. 37

[4] Nesher G, Nesher R. Giant cell arteritis and polymyalgia rheumatica. In:Ball GV, Bridges Jr SL, editors. Vasculitis. 2nd ed. Oxford University Press; 2008.

[5] National Academies Press (US); 2020 Apr 21. 5, Musculoskeletal Disorders. Available from: https://www.ncbi.nlm.nih.gov/books/NBK559512/

[6] Cup, Edith H., et al. "Exercise therapy and other types of physical therapy for patients with neuromuscular diseases: a systematic review." *Archives of physical medicine and rehabilitation* 88.11 (2007): 1452-1464

[7] Miguel A González-Gay, Eric L Matteson, Santos Castañeda, "Polymyalgia rheumatica", The Lancet, Volume 390, Issue 10103, 2017, Pages 1700-1712, ISSN 0140-6736, https://doi.org/10.1016/S0140-6736(17)31825-1.

[8] Yates M, Graham K, Watts RA, MacGregor AJ. "The prevalence of giant cell arteritis and polymyalgia rheumatica in a UK primary care population". BMC Musculoskeletal Disorder 2016; 17: 285.

[9] Salvarani C, Cantini F, Hunder GG. "Polymyalgia rheumatica and giant-cell arteritis". *Lancet*.2008;372(9634):234-245.

[10] John Haughton, Central Health Physiotherapy, Polymyalgia Rheumatica Available from: https://www.central-health.com/blog

[11] Fraser, J Alexander et al. "The treatment of giant cell arteritis." *Reviews in neurological diseases* vol. 5,3 (2008): 140-52

[12] Pirker, Walter, and Regina Katzenschlager. "Gait disorders in adults and the elderly: A clinical guide." *Wiener Klinische Wochenschrift* 129.3-4 (2017): 81-95.

[13] Miller, Robert A., et al. "Components of EMG symmetry and variability in parkinsonian and healthy elderly gait." *Electroencephalography and Clinical Neurophysiology/Electromyography and Motor Control* 101.1 (1996): 1-7.

[14] D. A. Winter, Biomechanics and Motor Control of Human Movement: Fourth Edition. 2009

[15] Brancati, Renato, et al. "Experimental measurement of underactuated robotic finger configurations via RGB-D sensor." *International Conference on Robotics in Alpe-Adria Danube Region*. Cham: Springer International Publishing, 2018.

[16] Müller, Björn, et al. "Validation of enhanced Kinect sensor based motion capturing for gait assessment." *PloS one* 12.4 (2017): e0175813.

[17] Prathap C and S. Sakkara, "Gait Recognition using skeleton data," 2015 International Conference on Advances in Computing, Communications and Informatics (ICACCI), Kochi, India, 2015, pp. 2302-2306, doi: 10.1109/ICACCI.2015.7275961.

[18] A. S. M. H. Bari and M. L. Gavrilova, "Artificial Neural Network Based Gait Recognition Using Kinect Sensor," in *IEEE Access*, vol. 7, pp. 162708-162722, 2019, doi: 10.1109/ACCESS.2019.2952065.

[19] A. Amini, K. Banitsas and S. Hosseinzadeh, "A new technique for foot-off and foot contact detection in a gait cycle based on the knee joint angle using microsoft kinect v2," *2017 IEEE EMBS International Conference on Biomedical & Health Informatics (BHI)*, Orlando, FL, 2017, pp. 153-156, doi: 10.1109/BHI.2017.7897228.

[20] S. Bei, Z. Zhen, Z. Xing, L. Taocheng and L. Qin, "Movement Disorder Detection via Adaptively Fused Gait Analysis Based on Kinect Sensors," in *IEEE Sensors Journal*, vol. 18, no. 17, pp. 7305-7314

[21] Aleš Procházka, Oldřich Vyšata, Martin Vališ, Ondřej Ťupa, Martin Schätz, Vladimír Mařík, "Bayesian classification and analysis of gait disorders using image and depth sensors of Microsoft Kinect," Digital Signal Processing, Volume 47, 2015,Pages 169-177,ISSN 1051-2004

[22] A. Ismail, H. Shouman, A. Cherry and M. Hajj-Hassan, "Torwads real time kinect anlysis system for early diagnosis of gait cycle abnormalities," 2017 Fourth International Conference on Advances in Biomedical Engineering (ICABME), Beirut, 2017, pp. 1-4, doi: 10.1109/ICABME.2017.8167576.

[23] Setsuki Tsukagoshi, Minori Furuta, Kimitoshi Hirayanagi, Natsumi Furuta, Shogo Nakazato, Motoaki Fujii, Yasushi Yuminaka, Yoshio Ikeda,"Noninvasive and quantitative evaluation of movement disorder disability using an infrared depth sensor" Journal of Clinical Neuroscience, Volume 71, 2020, Pages 135-140, ISSN 0967-5868

[24] Kozlow P, Abid N, Yanushkevich S. Gait Type Analysis Using Dynamic Bayesian Networks. *Sensors*. 2018; 18(10):3329. https://doi.org/10.3390/s18103329.

[25] D. -W. Lee, K. Jun, S. Lee, J. -K. Ko and M. S. Kim, "Abnormal Gait Recognition Using 3D Joint information of Multiple Kinects System and RNN-LSTM," 2019 41st Annual International Conference of the IEEE Engineering in Medicine and Biology Society (EMBC), Berlin, Germany, 2019, pp. 542-545, doi: 10.1109/EMBC.2019.8857607

[26] A. Elkholy, M. E. Hussein, W. Gomaa, D. Damen and E. Saba, "Efficient and Robust Skeleton-Based Quality Assessment and Abnormality Detection in Human Action Performance," in IEEE Journal of Biomedical and Health Informatics, vol. 24, no. 1, pp. 280-291, Jan. 2020, doi: 10.1109/JBHI.2019.2904321.

[27] Nüesch, Corina, et al. "Gait patterns of asymmetric ankle osteoarthritis patients." *Clinical Biomechanics* 27.6 (2012): 613-618

[28] Z. Kang, M. Deng and C. Wang, "Frontal-view human gait recognition based on Kinect features and deterministic learning," *2017 36th Chinese Control Conference (CCC)*, Dalian, 2017, pp. 10834-10839, doi: 10.23919/ChiCC.2017.8029085

[29] System, D. Delsys Europe. 2021. Available online: https://delsys.com/trigno-avanti/ (accessed on 4 June 2022)

[30] Anwary, Arif Reza, Hongnian Yu, and Michael Vassallo. "An automatic gait feature extraction method for identifying gait asymmetry using wearable sensors." *Sensors* 18.2 (2018): 676

[31] Di Nardo, Francesco, et al. "A new parameter for quantifying the variability of surface electromyographic signals during gait: The occurrence frequency." *Journal of Electromyography and Kinesiology* 36 (2017): 25-33.

[32] Y. Guo, R. Gravina, X. Gu, G. Fortino and G. -Z. Yang, "EMG-based Abnormal Gait Detection and Recognition," 2020 IEEE International Conference on Human-Machine Systems (ICHMS), 2020, pp. 1-6, doi: 10.1109/ICHMS49158.2020.9209449

[33] Cole, Bryan T., Serge H. Roy, and S. Hamid Nawab. "Detecting freezing-of-gait during unscripted and unconstrained activity." *2011 Annual International Conference of the IEEE Engineering in Medicine and Biology Society*. IEEE, 2011

[34] Nor, MN Mohd, R. Jailani, and N. M. Tahir. "Analysis of EMG signals of TA and GAS muscles during walking of Autism Spectrum Disorder (ASD) children." *2016 IEEE Symposium on Computer Applications & Industrial Electronics (ISCAIE)*. IEEE, 2016.

[35] Mazzetta, Ivan, et al. "Wearable sensors system for an improved analysis of freezing of gait in Parkinson's disease using electromyography and inertial signals." *Sensors* 19.4 (2019): 948.

[36] S. Potluri, S. Ravuri, C. Diedrich and L. Schega, "Deep Learning based Gait Abnormality Detection using Wearable Sensor System," 2019 41st Annual International Conference of the IEEE Engineering in Medicine and Biology Society (EMBC), 2019, pp. 3613-3619, doi: 10.1109/EMBC.2019.8856454

[37] Chakraborty, Jayeeta, and Anup Nandy. "Discrete wavelet transform based data representation in deep neural network for gait abnormality detection." *Biomedical Signal Processing and Control* 62 (2020): 102076.

[38] Nair, Sumitra S., et al. "The application of machine learning algorithms to the analysis of electromyographic patterns from arthritic patients." *IEEE Transactions on Neural Systems and Rehabilitation Engineering* 18.2 (2009): 174-184.

[39] Vijayvargiya, Ankit, et al. "A hybrid WD-EEMD sEMG feature extraction technique for lower limb activity recognition." *IEEE Sensors Journal* 21.18 (2021): 20431-20439.

[40] Alexandra Villa-Forte Tests for Musculoskeletal Disorders Sept, 2022 Available Tests for Musculoskeletal Disorders - Bone, Joint, and Muscle Disorders - MSD Manual Consumer Version (msdmanuals.com)

[41] Shin Y, Yang J, Lee YH, Kim S. Artificial intelligence in musculoskeletal ultrasound imaging. Ultrasonography. 2021 Jan;40(1):30-44. doi: 10.14366/usg.20080. Epub 2020 Sep 6. PMID: 33242932; PMCID: PMC7758096.

[42] Gideon Nesher,"Polymyalgia rheumatica –Diagnosis and classification" Journal of Autoimmunity, Volumes 48–49, 2014, Pages 76-78,ISSN 0896-8411, https://doi.org/10.1016/j.jaut.2014.01.016.

[43] Dario Camellino, Christina Duftner, Christian Dejaco, New insights into the role of imaging in polymyalgia rheumatica, *Rheumatology*, 2020;, https://doi.org/10.1093/rheumatology/keaa646

[44] Nesher G, Nesher R. Giant cell arteritis and polymyalgia rheumatica. In:Ball GV, Bridges Jr SL, editors. Vasculitis. 2nd ed. Oxford University Press; 2008.

[45] Dasgupta, Bhaskar, et al. "2012 provisional classification criteria for polymyalgia rheumatica: a European League Against Rheumatism/American College of Rheumatology collaborative initiative." *Arthritis & Rheumatism* 64.4 (2012): 943-954.

[46] Fors, Charlotta, et al. "Validity of polymyalgia rheumatica diagnoses and classification criteria in primary health care." *Rheumatology Advances in Practice* 3.2 (2019): rkz033.

[47] Wu, Changcheng, et al. "A low-cost surface EMG sensor network for hand motion recognition." *2018 IEEE 1st International Conference on Micro/Nano Sensors for AI, Healthcare, and Robotics (NSENS)*. IEEE, 2018.

[48] Fu, Jianting, et al. "Design of a low-cost wireless surface EMG acquisition system." *2013 6th International IEEE/EMBS Conference on Neural Engineering (NER)*. IEEE, 2013.

[49] Supuk, Tamara Grujic, Ana Kuzmanic Skelin, and Maja Cic. "Design, development and testing of a low-cost sEMG system and its use in recording muscle activity in human gait." *Sensors* 14.5 (2014): 8235-8258.

[50] Dombele, Christopher, and Chen-Hsiang Yu. "MusCare: A Mobile Design for Muscle Monitoring." *2020 IEEE MIT Undergraduate Research Technology Conference (URTC)*. IEEE, 2020.

[51] Walter Lee (2018), An Unofficial Introductory Tutorial to MyoWare muscle sensor development kit. Available [Online] https://medium.com/@leex5202/an-unofficial-introductory-tutorial-to-myoware-muscle-sensor-development-kit-e2169948e63 Accessed June 2021

[52] Bluetooth Module, Available [Online] https://www.geeksforgeeks.org/all-about-hc-05-bluetooth-module-connection-with-android/ Accessed July 2021.

[53] Zanella, Andrea. "A mathematical framework for the performance analysis of Bluetooth with enhanced data rate." *IEEE Transactions on Communications* 57.8 (2009): 2463-2473.

[54] Arduino Uno Specification, Available [Online] https://www.elprocus.com/what-is-arduino-uno-r3-pin-diagram-specification-and-applications/ Accessed July 2021

[55] Reaz, Mamun Bin Ibne, M. Sazzad Hussain, and Faisal Mohd-Yasin. "Techniques of EMG signal analysis: detection, processing, classification and applications." *Biological procedures online* 8 (2006): 11-35.

[56] Gupta, Ashutosh, et al. "EMG signal analysis of healthy and neuropathic individuals." *IOP Conference Series: Materials Science and Engineering*. Vol. 225. No. 1. IOP Publishing, 2017.

[57] Heywood, Sophie, et al. "Low-cost electromyography–Validation against a commercial system using both manual and automated activation timing thresholds." *Journal of Electromyography and Kinesiology* 42 (2018): 74-80.

[58] Fuentes del Toro, Sergio, et al. "Validation of a low-cost electromyography (EMG) system via a commercial and accurate EMG device: Pilot study." *sensors* 19.23 (2019): 5214.

[59] Toro, Sergio Fuentes del, et al. "Is the use of a low-cost sEMG sensor valid to measure muscle fatigue?." *Sensors* 19.14 (2019): 3204.

[60] Molina-Molina, Alejandro, et al. "Validation of mDurance, a wearable surface electromyography system for muscle activity assessment." *Frontiers in Physiology* (2020): 1556.

[61] Plichta, Stacey B., and Elizabeth A. Kelvin. "Munro's statistical methods for health care research." (2013).

[62] Chaokromthong, Kajohnsak, and Nittaya Sintao. "Sample Size Estimation using Yamane and Cochran and Krejcie and Morgan and Green Formulas and Cohen Statistical Power Analysis by G* Power and Comparisions." *APHEIT International Journal* 10.2 (2021): 76-86.

[63] Delsys, I. EMGworks Analysis; Delsys Inc.: Natick, MA, USA, 2019

[64] Farina, Dario, and Aleš Holobar. "Characterization of human motor units from surface EMG decomposition." *Proceedings of the IEEE* 104.2 (2016): 353-373.

[65] De Luca, Carlo J., et al. "Filtering the surface EMG signal: Movement artifact and baseline noise contamination." *Journal of biomechanics* 43.8 (2010): 1573-1579.

[66] Raez MB, Hussain MS, Mohd-Yasin F. "Techniques of EMG signal analysis: detection, processing, classification and applications." Biol Proced Online. 2006;8:11-35. doi: 10.1251/bpo115. Epub 2006 Mar 23. Erratum in: Biol Proced Online. 2006;8:163. PMID: 16799694; PMCID: PMC1455479.

[67] Finsterer, Josef. "EMG-interference pattern analysis." *Journal of Electromyography and Kinesiology* 11.4 (2001): 231-246.

[68] Chowdhury, Rubana H., et al. "Surface electromyography signal processing and classification techniques." *Sensors* 13.9 (2013): 12431-12466.

[69] Al-Ayyad, Muhammad, et al. "Electromyography Monitoring Systems in Rehabilitation: A Review of Clinical Applications, Wearable Devices and Signal Acquisition Methodologies." *Electronics* 12.7 (2023): 1520.

[70] Gupta, Ashutosh, et al. "EMG signal analysis of healthy and neuropathic individuals." *IOP Conference Series: Materials Science and Engineering*. Vol. 225. No. 1. IOP Publishing, 2017.

[71] Fukuda, Thiago Yukio, et al. "Root mean square value of the electromyographic signal in the isometric torque of the quadriceps, hamstrings and brachial biceps muscles in female subjects." *J Appl Res* 10.1 (2010): 32-39.

[72] Phinyomark, Angkoon, et al. " Feature extraction of the first difference of EMG time series for EMG pattern recognition." *Computer methods and programs in biomedicine* 117.2 (2014): 247-256.

[73] Scott Frothingham, Gregory M., https://www.healthline.com/health/muscles-imbalance, Feb(2020), Accessed October 18,2022

[74] Wojdala, Grzegorz, et al. "Impact of the “Sling Shot” Supportive Device on Upper-Body Neuromuscular Activity during the Bench Press Exercise." *International Journal of Environmental Research and Public Health* 17.20 (2020): 7695

[75] Teixeira, Jorge, et al. "Isokinetic assessment of muscle imbalances and bilateral differences between knee extensores and flexores’ strength in basketball, football, handball and volleyball athletes." *Int J Sports Sci* 4.1 (2014): 1-6.

[76] Arab, Amir M., and Mohammad R. Nourbakhsh. "The relationship between hip abductor muscle strength and iliotibial band tightness in individuals with low back pain." *Chiropractic & osteopathy* 18.1 (2010): 1-5.

[77] Nadler, Scott F., et al. "The relationship between lower extremity injury, low back pain, and hip muscle strength in male and female collegiate athletes." *Clinical Journal of Sport Medicine* 10.2 (2000): 89-97.

[78] Meldrum, Dara, et al. "Maximum voluntary isometric contraction: reference values and clinical application." *Amyotrophic Lateral Sclerosis* 8.1 (2007): 47-55.

[79] Omuya, Erick Odhiambo, George Onyango Okeyo, and Michael Waema Kimwele. "Feature selection for classification using principal component analysis and information gain." *Expert Systems with Applications* 174 (2021): 114765.

[80] P. Diehl and G. Cauwenberghs, “Svm incremental learning, adaptation and optimization,” in Proceedings of the International Joint Conference on Neural Networks, 2003., vol. 4, pp. 2685–2690, IEEE, 2003

[81] H. H. Patel and P. Prajapati, “Study and analysis of decision tree-based classification algorithms,” International Journal of Computer Sciences and Engineering, vol. 6, no. 10, pp. 74–78

[82] M. Atzori, M. Cognolato, and H. Muller, “Deep learning with convolutional neural networks applied to electromyography data: A resource for the classification of movements for prosthetic hands,” Frontiers in neurorobotics, vol. 10, p. 9, 2016.

[83] Q. Zhang, L. T. Yang, Z. Chen, and P. Li, “A survey on deep learning for big data,” Information Fusion, vol. 42, pp. 146–157, 2018.

[84] D. Xiong, D. Zhang, X. Zhao, and Y. Zhao, “Deep learning for emg- based human-machine interaction: A review,” IEEE/CAA Journal of Automatica Sinica, vol. 8, no. 3, pp. 512–533, 2021.

[85] F. Quivira, T. Koike-Akino, Y. Wang, and D. Erdogmus, “Translating semg signals to continuous hand poses using recurrent neural networks,” in 2018 IEEE EMBS International Conference on Biomedical & Health Informatics (BHI), pp. 166–169, IEEE, 2018

[86] T. Sun, Q. Hu, P. Gulati, and S. F. Atashzar, “Temporal dilation of deep lstm for agile decoding of semg: Application in prediction of upper- limb motor intention in neurorobotics,” IEEE Robotics and Automation Letters, vol. 6, no. 4, pp. 6212–6219, 2021.

[87] Louart, Cosme, Zhenyu Liao, and Romain Couillet. "A random matrix approach to neural networks." *The Annals of Applied Probability* 28.2 (2018): 1190-1248.

[88] Simão, Miguel, Pedro Neto, and Olivier Gibaru. "EMG-based online classification of gestures with recurrent neural networks." *Pattern Recognition Letters* 128 (2019): 45-51.
[89] S. Kostadinov, Recurrent Neural Networks with Python Quick Start Guide: Sequential learning and language modeling with TensorFlow. Packt Publishing Ltd, 2018.
[90] Daroff, Robert B., and Michael J. Aminoff. *Encyclopedia of the neurological sciences*. Academic press, 2014.
[91] Reaz, Mamun Bin Ibne, M. Sazzad Hussain, and Faisal Mohd-Yasin. "Techniques of EMG signal analysis: detection, processing, classification and applications." *Biological procedures online* 8 (2006): 11-35.
[92] Mills, Kerry R. "The basics of electromyography." *Journal of Neurology, Neurosurgery & Psychiatry* 76.suppl 2 (2005): ii32-ii35.
[93] Petajan JH. AAEM minimonograph : motor unit recruitment. Muscle Nerve. 1991 Jun;14(6):489-502. doi: 10.1002/mus.880140602. PMID: 1852155.
[94] Chowdhury, Rubana H., et al. "Surface electromyography signal processing and classification techniques." *Sensors* 13.9 (2013): 12431-124
[95] Bolboacă, Roland, and Piroska Haller. "Performance Analysis of Long Short-Term Memory Predictive Neural Networks on Time Series Data." *Mathematics* 11.6 (2023): 1432.
[96] Vaswani, Ashish, et al. "Attention is all you need." *Advances in neural information processing systems* 30 (2017).
[97] Thickstun, John. "The transformer model in equations." *University of Washington: Seattle, WA, USA* (2021).
[98] Montazerin, Mansooreh, et al. "ViT-HGR: Vision transformer-based hand gesture recognition from high density surface EMG signals." *2022 44th Annual International Conference of the IEEE Engineering in Medicine & Biology Society (EMBC)*. IEEE, 2022.
[99] Jang, Myung Hun, et al. "Validity and reliability of the newly developed surface electromyography device for measuring muscle activity during voluntary isometric contraction." *Computational and mathematical methods in medicine* 2018 (2018).
[100] Hides, Julie A., et al. "The effect of low back pain on trunk muscle size/function and hip strength in elite football (soccer) players." *Journal of Sports Sciences* 34.24 (2016): 2303-2311.
[101] Jinnovart, Thanaporn, Xiongcai Cai, and Kundjanasith Thonglek. "Abnormal gait recognition in real-time using recurrent neural networks." *2020 59th IEEE Conference on Decision and Control (CDC)*. IEEE, 2020.
[102] Fricke, Christopher, et al. "Evaluation of three machine learning algorithms for the automatic classification of EMG patterns in gait disorders." *Frontiers in neurology* 12 (2021): 666458.
[103] Zawawi, T. N. S. T., et al. "Classification of EMG signal for health screening task for musculoskeletal disorder." *Int. J. Eng. Technol* 8.1.7 (2019): 219-226.
[104] Montazerin, Mansooreh, et al. "ViT-HGR: Vision transformer-based hand gesture recognition from high density surface EMG signals." *2022 44th Annual International Conference of the IEEE Engineering in Medicine & Biology Society (EMBC)*. IEEE, 2022.
[105] Shen, Shu, et al. "Movements classification through sEMG with convolutional vision transformer and stacking ensemble learning." *IEEE Sensors Journal* 22.13 (2022): 13318-13325.

[106] Zhang, Hanyang, et al. "ViT-LLMR: Vision Transformer-based lower limb motion recognition from fusion signals of MMG and IMU." *Biomedical Signal Processing and Control* 82 (2023): 104508.

[107] Houglum, Peggy A. "*Therapeutic exercise for musculoskeletal injuries 4th edition*." Human Kinetics, 2016.

Appendix

Appendix A: Ethical Approval from Brunel University

University Research Ethics Committee
Brunel University London
Kingston Lane

10 June 2022

LETTER OF CONDITIONAL APPROVAL

APPROVAL HAS BEEN GRANTED FOR THIS STUDY TO BE CARRIED OUT BETWEEN 10/06/2022 AND 30/09/2022

Applicant (s): Mr. Anthony Bawa, Dr. Mensah Yeboah, Dr. Evans Ansu-Yeboah

Project Title: GAIT ASSESSMENT OF PATIENTS WITH RHEUMATIC CONDITIONS USING ELECTROMYGRAPHY SENSOR NETWORK.

Reference: 35807-MHR-Apr/2022- 39291-3

Dear Mr. Anthony Bawa

The Research Ethics Committee has considered the above application recently submitted by you.

The Chair, acting under delegated authority has agreed that there is no objection on ethical grounds to the proposed study. Approval is given on the understanding that the conditions of approval set out below are followed:

- This approval is subject to approval being granted by the local IRB. Please provide evidence of this once received (prior to commencement of the study) via email to res-ethics@brunel.ac.uk.
- When approaching potential control subjects, please ensure that you communicate the inclusion/exclusion criteria as you may not know immediately whether hospital employees will be eligible to take part (i.e., that they do not have any health conditions which may impact results or place them at risk).
- The agreed protocol must be followed. Any changes to the protocol will require prior approval from the Committee by way of an application for an amendment.
- Please ensure that you monitor and adhere to all up-to-date local and national Government health advice for the duration of your project.

Please note that:

- Research Participant Information Sheets and (where relevant) flyers, posters, and consent forms should include a clear statement that research ethics approval has been obtained from the relevant Research Ethics Committee.

- The Research Participant Information Sheets should include a clear statement that queries should be directed, in the first instance, to the Supervisor (where relevant), or the researcher. Complaints, on the other hand, should be directed, in the first instance, to the Chair of the relevant Research Ethics Committee.
- Approval to proceed with the study is granted subject to receipt by the Committee of satisfactory responses to any conditions that may appear above, in addition to any subsequent changes to the protocol.
- The Research Ethics Committee reserves the right to sample and review documentation, including raw data, relevant to the study.
- If your project has been approved to run for a duration longer than 12 months, you will be required to submit an annual progress report to the Research Ethics Committee. You will be contacted about submission of this report before it becomes due.
- You may not undertake any research activity if you are not a registered student of Brunel University or if you cease to become registered, including abeyance or temporary withdrawal. As a deregistered student you would not be insured to undertake research activity. Research activity includes the recruitment of participants, undertaking consent procedures and collection of data. Breach of this requirement constitutes research misconduct and is a disciplinary offence.

Kind regards,

Dr Derek Millard-Healy

Chair of the University Research Ethics Committee

Brunel University London

Appendix B: Ethical Approval from KATH hospital

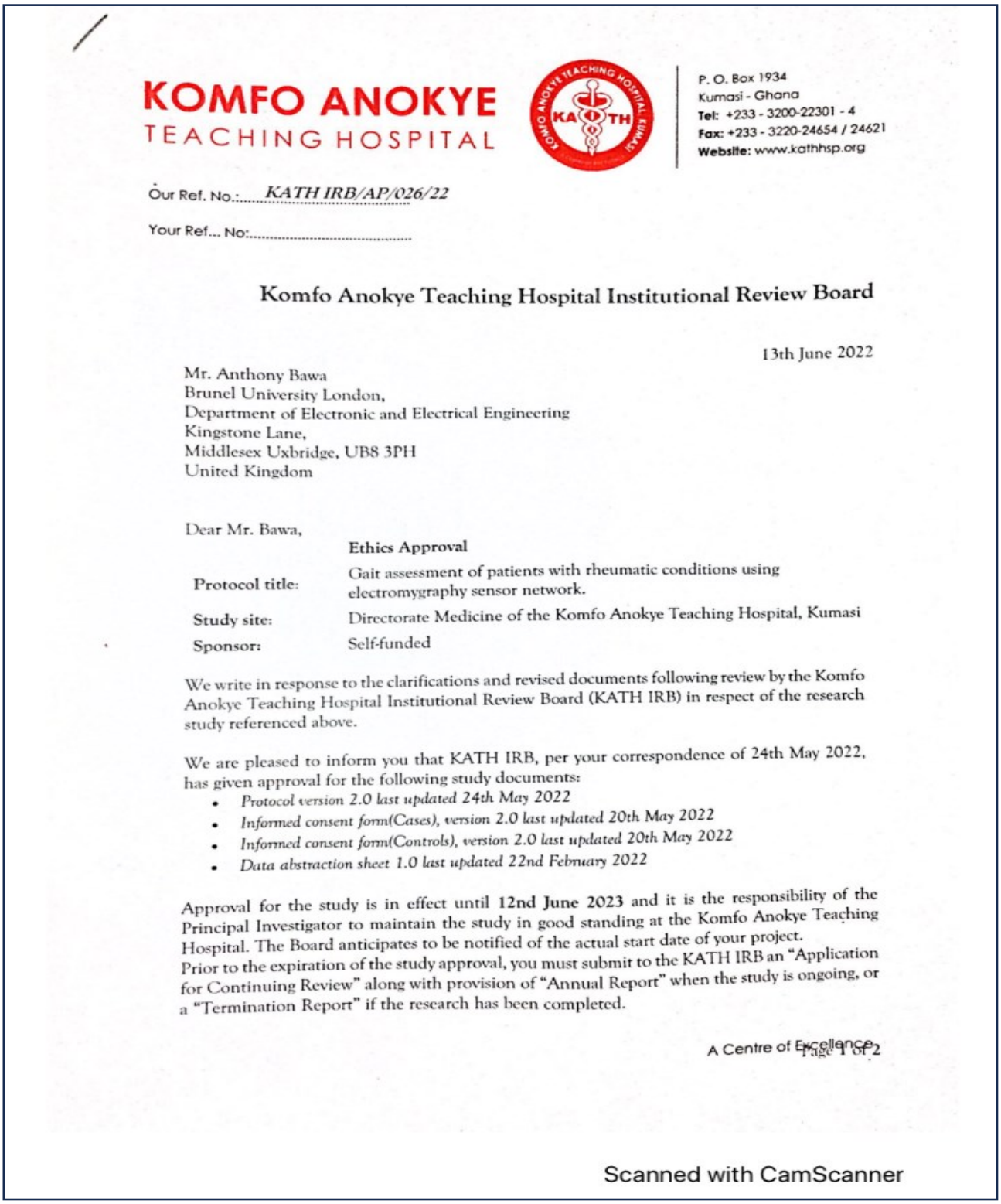

KOMFO ANOKYE
TEACHING HOSPITAL

P. O. Box 1934
Kumasi - Ghana
Tel: +233 - 3200-22301 - 4
Fax: +233 - 3220-24654 / 24621
Website: www.kathhsp.org

Our Ref. No.: *KATH IRB/AP/026/22*

Your Ref... No:.....

Komfo Anokye Teaching Hospital Institutional Review Board

13th June 2022

Mr. Anthony Bawa
Brunel University London,
Department of Electronic and Electrical Engineering
Kingstone Lane,
Middlesex Uxbridge, UB8 3PH
United Kingdom

Dear Mr. Bawa,

Ethics Approval

Protocol title:	Gait assessment of patients with rheumatic conditions using electromygraphy sensor network.
Study site:	Directorate Medicine of the Komfo Anokye Teaching Hospital, Kumasi
Sponsor:	Self-funded

We write in response to the clarifications and revised documents following review by the Komfo Anokye Teaching Hospital Institutional Review Board (KATH IRB) in respect of the research study referenced above.

We are pleased to inform you that KATH IRB, per your correspondence of 24th May 2022, has given approval for the following study documents:

- *Protocol version 2.0 last updated 24th May 2022*
- *Informed consent form(Cases), version 2.0 last updated 20th May 2022*
- *Informed consent form(Controls), version 2.0 last updated 20th May 2022*
- *Data abstraction sheet 1.0 last updated 22nd February 2022*

Approval for the study is in effect until **12nd June 2023** and it is the responsibility of the Principal Investigator to maintain the study in good standing at the Komfo Anokye Teaching Hospital. The Board anticipates to be notified of the actual start date of your project.
Prior to the expiration of the study approval, you must submit to the KATH IRB an "Application for Continuing Review" along with provision of "Annual Report" when the study is ongoing, or a "Termination Report" if the research has been completed.

Scanned with CamScanner

You must hastily report to the KATH IRB should a modification to the research be proposed, and without delay if an unanticipated development occurs before the next required review. Regulations do not permit you to modify conduct of the study in its present form prior to ethics approval; except where urgent action is required to eliminate an apparent immediate hazard to a study subject or other person. It is of utmost importance data generated from this study must be used for the intended purposes only.

Thank you.

Sincerely,

Prof. Kwabena Antwi Danso, BSc, MB ChB, FWACS, FGCS, FACOG
Chairman, KATH IRB

Appendix C: Patients Consent Form

CONSENT FORM (PATIENT)

TITLE: GAIT ASSESSMENT OF PATIENTS WITH RHEUMATIC CONDITIONS USING ELECTROMYGRAPHY SENSOR NETWORK

PRINCIPAL INVESTIGATOR: ANTHONY BAWA

APPROVAL HAS BEEN GRANTED FOR THIS STUDY TO BE CARRIED OUT BETWEEN 04/07/2022 AND 30/09/2022

The participant should complete the whole of this sheet.		
	YES	NO
Have you read the Participant Information Sheet?	☐	☐
Have you had an opportunity to ask questions and discuss this study?	☐	☐
Have you received satisfactory answers to all your questions?	☐	☐
Who have you spoken to about the study?		
Do you understand that you will not be referred to by your name in any report concerning this study?	☐	☐
Do you understand that:		
• You are free to withdraw from this study at any time	☐	☐
• You don't have to give any reason for withdrawing.	☐	☐
• Your medical record will not be accessed in the study.	☐	☐
• You can withdraw your data any time up to 08/09/2022	☐	☐
I agree to my gait simulation being video recorded.	☐	☐
I agree to the electromyography sensor placed on my muscle surface to record the muscle signals.	☐	☐
The procedures regarding confidentiality have been explained to me	☐	☐
I agree that my anonymized data can be stored and shared with other researchers for use in future projects.	☐	☐

I agree to take part in this study.	☐	☐

Signature of research participant:	
Print name:	Date:

Appendix D: Participant Information Sheet

PARTICIPANT INFORMATION SHEET (PATIENT)

Study title: Gait Assessment of Patients with Polymyalgia Rheumatica Using Electromyography Sensor Network**.**

Invitation Paragraph

You are invited to participate in this academic study on gait assessment of patients with rheumatic conditions using surface electromyography sensor. The main aim of this study is to conduct gait assessment of patients with rheumatic conditions to determine if there is any gait abnormality. All the standard protocols for a clinical experiment will be duly followed. The study is being conducted by Anthony Bawa, a doctoral researcher in the department of Electronic and Electrical Engineering at Brunel University London.

Principal Supervisor: Dr. Konstantinos Banitsas.

What is the purpose of the study?

The main aim of the study is to conduct gait assessment of patients with rheumatic conditions to determine if there is any gait abnormality. This is to investigate how the muscular activities of patients with rheumatic conditions affects their movement. It will conduct an in-depth gait assessment of patients with rheumatic conditions using the electromyography sensor. The study would also seek to find out if there is any muscular imbalance for patients with the condition.

Why have I been invited to participate as a patient?

You are invited to participate in this study because this study is targeted at patients who have rheumatic musculoskeletal disease. You are chosen as a participant because it is believed you can provide the essential data required for the study. You are expected to freely agree to sign a consent form and have the option to opt out at any point in the experiment period. There is no direct benefit to the participant, and this will not affect your treatment for not taking part in the study.

Do I have to take part?

Your participation is voluntary, it is up to you to decide whether you want take part in this clinical experiment. If you decide to part take in this study, you would be providing the essential data in the experiment. All the procedure and the information required will be explained into details in English language for your understanding. A consent form is to be signed before participating in the experiment.

What will happen to me if I take part?

You would be needed for the research study for a period of one day to conduct the experiment. There would be preparation of participants before the actual experiment. The experiment should last for a

minimum period of 30 mins and a maximum of an hour. During the experiment process you would be doing some walking and performing simple activities. Whiles performing these activities, the EMG sensor will be attached to the desired specific muscles to read the muscle signals. There would be Kinect sensor in the room to record the movement, however patients' image will be protected. All the safety measures and standard protocols in the laboratory experiment will be strictly adhered to.

Are there any lifestyle restrictions?

There are no lifestyle restrictions for participants involved during the study or after the experiment.

What are the possible disadvantages and risks of taking part?

Some of the risks anticipated might be participants may slip and fall in the process of gait simulation. If allergic, some participants may react to the sticky plaster of the EMG sensor that would be attached to the skin surface. This may create some discomfort for some participants. If something happens, immediate measures would be taken to ensure the safety of all participants in this study. The medical team collaborating with the principal investigator.

Are the any risks of contracting Covid-19?

There may be possible risks of contracting Covid-19. However, all the safety protocols will be strictly adhered to in the hospital facility and there would be no crowding.

What are the safety protocols to mitigate the risks of contracting Covid-19?

Safety protocols and measures to be put in place at location Centre of the hospital where the research will be contacted are.

- Wash and sanitize the hands frequently during the day.
- Avoid handshakes and close contact with others.
- Avoid touching the face, nose, and mouth.
- Wearing mask at all times.
- Observe physical distancing and maintain a two-metre gap.
- Use tissue to cover up mouth and nose when sneezing or coughing.
- Ensure the room is well ventilated and windows open.

What are the safety measures put in place for gait simulation?

There are some safety measures put in place to ensure the safety of patients who agree to participate in the study. The gait simulation room will be cleared of any obstructive objects that can cause a fall. The floor will be kept dry and clean to allow patients work freely. For participants who react to the sticky plaster from the Surface EMG sensor the medical team will be available to apply anti-itching solutions to the participants.

What are the possible benefits of taking part?

There are no direct benefits to the participants. Even though there are no direct benefits to participants, the study would contribute knowledge to understanding the gait of patients with rheumatic conditions. If you decide not to take part, it will not affect your treatment at the hospital.

What if something goes wrong?

The study does anticipate anything to go wrong that could result in injury to the patient. However, in the unlikely event that something goes wrong, there are structures in place to address any issues. Concerns can be sent to department email: cedps-research@brunel.ac.uk

Will my taking part in this study be kept confidential?

The information taken from the study would be kept highly confidential. The type of data to be collected will be EMG signals data captured from participants. There is maximum data integrity and essential data collected for patients will be secured with the standard protocols set up by Brunel University London.

Will I be recorded, and how will the recording be used?

Participants will be video recorded during the experiment process. Participants will be recorded because we may need to extract skeletal features of participants in motion. Participants will be video record with motion capturing devices such a Kinect Azure to extract the gait features.

What will happen to the results of the research study?

The findings would also be given to a medical officer at the KATH hospital. The qualified clinician would be competent to interpret the outcome of the study to participants.

What are the indemnity arrangements?

Ghana scholarship secretariat would provide the insurance cover for the study. Insurance package will be included according to the Ghanaian law and the standards required at KATH.

Who has reviewed the study?

The IRB from KATH will be reviewing the study.

Contact for information and complaints.

Researcher name and details: Anthony Bawa, Email: Anthony.bawa@brunel.ac.uk Tel: +233202197777

Chair of the University Research Ethics Committee Dr Derek Millard-Healy

Brunel University London, Email: res-ethics@brunel.ac.uk.

Appendix E: Sample codes with python language

```
import numpy as np
import pandas as pd
from sklearn.preprocessing import MinMaxScaler
import tensorflow as tf
from tensorflow.keras.models import Sequential
from tensorflow.keras.layers import Dense, LeakyReLU,
BatchNormalization
from tensorflow.keras.optimizers import Adam

num_samples = int(input('How many sample you want to generate?  : '))
dataset_name =  input('Enter dataset name: (e.g.
NewGait_DatasetFive.csv)')


dfs = []
import pandas as pd
from google.colab import drive
drive.mount('/content/drive')

#datam = pd.read_csv('/content/drive/My Drive/dataset(anthony)/'
+dataset_name)
datam = pd.read_excel('/content/drive/My Drive/dataset(anthony)/'
+dataset_name)

labels = [0, 1, 2]

for label in labels:
  datax = datam[datam['Label '] == label]
  ecg_data = datax.drop(['Label '], axis=1)
  dim  = ecg_data.shape[1]
  print(dim)

  # Define the generator model
  def create_generator():
      model = Sequential()
      model.add(Dense(100, input_dim=100))
      model.add(LeakyReLU(0.2))
      model.add(Dense(200))
      model.add(LeakyReLU(0.2))
```

```
        model.add(Dense(dim, activation='tanh')) # Adjust this layer to
match your sequence length
        return model

    # Define the discriminator model
    def create_discriminator():
        model = Sequential()
        model.add(Dense(200, input_dim=dim)) # Adjust this layer to match
your sequence length
        model.add(LeakyReLU(0.2))
        model.add(Dense(100))
        model.add(LeakyReLU(0.2))
        model.add(Dense(1, activation='sigmoid'))
        return model

    # Create the GAN
    def create_gan(discriminator, generator):
        discriminator.trainable = False
        gan_input = tf.keras.Input(shape=(100,))
        x = generator(gan_input)
        gan_output = discriminator(x)
        gan = tf.keras.Model(inputs=gan_input, outputs=gan_output)
        return gan


    # Normalize the data to be between -1 and 1
    scaler = MinMaxScaler(feature_range=(-1, 1))
    ecg_data_normalized = scaler.fit_transform(ecg_data)

    # Convert data to numpy array
    ecg_data_normalized = np.array(ecg_data_normalized)

    # Function to get real data
    def get_real_data(batch_size):
        random_indexes = np.random.randint(0, len(ecg_data_normalized),
batch_size)
        return ecg_data_normalized[random_indexes]

    # Training parameters
    epochs = 100
    batch_size = 128

    # Create the discriminator, generator and GAN
    discriminator = create_discriminator()
    discriminator.compile(loss='binary_crossentropy', optimizer=Adam())
    generator = create_generator()
```